Paired $\delta^{18}O$ and Sr/Ca records of *Porites* corals from Tahiti (French Polynesia) and Timor (Indonesia)

Dissertation

Zur Erlangung des Doktorgrades
der Mathematisch-Naturwissenschaftlichen Fakultät
der Christian-Albrechts-Universität
zu Kiel

Vorgelegt von
Sri Yudawati Cahyarini

Kiel 2006

Referent/in: :.....

Koreferent/in :.....

Tag der mündlichen Prüfung :.....

Zun Druck genehmigt : Kiel, den.....

to my parents:
Koessantjojo Oemar and Sri Marmini

He has let loose the two seas (the salt and fresh water) meeting together. Between them is a barrier which none of them can transgress. Then which of the Blessings of your Lord will you deny? Out of them both come out pearl and coral. Then which of the Blessings of your Lord will you deny?
(Qur'an 55:19-23)

ABSTRACT

In order to better understand natural climate variability, as well as the impact of anthropogenic influences on 20th century climate, long records of important climate variables covering the past hundreds to thousand years are needed. The instrumental database is too short to provide this information. Geochemical proxies measured in Scleractinian coral skeletons are an ideal tool to reconstruct seasonal, interannual and decadal to centennial climate variations. Furthermore, corals live throughout the tropical oceans and their skeletons have annual density bands providing a precise chronological control. The aragonite coral skeletons incorporate a diverse suite of isotopic and trace elemental proxies during their formation tracking ambient water temperature, salinity, and other environmental processes, e.g., turbidity and runoff.

Sea surface temperature (SST) is the most important climatic parameter. Despite the fact that there are still some differences in published coral Sr/Ca-SST calibrations, many studies have confirmed that coral Sr/Ca is a reliable temperature proxy. Another important climate parameter is sea surface salinity (SSS). SSS can not be measured directly from coral aragonite. Coral $\delta^{18}O$, however, records both ambient water temperature and seawater $\delta^{18}O$ ($\delta^{18}O_{sw}$). The latter is assumed to correlate linearly with SSS. Thus, paired measurements of coral Sr/Ca and $\delta^{18}O$ can be used to reconstruct SSS over the past several centuries. However, the statistical methods that are being used for $\delta^{18}O_{sw}$ (SSS) calculations from paired coral Sr/Ca and $\delta^{18}O$ measurements have been a matter of intense debate during the past few years. The problem is amplified by the fact that the reliability of $\delta^{18}O_{sw}$ reconstructions inferred from paired coral Sr/Ca and $\delta^{18}O$ measurements is difficult to assess due to the lack of continuous time series of $\delta^{18}O_{sw}$ and the poor quality of the instrumental salinity datasets currently available.

The aims of this thesis are to evaluate the coral Sr/Ca -SST relationship, and the reliability of coral-based seawater $\delta^{18}O$ reconstructions as indicators of SSS variations on seasonal to centennial time scales covering more than hundreds years. Furthermore, the potential of the corals to record major climate phenomena such as the El Niño Southern Oscillation (ENSO) will be evaluated. For this purpose, we have analyzed coral cores from the western Pacific warm Pool (Timor, Indonesia) and the central Pacific (Tahiti, French Polynesia).

(1) Coral Sr/Ca-SST calibrations are calculated and compared using several coral Sr/Ca records and various instrumental SST datasets. The Tahiti Sr/Ca records are used as examples, because there are several coral Sr/Ca records from different coral cores available in this area. Usually only one Sr/Ca record from a single coral core is calibrated with an SST dataset selected from the different data products currently available. SST datasets from global SST data products refer to a defined area and have grid-box resolution. The SST record inferred from coral Sr/Ca is local and represents a point measurement. Therefore, using the regression equation by calibrating Sr/Ca with grid-SST data may lead to a bias in reconstructed SST. I calibrate Sr/Ca with grid-SST using several Sr/Ca records from Tahiti, i.e., three single Sr/Ca records and average Sr/Ca records from several cores. Different SST datasets are used. The results show that averaging proxy measurements from multiple coral colonies improves the correlation coefficients of the proxy and SST, provides a better estimate of the SST variance, and minimizes the residual SST. SST reconstructions using average proxy records are suggested to be more representative of regional SST variations.

(2) The methods of coral-based seawater $\delta^{18}O$ reconstructions from paired coral $\delta^{18}O$ and Sr/Ca measurements proposed by Gagan et al. (1994, 1998) and Ren et al. (2002) are evaluated and a new simpler and statistically correct method is proposed. Coral $\delta^{18}O$ and Sr/Ca measurements at Tahiti are used as examples. I find that the Gagan et al. (1994, 1998) method contains a methodological error, because coral $\delta^{18}O$ is calibrated with SST only, and if SST and SSS co-vary, there will be a bias in the slope estimate of coral $\delta^{18}O$ vs. SST. The Ren et al. (2002) method requires the calculation of the first derivatives from measured coral $\delta^{18}O$ and Sr/Ca and can be simplified using the centering method (i.e., by removing the mean values from the variables) proposed in this study. $\delta^{18}O_{sw}$ variations calculated using either the Ren et al. (2002) or Centering method are the same. Ideally, a multiple linear regression (MLR) of coral $\delta^{18}O$ vs. SST and SSS should be used for the calculation of $\delta^{18}O_{sw}$ and SSS. The MLR can account for covariant SST and SSS changes in the regression. To omit the regression constant in the MLR, I propose to center the MLR equations. The statistical error propagation of reconstructed $\delta^{18}O_{sw}$ is calculated to assess our ability to resolve past variations in $\delta^{18}O_{sw}$ (SSS). Only variations that are larger than the combined analytical uncertainty of coral $\delta^{18}O$ and Sr/Ca can be resolved.

(3) Further, the climatic variations recorded in the coral proxy records from Tahiti and Timor are carefully examined.

(a.) Tahiti is located in the south western tropical Pacific (SWTP) (24°S-10°S and 160°E-140°W) which is characterized by a horizontal SSS gradient between a south-eastward oriented tongue of fresh water featuring the warm pool and a westward oriented tongue of high salinity water advected by the southern branch of the south equatorial current coming from the central south Pacific. SSS variations in this area arise from the displacement of this salinity front. The salinity front separates the high salinity waters formed in the subtropical region (20°S, 120°W), where evaporation exceeds precipitation, and the low salinity waters of the warm pool area, where precipitation exceeds evaporation. The frontal region is located under the south Pacific convergence zone (SPCZ) which plays a significant role in global atmospheric circulation. The movement of SPCZ also influences the climate in this region. In the SWTP, ENSO related SST anomalies are an order of magnitude smaller than seasonal anomalies, while the magnitude ENSO-related SSS anomalies is twice as large as the seasonal signal. Tahiti is located exactly at the eastern margin of the SWTP.

Coral Sr/Ca records of the Tahiti cores show local SST. However, the coral Sr/Ca based SST reconstruction from Tahiti shows much larger variation on interannual times scales than grid-SST, i.e., the variance of the annual mean SST reconstruction based on the monthly Sr/Ca-SST calibration differs from instumental grid-SST. This reflects the different spatial scales of the proxy and grid-SST and is a serious problem to any attempt to assess the magnitude of regional SST variations from fossil corals. Seasonal SSS variations at Tahiti can not be resolved because the signal is smaller than the combined analytical uncertainty of coral $\delta^{18}O$ and Sr/Ca. At Tahiti, coral Sr/Ca and $\delta^{18}O$ are poor indicators of ENSO variability. This is not surprising, since Tahiti is located close to a zero line of the ENSO-related SST anomaly pattern in the tropical Pacific. However, the coral Sr/Ca records from Tahiti appear to record the SST anomalies in the Niño 4 region at interannual scales. In the Niño 4 region, the leading SST mode is a decadal mode, which may be captured in the proxy records from Tahiti.

The results of this thesis contribute significantly to coral paleoclimatology studies at Tahiti which will follow the IODP Tahiti expedition in 2005.

(b.) Timor is located in the western Pacific warm pool (WPWP) which is characterized by the warmest ocean water on the earth and is an important driver of the tropical atmospheric circulation. The system of currents transporting warm water out of the WPWP and into the Indian ocean is called the Indonesian Throughflow (ITF). The ITF plays an important role in

the global climate system and also in modulating and terminating warm ENSO events and it is also influences the Australasian monsoon, which in turn drives the climate in the WPWP. The Timor coral site is located in an ITF exit passage (Ombai strait). The ITF, the Australasian monsoon, and the ENSO phenomenon are all influencing the climatic conditions in this area.

At Timor, coral Sr/Ca shows SST, while $\delta^{18}O$ is influenced both by SST and $\delta^{18}O_{sw}$ (SSS). Seasonal SSS variations can be reconstructed from paired $\delta^{18}O$ and Sr/Ca measurements. Coral Sr/Ca and $\delta^{18}O$ do not show a clear correlation with El Niño. Filtering of the Timor records in the ENSO frequency bands does not improve the correlation of the Timor coral proxy records with Niño 3.4. However, spectral analysis shows significant coherence between Timor coral Sr/Ca and the Niño 3.4 index at interannual periods. At decadal time scales, coral Sr/Ca and SST show similar trends. Spectral analysis of the Timor Sr/Ca record shows significant power at decadal periods. A running correlation between coral Sr/Ca and the Pacific Decadal Oscillation (PDO) index shows a high correlation for November to February average months.

ZUSAMMENFASSUNG

Um natürliche Klimavariabilität und die Auswirkungen anthropogener Einflüsse auf das Klima des 20. Jahrhunderts besser zu verstehen, sind lange Aufzeichnungen/Rekonstruktionen der wichtigen Klimavariablen für die letzten einhundert bis tausend Jahre erforderlich. Die instrumentelle Datenbank ist zu kurz, um diese Informationen zur Verfügung zu stellen.

An skleraktinen Korallenskeletten gemessene geochemische Proxies sind ein ideales Werkzeug für die Rekonstruktion von Klimaveränderungen auf saisonalen, interannuellen und dekadischen Zeitskalen. Die Verbreitung von Korallen erstreckt sich über alle tropischen Ozeane. Aragonitische Korallenskelette zeigen jährliche Dichtebänder, die eine exakte chronologische Einordnung erlauben. Während des Wachtums bauen Korallen ein breites Spektrum von Isotopen und Spurenelementen in ihr Skelett ein und zeichnen so die Temperatur und den Salzgehalt des umgebenden Meerwassers auf und können wichtige Daten über andere Prozesse (z.B. Wassertrübung und Flusseintrag) speichern.

Meeresoberflächentemperatur (SST) stellt den wichtigsten Klimaparameter dar. Viele Studien haben gezeigt, dass Sr/Ca aus Korallen ein verlässlicher Proxy für Temperatur ist, wenngleich die bisher veröffentlichten Sr/Ca-Temperatur (SST) Kalibrationen auch Differenzen aufweisen. Ein weiterer wichtiger Klimaparameter ist der Salzgehalt an der Meeresoberfläche (SSS). Der Salzgehalt kann nicht direkt am Aragonit des Korallenskeletts gemessen werden. Jedoch zeichnet das $\delta^{18}O$ in Korallen sowohl die umgebende Wassertemperatur, als auch das $\delta^{18}O$ des Meerwassers ($\delta^{18}O_{sw}$) auf, von dem angenommen wird das es linear mit dem Salzgehalt (SSS) korreliert. Folglich können gepaarte Messungen von Sr/Ca und $\delta^{18}O$ an der Koralle dazu verwendet werden, um den Salzgehalt des Meeres für die vergangenen Jahrhunderte zu rekonstruieren. Allerdings waren die statistischen Methoden, die zur Berechnung von $\delta^{18}O_{sw}$ (SSS) verwendet werden, in den letzten Jahren Gegenstand zahlreicher Auseindandersetzungen/Debatten /Diskussionen. Dieses Problem wird noch zusätzlich verstärkt, da aufgrund fehlender kontinuierlicher $\delta^{18}O_{sw}$ Zeitreihen und der schlechten Qualität der gegenwärtig verfügbaren instrumenteller Salzgehaltsdaten die Verlässlichkeit der auf gepaarten Sr/Ca und $\delta^{18}O$ Messungen basierenden $\delta^{18}O_{sw}$ Rekonstruktionen schwer zu beurteilen/nachzuprüfen ist.

Die Ziele dieser Arbeit sind die Evaluierung der Beziehung zwischen Sr/Ca aus Korallen und SST, und die Verlässlichkeit/Zuverlässigkeit der auf Korallen basierenden $\delta^{18}O$-Meerwasser Rekonstruktionen als Indikator für Variationen im Salzgehalt auf saisonalen bis hundertjährigen Zeitskalen. Desweiteren untersuchen wir, inwieweit Korallen dazu geeignet sind wichtige Klimaphänomene wie die El Niño Southern Oscillation (ENSO) aufzuzeichnen. Zu diesem Zweck haben wir Korallenkerne aus dem "Western Pacific Warm Pool" (Timor, Indonesien) und dem zentralen Pazifik (Tahiti, Französich Polynesien) untersucht.

(1) Verschiedene Sr/Ca Zeitreihen aus Korallen und instrumentelle SST Daten wurden verwendet um Korallen Sr/Ca-SST Kalibrationsgleichungen zu berechnen. Da aus Tahiti mehrere Sr/Ca Zeitreihen aus verschiedenen Korallenkernen vorliegen, werden diese als Beispiel dienen. Gewöhnlich wird eine Sr/Ca Zeitreihe aus einem Korallenkern unter Verwendung eines SST Datensatzes kalibriert, der sich auf ein definiertes Gebiet (Planquadrat) bezieht und eine bestimmte räumliche Auflösung aufweist. Die aus dem Korallen Sr/Ca abgeleitete Temperatur-Zeitreihe ist lokal, d.h. sie repräsentiert eine Punktmessung. Deshalb kann die Kalibration der Sr/Ca Zeitreihe mit instrumenteller SST (Grid-SST), die eine geringe räumliche Auflösung aufweist (/über ein grösseres Gebiet gemittelt wurde), zur Verfälschung der rekonstruierten SST führen. Deshalb werden für die Sr/Ca-SST Kalibration mehrere Sr/Ca Zeitreihen aus Tahiti (drei einzelne Sr/Ca Zeitreihen) verwendet, der Mittelwert aus verschiedenen Kernen berechnet, und mehrere SST Datensätze benutzt. Die Ergebnisse zeigen, dass das Mitteln von Proxy Zeitreihen aus verschiedenen Korallenkolonien sowohl die Korrelationskoeffiezienten zwischen Proxy und SST erhöht, als auch die Abschätzung der SST Varianz verbessert und das SST Residuum minimiert. Deshalb sind auf gemittelten Proxy Zeitreihen basierende SST Rekonstruktionen vermutlich besser geeignet um regionale SST Variationen anzuzeigen.

(2) Wir evaluieren die auf gepaarten Messungen von $\delta^{18}O$ und Sr/Ca aus Korallen basierenden Methoden zur Rekonstruktion von $\delta^{18}O$ Meerwasser von Gagan et al. (1994, 1998) und Ren et al. (2002), und stellen eine neue, einfachere und statistisch korrekte Methode vor. Korallen $\delta^{18}O$ und Sr/Ca aus Tahiti werden als Beispiel verwendet. Wir haben festgestellt das die Methode von Gagan et al. (1994, 1998) einen methodischen Fehler enthält, da darin das $\delta^{18}O$ aus Korallen nur mit SST kalibriert wird. Im Falle einer Kovarianz von SST und SSS würde dies zu einem Fehler in der berechneten Steigung der Korallen $\delta^{18}O$-SST Kalibrationsgleichung führen. Die von Ren et al. (2002) vorgeschlagene Methode erfordert

die Berechnung der ersten Ableitung aus den gemessenen Korallen $\delta^{18}O$ und Sr/Ca Werten, dies kann durch die Anwendung der hier vorgestellten Centering-Methode vereinfacht werden (durch die Entfernung der Mittelwerte aller Variablen). Die mit Hilfe der Ren et al. (2002) - Methode und Centering-Methode berechneten d18Osw-Werte sind identisch. Idealerweise sollte eine Multiple Lineare Regression (MLR) von Korallen $\delta^{18}O$ gegen SST und SSS für die Berechnung von $\delta^{18}O_{sw}$ und SSS verwendet werden. Die MLR kann kovariante Änderungen von SST und SSS in der Regression erfassen. Um die Regressionskonstanten in der MLR zu auszusparen, schlage ich vor die Centering-Methode auf die MLR Gleichungen anzuwenden. Die statistische Fehlerfortpflanzung im rekonstruierten $\delta^{18}O_{sw}$ wird berechnet um abzuschätzen inwieweit Variationen im $\delta^{18}O_{sw}$ (SSS) aufgelöst werden können. Es können nur Schwankungen aufgelöst werden, die grösser sind als die kombinierte analytische Unsicherheit für das $\delta^{18}O$ und Sr/Ca aus den Korallen.

(3) Ausserdem untersuchen wir die in den Proxy Zeitreihen der Korallen aus Timor und Tahiti aufgezeichnete Klimavariabilität.

(a.) Tahiti liegt im südwestlichen tropischen Pazifik (SWTP) (24°S-10°S und 160°E-140°W), der durch einen horizontalen SSS Gradienten zwischen einer südostwärts orientierten Frischwasserzunge des "West Pacific Warm Pools" und einer westwärts gerichteten Zunge höhersalineren Wassers, das vom südlichen Teil der aus dem südzentralen Pazifik kommenden Südequatorialströmung transportiert wird, gekennzeichnet ist. Salzgehaltsänderungen in diesem Gebiet resultieren aus der Verschiebung der Salinitätsfront. Die Salinitätsfront trennt hochsalines, in den Subtropen (20°S, 120°W) gebildetes Wasser (Evaporationsrate übersteigt die Niederschlagsrate) und niedrigsalines Wasser aus dem Gebiet des Warm Pools (Niederschlagsrate übertrifft die Evaporationsrate). Die Frontregion befindet sich unter der südpazifischen Konvergenzzone (SPCZ), die eine wichtige Rolle in der globalen atmosphärischen Zirkulation einnimmt. Die Verschiebung der SPCZ beeinflusst das Klima in dieser Region. In der SWTP sind ENSO bedingte SST Anomalien um eine Größenordung kleiner als saisonale Anomalien, wohingegen die Größenordung der ENSO bedingten SSS Anomalien doppelt so gross ist wie das saisonale Signal. Tahiti befindet sich exakt am östlichen Rand des SWTP.

Die Sr/Ca-Zeitreihen der Tahiti Kerne zeigen lokale SST. Jedoch zeigt die auf das Sr/Ca gestützte SST Rekonstruktion aus Tahiti sehr viel grössere Schwankungen auf interannuellen

Zeitskalen im Vergleich zur instrumentellen SST, d.h. die Varianz der jährlich gemittelten SST Rekonstruktion (basierend auf den monatlichen Sr/Ca-SST Kalibration) weicht von der instrumentellen SST ab. Dies spiegelt die unterschiedlichen räumlichen Maßstäbe von Proxy und instrumenteller SST (grid-SST) wider und stellt ein ernstzunehmendes Problem für zukünftige Ansätze dar, die die Rekonstruktion saisonaler SST Schwankungen aus fossilen Korallen zum Ziel haben. Saisonale SSS Schwankungen in Tahiti können nicht aufgelöst werden, da das Signal kleiner ist als der kombinierte analytisch bedingte Fehler der Korallen $\delta^{18}O$ und Sr/Ca Messungen. Aufgrunddessen ist an Korallen aus Tahiti gemessenes $\delta^{18}O$ und Sr/Ca nur bedingt als Indikator für ENSO Variabilität geeignet. Diese Erkenntnis ist nicht überraschend, da Tahiti nahe an einer Nulllinie des ENSO bedingten SST Anomaliefeldes im tropischen Pazifik liegt. Jedoch scheinen die Sr/Ca Zeitreihen aus den Korallen von Tahiti die SST Anomalien in der Niño 4 Region auf interannuellen Zeitskalen widerzuspiegeln. Das Haupt-SST-signal in der Niño 4 Region ist dekadisch, und könnte deshalb in den Proxy Zeitreihen aus Tahiti aufgezeichnet sein.

Die Ergebnisse dieser Arbeit leisten einen wichtigen Beitrag zu den im Anschluss an die IODP Tahiti Expedition (2005) folgenden Studien zur Paläoklimatologie aus Korallen.

(b.) Timor befindet sich im "Western Pacific Warm Pool" (WPWP), der gekennzeichnet ist durch die weltweit wärmsten Meereswassertemperaturen und den eine wichtige Rolle in der atmosphärischen Zirkulation in den Tropen spielt. Das System von Strömungen, dass warmes Wasser vom WPWP in den Indischen Ozean transportiert wird Indonesian Throughflow (ITF) genannt. Der ITF spielt eine wichtige Rolle im globalen Klimasystem und moduliert und terminiert warme ENSO Ereignisse. Ausserdem beeinflusst die ITF den australischen Monsun, der wiederum das Klima im WPWP antreibt. Das Arbeitsgebiet in Timor befindet sich an einer Ausgangspassage des ITF, der sog. Ombai strait. Die Klimabedingungen in diesem Gebiet werden vom ITF, dem australischen Monsun und dem ENSO Phänomen gleichermaßen beeinflusst.

Korallen Sr/Ca aus Timor zeigt SST, während das d18O der Koralle sowohl von SST als auch vom $\delta^{18}O$ des Meerwassers (SSS) beeinflusst wird. Saisonale SSS Schwankungen können mit Hilfe gepaarter $\delta^{18}O$ und Sr/Ca Messungen rekonstruiert werden. Sr/Ca und $\delta^{18}O$ zeigen keine deutliche Korrelation zu El Niño, auch durch das Herausfiltern des ENSO Bands aus den Korallen Proxies kann keine höhere Korrelation mit dem Niño 3.4 Index erzielt werden.

Jedoch zeigt eine Spektralanalyse eine signifikante Kohärenz zwischen der Sr/Ca Zeitreihe der Timor Koralle und dem Niño 3.4 Index auf interannuellen Zeitskalen. Auf dekadischen Zeitskalen zeigen das Sr/Ca der Koralle und die SST ähnliche Trends. Eine Spektralanalyse der Timor Sr/Ca Zeitreihe zeigt signifikante Varianz auf dekadischen Zeitskalen. Eine gleitende Korrelation zwischen dem Korallen Sr/Ca und der Pacific Decadal Oscillation (PDO) erzielt eine hohe Korrelation für die Monate November bis Februar.

ACKNOWLEDGEMENTS

All the praises and thanks be to Allah, the Lord of '*Alamin* (mankind, jinn and all that exists) and peace be upon the Master of the Messengers, Muhammad صلى الله عليه و سلم.

This work would not be realized without any support of many people, and I would like to thank all of them:

1. I am very grateful to Christian Dullo for his believe to me working in completely new topic for me, giving me opportunity to carry out this work. I am greatly indebt for his supervising, took time to read my draft, for his suggestion, critical questions and continuing support during writing my thesis.
2. I am indebted to Miriam Pfeiffer for her guidance in the first years of confusion, for spending time reading my first draft, offering many suggestions, questions which provoked me to more careful and scrutiny of concept, analysis and interpretation. Discussing with her, stimulates me always to develop better idea. I am gratefully also to her for introducing me about German culture and life which make my life easier and enjoyable in Germany. Thanks also for offering good friendship throughout my stay in Kiel.
3. I thank to Anton Eisenhauer for his letter of recommendation to extent my scholarship.
4. Greatly thanks to Dieter Garbe-schönberg for the discussion and an overview about trace element measurement technique.
5. Lutz Haxhiaz, Karin Kiessling, Ana Kolevica for the assistance during laboratory works. I am very grateful to them.
6. I thank to Steffen Hetzinger for the discussion and assistance during the field works and also to Dudi Prayudi, NGO 'Minang Bahari'- Padang, West Sumatra Province and Coral Reef Information and Training Centre (CRITC)- Kupang, East Nusatenggara Province for providing logistic in the field.
7. Special thank to Oliver Timm, Jen Zinke, Noel Kenlyside for discussion and giving me plenty of useful feedback and also to Lars Reuning, Marcus Regenberg, John Reijmer who took time to read and offer critical discussions on my draft. I have benefited greatly from discussion with them. I thanks also to Hendrik Lanzth, Aaron Gaal, Andress Ruegeberg, Sven Roth, Sybille Noe, Steffi, Jenny Kandiano, Nicolas Neuwihenhoe, Caroline. They all are wonderful people and their supports make my life enjoyable in IFM-GEOMAR. With them I had pleasure time during my stay in Germany.

8. Special thank to Indah E. Wijayanti for the discussion about basic Algebra, PPI-Kiel, and Indonesian DAAD scholar holder 2001/2002 for nice time spending together far away from home.
9. I am grateful to *Deustcher Akademischer Austauschdienst* (DAAD) for financing my study and my stay in Kiel.
10. I acknowledge to Geotechnology R & D, Indonesian Institute of Sciences (LIPI) for the permission leaving office to study abroad.
11. Finally, I can't thank enough for their unfailing support: my mother, my brother Andung and Upik, my sister Rini and Mika and also my late father whose spirit informs this work and my life.

CONTENTS

Abstract i

Acknowledgements x

CHAPTER I **Introduction**..... 1-1

1. Corals as climate archives..... 1-1

2. Oxygen isotopes..... 1-3

3. Oxygen isotopes in seawater..... 1-5

4. Sr/Ca ratios..... 1-6

5. El Niño Southern Oscillation 1-8

6. Geographic, climatic and oceanographic settings of the study area..... 1-10

6.1. Geographic description 1-10

6.1.1. South Central Pacific: French Polynesia..... 1-10

6.1.2. West Pacific warm pool: Indonesia..... 1-10

6.2 Climatic and oceanographic setting..... 1-11

6.2.1. South Central Pacific: French Polynesia..... 1-11

6.2.2. West Pacific warm pool: Indonesia..... 1-14

7. Western and Central Pacific corals..... 1-17

8. Aims and objectives..... 1-18

9. Thesis structure..... 1-20

CHAPTER II **Material and Methods**..... 2-1

1. Coral collection..... 2-1

2. Sample preparation..... 2-1

3. Oxygen isotope analysis..... 2-3

3.1. Technical preparation..... 2-4

4. Sr/Ca ratio analysis..... 2-4

4.1. Technical preparation..... 2-4

5. Age model development..... 2-5

6. Time series analysis..... 2-5

6.1. Software packages..... 2-5

6.2. Linear regression analysis..... 2-6

7. Linear extension analysis..... 2-7

CHAPTER III

Calibration of Sr/Ca with sea surface temperature (SST) and Sr/Ca-based SST reconstructions: Records from Tahiti (French Polynesia)..... 3-1

1. Introduction..... 3-1

2. Climatic and oceanographic setting of the study area..... 3-2

3. Material and methods..... 3-3

3.1. SST datasets..... 3-5

3.1.1. ERSST..... 3-6

3.1.2. NCEP SST..... 3-6

3.1.3. IRD SST and Delcroix SST..... 3-6

3.2. Age model development..... 3-7

4. Results and discussion..... 3-7

4.1. Comparison of the SST datasets..... 3-7

4.2. Comparisons of the two age models..... 3-8

4.3. Monthly calibrations of coral Sr/Ca vs. sea surface temperature (SST) 3-9

4.3.1. Temperature as independent and dependent variable..... 3-9

4.3.2. Single records of coral Sr/Ca ratios vs. SST..... 3-10

4.3.3. Averaging coral Sr/Ca records measured in the same colony..... 3-13

4.3.4. Averaging coral Sr/Ca records from different colonies..... 3-13

4.4. Coral Sr/Ca-based SST reconstruction..... 3-15

4.4.1. SST reconstruction based on single coral Sr/Ca records 3-15

4.4.2. SST reconstruction based on average coral Sr/Ca..... 3-17

4.5. The linear extension rate..... 3-18

4.6 Annual mean coral Sr/Ca calibration..... 3-23

5. Concluding remarks..... 3-24

CHAPTER IV

Reconstructing seawater $\delta^{18}O$ from paired coral $\delta^{18}O$ and Sr/Ca ratios: Methods, Error Analysis and Problems, with examples from Tahiti (French Polynesia)..... 4-1

1. Introduction..... 4-1

2. Climatic and oceanographic setting of Tahiti..... 4-3

3. Material and methods..... 4-4

3.1. Sample collection and analytical procedures..... 4-4

3.2. Historical data..... 4-7
4. The reconstruction of $\delta^{18}O$ seawater..... 4-7
4.1. Methodologies..... 4-7
4.1.1. The method of Gagan et al. (1994, 1998) 4-9
4.1.2. The method of Ren et al. (2002)..... 4-9
4.1.3. The Centering method..... 4-11
4.1.4. Multiple linear regression..... 4-12
4.1.5. Centering of multiple linear regression equations..... 4-13
4.2 Error Propagation..... 4-13
4.2.1. Error calculation for the method of Ren et al. (2002) and centering.... 4-14
4.2.2. Error calculation for the multiple linear regression..... 4-14
4.2.3. Error calculation for the centered multiple linear regression..... 4-15
5. Discussion..... 4-15
5.1. Examples: Tahiti records..... 4-15
5.1.1. Calibration: seasonal coral Sr/Ca ($\delta^{18}O$) variations vs. SST..... 4-16
5.1.2. Reconstructing seawater $\delta^{18}O$ using the method of Ren et al. (2002) and centering..... 4-16
5.1.3. Error Propagation: Ren et al. (2002) and centering methods..... 4-19
5.1.4. Example of multiple linear regression analysis..... 4-20
5.2. Reconstructed $\delta^{18}O_{sw}$ (SSS) vs. sea surface salinity (SSS)..... 4-22
5.3. Methods of reconstructing $\delta^{18}O_{sw}$..... 4-26
6. Conclusions..... 4-29

CHAPTER V

Assessing the fidelity of coral $\delta^{18}O$ and Sr/Ca ratios from modern Tahiti corals as recorders of interannual and interdecadal climate variability in the tropical Pacific..... 5-1
1. Introduction..... 5-1
2. Oceanic and climatic setting of Tahiti..... 5-4
3. Material and methods..... 5-4
4. Results and discussion..... 5-8
4.1. Coral Sr/Ca..... 5-8
4.2. Coral $\delta^{18}O$..... 5-10

4.3. Reconstructed seawater $\delta^{18}O$ (SSS)..... 5-13
4.4. Coral Sr/Ca ($\delta^{18}O$) and ENSO..... 5-15
4.5. Interdecadal coral Sr/Ca ($\delta^{18}O$) variations..... 5-22
5. Conclusions..... 5-25

CHAPTER VI
Paired coral $\delta^{18}O$ and Sr/Ca measurements at a Timor coral: salinity variations in an exit passage of the Indonesian Throughflow..... 6-1
1. Introduction..... 6-1
2. Climatic and oceanographic setting..... 6-3
3. Material and methods..... 6-6
4. Results..... 6-8
4.1. Coral Sr/Ca ($\delta^{18}O$)..... 6-8
4.2. Calibration of coral Sr/Ca-SST..... 6-8
4.3. Calibration of coral $\delta^{18}O$ -SST..... 6-9
5. Discussion..... 6-10
5.1. Coral Sr/Ca-SST relationship..... 6-10
5.2. Coral $\delta^{18}O$ variations..... 6-14
5.3. Reconstructed SSS..... 6-15
5.4. ENSO signature in Timor coral Sr/Ca..... 6-19
5.5. El Niño and SSS at Timor..... 6-24
5.6. Interdecadal variations of coral Sr/Ca ($\delta^{18}O$) and the Pacific Decadal Oscillation..... 6-27
6. Concluding remarks..... 6-28

CHAPTER VII
Summary of chapter III-VI, conclusions and further studies..... 7-1
1. Summary of chapter III-VI..... 7-1
2. Conclusions..... 7-3
3. Further studies..... 7-5

REFFERENCES..... 8-1

APPENDICES

Appendix I Core TH1 (Tahiti)

Appendix II Core TH1B (Tahiti)

Appendix III Core TH2 (Tahiti)

Appendix IV Core KP1 (Timor)

CHAPTER I

Introduction

Geochemical proxies measured in corals are a promising tool for paleoclimatic studies, because they can provide long time series of climate parameters extending back hundreds of years, which can not be provided by the available historical dataset. The main objective this thesis is to assess the reliability of coral proxies as records of climate phenomena such as the El Niño -Southern Oscillation (ENSO). ENSO is the prominent climate phenomenon of the tropics and is centered in the Pacific Ocean. The atmospheric-component of ENSO is recorded by the sea level pressure (SLP) difference between Tahiti and Darwin, and is known as the Southern Oscillation Index. Therefore, it is expected that corals from Tahiti (French Polynesia) and Timor, which is close to Darwin, will record ENSO. $\delta^{18}O$ and Sr/Ca are well-known and promising coral proxies for climate. Until now, there are no paired coral $\delta^{18}O$ and Sr/Ca records available from Tahiti and Timor. In this study, modern coral cores from Tahiti and Timor are analyzed for $\delta^{18}O$ and Sr/Ca. The reliability of paired coral $\delta^{18}O$ and Sr/Ca as recorders of climatic variations will be assessed. In this chapter, the use of corals as a climate archives will be followed by a description of $\delta^{18}O$ and Sr/Ca in corals. The ENSO phenomenon is also described in this session. A detailed description of the geographic, climate and oceanographic setting of the study areas is given. The most important results of coral-based studies from the Pacific are summarized followed by a detailed description of the aims and objectives of this thesis and the structure of thesis.

1. Corals as Climate Archive

Massive scleractinian corals from the tropical oceans are paleoclimatic archives, which provide information of the seasonal, annual and interannual climate variability on time scales ranging from several decades to hundreds of years. Most scleractinian coral live in the tropical oceans and grow at rates of 0.6-2 cm/year. Massive growing corals such as those are belonging to the genus *Porites* are particularly well suited for climate reconstructions. *Porites* corals typically grow by about 1-2 cm per year. Scleractinian corals produce annual density bands that provide time markers for the development of long chronologies. A pair of high-and low density bands represents one year of coral growth. The density variations result from changes in the rate of coral calcification and/or linear extension. A preliminary age model is based on counting the density bands, which are visible in X-radiographs of the coral slabs.

This preliminary chronology is then refined using high-resolution coral isotope or trace element profiles, that reflect the seasonal cycle of sea surface temperature and/or salinity (Quinn, et al., 1996; Charles, et al., 1997). A sample spacing of 1 mm allows approximately monthly resolution.

The isotopic and trace elemental signatures of scleractinian corals are a function of environmental changes in the ambient water masses, such as sea surface temperature (SST), salinity (SSS), turbidity and upwelling intensity. However, only few coral records have been calibrated by multi-year in situ monitoring studies located directly at the coral sites. Usually, one relies on the correlation (both near field or far-field) between the proxies and gridded SST, rainfall or salinity data sets or standardized indices of major climate phenomena such as ENSO.

Several paleoclimatic records which are based on $\delta^{18}O$ and or Sr/Ca determinations in modern corals have been published, e.g. a 347 year coral stable isotope and trace element record from a Galapagos coral (Dunbar et al., 1994), a 271 year Sr/Ca records from a Rarotonga coral (Linsley et al., 2000), several $\delta^{18}O$ records from western Indian ocean corals, i.e. Seychelles and La Reunion (Charles et al., 1997; Pfeiffer et al., 2004; Pfeiffer and Dullo, in press), as well as two $\delta^{18}O$ record from Bali and Bunaken Indonesia corals (Charles et al., 2003). Most of these records correlate with local and regional climate indices and also reflect large-scale climate phenomena. Modern coral records usually span up to 200-500 years. The reconstruction of past climate variability throughout the last millennium is possible only using dead and fossil corals. Such a seasonal-resolved coral $\delta^{18}O$ and Sr/Ca record providing a 84 yrs time series from the 16th century was published by Kuhnert et al. (2002). The exceptional monthly coral $\delta^{18}O$ records from Palmyra provide time window of central Pacific climatic variability and ENSO during the last 100 year (Cobb et al., 2001, 2003a). These long records from Palmyra were obtained by overlapping time series of a few hundred years old from modern and dead corals (Cobb et al., 2003a) in a manner similar to the way tree ring time series have been spliced together from individual trees. Palmyra is in a prime location to provide a record of past ENSO variability in the coral $\delta^{18}O$ record. Modern corals from this location correlate well with the Niño 3.4 index, particularly in the ENSO band (Cobb et al., 2003a). Several coral proxy records well the ENSO signal (e.g. Charles et al., 1997; Cobb et al., 2003a; Kilbourne et al., 2004; Zinke et al., 2004; Timm et al., 2005). Figure 1.1 shows several sites of coral proxy studies in the Pacific and Indian oceans.

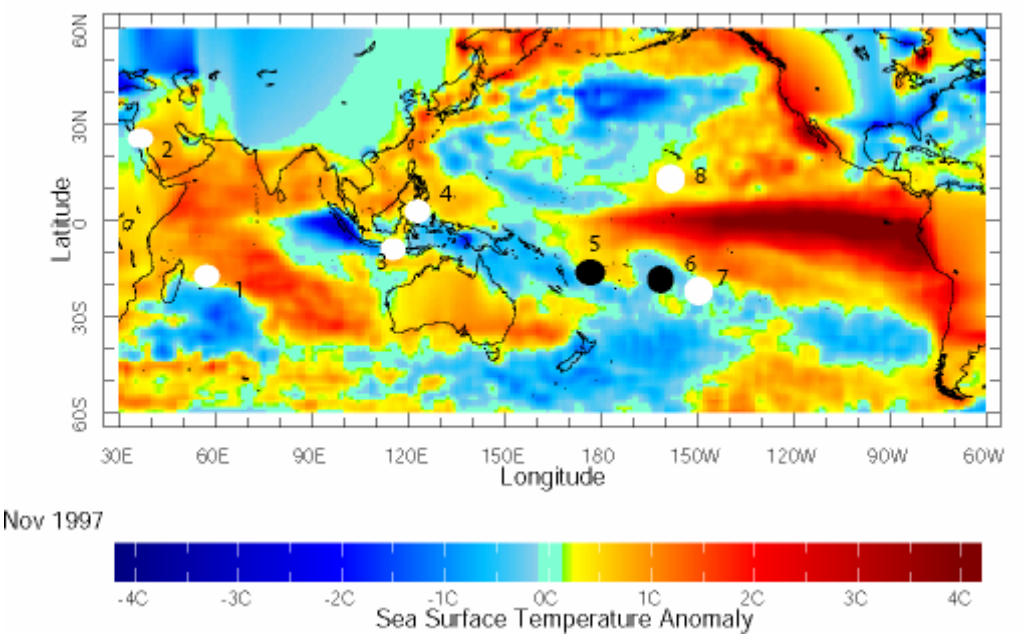

Figure 1.1 Map showing sea surface temperature anomaly for November 1997 (colors) and sites of coral proxy studies (points): coral $\delta^{18}O$ (white dot) and paired coral $\delta^{18}O$ and Sr/Ca (black dot). 1. Seychelles coral, 2. Red Sea coral, 3. Bali coral, 4. Bunaken coral, 5. Fiji coral, 6. Rarotonga coral, 7. Moorea coral, 8. Palmyra coral.

2. Oxygen isotopes

The partitioning of ^{16}O and ^{18}O between seawater and biological carbonate has been a focus of research for decades. The partitioning of isotopes between substances with different isotopic compositions has been known as isotopic fractionation. The fractionation factor α quantifying isotopic fractionation between two substances A and B and is defined as :

$$\alpha_{AB} = R_A/R_B \qquad (1)$$

Where R_A/R_B is the ratio of the heavy /light isotope of any two isotopic systems (e.g $^{18}O/^{16}O$) in the chemical compounds A and B. The fractionation factor α can also be expressed as the difference of the delta value of the compounds A and B:

$$\delta_A - \delta_B = \Delta_{A-B} = 10^3 \ln \alpha_{A-B} \qquad (2)$$

The isotopic composition of two compounds A and B is expressed as "delta value " (δ) in ‰ (permil), that can be defined as:

$$\delta_A = (R_A/R_{standard} - 1) \times 10^3 \text{ (‰)} \qquad (3)$$

$$\delta_B = (R_B/R_{standard} - 1) \times 10^3 \text{ (‰)} \quad (4)$$

The oxygen isotopic composition of carbonates precipitated from any fluid comprises a temperature dependent isotope fractionation factor (McCrea, 1950), and also depends on the isotopic composition of the ambient fluid. Shell-secreting organisms can be used for paleotemperature studies when its carbonate precipitation is in isotopic equilibrium with the seawater where they live. Coral $\delta^{18}O$ in skeletal carbonate is precipitated in isotopic disequilibrium with seawater $\delta^{18}O$ due to 'vital effec'. However, the offset between the coral oxygen isotopic composition and isotopic equilibrium is constant for individual corals.

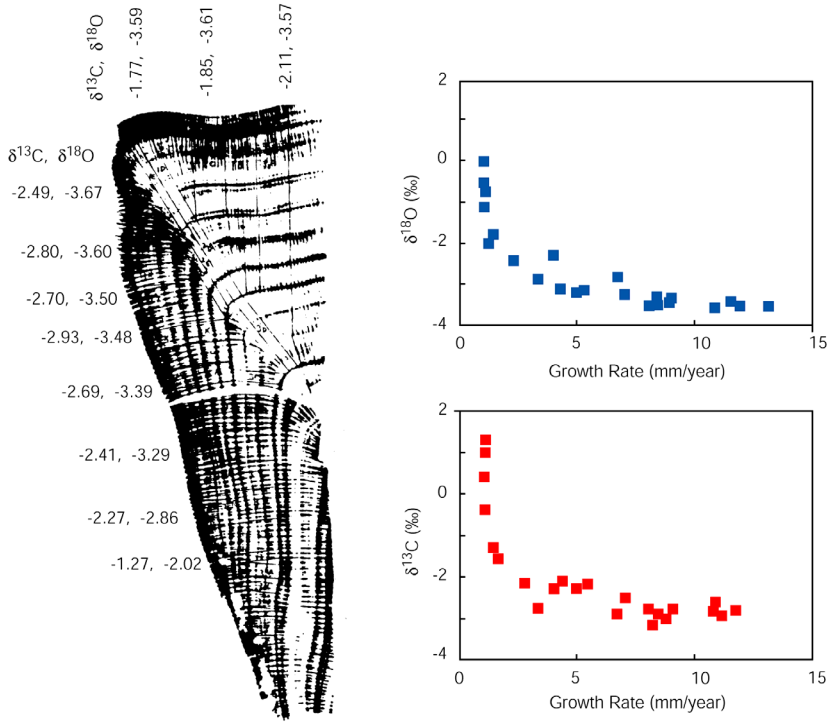

Figure 1.2 Left: X-ray of a *Pavona clavus* coral head from Punta Pitt, San Cristobal Island (Galapagos), sampled horizontally. The numbers represent $\delta^{18}O$ and $\delta^{13}C$ for skeletal aragonite deposited over the 1979-1982 periods. The upper surface of the coral head received more sunshine than the lateral surfaces, grew faster and was relatively depleted in ^{18}O. Right: Correlation between skeletal $\delta^{18}O$ (top) and $\delta^{13}C$ (bottom) and growth rate for *Pavona clavus* head sampled horizontally (redrawn from McConaughey, 1989a)

Weber and Woodhead (1972) compared oxygen isotope determinations from coral skeletons with the expected equilibrium isotopic fractionation. The results showed that there is an "isotopic offset" which indicates that non equilibrium isotopic partitioning occurs during the formation of coral skeletal aragonite. Kinetic and metabolic factors are thought to lead to the isotopic disequilibrium during biological calcification (McConnaughey, 1989a,b). The coral

$\delta^{18}O$ composition is offset below values predicted for equilibrium precipitation at any given temperature. The lower $\delta^{18}O$ values are believed to result from kinetic effects due to the slow reaction kinetics of molecules containing ^{18}O during CO_2 hydration and hydroxylation. Strong kinetic disequilibrium is often associated with rapid calcification in both photosynthetic and non-photosynthetic organisms. The absolute offset in photosynthesis corals is due to kinetic effects and it is constant in the rapidly growing portions of the coral skeleton (McConnaughey, 1989a) (Figure 1.2). However, the magnitude of the offset varies between colonies of the same genus (Figure 1.3) (Linsley et al., 1999; Suzuki et al., 2005). Time dependent variations are controlled by thermodynamic laws and reflect changes in environmental conditions. The $\delta^{18}O$ of calcium carbonate precipitated in equilibrium with seawater decreases by about 0.22 ‰ for every 1° C rise in water temperature (Epstein et al., 1953).

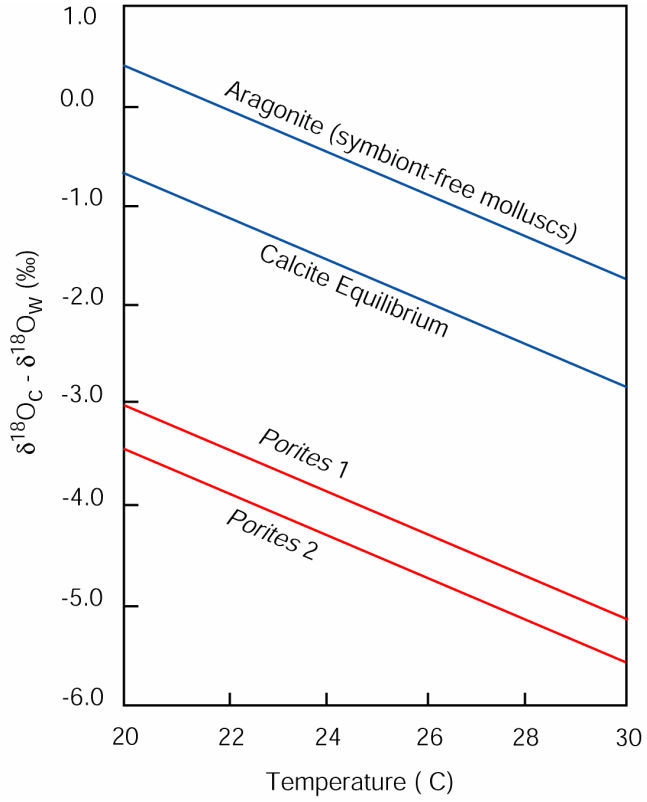

Figure 1.3. Temperature dependency of oxygen isotope fractionation over the temperature range from 20 to 30 °C for equilibrium calcite and selected biogenic aragonites. $\delta^{18}O$ offsets occur between corals from the same genus (*Porites*). From Aharon (1991).

3. Oxygen isotopes in seawater

The $\delta^{18}O$ seawater-salinity relationship is an important factor in paleoclimatology. On the global scale, $\delta^{18}O$ seawater co-varies with salinity. There is a strong correlation between

salinity and the oxygen isotopic composition of surface waters. High salinity and $\delta^{18}O$ seawater value characterize areas where evaporation exceeds precipitation. However, at a regional scale, the $\delta^{18}O$ seawater-salinity slopes vary (Delaygue et al. 2000). The slope of the $\delta^{18}O$ seawater-salinity relationship is determined by the local precipitation-evaporating balance and oceanic advection. On an ocean basin scale, the seawater $\delta^{18}O$-salinity relationship appears to be stable. Seawater $\delta^{18}O$ is enriched in the subtropics and depleted in the higher latitude. This results in a strong latitudinal gradient (Delaygue, at al., 2000). The slope of the $\delta^{18}O$-salinity relationship increases with latitude (Craig & Gordon, 1965). Observed slope values of seawater $\delta^{18}O$- salinity relationship in the surface oceans range 0.49 and 0.47 in the Northern Pacific and Southern Pacific ocean, from 0.1 to 0.5 in the sub tropic (Delaygue et al., 2000). Low slope values are found in the Intertropical Convergence Zones (ITCZ) and high slope value in the subtropical region. Figure 1.4 shows the regression lines of $\delta^{18}O$ seawater-salinity for tropical- extra tropical oceans.

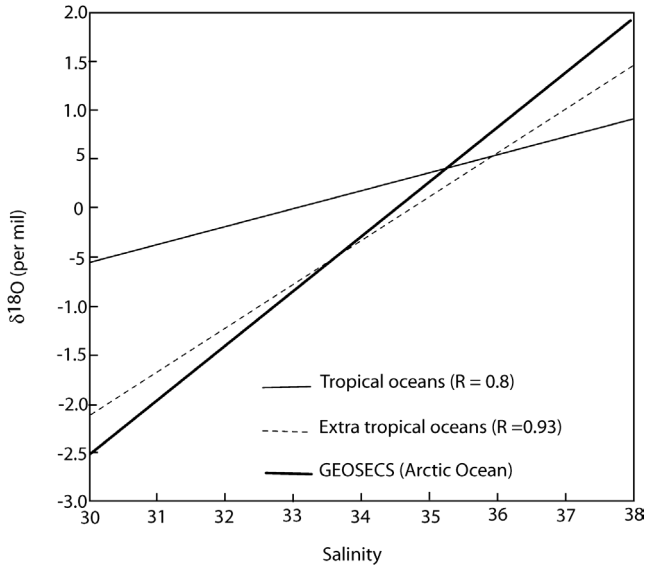

Figure 1.4. The relationship between the average $\delta^{18}O_{sw}$ and salinity for all surface water in the tropical oceans, extra tropical ocean and arctic ocean. (redraw from Schmidt, 1998)

4. Sr/Ca ratios

Scleractinian corals secrete skeletons composed of aragonit ($CaCO_3$), which incorporates both Sr and Ca into its structure. Sr^{2+} mainly substitutes for Ca^{2+} in the crystal lattice (Kinsman and Holland, 1969). The chemistry of Sr^{2+} is very similar to Ca^{2+} and therefore their behaviour is similar. The ratio of the incorporation of Sr to Ca is controlled by two factors: (1) The Sr/Ca activity of the ocean water, (2) the Sr/Ca distribution coefficient between aragonite and

seawater. When a compatible trace component substitutes for lattice calcium in aragonite (a guest/host substitution) the concentration of that trace element can be predicted by its distribution coefficient (D_{Sr}):

$$D_{sr} = \frac{[Sr]/[Ca]_{coral}}{[Sr]/[Ca]_{seawater}}$$

The distribution coefficient strongly depends on the temperature of the seawater where the coral grows (Kinsman & Holland, 1969; Beck et al., 1992). Because of the long residence times of Sr and Ca in the ocean, i.e 4-5 million years (Beck et al., 1992; Guilderson et al., 1994), it has generally been assumed that the Sr/Ca ratio in seawater has remained constant over the past 100.000 years or so. Several studies confirm that the value of D_{Sr} has remained constant. For example, Weber (1973) used several genera of hermatypic corals growing in shallow water and obtained D_{Sr} = 1.01 ± 0.03. Shen et al. (1996) used *Porites* corals from Taiwan and obtained D_{Sr} = 1.056 ± 0.03. Also using *Porites,* Marshall & McCulloch (2002) obtained D_{Sr} = 1.06. These studies justify the assumption, that the Sr/Ca ratios of seawater is constant. Thus, variations of the distribution coefficient, and hence variations in coral Sr/Ca, are determined by ambient water temperature. Thus, coral Sr/Ca can be used to reconstruct temperature.

The Sr/Ca incorporation in corals could also be affected by the calcification rate (coral density multiplied with linear extension) if the partitioning of Sr/Ca in corals is under kinetic control (Weber, 1973). Several studies on inorganic aragonite found no relationship between strontium incorporation and precipitation (Kinsman & Holland, 1969; Mucci et al., 1989). De Villiers et al (1994), in contrast, found that Sr/Ca values were lower in the faster growing sections of corals. Shen et al (1996) and Alibert and McCulloch (1997) confirmed that linear extension and calcification has little effect on coral Sr/Ca as long as a main growth axis is sampled. Sampling outside of the main growth axis results in higher Sr/Ca values (Alibert and McCulloch, 1997). However, published Sr/Ca and SST calibrations show rather large differences (e.g. Beck et al., 1992; de Villiers et al., 1994; Heiss and Dullo, 1997; Shen et al., 1996; Alibert and McCulloch, 1997; Gagan et al., 1998; Linsley et al., 2003) (Figure 1.5). The slope values usually range between -0.04 to -0.08 mmol/mol/°C. The intercepts show even larger differences. The different calibrations can at least partly be attributed to the different methods used for the Sr/Ca analysis (TIMS, ICP AES, and ICP MS) and also to the fact that

different local SST datasets were used to calibrate Sr/Ca. For example, de Villiers et al. (1994) use local SST measurements approximately 100 km away from the coral site; Beck et al. (1992) calibrate coral Sr/Ca with coral $\delta^{18}O$. Many other studies used gridded temperature datasets from ship or satellite measurements (Heiss and Dullo, 1997, Gagan et al, 2000, Marshall & Mc Culloch, 2002).

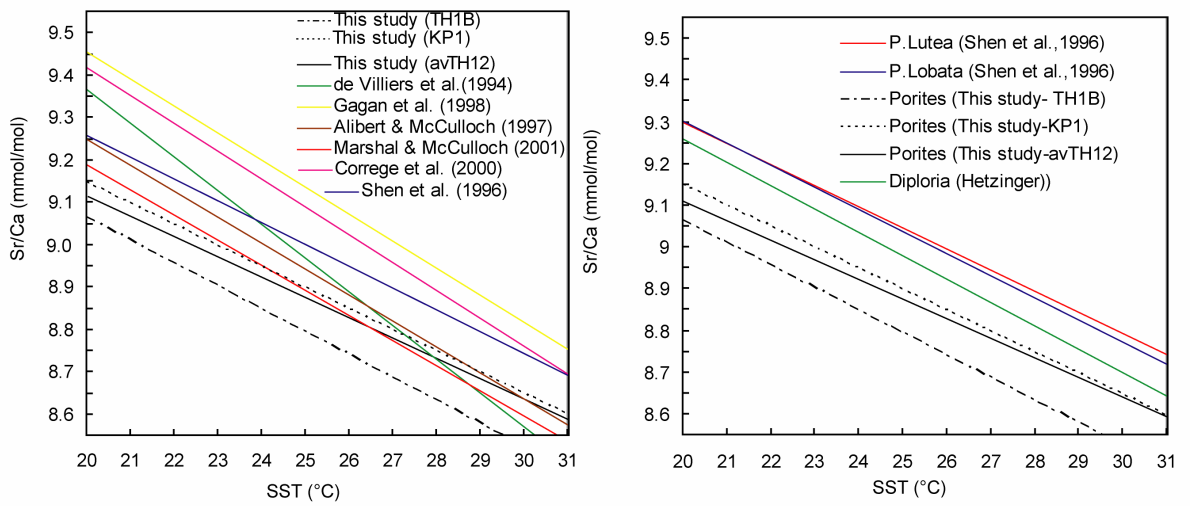

Figure 1.5. (Left) Published Sr/Ca-SST calibrations. Note the different regression slopes and constant. (Right) Calibration of Sr/Ca-SST from different coral genera and species.

5. El Niño-Southern Oscillation

The El Niño Southern Oscillation (ENSO) is a coupled instability of the ocean-atmosphere system in the tropical Pacific with global impact. El Niño is the warm phase of ENSO, and the opposite cold phase is termed La Nina. During normal conditions, the thermocline is near the surface in the eastern Pacific and sea surface temperatures are cold. The easterly trades are strong. The stronger winds pull the thermocline up and therefore increase upwelling. The strong east-west SST gradient in the tropical Pacific creates a strong east-west sea level pressure (SLP) gradient. This SLP gradient is captured by an index based on the SLP difference between Darwin (Australia) and Tahiti (French Polynesia) and is known as the Southern Oscillation Index (SOI). Negative values of the SOI indicate El Niño episodes and positive values indicate La Niña episodes. During El Niño, the trade winds relax, the thermocline deepens in the eastern tropical Pacific and SSTs warm. The SST and SLP gradients decrease, weakening the trade winds even further and the warm state is reinforced (see Trenberth, 1997, and Cane, 2005 for a detailed discussion). El Niño is an important climate phenomenon since it has consequences for global climate. El Niño events are usually

accompanied by severe drought in Indonesia and Australia, together with a weakened summer monsoon rainfall over south Asia (Webster and Palmer, 1997). Flooding often occurs along the Pacific coast of South America and fish stocks disappear as ocean upwelling, containing high-nutrient cold water, diminishes. El Niño also influences tropical cyclones, reducing their frequency in the Atlantic, but increasing it in parts of the Pacific (Webster and Palmer, 1997). Several coral studies have shown that coral proxy records capture the El Niño signal (e.g., Charles et al., 1997; Cobb et al., 2003a; Kilbourne et al., 2004; Zinke et al., 2004; Timm et al., 2005, Pfeiffer and Dullo, in press) and also show decadal/interdecadal variations in the tropical Pacific (e.g., Correge et al., 2000; Cobb et al., 2001).

The Indian Ocean Dipole (IOD) is another climate phenomena centered in the tropical Indian Ocean, outside the Pacific, which was discovered recently by Saji et al. (1999). The Dipole Mode Index is defined as the SST anomaly difference between the eastern and the western tropical Indian Ocean. The changes in SST during IOD events are found to be associated with changes in the surface wind field of the central equatorial Indian Ocean. In fact, the direction of winds reverses from westerlies to easterlies during positive IOD events when SST cool, in the east and warm in the west (Saji et al., 1999; Behera and Yamagata, 2001). Coral $\delta^{18}O$ records from the western coast of Sumatra (eastern Indian Ocean) appear to record the IOD events (Abram et al., 2003). Saji et al (1999) argue that the dipole mode is independent from ENSO centered in the Pacific Ocean.

However, there is still scientific debate whether the IOD exist, and whether it is independent of ENSO or not. Some IOD events are coincident with strong ENSO events while others not (Saji et al., 1999; Rao et al., 2002). Grodsky et al. (2001) find that the eastern equatorial Indian Ocean dynamics are intimately related to ENSO forcing at least during the decade of the 1990s, while Dommenget and Latif (2001) question the existence of the IOD and suggest that it is only an artifact of statistical analysis and does not represent a physical mode. Juneng and Tangang (2005) argue that the strengthening and weakening of SST in the western Pacific, the changing sign of anomalous SST in the Java Sea and the warming in the Indian Ocean and South China Sea are all part of ENSO-related changes and are all linked to Southeast Asian rainfall. Although Timor coral lied on the Indian oceans, but in this thesis the IOD in Timor coral is not studied. In this thesis I will therefore focus on Timor and Tahiti coral proxy records and their relationship to ENSO.

6. Geography, climate and oceanographic setting of the study areas

6.1 Geographic setting

6.1.1 South Central Pacific: French Polynesia

French Polynesia extends over ca 2.500.000 sq. km of ocean from 134°28`W to 154°40`W and from 7°50`S to 27°36`S. The age of the islands decreases from north-west to south east and they form five distinctive archipelagos: Society, Tuamotu, Gambier, Marquesas and Austral Islands. There are atolls, and volcanic islands, the latter often being very mountainous with inaccessible interiors (UNEP/IUCN, 1998).

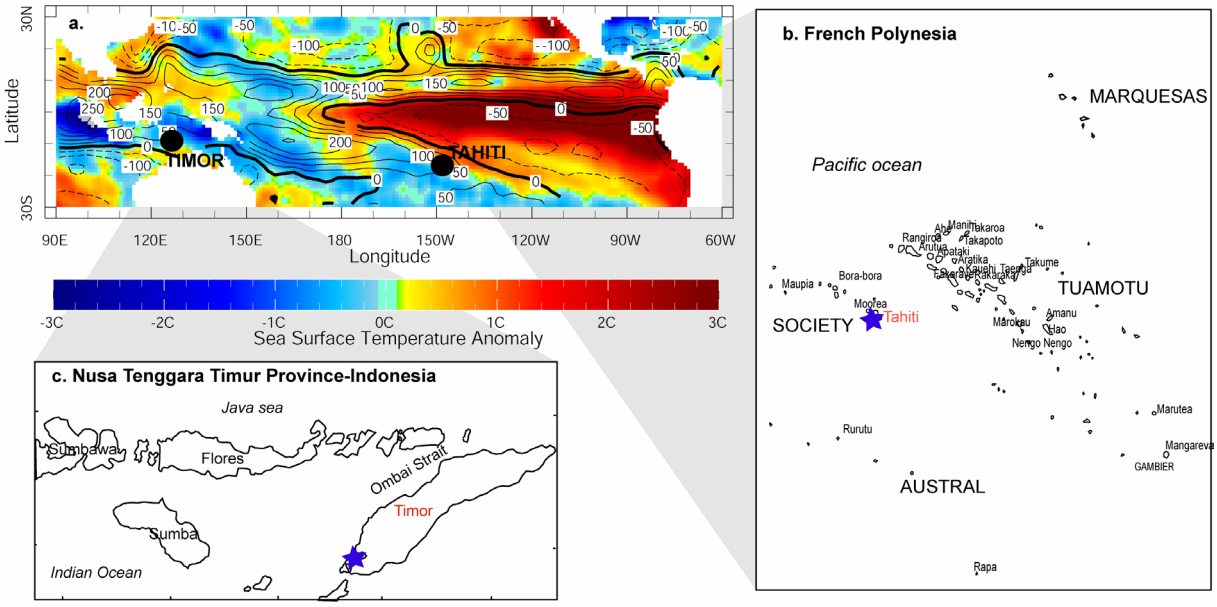

Figure 1.6. (a) Sea surface temperature anomalies during the El Niño of 1997/1998 (colors) and E-P balance (contours). Coral sites are marked by black dots. (b) Tahiti island and the Society archipelago, French Polynesia. (c) Timor island and the province of Nusa Tenggara Timur, Indonesia. Coral drilling locations at Timor and Tahiti islands are marked by a blue star.

Tahiti (149°20' W 17°4`E), where the corals were drilled (Figure 1.6) is part of the Society archipelago (French Polynesia). Tahiti island covers around 1042 sq km and is a high volcanic island with peaks at 2241 m and 1323 m. The marine environment in this area is characterized by discontinuous fringing reefs and frequently interrupted chains of barrier reefs enclosing a lagoon in some places (Chevalier, 1971 in UNEP/IUCN, 1998).

6.1.2. West Pacific warm pool: Indonesia

The Indonesian archipelago consists of more than 13 600 islands, stretching from 6°N to 10°S and from 95° to 142 °E (UNEP/IUCN, 1998) and coral reefs are estimated to extend over

more than 51 000 km (Burke et al., 2002). The coral core was taken from Kupang bay (10°12'S, 123°31'), Timor Island, East Nusatenggara province (Figure 1.6). Coral fringing reefs spread along the northern and southern shore of Timor island.

6.2 Climatic and oceanographic setting

6.2.1 Central Pacific: French Polynesia

In the tropical Pacific Ocean, the trade winds cause the water masses to flow from east to west, and drive the Equatorial Current (EC). The water accumulated in the west tends to flow back towards the east, and this reflux leads to the Equatorial Counter-Currents (ECC). South of latitude 30°S, the prevalent westerly winds drive an eastward flow of tropical and sub-tropical waters within the South Pacific Current (SPC), which is an extension of the Eastern Australian and Tasmanian currents. Farther south, below 45°S, is the region of the Circumpolar Antarctic Current (CAC), which transports an enormous volume of water. As this current approaches the South American continent, part of the water mass is deviated northwards and forms the Humbolt Current, which enters the equatorial zone. This is how the easterly trade winds in the subtropics and the prevailing westerlies in the mid-latitude together drive a swirling anti-cyclonic stream. The entire current system is called the South Pacific Eddy.

The French Polynesian archipelago lies in the South Pacific Gyre. The convergent nature of the circular flow in the South Pacific Gyre leads to an accumulation of waters in the centre of the Gyre. The extremely strong solar insolation which occurs under subtropical climatic conditions contributes to maintaining high temperature and salinity levels, and a relatively homogenous water mass is formed that behaves like a floating disk some 200 metres thick, supported by even denser, deeper ocean water. The great vertical stability resulting from this stratification, isolates the tropical waters from the surrounding ocean (Rougerie and Wanty, 1993).

The salinity profile observed in the South Pacific during the Austral summer and Austral winter differs between the eastern and western regions of French Polynesia. During the Austral summer the SST is higher than 28°C and the salinity is less than 36 psu in the western regions (Society archipelago). During the Austral winter the SST in the Society and northern Tuamotu archipelagos ranges between 25°-28°C, and the salinity is higher than 36 psu (Rougerie and Wanty, 1993) (Figure 1.7).

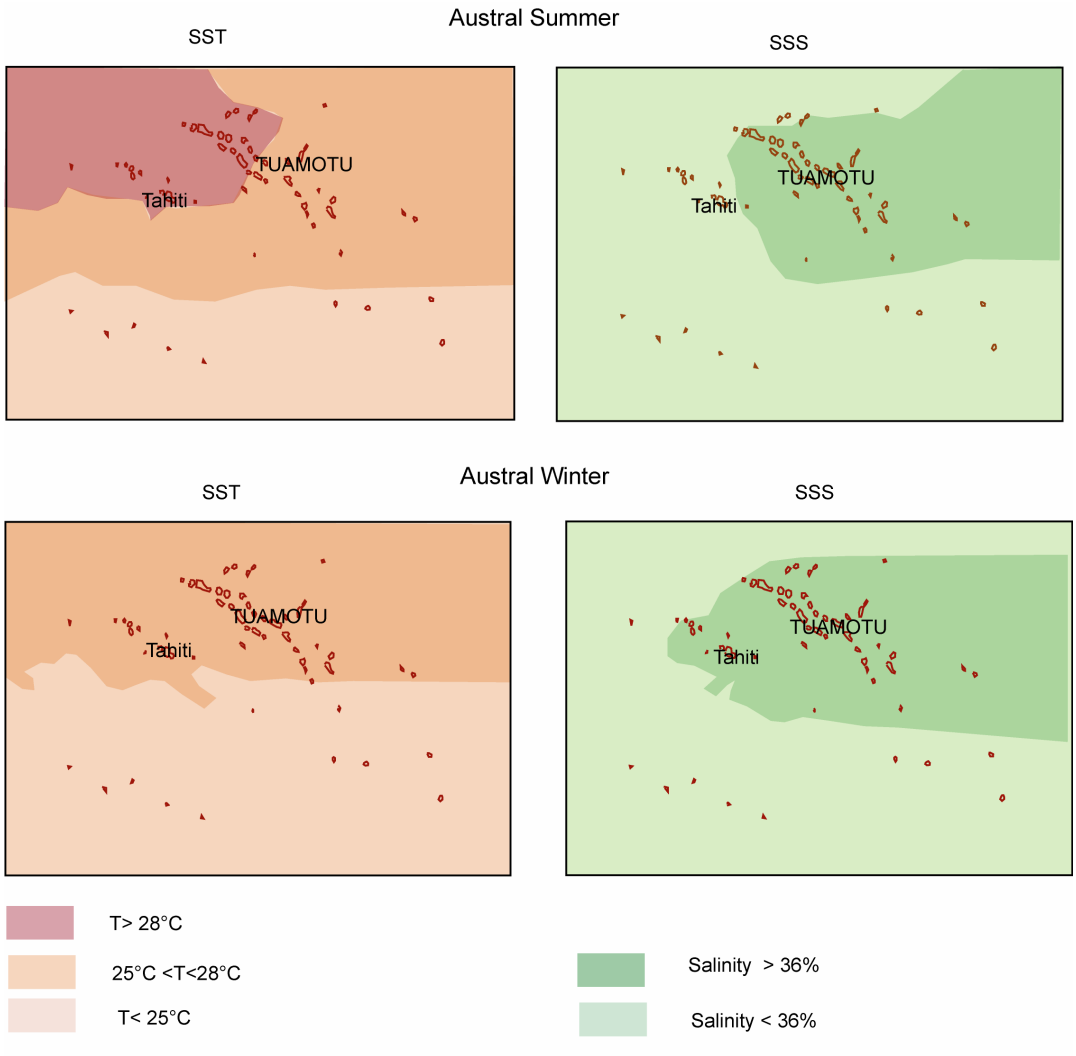

Figure 1.7. SSS and SST at French Polynesia during Austral Summer and Austral Winter (source: Rougerie and Wanty, 1993).

Tahiti is located near the eastern margin of the South Western Tropical Pacific (SWTP) region (24°S-10°S and 160°E-140°W) (Gouriou & Delcroix, 2002). The SWTP is characterized by a horizontal SSS gradient between the south-eastward oriented tongue of fresh water featuring the warm pool in the north-west of the SWTP region, and the westward oriented tongue of high salinity water advected by the southern branch of the south equatorial current, which flows westward from the central south Pacific. Seasonal and interannual variability is apparent in monthly time series of SSS averaged over the SWTP region. The interannual variability is clearly linked to ENSO. The greatest SSS anomalies occurred during the 1982/1983 El Niño (Gouriou & Delcroix, 2002). For SST, the amplitude of interannual variations is small relative to seasonal variations. The displacements of the salinity front results in seasonal SSS variations in the eastern region of the SWTP where Tahiti is located.

During Austral summer, the 36 psu SSS contour lies to the east of Tahiti, while during Austral winter it lies to the west (Rougerie and Wanty, 1993).

Annual rainfall in French Polynesia affects the mean temperatures, and a warm rainy season lasts from November to April and a relatively cool and dry season from May to October. The eastern trade winds predominate from October to March. A long calm period last from April to June, and is interrupted by occasional cyclones which generally arrive from the north-east and north-west. Sea surface temperatures decrease southward and eastward of Rapa Island (25°S, 145°W), where the minimum temperatures suitable for coral growth in the Polynesia are reached. Average summer temperatures reach 26°-30°C while winter temperatures range between 20°-22°C. Within this general pattern there are significant differences between the archipelagos (Tessier, 1969 in UNEP/IUCN, 1998).

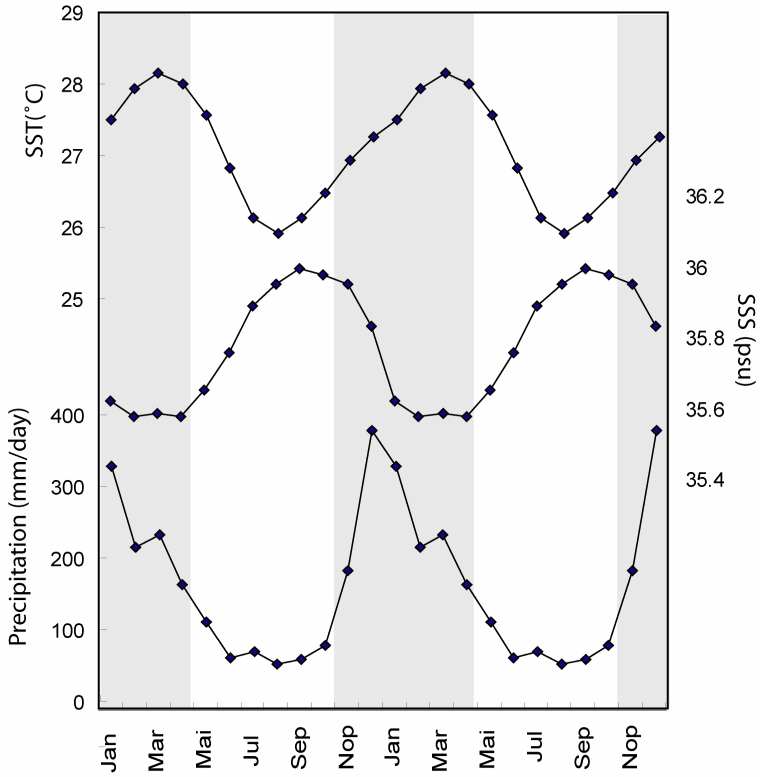

Figure 1.8. Mean seasonal cycle climatic variables at Tahiti for the period of 1979-1990 of (a) sea surface temperature (SST), (b) sea surface salinity (SSS), (c) Precipitation. Shading marks the wet season during November-April. Data source: L'Institut français de Recherche scientifique pour le Développement en coopération (IRD).

Tahiti is a large island with a high volcano. The trade winds flow around this mountain obstacle and largest rainfall is found on the windward side. Daytime convection on the leeward side leads to cloud developments at the edges between the sea breeze and the trade

wind systems. The maximum SST, precipitation and the minimum SSS at Tahiti occur during the rainy season (November-April). Based on climatological data the maximum (minimum) SST in Tahiti occurs in March (August) (Figure 1.8). The mean seasonal SST ranges from 27° to 28°C during the rainy season (Nov-April) and from 26° to 28°C during the dry season (May-October).

6.2.2 West Pacific warm pool: Indonesia

The West Pacific Warm Pool (WPWP) is characterized by the warmest surface ocean water of the world oceans (Levitus et al., 1994), driving the tropical atmospheric circulation. Latent heat release over these warm waters leads to the formation of convective cloud systems which drive the Walker circulation. During El Niño events, this centre of ocean heating and the accompanying convective precipitation moves eastward producing severe droughts in Indonesia, while bringing high rainfall anomalies to the central Pacific. The El Niño induced droughts in the WPWP region result from a reduction in precipitation, due to a weakening of the trade winds. Conversely, during La Niña (ENSO cool phase), when the Walker circulation is intensified, positive rainfall anomalies appear in this region due to a strengthening of the trade winds.

The impact of large-scale climate phenomena such as ENSO varies across the Indonesian region due to island topography and/or ocean-atmosphere fluxes. The average annual SST varies from 28.2°C to 29.2°C and the average annual salinity in this region is the lowest in the tropical oceans and varies from 32.5 psu to 33.8 psu (Levitus et al., 1994) (Figure 1.9). Rainfall in Indonesia is high all year around. A peak appears in the wet season in January and a minimum in August, which is the dry season (Hendon, 2003). Based on the rainfall distribution, Indonesia is divided into three climate regimes (Hamada et al., 2002; Aldrian & Susanto, 2003). Kupang bay at Timor island, where the coral was drilled, lies in the area where rainfall variability correlates significantly with SST (Aldrian & Susanto, 2003; Hamada et al., 2002). Based on climatological data from the Extended Reconstructed global SST (ERSST) dataset (Kupang-Timor Island (10°12'S, 123°31')), the maximum SST occurs in December and the minimum SST in August. The seasonal mean salinity cycle of Kupang-Timor Island from the Levitus dataset (1982) shows a maximum in January and a minimum in May (Figure 1.10). That is, the maximum (minimum) salinity coincides with maximum (minimum) precipitation, suggesting that salinity in the Timor region is not governed by precipitation.

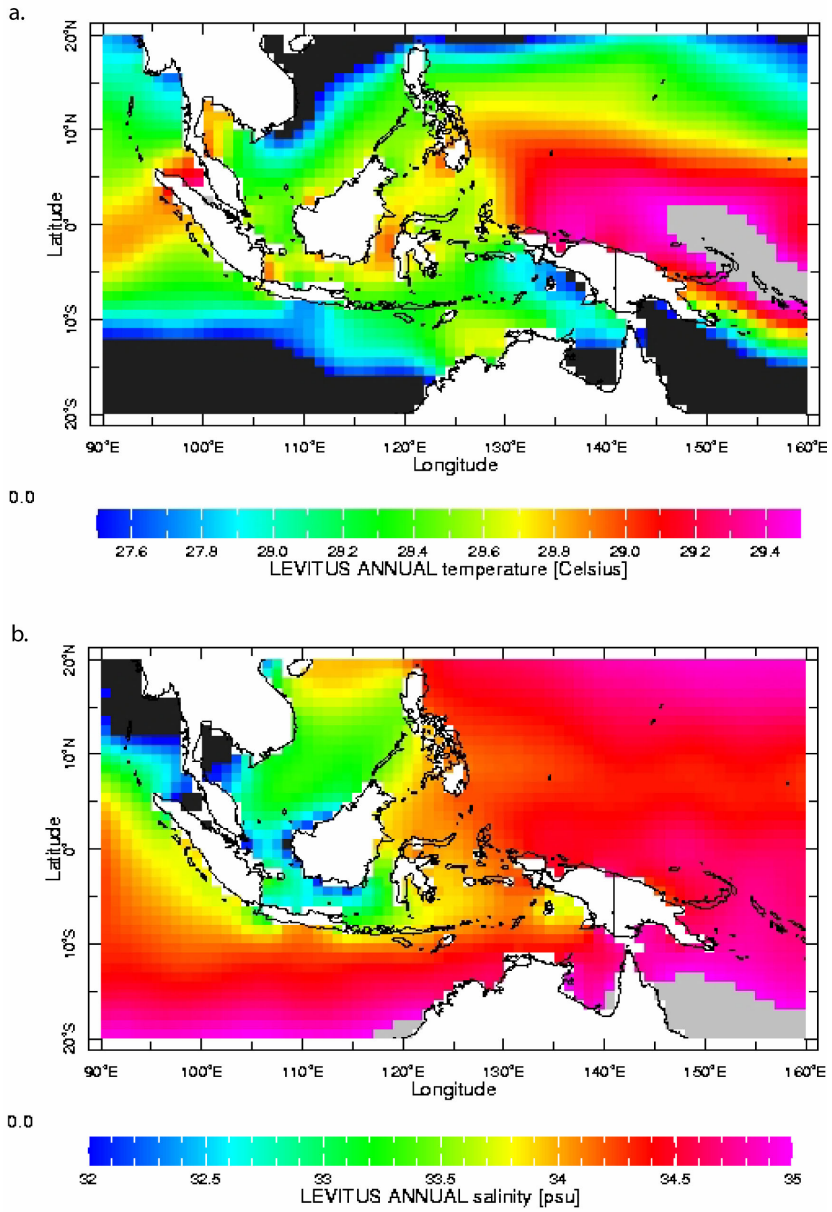

Figure 1.9. Annual mean SST (a) and SSS (b) in the West Pacific Warm Pool. Data from Levitus (1994).

ENSO influences rainfall in the Indonesian region. The ENSO signal is strongest during the dry season (June to September) because higher SSTs in the central Pacific will lower the rainfall amount over the Indonesian region due to the eastward migration of the Indonesian low (Aldrian & Susanto, 2003; Hendon, 2003). Lower rainfall during El Niño events causes drought conditions over Indonesia, because the SSTs surrounding Indonesia are cooler than normal and the Walker circulation is weakened. The opposite tends to occur during La Niña events (Hendon, 2003).

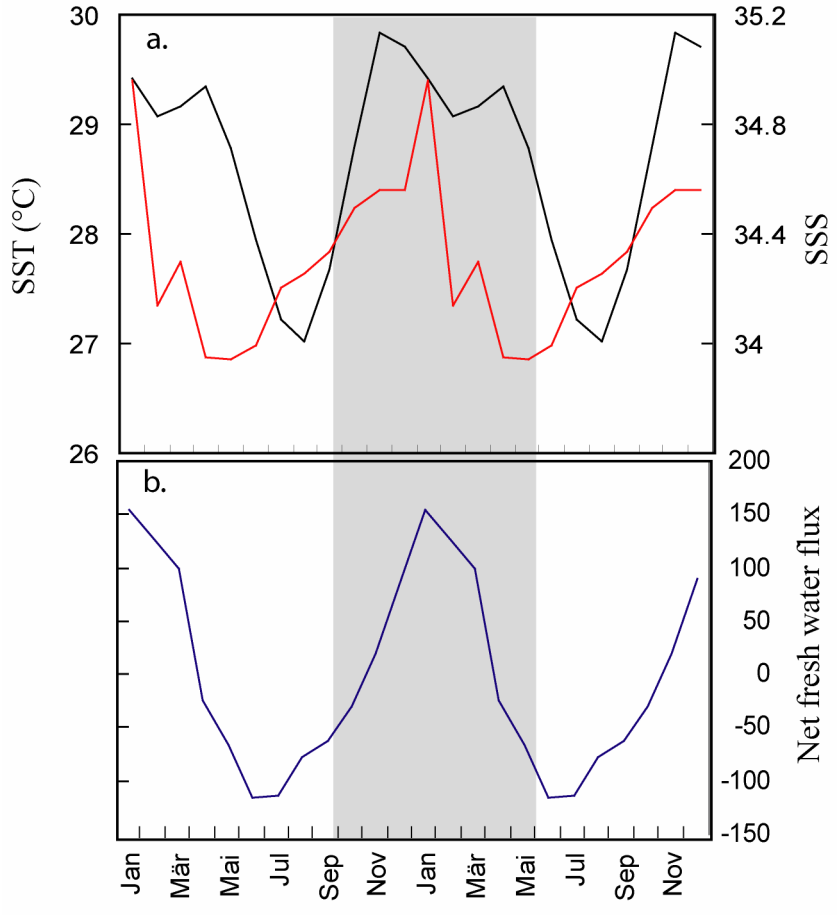

Figure 1.10. Climatological data of Timor (a) SST (ERSST, Smith & Reynolds, 2004) (black dashed line) and SSS (Levitus et al., 1994) (red solid line). (b) Net fresh water flux (data from Oberhuber, 1988). Shading indicates the wet season in the Indonesian region, which peaks in January.

The Indonesian Throughflow (ITF), which carries the heat and freshwater from the Pacific into the Indian Ocean, substantially affects the atmosphere-ocean coupling on a global scale. From the Banda sea, the main exit passages of ITF water into the eastern Indian ocean are Ombai strait and Timor passage (Sprintall et al., 2003) (Figure 1.11).

During the warm, wet summer months of the northwest monsoon that last from November to March, the upper ocean temperatures rise and salinity falls around Indonesia. During the cooler, drier and windier southeast monsoon, temperature falls and salinity increases. The semi-annual cycle dominates the timeseries of temperature and salinity in Ombai strait and in the Sumba strait as a result of an eastward flow of freshwater in the south Java current that is advected into the Savu sea (Sprintall et al., 2003).

Interannual variations in the heat and water mass transport of the Indonesian Throughflow are linked to interannual climate anomalies such as ENSO. This leads to regional variations in surface water temperature and salinity. From mid-1997 to early 1998 the upper ocean was cooler and saltier than normal due to the strong 1997-1998 El Niño event in the tropical Pacific. The outflow passages respond to the lower precipitation, and lower transport of the fresh, warm Throughflow water (Sprintall et al., 2003).

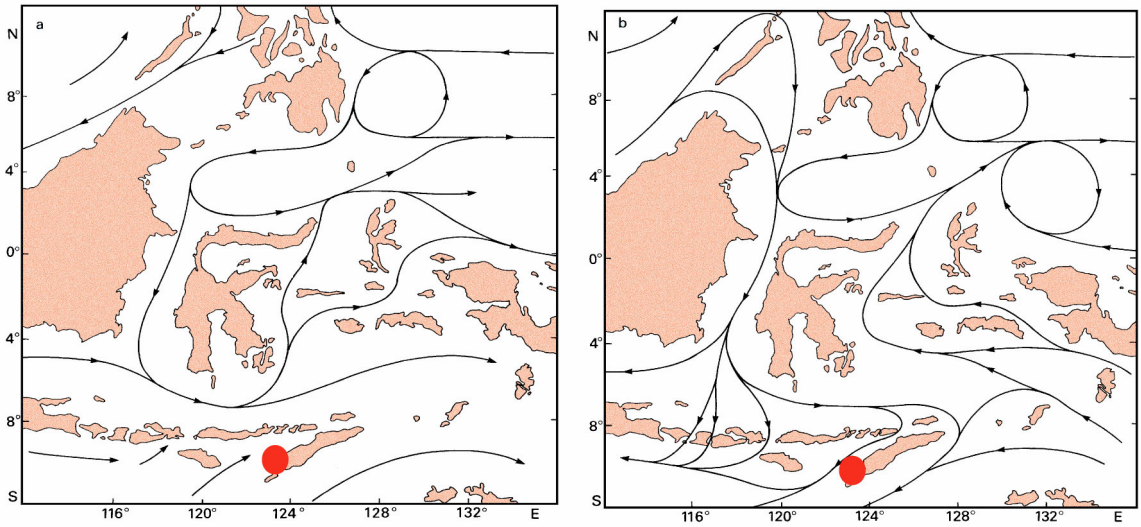

Figure 1.11. Surface currents in the Indonesian sea: (a) In February (minimum throughflow), (b) in August (maximum throughflow). Redrawn from Tomczack & Godfrey (2003). Coral drilling location is marked by the red dot.

7. Western and central Pacific corals

The coral-based climate reconstructions from the central equatorial Pacific, e.g. north Kiribati (Cole and Fairbanks, 1990; Cole et al., 1993; Shen et al., 1992), show that a combination of warm SST and rainfall anomalies during ENSO warm phases that work in phase to generate lower coral skeletal $\delta^{18}O$. The $\delta^{18}O$ records from Tarawa (Cole et al., 1993) correlate with instrumental ENSO indices. The Tarawa records show that seasonal and interannual variability have varied together over the past century with stronger seasonal cycles accompanying periods of reduced ENSO amplitude. Interannual variations in coral $\delta^{18}O$ records from Moorea in the SWTP (17°30'S, 149°50'W) (Boiseau et al., 1998) also appear to be associated with ENSO. During El Niño events the SPCZ moves northeastward and causes high rainfall in this area, which is reflected in reduced coral $\delta^{18}O$ values. Coral Sr/Ca records from Rarotonga (Linsley et al., 2000) show that seasonal and interannual variability is coherent with local SST, while interdecadal variation are moderately coherent with Pacific decadal oscillation (PDO) indices.

Two coral $\delta^{18}O$ records from Indonesia (Bunaken and Bali) have been studied by Charles et al. (2003). The annual cycle of coral $\delta^{18}O$ from Bunaken (1°30' N, 124°50'E) reflects the seasonal cycle of both salinity and temperature in the surrounding seawater. The $\delta^{18}O$ record from the Bunaken coral correlates with local precipitation (r = 0.59) on an interannual scale. The record also captures the warm ENSO phases as observed by Darwin Sea Level Pressure Anomalies (SLPA). The second $\delta^{18}O$ records has been developed from a Bali coral (8°15`S, 115°30`E) (Charles et al., 2003), which shows a much stronger seasonal variation of coral $\delta^{18}O$ than the Bunaken record. Significant interannual variability shows a general sensitivity to ENSO with the same polarity as Indonesia: ENSO warm phases are marked by positive $\delta^{18}O$ excursions, reflecting the weakening and dislocation of the Indonesian low-pressure cell (Charles et al., 2003). The Bali coral records local climatic influences, which are not necessarily a direct reflection of ENSO-related rainfall variability only. Comparing the Pacific corals, Charles et al. (2003) show that the amplitude of the biennial cycle in the Pacific does not vary inversely with the strength of ENSO, as might be expected from some models of monsoonal feedback on the central Pacific. The biennial variability shows modulations on decadal timescales throughout most parts of the Pacific.

8. Aims and Objectives

Coral Sr/Ca is believed to be a promising temperature proxy for paleoclimate studies. However, there are still differences in temperature calibrations between different studies (e.g., Beck et al., 1992; de Villiers et al., 1994; Marshall & McCulloch, 2002). These could be due to different methods used for Sr/Ca analysis (e.g TIMS, ICP AES, ICP MS) and also the different temperature datasets that are used to calibrate Sr/Ca (e.g. Beck et al., 1992; de Villiers et al., 1994; Heiss and Dullo, 1997, Gagan et al., 2000, Marshall & McCulloch, 2002).

Question: Which calibration is best for proxy based SST estimates at Tahiti and Timor? How realistic is reconstructed SST based on coral Sr/Ca compared to measured SST?

Salinity is an important parameter in climate and oceanography. SSS measurements are few. Reanalysis data is available back until 1958. However, SSS records covering longer time scales are needed to understand decadal to centennial variations and what drives them. Since coral $\delta^{18}O$ shows temperature and $\delta^{18}O_{sw}$ while coral Sr/Ca shows temperature only, one can

reconstruct $\delta^{18}O_{sw}$ from paired coral Sr/Ca and $\delta^{18}O$. Furthermore, assuming that $\delta^{18}O_{sw}$ and SSS are linearly correlated, it is possible to reconstruct SSS from paired coral $\delta^{18}O$ and Sr/Ca. However, currently there are still debates regarding the methods that should be used for $\delta^{18}O_{sw}$ (SSS) reconstruction (e.g., Gagan et al., 1994, 1998; Ren et al., 2002; Hupert & Sollow, 2004).

Question: What is the reliable method for $\delta^{18}O_{sw}$ (SSS) reconstructions?

The periodic warming and cooling of SST in the equatorial Pacific during El Niño /La Niña events leaves a fingerprint in the sea level pressure difference between the western Pacific (Darwin, Australia) and the central Pacific (Tahiti). Timor is located close to Darwin, approximately 450 miles to the north, and the climate dynamics at Darwin and Timor should be similar. Timor is also located in an exit passage of the Indonesian Throughflow (ITF), and El Niño events also influence the ITF transport (Sprintall et al., 2003). ENSO- related rainfall anomalies in this region have been studied by Aldrian and Susanto (2003), who find decreasing rainfall during El Niño. However, there is still a lack of coral studies from the ITF exit passages. Tahiti lies in the SWTP, which is affected by the SPCZ. At present, there are few coral proxy records from this region. Yet, fossil corals from Tahiti have been drilled by International Ocean Drilling Project (IODP) and will be analyzed in order to reconstruct El Niño. Therefore, I will carefully analyze the ENSO-signature in the coral proxy records from Timor and Tahiti.

Question: Are El Niño events recorded in the corals from Tahiti and Timor?

In summary, the main objectives of this study are (1) to obtain the best calibration of Sr/Ca-SST, (2) to reconstruct seawater $\delta^{18}O$ from paired coral Sr/Ca and $\delta^{18}O$ measurements and (3) to study the signature of ENSO-related climate anomalies in the coral proxy records of Timor, Indonesia and Tahiti, French Polynesia. For this purpose, I analyze coral Sr/Ca and $\delta^{18}O$ from Tahiti and Timor coral cores. Several SST datasets are used for calibration. Several methods of chronology development are applied and compared to reduce chronological errors which may reduce the quality of the calibration. The methods proposed for seawater $\delta^{18}O$ reconstruction from paired coral Sr/Ca and $\delta^{18}O$ (Gagan et al., 1994, 1998; Ren et al., 2002) are compared and evaluated. I propose a new, more appropriate method for seawater $\delta^{18}O$ reconstruction from paired coral Sr/Ca and $\delta^{18}O$ measurements. Seawater $\delta^{18}O$ will be

calculated from paired coral Sr/Ca and $\delta^{18}O$ measurements of Tahiti and Timor corals. Coral Sr/Ca ($\delta^{18}O$) and reconstructed seawater $\delta^{18}O$ (SSS) will be calibrated with local SST and salinity data, and with instrumental ENSO indices. Furthermore, the results of the Tahiti corals will provide a basis for coral-based paleoclimatology studies at Tahiti which will be done following the IODP Tahiti expedition in 2005. The Timor record presented in this study is the first paired coral proxy record available from an ITF exit passage. Also, the SSS reconstruction based on paired coral proxy measurements at Timor will provide a basis for coral-based paleoceanographic reconstructions at the ITF exit passages.

9. Thesis Structure

This Thesis consists of 7 chapters. Chapter I describes the basic theories of corals and their use as climate archive. The most important coral proxies, i.e., Sr/Ca and $\delta^{18}O$, are discussed, followed by a detailed description of the study areas. The main objectives of this thesis are summarized. In chapter II, the methods and materials used in this study are described. The chapters III-VI are designed in a paper format suitable for publication. Thus, it is possible that there is some duplication in these chapters. Chapter III discusses the chronology development of the proxy time series and focuses on the calibration of Sr/Ca vs. SST which further is used to reconstruct SST from Sr/Ca. Tahiti coral Sr/Ca is used as a case study. Chapter IV discusses the methods proposed for seawater $\delta^{18}O$ reconstructions from paired coral Sr/Ca and $\delta^{18}O$ (i.e procedures and problems) and provides example using the Tahiti proxy record. I also propose a new method for seawater $\delta^{18}O$ and SSS reconstructions. Chapter V and Chapter VI discuss the climate signals recorded in the coral proxy records from Tahiti and Timor, respectively. A particular focus is on the ENSO signature in the proxy time series. Chapter VII provides a summary of chapters III-VI and highlights the main conclusions of this thesis.

CHAPTER II

Materials and Methods

This chapter provides a comprehensive summary of the materials and methods used for analyzing the samples, and for processing the proxy data. The following chapters have been written in a format suitable for publication and some parts of this chapter may be repeated.

1. Coral collection

Cores were drilled from massive coral colonies of *Porites* in July 1995 at Teahupoo and at Vairao, in the south eastern part of the lagoon of Tahiti (French Polynesia) (Figure 1.3, see Chapter I). At Teahupoo (Tahiti) the base of the coral colony is at approximately 2.40 m water depth. This colony was drilled vertically (TH1) as well as horizontally (TH1B). The vertical core is approximately 180 cm long and the horizontal core is approximately 26 cm long. At Vairao, the base of the coral colony drilled is at approximately 3.80 m water depth. This core (TH2) was drilled vertically and is approximately 342 cm long. At Timor (Indonesia), corals were drilled vertically following the main growth axis in June 2004 at Kupang bay (Figure 1.3 see Chapter I). This core is a 180 cm long (KP1) and the base of the corals is at 3 m depth.

The drilling equipment used consists of a diamond-tipped steel tube 3.6 cm in diameter and 30 cm long, which is attached to a pneumatic drilling pistol powered by SCUBA tanks. By using extension rods of 3.5 cm diameter and 30 cm length, it is possible to recover cores of up to 4 m length.

2. Sample preparation

The coral cores were cleaned and cut into 4 mm thick slabs using a diamond rock saw. The 4 mm thick slabs were then cleaned in an Ultrasonic bath, rinsed with distilled water, and dried at 50^{o} C. Then they were X-rayed using 35 kvp 12 minutes to reveal the annual banding. Figure 2.1 shows the X-ray images of the coral samples from Tahiti and Kupang: TH1 (Figure 2.1a), TH2 (Figure 2.1b), KP1 (Figure 2.1c). A comparison of the X-ray images of TH1B (horizontal core) and the core top of TH1 (vertical core from the same colony) is shown in Figure 3.11 (see Chapter III). The X-rays are used to develop a first chronology by counting the density bands, to measure the annual mean linear extension rate and to determine the

optimal sampling profile for trace elements and stable isotope analysis. Slabs were sub sampled manually using a hand-held drill with a drilling bit of 1 mm along the growth axis at ± 1 mm interval to get monthly resolution. The sample powders were then splitted for $\delta^{18}O$ and Sr /Ca analysis.

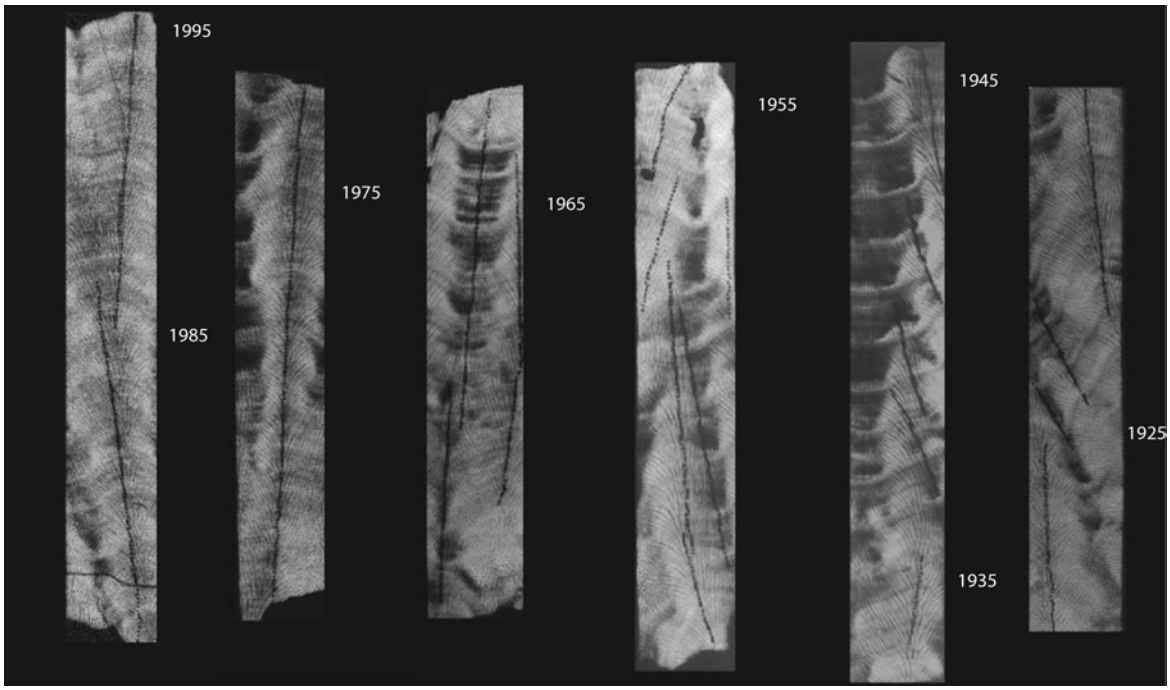

Figure 2.1a The X-Radiographs of core TH1. The dark lines are the sampling transects for stable isotope and trace element analysis.

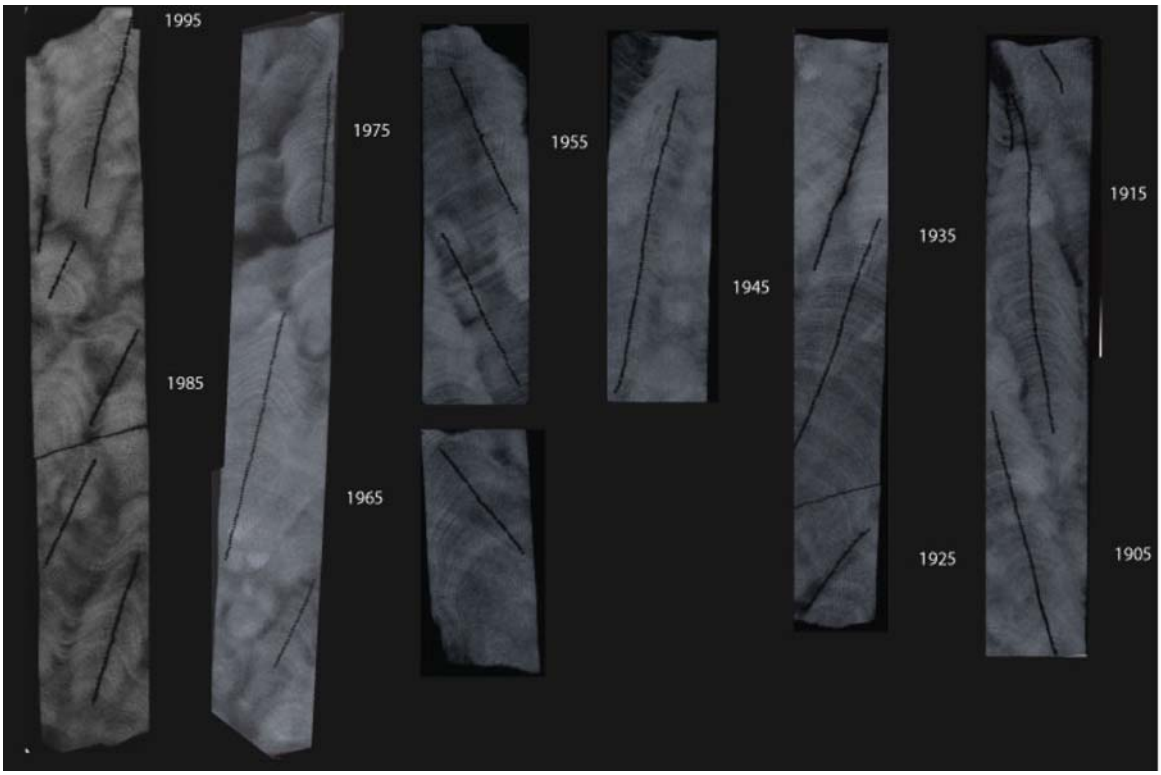

Figure 2.1b The X-Radiographs of core TH2. The dark lines are the sampling transects for stable isotope and trace element analysis.

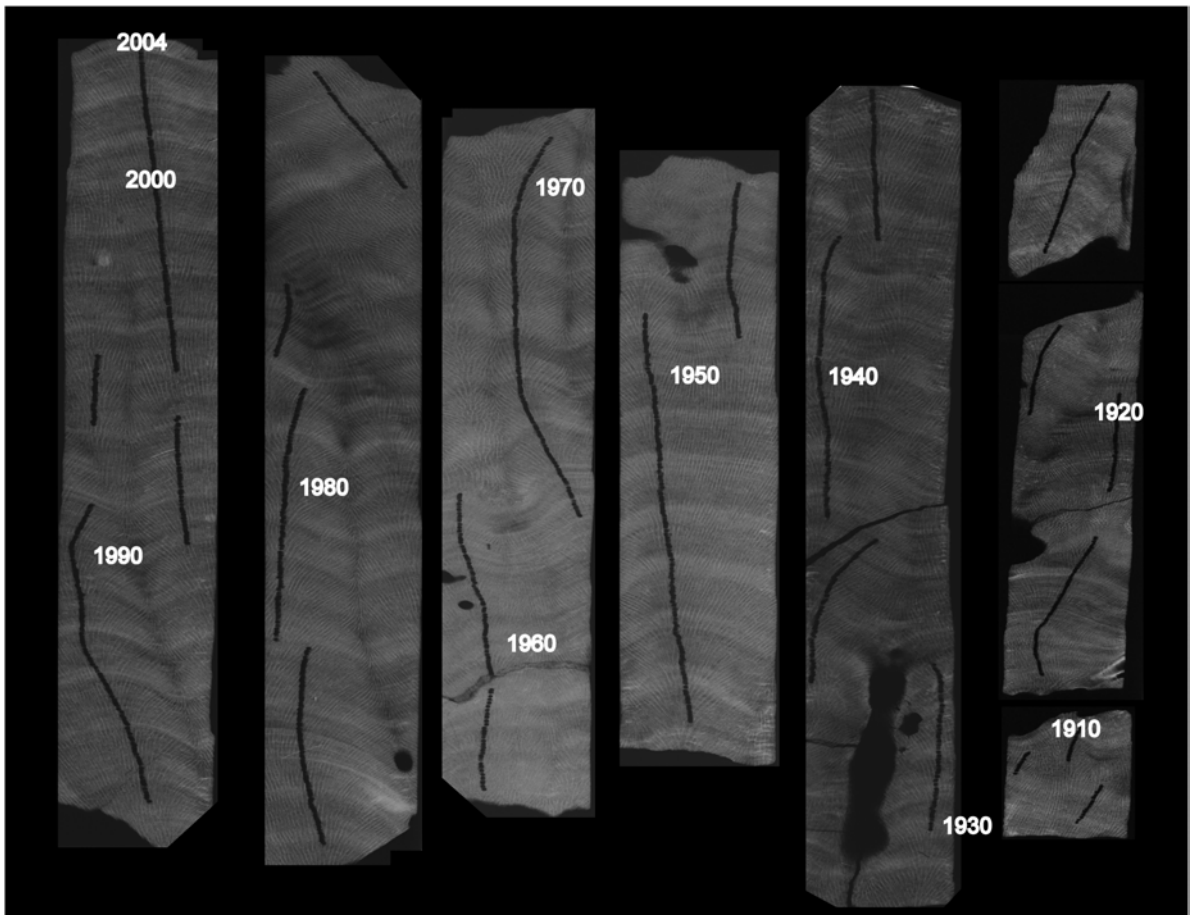

Figure 2.1c. The X-Radiographs of core KP1. The dark lines are the sampling transects for stable isotope and trace element analysis.

3. Oxygen isotope analysis

The oxygen isotopic composition of coral aragonite is expressed as delta ^{18}O ($\delta^{18}O$) values in parts per thousands (‰). $\delta^{18}O$ is measured as ratio of $^{18}O/^{16}O$ in the sample relative to an international reference standard:

$$\delta^{18}O = (R_{sample}/R_{standard} - 1) \times 10^{3} \text{ (‰)} \quad (1)$$

where R_{sample} is the isotope ratio ($^{18}O/^{16}O$) of the sample and $R_{standard}$ is the isotope ratio of the standard sample (Hoefs, 1997). The stable isotopes of oxygen and carbon are analyzed by mass spectrometric determination of the mass ratios of carbon dioxide (CO_2) obtained from the sample, with reference to a standard carbon dioxide gas of known composition. The CO_2 is produced by reaction of the carbonate with phosphoric acid :

$$CaCO_3 + H_3PO_4 \Leftrightarrow CaHPO_4 + CO_2 + H_2O$$

Quantitative results are obtained by comparing the isotope ratio of a given sample with the isotopic ratio of a known external standard.

For example :

$$\delta^{18}O‰ = \frac{\left(\frac{^{18}O}{^{16}O}\right)_{sample} - \left(\frac{^{18}O}{^{16}O}\right)_{standard}}{\left(\frac{^{18}O}{^{16}O}\right)_{standard}} x1000$$

3.1 Technical preparation

The oxygen isotopes were measured at the IFM-GEOMAR using a Finnigan MAT 252 Mass spectrometer for analyzing the $\delta^{18}O$ of TH1 and a Thermo Finnigan MAT DELTA Plus Gasbench II for analyzing the $\delta^{18}O$ composition of TH2 and KP1.

The powdered samples were reacted with H_3PO_4 and the resulting CO_2 gas was analyzed in the mass spectrometer. The standard used for $\delta^{18}O$ is NBS-19. The standard deviation of multiple sample of the international reference standard NBS-19 was ±0.06‰ for $\delta^{18}O$. All samples are reported in ‰ relative to Vienna Pee Dee Belemnite (VPDB) by assigning a $\delta^{18}O$ value of - 2.2 ‰ to NBS-19.

4. Sr/Ca ratio analysis

Sr/Ca ratios are measured in an inductively coupled plasma optical emission spectro-photometer (ICP-OES) at the Geological Institute of the University of Kiel following a combination of the techniques described in detail by Schrag (1999) and de Villiers et al. (2002). Sr and Ca intensity lines used are 407 nm and 317 nm, respectively. The intensities of Sr and Ca are then converted into Sr and Ca ratio in mmol/mol. An in-house reference standard is used for a drift-correction of the measured Sr/Ca ratios.

4.1 Technical preparation

The sample solution was prepared by dissolving 0.5 mg coral powder in 1 ml HNO_3 2%. The working solutions were prepared by a serial dilution of the sample solution with HNO_3 2% to get a concentration of about 8 ppm Ca. The standard solution was prepared by dilution of 1ml from a stock solution (0.52 gram of coral powder from a Mayotte coral in 250 ml HNO_3 2% with 2 ml HNO_3 2%). The relative standard deviation (RSD) of multiple measurements on the same day and on different days is about ±0.15%.

5. Age model development

The coral oxygen isotope and Sr/Ca records are measured in the depth domain (distance from core top) and must be converted into the time domain (sample per year) to facilitate a comparison with instrumental data. In a first step, calendar years are assigned to the coral density bands. Low and high density band couples (one light and dark color band in the X-ray) is defined as one year. In a second step, this age model is refined using the seasonal cycle in Sr/Ca. The measured skeletal Sr/Ca minimum (maximum) is assigned to the average seasonal SST maximum (minimum). The Sr/Ca ratios are then interpolated using these anchor points (e.g. Charles et al., 1997). To obtain equidistant time series, i.e., 12 points per year and therefore a monthly time series, a second interpolation is performed. This approach introduces an error of 1 or 2 month in any given year, but the resulting time series is independent of instrumental climate data. For the interpolation of coral $\delta^{18}O$, the same anchor points as for Sr/Ca are used. For comparison, the ``peak matching`` method between Sr/Ca and measured SST data is also applied for age model development. The maximum (minimum) of the measured Sr/Ca ratios are overlayed and matched with the minimum (maximum) of instrumental SST, assuming that peaks and troughs in the coral proxy series correspond exactly to the instrumental SST values. Using the peak matching method, the resulting time series will not be independent of the instrumental climate data.

6. Time series analysis

Time series analysis was performed using various programs which are distributed freely on the World Wide Web. A detailed description of the programs, methods and theories can be found in the references cited.

6.1 Software packages

The Analyseries software package (Paillard et al., 1996) is available at http://www.ngdc.noaa.gov/paleo/softlib.html. Analyseries is graphically oriented program and run under Macintosh operating systems. This package is designed to facilitate the study of paleoclimatic records using the approach and methods defined by the SPECMAP group (Imbrie et al., 1989). It addresses the problem of transforming data vs. depth into data vs. age records, and spectral and cross spectral analysis of the paleoclimatic records to study the relationship of paleoclimatic records with other climatic records in the frequency domain. In this study the

software is mainly used to interpolate the proxy records and to match the proxy data with the instrumental climate data.

Microsoft Excel is a spread sheet package running under Windows and Macintosh Operating system. This program provides a large set of statistical data analysis tools, e.g. correlation analysis, linear regression, ANOVA, and residual plots. Graphic presentations of the results were also performed using MS Excel.

Several statistical correlation analysis tools e.g., running correlation, field correlations etc. were performed using the Royal Netherlands Meteorological Institute (KNMI) time series web page developed by Oldenborgh and Burgers (2005). This web page can be found at http://www.knmi.nl.

The SSA-MTM Toolkit is used to perform spectral analysis of the proxy data. Four methods of spectral analysis are provided: the Blackman-Tuckey correlogram, the Maximum Entropy method, the Multi-Taper method and Singular Spectrum Analysis (for details see Dettinger et al., 1995). This package is available at http://www.atmos.ucla.edu/tcd/ssa.

A wavelet spectral analysis and wavelet cross coherency analysis package running under MATLAB is provided by Grinsted et al. (2004) and Torrence and Compo (1998), respectively. The wavelet power spectrum (Torrence and Compo, 1998) gives a measure of the time series variance at each period and at each time (available at http:// paos.colorado.edu/research/wavelets/). The wavelet coherency spectrum can identify significant coherency between two time series even though their common power is low. The wavelet coherency software package developed by Grinsted et al (2004) is available at http:// www.pol.ac.uk/ home/ research/ waveletcoherence/.

6.2 Linear regression analysis

Linear regression analysis of proxy measurements against instrumental SST datasets is commonly performed to quantify the coral proxy - SST relationship. In this study, the calculated temperatures based on the regression equation considering temperature as the independent variable have higher variations than the measured temperatures. On the other hand, considering temperature as the dependent variable results in calculated temperature variations that are lower than those of the measured temperature (Figure 3.4 see Chapter III).

The error of the regression (σ) regarding temperature as the independent variable is smaller than the error regarding temperature as the dependent variable (see Table 3.3 see chapter III). In this thesis, the linear regression analysis considering temperature as the independent variable is used. Multiple linear regression is applied to represent the relationship of coral $\delta^{18}O$ with SST and sea surface salinity (SSS), assuming that coral $\delta^{18}O$ is influenced by both SST and SSS variations.

7. Linear extension analysis

The linear extension rates of TH1 and TH1B were calculated using the Coral X-radiograph Densitometry System (Coral*XDS*) from NSUOC (National Coral Reef Institute Nova South Eastern University Oceanographic Center) (http://www.nova.edu/ocean/coralxds/). Coral*XDS* is a Windows-based program which provides a tool for the measurement of linear extension, density, and calcification from coral X-radiographs. These quantities are determined from high-density, low-density, and annual bands. In this study the extension/luminance mode to measure only the linear extension is used. The extension/luminance mode requires only a coral x-ray image and the knowledge of the scaling parameter (pixels per centimeter) used for the image. Coral*XDS* allows user specification of transect location and orientation on the coral image, and provides several options for automated and manual band selection. The output measurements are provided as plots and datasets. The full mode allows the user to measure density and calcification, but this mode is more complicated than the extension mode and the results are still uncertain. The full mode requires the input of dimensions and density of an aluminum wedge, thickness of the coral slab, the relative mass absorption coefficient ratio, images of the coral X-radiograph, and images of a scale bar/ruler. A detailed description of CoralXDS is provided in Helmle et al. (2002).

CHAPTER III

Calibration of Sr/Ca-sea surface temperature (SST) and Sr/Ca-based SST reconstructions: Records from Tahiti (French Polynesia)

Abstract

We reconstruct SST from coral Sr/Ca ratios measured at coral cores taken from the lagoon of Tahiti (French Polynesia). We have calculated the Sr/Ca-SST regression equations using several different instrumental datasets and we compare their statistical parameters such as correlation coefficients and variance (σ^2). We use several proxy records: (1) single records from a given coral core (TH1, TH1B and TH2), (2) average proxy records derived from two cores from the same colony (TH1 and TH1B), (3) average proxy records including data from a different colony taken from the same location (TH1, TH1B and TH2), and (4) an averaging proxy record from different colonies taken from different locations (TH1, TH1B, TH2 and Rarotonga (RRT)). Of the three Tahiti cores, TH1B, which was drilled horizontally, shows the best correlation with SST on an annual mean scale. On the annual mean scale, the average proxy record of TH1, TH1B, and TH2 does not show a better correlation with annual mean SST than TH1B alone. However, the calibration of the average proxy from Tahiti (149.2 ^{o}W 17.4 ^{o}S) and the record from Rarotonga (159.5^{o}W 21.5^{o}S), improves the correlation between coral Sr/Ca and regional SST. The variance of the SST reconstruction is more realistic and the residual is low. This suggests that reconstructing SST from average proxy records of different locations gives a better representation of regional SST variations.

1. Introduction

Sea surface temperatures (SSTs) are one of the most important climatic parameters. The strength of the relationship between coral Sr/Ca ratios with temperature is used as a basis for reconstructing past sea surface temperature variations. The instrumental SST dataset must be used to calibrate the coral proxies in order to reconstruct past SST. Linear regression analysis of Sr/Ca measurements against SST is applied commonly to quantify the coral Sr/Ca - SST relationship (e.g Juillet-Leclerc and Schmidt, 2001; Gagan et al., 2000; Linsley et al., 2000, 2004). Past reconstructed SST based on coral Sr/Ca are calculated based on the calibration with gridded SST (e.g Correge et al., 2004; Felis et al., 2004). This approach is important to evaluate the quality of the proxy as a monitor of regional scale SST variation. However, a large number of SST datasets is available, each covering a different time period and with

different spatial resolution. There is no general agreement on which SST datasets should be used for calibration (de Villiers, et al., 1994; Schrag, 1999; Linsley, et al., 2000, 2004). Usually, a single Sr/Ca record is calibrated with a SST dataset chosen from the many different available datasets. SST data refer to a defined area and grid box resolution. The data representing SST from the proxy is local and represents a point (1° to 5° grids are used). Therefore using grid-SST may lead to the bias in reconstructing SST based on the Sr/Ca-SST regression equation (Solow and Huppert, 2004). However, SST series from global datasets also have uncertainties (Hurrel and Trenberth, 1999). These are larger in regions with few *insitu* measurements.

Ideally, one should use a continuous time series of sea surface temperature (SST) directly from the site where the coral grew. However, the limited local SST measurements available have forced most studies to use grid-SST from various sources. In this study we calibrated Sr/Ca with several instrumental SST datasets, i.e., ERSST, NCEP SST, IRD SST, and Delcroix SST. We also compare several SST datasets. Furthermore we discuss the age model development of the coral records, which is also potential source of error, and the quality of coral Sr/Ca ratios as monitors for regional, grid-scale temperature variability.

2. Climatic and oceanographic setting of the study area

Tahiti is located in the central Pacific (149°20' W 17°4`S) (Figure 3.1), and is part of the Society archipelago (French Polynesia). Tahiti Island is measured around 1042 sq km with a high mountain top (2241 m and 1323 m). The trades wind flow around this mountain obstacle and largest rainfall is found on the windward side. Daytime convection on the leeward side develops clouds at the edges between the sea breeze and trade wind systems. In the central Pacific, in situ SST measurements are poor. The sampling error of the Extended Reconstructed global Sea Surface Temperature (ERSST) datasets at Tahiti increases markedly prior to 1950 (Smith and Reynolds, 2004). The insitu SST measured by *L'lnstitut français de Recherche scientifique pour le Développement en coopération* (IRD) are averaged SST on a monthly basis over a 2° latitude x 10° longitude grid (Gouriou and Delcroix, 2002). Due to the large areal averaged SST data in the region of Tahiti, the calibration of coral Sr/Ca -SST is difficult, which may lead to inaccurate SST reconstruction (Solow and Huppert, 2004).

The maximum SST at Tahiti occurs during the rainy season (November-April). Based on the mean seasonal SST, the maximum (minimum) SST in Tahiti falls in March (August) (Figure 3.2). Climatological SSTs vary during the rainy season (November-April) from 27° to 28°C and from 26° to 28°C during dry season (May-October). Interannual SST anomalies are associated with the El Niño-Southern Oscillation (ENSO). However, these anomalies are an order of magnitude smaller than the seasonal cycle (Delcroix et al., 2002)

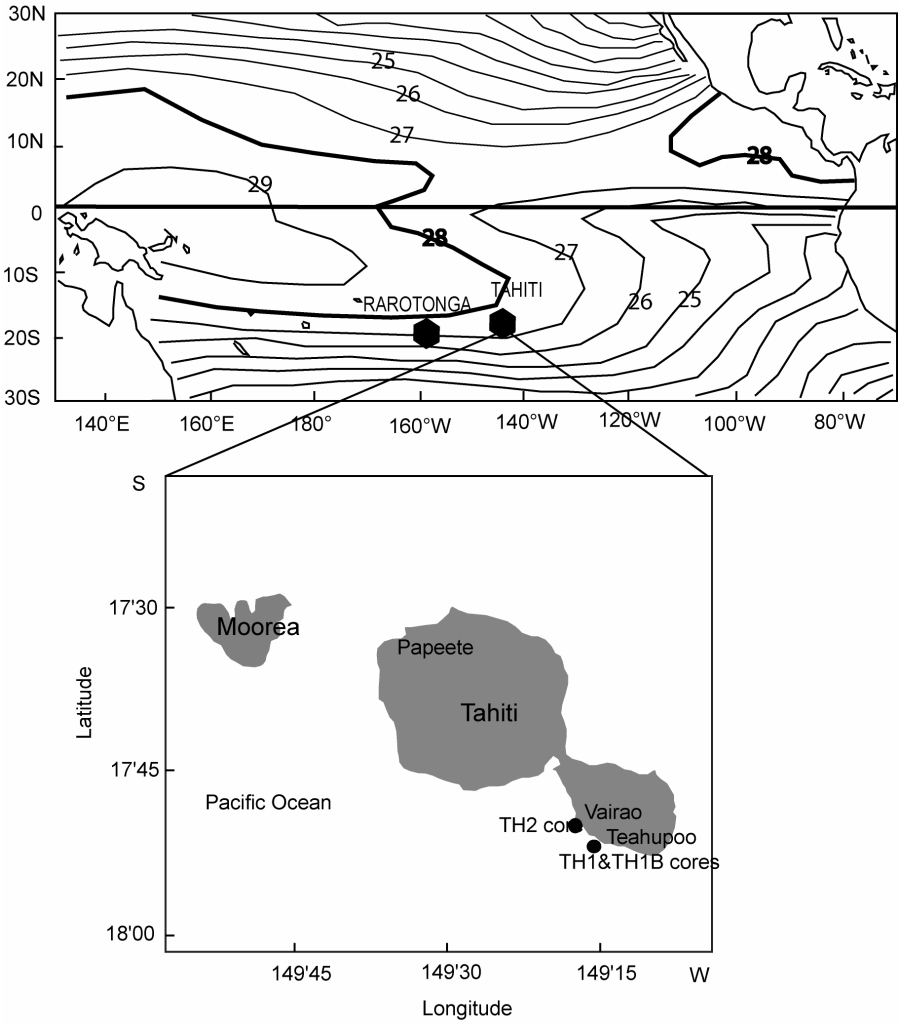

Figure 3.1. Mean annual SST at Tahiti from Gouriou and Delcroix, 2002 (top) and map of Tahiti with location of cores (TH1, TH2 and TH1B) (below).

3. Material and methods

In July 1995, three cores from massive colonies of the genus *Porites* were collected at Teahupoo and at Vairao, in the south-eastern part of Tahiti (French Polynesia) (Figure 3.1). Core TH1 and TH1B were drilled from a single colony growing in the lagoon of Teahupoo. The living surface of the coral almost reached the sea surface. The base is at 2.40 m water

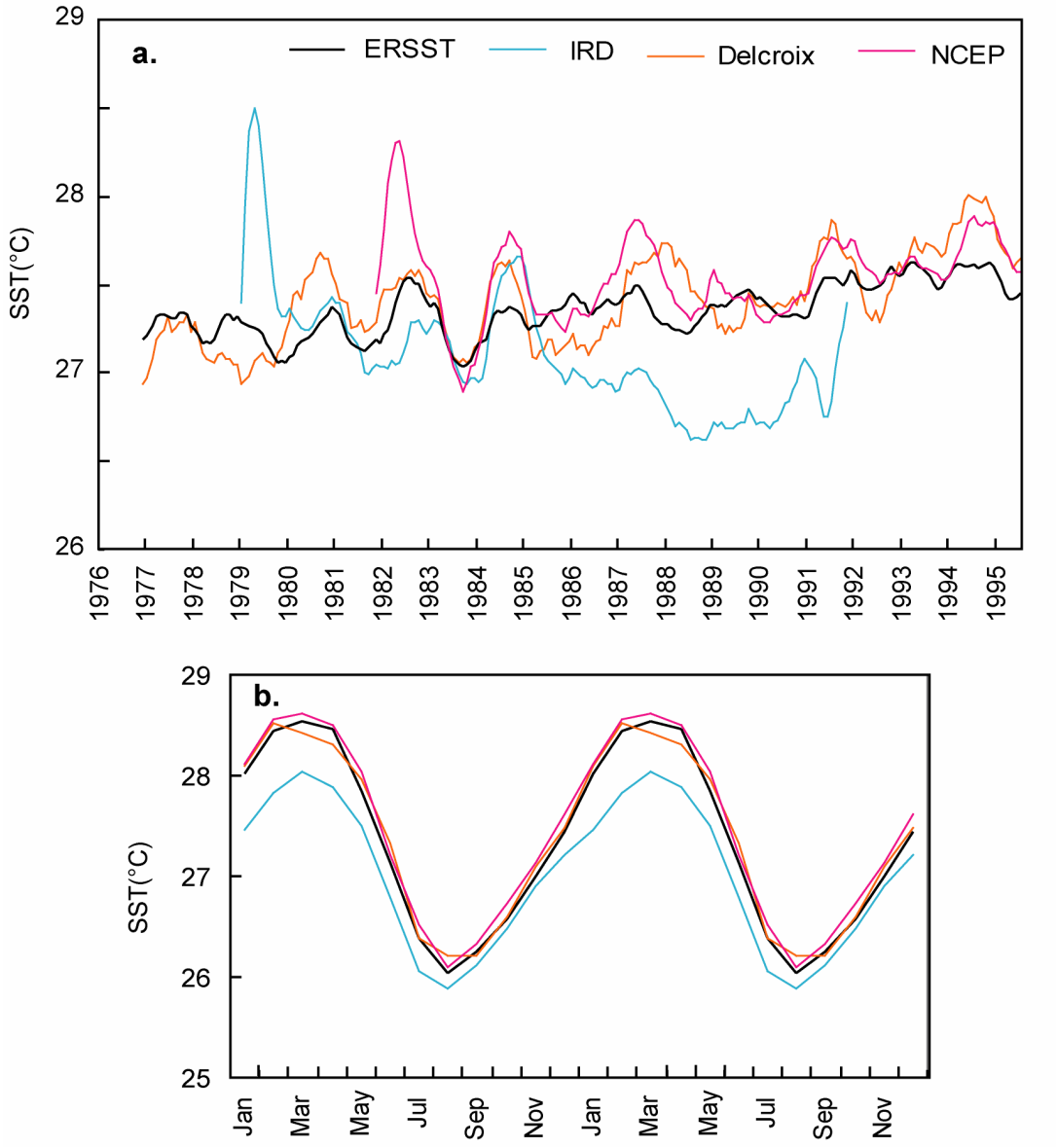

Figure 3.2. (a) Interannual SST variability (highlighted by 12 points running average) and (b) the SST climatologies from different data products.

depth. Core TH1 was drilled vertically and core TH1B was drilled horizontally. The vertical core is 180 cm long and the horizontal core is 26 cm long. Core TH2 was drilled vertically in a colony within the lagoon of Vairao and the base of the coral is at 3.80 m water depth. Core TH2 is 342 cm long and the uppermost 110 cm of this core are analyzed for Sr/Ca.

After drilling the cores were cut into 4 mm thick slabs. The 4 mm slabs were cleaned in an Ultrasonic bath and rinsed with distilled water, and dried at 50^{o} C for 24 hours. Then they were X-rayed using 35 kvp and an exposure time of 12 minutes to reveal the annual density bands. The mean growth rate is ± 2 cm/year. The samples were taken every 1 mm, using a

drilling bit of 1 mm following the main growth axis to get monthly resolution. The powdered samples were analyzed for Sr/Ca ratios. The Sr/Ca ratios were measured in an inductively coupled plasma atomic emission sprectro-photometer (ICP-OES) at the Geological Institute of the University of Kiel following a combination of the techniques described in detail by Schrag (1999) and de Villiers (2002). Sr and Ca lines, which were used for this measurement, are 407 nm and 317 nm respectively. The sample solution was prepared by dissolving ±0.5 mg of coral powder in 1.00 ml HNO_3 2%. The working solution is prepared by a serial dilution of the sample solution with HNO_3 2% to get a concentration of about 5 ppm Ca. The standard solution was prepared by dilution of 1.00 ml of the stock solution (0.52 gram coral powder from Mayotte sample in 250 ml HNO_3 2-3% with 2 ml HNO_3 2%). The relative standard deviation (RSD) of multiple measurements on the same day and on different days is about 0.15%.

The chronology of the coral cores was developed using the anchor point method (e.g. Charles et al., 1997). We used the anchor point Sr/Ca minimum (maximum) matched to the seasonal SST maximum (minimum) in March (August). We also used the peak matching method for comparison (see detail in session 3.2). The Analyseries software (Paillard et al., 1996) was used to match the coral Sr/Ca with SST and to interpolate the Sr/Ca data to monthly records. The Coral *XDS* software (X-radiograph Densitometry System) is used to measure the linear extension of the core top of TH1 and core TH1B. The Coral *XDS* software is obtained from NSUOC (National Coral Reef Institute Nova South Eastern University Oceanographic Center) (http:// www.nova.edu/ocean/coralxds/). The Coral *XDS* is a Windows-based program which provides a tool for measurement of linear extension, density, and calcification from coral X-radiographs. These quantities are determined from high-density, low-density, and annual bands. Mean linear extension of core top TH1 and TH1B calculated using coral XDS are 0.974 cm/year and 1.337 cm/year respectively.

3.1 SST datasets

To reconstruct past SSTs from coral Sr/Ca records, a linear regression between a given SST dataset chosen from a set of available products and the Sr/Ca ratios is performed. Consequently, the SST reconstructions depend on the SST dataset used. In this study, we use and compare SST datasets from four different sources: The Extended Reconstructed global Sea Surface Temperature (ERSST) of Smith & Reynolds (2004), the optimal interpolation

SST of NCEP (National Centre for Environmental Prediction) from Reynold and Smith (1994), the local SST from Tahiti (hereafter referred to as IRD SST) obtained from *L'lnstitut français de Recherche scientifique pour le Développement en coopération* (IRD) (Boiseau et al., 1998), and a regional SST dataset published by Delcroix, et al. (1996), Delcroix and McPhaden (2002), and Gouriou and Delcroix (2002) (hereafter referred to as Delcroix SST).

3.1.1 ERSST

The ERSST is based on the SST data from the Comprehensive Ocean Atmosphere Data Set (COADS) SST and uses improved statistical methods that allow a stable reconstruction using sparse data. This dataset covers the time period from January 1854 until present. Because of sparse data the analyzed signal is heavily damped before 1880. Afterwards the strength of the signal is more consistent over time. The sampling error in the area of Tahiti is large (more than 0.1°C) and increases from 1950 backward (Smith and Reynolds, 2004). The standard deviation of monthly SST over the period 1982-97 ranges from 0.2 °C to 0.6 °C (for a detailed discussion see Smith and Reynolds, 2004).

3.1.2 NCEP SST

The SST data from the National Centres for Environmental Prediction (NCEP) uses optimal interpolation to combine in situ and satellite-derived SST data. This method was described by Reynolds and Smith (1994). The dataset extends from November 1981 until present. The standard deviation of monthly SST anomalies from NCEP is larger in the equatorial Pacific, where large interannual variations occur that are associated with ENSO (Hurrell and Trenberth, 1999). These anomalies are well captured in the NCEP analysis. In contrast, for the remaining tropical oceans, the SST variations are much smaller and the noise level is larger (Hurrell and Trenberth, 1999).

3.1.3 IRD SST and Delcroix SST

The IRD SST is measured in Papeete, Tahiti (Boiseau et al., 1998). The SST measurements extend from 1979 until 1990. The mean SST, averaged from 1979 to 1990, is 27.1 ^{o}C. The SST data published by Delcroix et al. (1996), Delcroix and McPhaden (2002), and Gouriou and Delcroix (2002) is obtained from bucket measurements along regular shipping routes. The dataset extends from 1976-2000. For Tahiti we use the SST record from the grid box 150^{o}W-140^{o}W 16^{o}S-18^{o}S.

3.2. Age model development

The chronology of our coral proxy data is developed using anchor points (e.g. Charles et al., 1997), which are fixed at seasonal maximum and or minimum SST. It is assumed that the measured Sr/Ca minimum (maximum) corresponds to the seasonal SST maximum (minimum). Based on the SST climatologies for Tahiti (149.2°W 17.4°S) (Figure 3.2), the warmest temperatures (SST maximum) occur in March and the coolest temperatures (SST minimum) occur in August. To obtain age assignments for all Sr/Ca values, we linearly interpolated between the anchor points. A second interpolation was performed to obtain an equidistant time series, with 12 monthly values per year. Based on this chronology, core TH1 extends from February 1923 to July 1995, TH1B core from January 1974 to July 1995 and TH2 core from July 1903 to July 1995 (Figure 3.3). For comparison, we also applied the peak matching method (Quinn et al., 1996; Felis et al., 2004) between measured Sr/Ca and SST data to develop the age model. By matching measured Sr/Ca maxima (minima) directly with SST minima (maxima), the resulting age model uncertainty should be lower than for the anchor point method, and the correlation between proxy and SST should be improve. For this comparison we used the SST data from NCEP and the ERSST for the time period from November 1981 until July 1995 as a basis for the peak matching.

4. Results and Discussion

4.1 Comparison of the SST datasets

The average of SST for the period from 1981-1990 is different from all datasets (ERSST, IRD, NCEP, Delcroix SST). IRD SST shows the coolest temperature (27°C), while the NCEP SST shows the warmest temperature (27.5°C) (Table 3.1).

SST Dataset	ERSST	IRD SST	NCEP SST	Delcroix SST
SST (°C)	27.3	27.0	27.5	27.4

Table 3.1. The average SST values from several SST datasets for the period 1981-1990.

The mean seasonal cycle of the four SST datasets is shown in Figure 3.2. The NCEP, Delcroix and ERSST datasets are more or less consistent, while the IRD dataset shows a lower seasonal amplitude with only 2°C. The mean seasonal cycle is 25°C for the period from 1981-1990. The interannual variations of the four SST dataset are shown in Figure 3.2. The records have been smoothed with a 12 points running average. The IRD SST that is measured close to our study area shows somewhat different trends than the other three SST datasets.

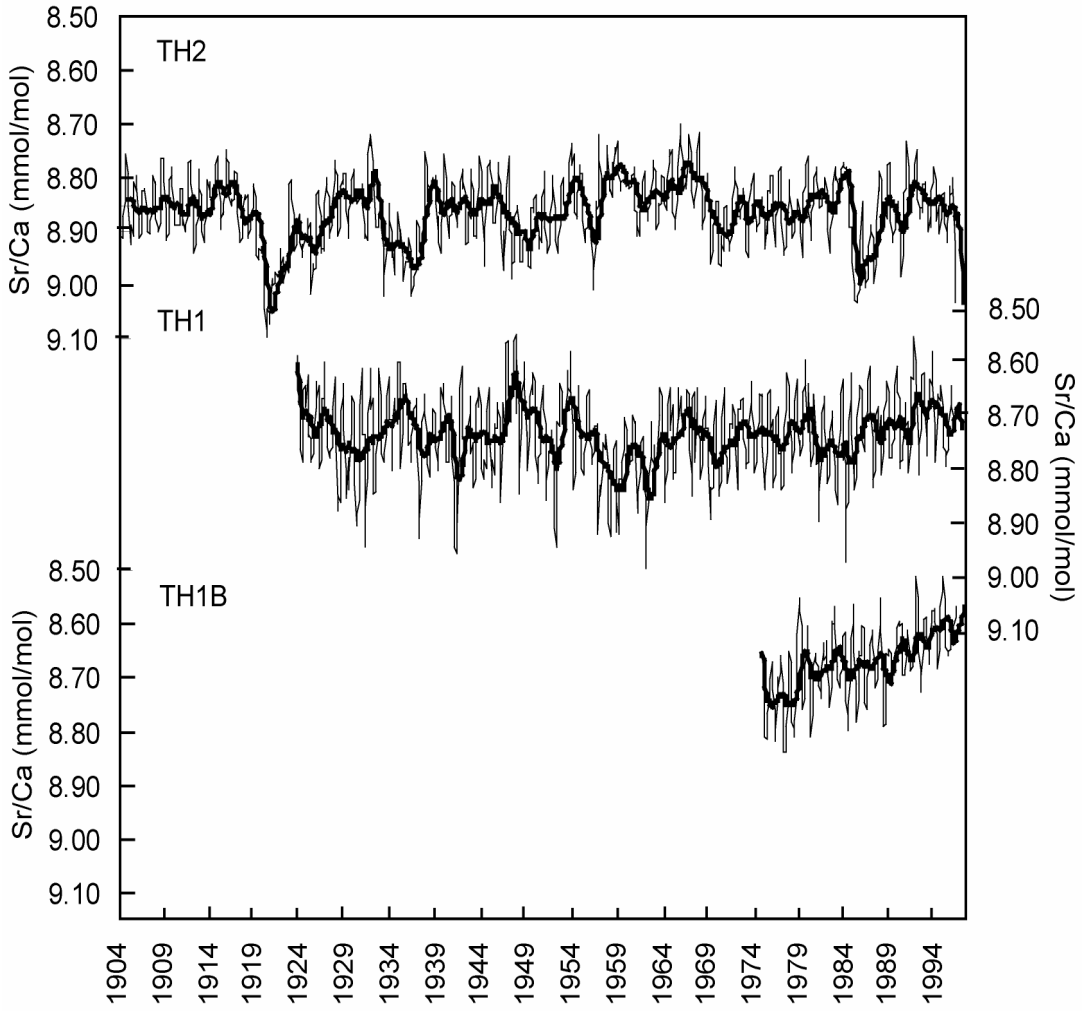

Figure 3.3. Monthly Sr/Ca time series of all three Tahiti cores (TH2, TH1, TH1B). Thick lines are 12 points running average.

4.2 Comparisons of the two age models

To check whether the peak matching method yields a better correlation between the coral proxy and SST than the anchor point method, we compared the correlation coefficients obtained by linear regression of monthly SST vs. the proxy data. The chronology of the proxy data was developed by: (1) Peak matching of the proxy with the ERSST (PM ERSST), (2) by peak matching of the proxy with the NCEP SST (PM NCEP) and (3) by fixing anchor points at maximum and minimum Sr/Ca values (AP MinMax). Method (1) and (3) were used to construct an age model from 1923 to 1995 and method (2) was used to construct an age model from 1981 to 1995. We use the coral Sr/Ca ratios data from TH1 to evaluate the two methods for the age model development. The results are shown in Table 3.2.

	ERSST		IRD		NCEP		Delcroix	
Chronology methods	1923-95	1981-90	1979-90	1981-90	1981-95	1981-90	1976-95	1981-90
1-PM ERSST	S=-0,051 R=0,624	S=-0,051 R= 0,638	S=-0,046 R=0,550	S=-0,041 R=0,482	S=-0,045 R=0,636	S=-0,044 R=0,592	S=-0,045 R=0,605	S=-0,041 R=0,552
2- PM NCEP	-	S=-0,065 **R=0,789**	-	S=-0,054 **R=0,619**	S=0,058 **R=0,779**	S=-0,060 **R=0,782**	-	S=-0,055 **R=0,717**
3-AP MinMax	S=-0,054 R=0,687	S=-0,056 R=0,732	S=-0,050 R=0,617	S=-0,049 R=0,600	S=-0,049 R=0,686	S=-0,046 R=0,650	S=-0,046 R=0,656	S=-0,042 R=0,605

Table 3.2. The correlation coefficients (R) and slopes of the monthly regressions of coral Sr/Ca ratios vs. SST from several datasets with different methods of chronologies development: PM= peak matching method, AP = anchor point method. S = slope of the regression equation Sr/Ca vs. SST, $p < 0.001$ for all analysis.

By comparing the R values of those three approaches for the period 1981-90 (see Table 3.2), we observe that matching coral Sr/Ca with the ERSST results in a lower correlation coefficient (R) than the anchor point method. In contrast, matching coral Sr/Ca with the NCEP SST resulted in a higher R value than with the anchor point method. We conclude that coral Sr/Ca chronologies based on peak matching do not always have a higher correlation with SST. The generally lower correlation coefficient between the proxy and the ERSST may effect the larger uncertainty of the SST data on longer time scales, particularly prior to the 1950, where in situ measurements are few. The NCEP record only ranges from 1981 until present, when data coverage is good. Therefore, the PM-NCEP method may result in slightly better correlations between the proxy and SST. For longer time scales, the anchor point method (AP MinMax) seems to be the most appropriate.

4.3. Monthly calibrations of coral Sr/Ca vs. sea surface temperature (SST)

4.3.1 Temperature as independent and dependent variable

Usually the SST is used as the dependent variable for the calibration equation. In order to choose the appropriate regression equation, we compared the linear regression analysis: (1) considering temperature as the independent variable and coral Sr/Ca as the dependent variable and (2) temperature as the dependent variable and coral Sr/Ca as the independent variable. We then compared the statistical error of the regression equations obtained by these two approaches. Table 3.3 shows the comparison of the regression equations of coral Sr/Ca $_{TH1}$ vs. SST that result from the two approaches.

T-dataset	Monthly	
	T independent	T dependent
ERSST n_m=870 n_a=73	Sr/Ca= -0.054±0.002 T + 10.219±0.053 (R = 0.69 σ = 0.053) (1)	T = -8.682±0.312 Sr/Ca + 103.143±2.723 (R = 0.69 σ = 0.665) (5)
NCEP n_m=165 n_a=14	Sr/Ca = -0.049±0.004 T + 10.070±0.112 (R = 0.69 σ = 0.051) (2)	T = -9.586±0.797 Sr/Ca + 111.129±6.952 (R = 0.69 σ = 0.714) (6)
IRD n_m=144 n_a=13	Sr/Ca = -0.050±0.005T + 10.077±0.144 (R = 0.62 σ =0.055) (3)	T = -7.689±0.823 Sr/Ca + 94.240±7.187 (R = 0.62 σ = 0.687) (7)
DELCROIX n_m =235 n_a= 20	Sr/Ca = -0.046±0.003T + 9.995±0.094 (R = 0.66 σ =0.052) (4)	T = -9.484±0.701 Sr/Ca + 110.16±6.121 (R= 0.66 σ = 0.740) (8)

Table 3.3. Comparison of regression equations obtained with SST as the independent variable and with SST as the dependent variable for coral Sr/Ca_{THI} vs. SST ($p < 0.001$ for all analysis).

The results show that the calculated temperatures based on the regression equation considering temperature as the independent variable have higher variations than the measured temperatures. On the other hand, considering temperature as the dependent variable results in calculated temperature variations that are lower than those of the measured temperature (Figure 3.4). The error of the regression (σ) concerning temperature as the independent variable is smaller than that of temperature as the dependent variable (see Table 3.3). However, the lower σ values do not mean that the estimated temperature variation, which is calculated from this equation, is more representative of the true temperature, despite the fact that this equation is more precise for calculating the temperatures. The lower σ values show that the deviation of the calculated and instrumental temperatures is small (Figure 3.4). Therefore, we will use the regression equation considering temperatures as the independent variable.

4.3.2 Single records of coral Sr/Ca ratios vs. SST

Sr/Ca ratios in corals are believed to be a function of temperature only (Beck et al, 1992; Mc Culloch et al., 1994; Marshall and McCulloch, 2002; Alibert, et al, 2003) and the regression equation of Sr/Ca vs. SST is used to reconstruct past SSTs. However, there are still differences in the Sr/Ca- temperature equation published in different studies. Many studies use different SST datasets. Beck et al. (1992) calibrated Sr/Ca not against the in situ instrumental SSTs record but used $\delta^{18}O$ -derived SST from the same sample. Their relationship between Sr/Ca and $SST_{\delta 18O}$ is Sr/Ca x 10^3 = 10.479-0.06245 x SST.

These results show a good relationship between the measured SST record from Noumea-Papeete and Sr/Ca –derived SST with an average difference of 0.34°C. Some other studies calibrate the Sr/Ca with the coral SST records that are up to 100 km away from the actual site (de Villiers et al., 1994).

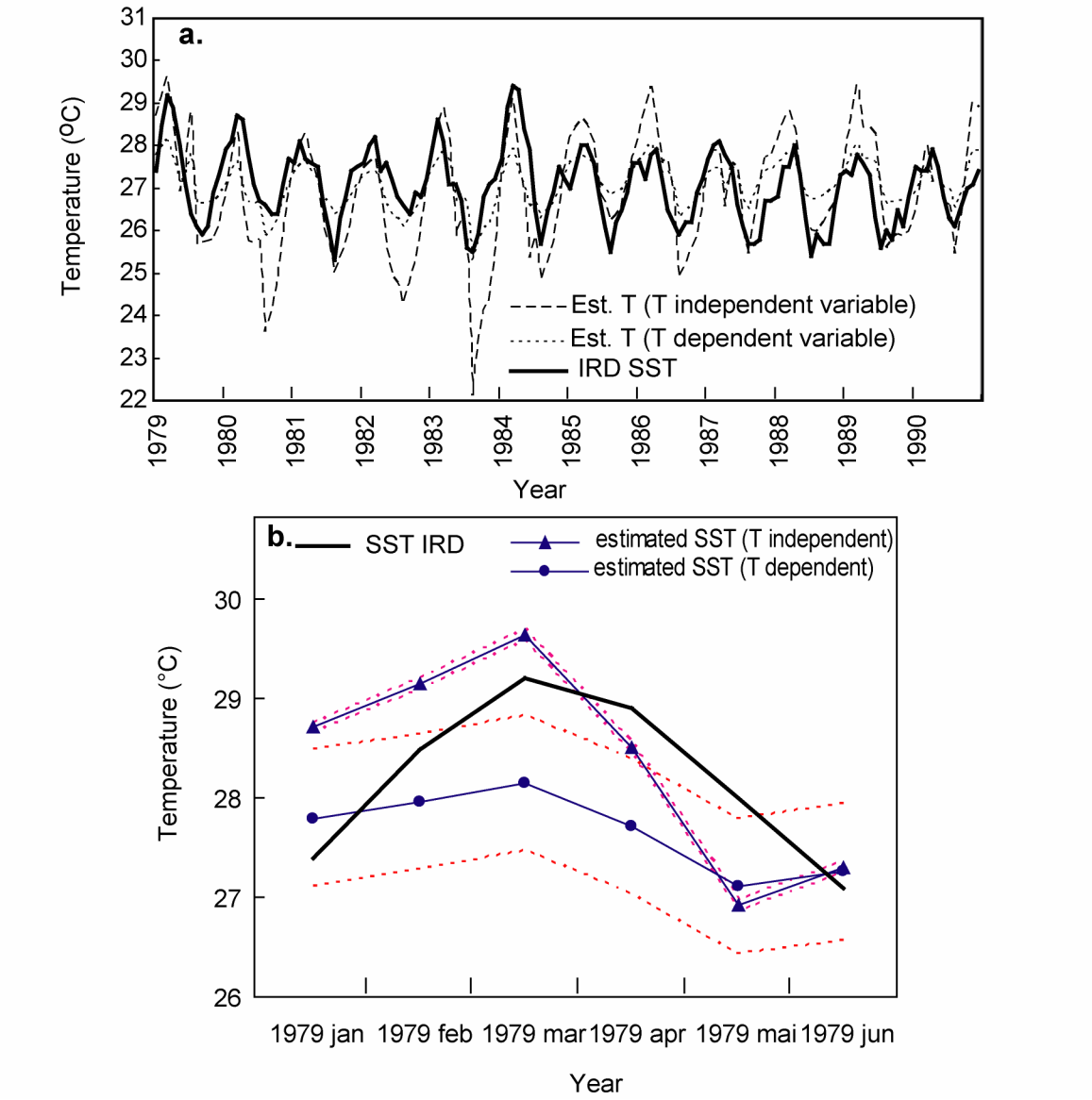

Figure 3.4 (a) Comparison of estimated SST based on the regression equations with SST as the dependent and as the independent variable. (b) Estimated SSTs using the equation considering SST as dependent variable have larger statistical uncertainties than SSTs obtained considering SST as independent variable. Equations is obtained from linear regression of IRD SST vs. Sr/Ca$_{THI}$ are used.

In this study, we used several SST datasets (ERSST, NCEP, IRD and Delcroix) to calibrate our monthly Sr/Ca records. The regression equations are obtained differ depending on the SST dataset used (Table 3.3). Table 3.4 shows the regression equation from coral TH2. Table

3.5 compares the various regression equations of the Sr/Ca-SST relationship from several sites in the central tropical Pacific.

	Regression equation		R
Sr/Ca_{TH2} vs. ERSST	Sr/Ca = -0.035 SST+ 9.815	(1)	0.51
Sr/Ca_{TH2} vs. IRD	Sr/Ca = -0.026 SST+ 9.564	(2)	0.32
Sr/Ca_{TH2} vs. NCEP	Sr/Ca = -0.029 SST + 9.592	(3)	0.38
Sr/Ca_{TH2} vs. Delcroix	Sr/Ca = -0.028 SST + 9.630	(4)	0.44

Table 3.4. Regression equations of monthly Sr/Ca records of TH2 vs. SST ($p < 0.001$ for all analysis).

Coral sites	Regression equation	R	SST dataset
Fiji (Correge et al, 2000 in Marshal & McCulloch, 2002)	Sr/Ca = 10.73-0.065 SST	-	-
Fiji (Linsley et al.,2004)	Sr/Ca = 10.65-0.053 SST	0.88	IGOSS
Fiji (Linsley et al.,2004)	Sr/Ca = 11.73-0.055 SST	0.84	CAC
Rarotonga, (Linsley et al.,2000)	Sr/Ca = 11.12-0.065 SST	0.87	IGOSS
Rarotonga (Linsley et al.,2004)	Sr/Ca = 11.07-0.063 SST	0.80	CAC

Table 3.5. Regression equations of monthly Sr/Ca vs. SST from several central tropical Pacific corals. CAC: Climate Analysis Centre. IGOSS: Integrated Global Ocean Service System.

The slopes of the calibration range from 0.046-0.054 (Table 3.3), which is in good in agreement with published slopes of the Sr/Ca - SST relationship, which range from 0.04 to 0.08 mmol/mol/^{o}C (e.g., Beck et al, 1992; de Villiers et al., 1994, 2002; Shen, et al, 1996; Alibert, et al., 2003; Marshall and McCulloch, 2002; Mitsuguchi et al., 2003), while the slope of Sr/Ca_{TH2} vs. SST is lower than published slope estimates (Table 3.4). The Fiji records (Linsley et al., 2004) show similar differences in the Sr/Ca-SST regression equations when calibrating with different SST datasets (CAC & IGOSS) (Table 3.5). This shows that Sr/Ca-based paleo-temperature estimates depend on the SST dataset used for calibration. The differences in Sr/Ca vs. SST from many studies can be dismissed as not being precise enough either with relation to Sr/Ca measurements or to the instrumental SST data (Marshall and McCulloch, 2002). The linear regression of Sr/Ca records vs SST data is shown in Figure 3.5. The differences between TH1 and TH2 can be attributed to the quality of the two coral records, or a local site-specific problem.

As corals grow upward, they extend into shallow water. This could bias the derived SST record (Heiss and Dullo, 1997). Therefore, the core (TH1B) was drilled horizontally from the same colony as core TH1. Based on the age model which was developed based on anchor point of the Sr/Ca records, TH1B extends from January 1974 to July 1995 (Figure 3.3e). The correlation coefficient for the period 1974 to 1995 of the horizontal core (TH1B) and the vertical core (TH1) is not significantly different (Figure 3.5). The difference of the intercept values between coral Sr/Ca records from the top of TH1 (vertical core) and TH1B (horizontal core) is ± 0.05-0.07 mmol/mol. Table 3.6 shows regression equations of Sr/Ca_{TH1B} vs. SST.

	Regression equation		R
Sr/Ca_{TH1B} vs. ERSST	Sr/Ca = -0.054 T + 10.144	(1)	0.73
Sr/Ca_{TH1B} vs. IRD	Sr/Ca = -0.043 T + 9.834	(2)	0.69
Sr/Ca_{TH1B} vs. NCEP	Sr/Ca = -0.046 T + 9.902	(3)	0.75
Sr/Ca_{TH1B} vs. Delcroix	Sr/Ca = -0.046 T + 9.931	(4)	0.70

Table 3.6 Regression equations of the monthly Sr/Ca records from the horizontal core (TH1B) with several SST dataset ($p < 0.001$ for all analysis).

4.3.3 Averaging coral Sr/Ca records measured in the same colony

The average Sr/Ca calculated from TH1B and TH1, hereafter referred to $Sr/Ca_{TH1-TH1B}$ (Table 3.7), improves the correlation coefficient compared to Sr/Ca_{TH1} vs SST, but not always compared to Sr/Ca_{TH1B} vs. SST. However, the lower correlation coefficient of Sr/Ca_{TH1B} vs Delcroix SST (R = 0.70) is not significantly different from the correlation coefficient of the average Sr/Ca records TH1 and TH1B vs. Delcroix SST (R = 0.69).

	Regression equation		R
$Sr/Ca_{TH1-TH1B}$ vs. ERSST	Sr/Ca = -0.055T + 10.213	(1)	0.82
$Sr/Ca_{TH1-TH1B}$ vs. IRD	Sr/Ca = -0.046 T + 9.956	(2)	0.71
$Sr/Ca_{TH1-TH1B}$ vs. NCEP	Sr/Ca = -0.047 T + 9.986	(3)	0.76
$Sr/Ca_{TH1-TH1B}$ vs. Delcroix	Sr/Ca = -0.042 T + 9.849	(4)	0.69

Table 3.7. Linear regression equations of average monthly coral Sr/Ca records from TH1 and TH1B vs. SST ($p < 0.001$ for all analysis).

4.3.4 Averaging coral Sr/Ca records from different colonies

We assume that coral cores taken from different colonies in the same area are influenced concomitantly by environmental changes (e.g. SST variations) while other potential influences on coral Sr/Ca (e.g. "vital effects", site specific problem) should differ for each core. Hence, averaged proxy record from multiple cores should better record regional environmental changes than a single core. Since grid- SST represent a large region and not a

spot measurement, their regression with the average intercolony proxy record should result in a better correlation with SST than a single record.

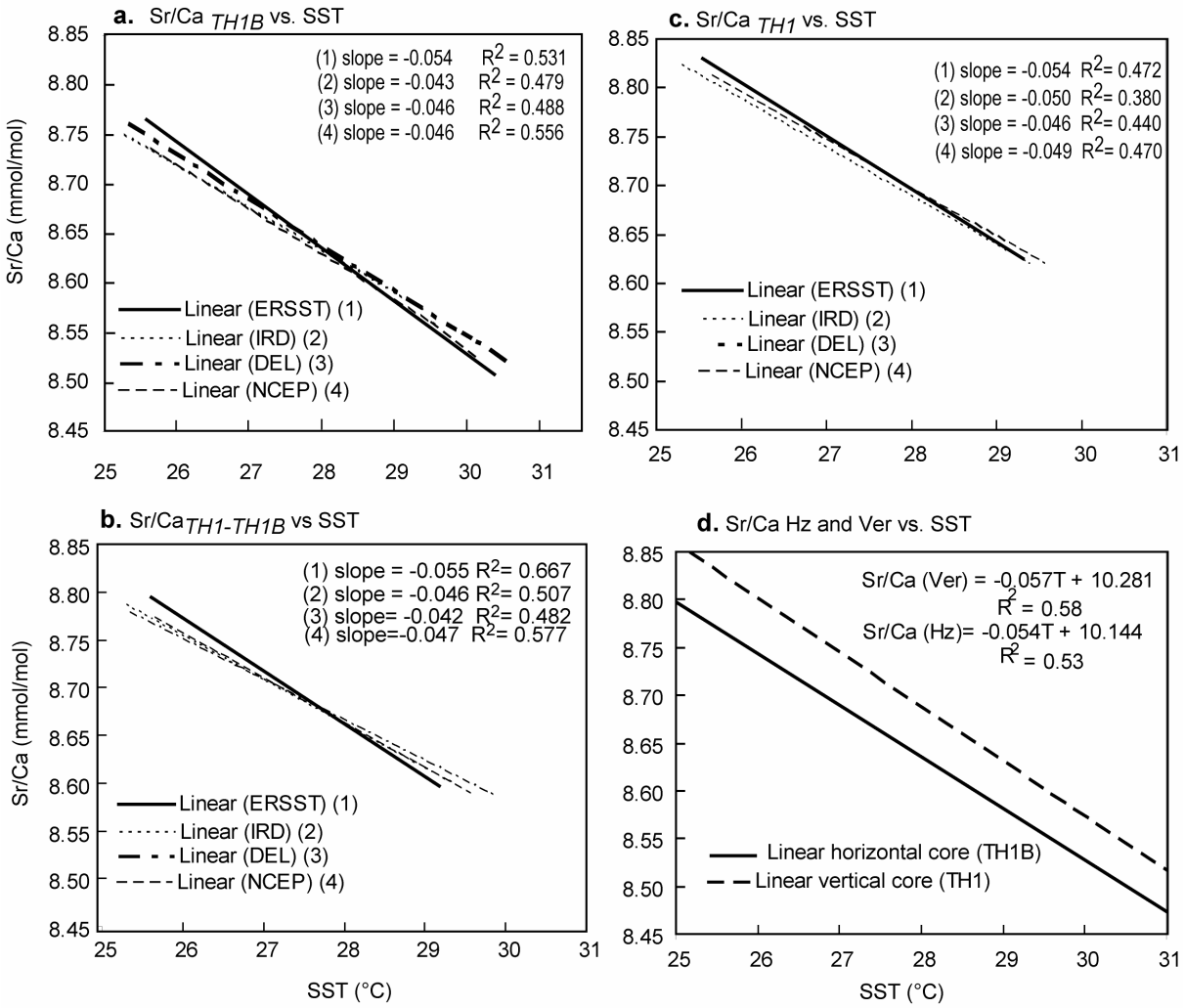

Figure 3.5. (a) Monthly linear regression of Sr/Ca TH1B vs. SST, (b) of average Sr/CaTH1-TH1B vs. SST, (c) and of Sr/CaTH1 vs. SST. (d) Monthly linear regression for the period of 1974 to 1995 of horizontal core (TH1B) and vertical core TH1 vs. SST (ERSST). The absolute offset is approximately 0.07 mmol/mol.

	Regression Equation		R
Sr/Ca_{TH12B} vs. ERSST	Sr/Ca = -0.047 T + 10.050	(1)	0.83
Sr/Ca_{TH12B} vs. IRD	Sr/Ca = -0.039 T + 9.825	(2)	0.70
Sr/Ca_{TH12B} vs. NCEP	Sr/Ca = -0.043 T + 9.854	(3)	0.76
Sr/Ca_{TH12B} vs. Delcroix	Sr/Ca = -0.0403 T + 9.856	(4)	0.77

Table 3.8. Linear regression equations of average monthly coral Sr/Ca record calculated from TH1, TH1B and TH2 vs. SST ($p < 0.001$ for all analysis).

Core TH2 is drilled in the lagoon of Vairao and from a different colony than core TH1 (drilled in the lagoon of Teahupoo), but both cores are still located within the same grid

(Figure 3.1). The linear regression of the single coral Sr/Ca record of TH2 (Table 3.4) shows a lower correlation with SST than either TH1 or TH1B.

By averaging the measured Sr/Ca from TH1, TH1B and TH2, hereafter mentioned as Sr/Ca_{TH12B}, we obtained a better correlation coefficient with SST than for the single record of TH1, TH2 and TH1B. Table 3.8 shows the regression equation of the averaging intercolony Sr/Ca record vs. SST. Figure 3.6 shows the regression plot of single proxy calibrations and of the average proxy measurements from different colonies (TH1, TH1B and TH2) and from the same colonies (TH1 and TH1B). Most of the calibrations lie on the slope range from -0.045 to -0.050 and in the intercept range from 9.90 to 10.10. However, we have shown that averaging proxy data will result in a higher correlation with SST (Table 3.8). Sr/Ca from Tahiti is also averaged with a published coral Sr/Ca record from Rarotonga (159.82°W; 21.23°S) (Linsley et al., 2000) (hereafter mentioned as $Sr/Ca_{THT\text{-}RRT}$), which is located to the west of Tahiti, although it is not located in the same grid. We use the available SST Rarotonga from ERSST and NCEP SST dataset. We average grid-SST obtained from 159.82°W; 21.23°S (Rarotonga) and 149.2°W;17.4°S (Tahiti) and regressed them with the average Sr/Ca from Tahiti and Rarotonga. Table 3.9 shows the regression equation of average SST vs. the average Sr/Ca record from Tahiti and Rarotonga.

	Regression Equation		R
$Sr/Ca_{THT\text{-}RRT}$ vs. ERSST	Sr/Ca = -0.044 T + 10.088	(1)	0.88
$Sr/Ca_{THT\text{-}RRT}$ vs. IRD	Sr/Ca = -0.05 T + 10.332	(2)	0.74
$Sr/Ca_{THT\text{-}RRT}$ vs. NCEP	Sr/Ca = -0.053T+ 10.380	(3)	0.83
$Sr/Ca_{THT\text{-}RRT}$ vs. Delcroix	Sr/Ca = -0.05 T + 10.295	(4)	0.80

Table 3.9. Linear regression equations of $Sr/Ca_{THT\text{-}RRT}$ vs. SST ($p < 0.001$ for all analysis).

We find that averaging the Tahiti and Rarotonga records improves the correlation with SST. (compare Table 3.8 & 3.9). This suggests that regional SST variations as recorded by gridded SST data, can be more adequately captured by multiple core averages from different sites.

4.4 Coral Sr/Ca-based SST reconstruction

4.4.1 SST reconstruction based on single coral Sr/Ca records

In this section we use Sr/Ca from TH1 and its calibration with ERSST (Table 3.3 equation 1) for illustration of the reconstructed SST based on a single proxy. We reconstructed the SST

based on the regression of Sr/Ca_{TH1} vs. ERSST (Table 3.3 equation 1). The variation of reconstructed SST is apparently larger than the SST dataset (Figure 3.7). The variance (σ^2_{recSST}) of the reconstructed SST data for the periods from 1923 to 1995 is 1.80 (^oC). We calculated the regression of Sr/Ca_{TH1} vs. ERSST by taking only the maximum (coolest month) and the minimum value

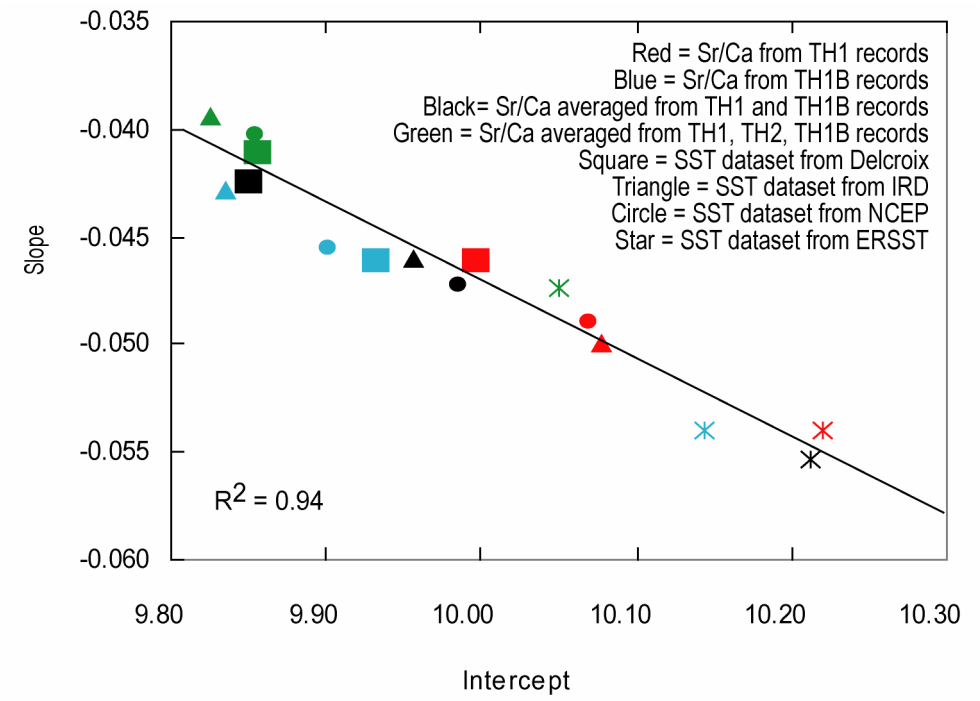

Figure 3.6. Regression plot of several regression equations of TH1, TH2, TH1B and average records

(warmest month) of the Sr/Ca and SST dataset following the method of Correge et al. (2004) (Sr/Ca_{TH1} vs. ERSST: Sr/Ca = -0.075 SST + 10.771 $p > 0.001$ R = 0.89, hereafter refered to an equation 9). We assume that this method will reduce the noise due to age model uncertainties. We then used this equation to reconstruct the SST from Sr/Ca_{TH1} and compare the result with reconstructed SST based on equation 1 Table 3.3. By applying equation 9, we expected to obtain a lower residual SST than applying equation 1. Figure 3.7 shows the result. The variance of the reconstructed SST based on equation 9 is $\sigma^2_{recSST} = 0.94$, which is lower than the variance of reconstructed SST based on equation 1 Table 3.3 ($\sigma^2_{recSST} = 1.80$). However, the lower variance of the reconstructed SST only shows the precision of the SST that is reconstructed from the regression of the proxy and the grid SST. We suggest by regressing the value of the maximum and the minimum of the data we will improve the

variance of reconstructed SST but we will not significantly reduce the residual SST (Figure 3.7), which is more or less the same as obtained by applying monthly calibration (equation 1 Table 3.3).

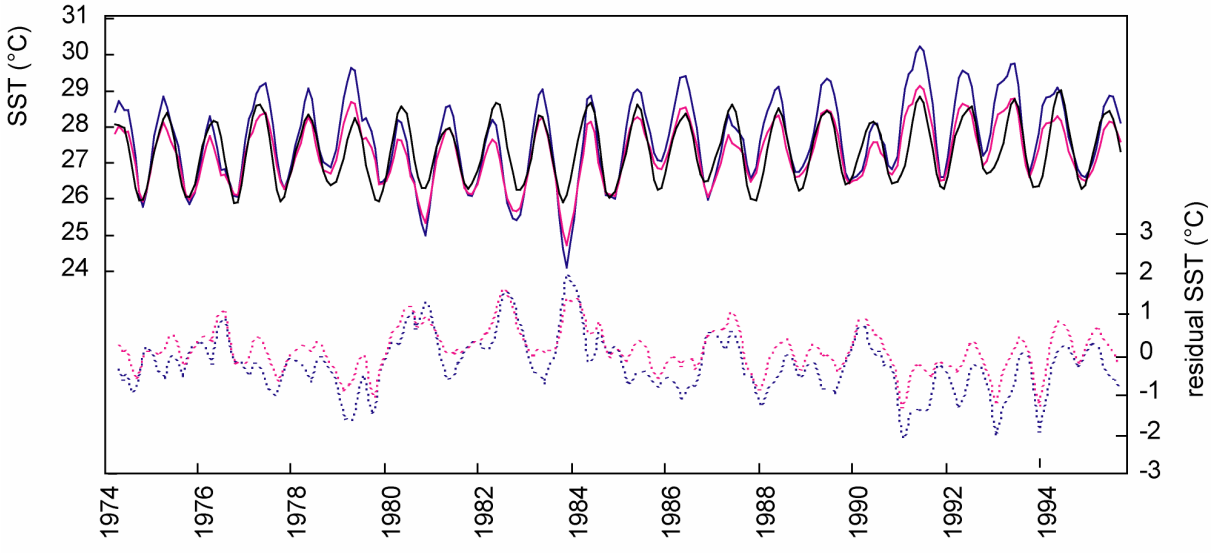

Figure 3.7. Comparison of reconstructed SST based on the regression of Sr/Ca$_{TH1}$ vs. ERSST (blue solid line R= 0.69 s = 0.053), of reconstructed SST based on the regression of minimum and maximum values of Sr/Ca$_{TH1}$ vs. ERSST (red solid line R= 0.89 s = 0.048) and ERSST (black solid line). The residual SST is obtained by substracting the ERSST from the reconstructed SST of Sr/Ca$_{TH1}$ (blue dashed line) and the reconstructed SST of the minimum and maximum values of Sr/Ca$_{TH1}$ (red dashed line).

We validated the Sr/Ca$_{TH1}$ with the ERSST data and compared the trend of SST and the proxy by regressing the coral Sr/Ca$_{TH1}$ vs ERSST covering 1950 to 1995. The regression equation of coral Sr/Ca$_{TH1}$ vs. ERSST for 1950-1995 is Sr/Ca = -0.052 ±0.002 SST + 10.17±0.066 R = 0.68 σ=0.052 (hereafter refer to equation 10). The slope and the intercept are not significantly different from the slope of the regression equation from the entire period data (equation 1 Table 3.3 slope= -0.054 intercept = 10.23). We then reconstructed SST based on equation 10 to validate the proxy. The result shows that comparing to the ERSST, the trend of the reconstructed SST in the validation period is not different from the trend in the calibration period (Figure 3.8). The similar trend in the calibration period (1950-1995) and validation period is also shown by record TH2.

4.4.2 SST reconstruction based on average coral Sr/Ca

We applied the regression of the averaging Sr/Ca record of TH1-TH1B (equation 1 Table 3.7) to convert Sr/Ca to SST. Figure 3.9 shows the result of reconstructed SST based on average

Sr/Ca TH1-TH1B. The residual SST is obtained by subtracting the instrumental SST from the reconstructed-SST. This residual is suggested to be noise. Using the average Sr/Ca from TH1 and TH1B, the residual SST varies from ± 2 ^{o}C to ± -2 ^{o}C, while the residual SST calculated from both single proxy records varies from ± 2 ^{o}C to ± -3 ^{o}C. SST reconstruction from averaging proxy records measured in different core from the same colony (TH1 and TH1B records) reduces the variance of the residual SST.

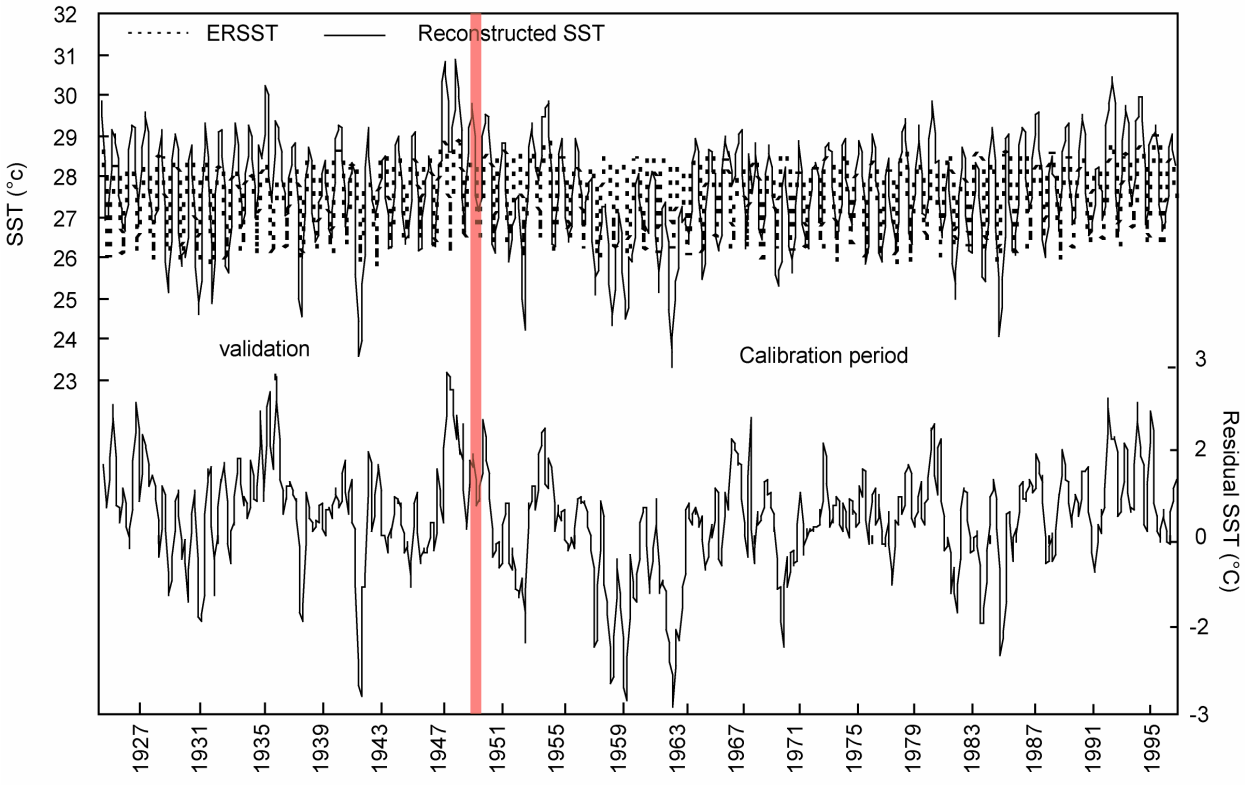

Figure 3.8. Reconstructed SST based on the regression of monthly Sr/Ca vs ERSST covering the time period of 1950 to 1995 (Sr/Ca = 0.052 SST + 10.17; R= 0.68; $p < 0.001$). The residual SST is obtained by substracting the ERSST from the reconstructed SST with the ERSST.

We also reconstruct past SST variation from average proxy TH1, TH1B and TH2 (equation 1 Table 3.8). The result is shown in Figure 3.9. For the intercolony average (TH1, TH1B and TH2) the variance of reconstructed SST is $\sigma^2 = 1.20$. For the single colony average (TH1 and TH1B) the variance is $\sigma^2 = 1.25$ (calculated using equation 1 Table 3.7). The residual of both averaging proxies records is not significantly different (Figure 3.9). The reconstructed SST based on average Sr/Ca ratios from Tahiti and Rarotonga has lower variation in the residual SST which vary from -1^{o} C to 1^{o} C (Figure 3.10).

4.5 The linear extension rate

For the periods 1974-1995, measured Sr/Ca values of TH1B range from 8.511 mmol/mol to 8.838 mmol/mol (mean value = 8.671 σ= 0.07), while Sr/Ca of TH1 range from 8.853 mmol/mol to 8.971 mmol/mol (mean value = 8.725 σ= 0.07). Previous studies suggested that such differences are a result of skeletal extension/calcification rate effects (e.g. de Villiers, 1994).

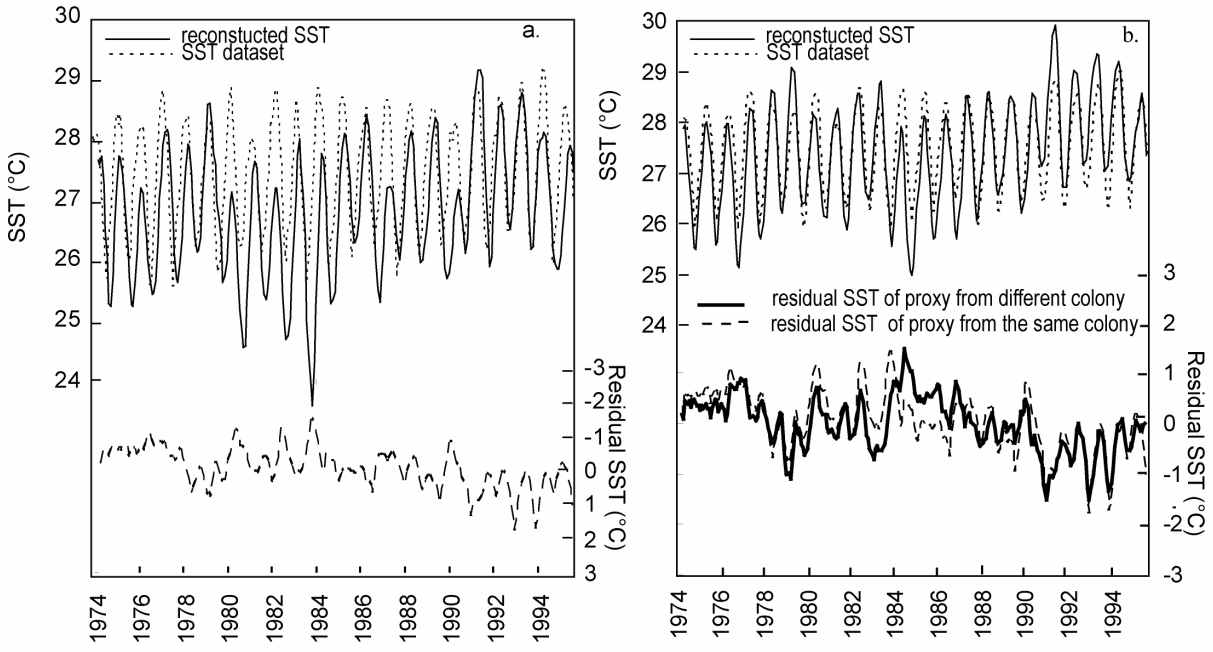

Figure 3.9. (a) Reconstructed SST (solid line) based on average Sr/Ca record from TH1 & TH1B vs. ERSST (dashed line) (R= 0.69). (b) Reconstructed SST (solid line) based on average Sr/Ca from TH1, TH2 & TH1B vs. ERSST (dashed line) (R= 0.67). The residual SST is calculated by substracting ERSST from the reconstructed SST, shown are 3 points running averages.

We use the coral XDS software (X-radiograph Densitometry System) from the National Coral Reef Institute of the Nova South Eastern University Oceanographic Center (NSUOC) to calculate the extension rates of the horizontal core (TH1B) and the top of the vertical core (TH1). The horizontal core is 25.08 cm long, and comprises approximately 21 years based on the Sr/Ca chronology. The core top of TH1 is 29.3 cm long and also comprises 21 years. Figure 3.11 shows the x-radiographs of both slabs. The linear extension rate is calculated based on the annual density bands. One coupled of high and low density bands is identified as one year of growth. The mean linear extension of the horizontal core (0.974 cm/year) is lower than that of the vertical core (1.337 cm/year). If higher mean Sr/Ca ratios are associated with

low extension rates (de Villiers et al., 1995) then the horizontal core analyzed in our study should have higher Sr/Ca values than the vertical core. However our results are different. We found that coral Sr/Ca ratios in the horizontal core are lower (8.511 to 8.838 mmol/mol) than in the vertical core (8.853 to 8.971 mmol/mol), although the extension rate of the horizontal core (0.974 cm/year) is lower than the extension of the vertical core (1.337 cm/year). Figure 3.12 shows the luminescence of the horizontal and the vertical core, where high luminescence values represent high density band.

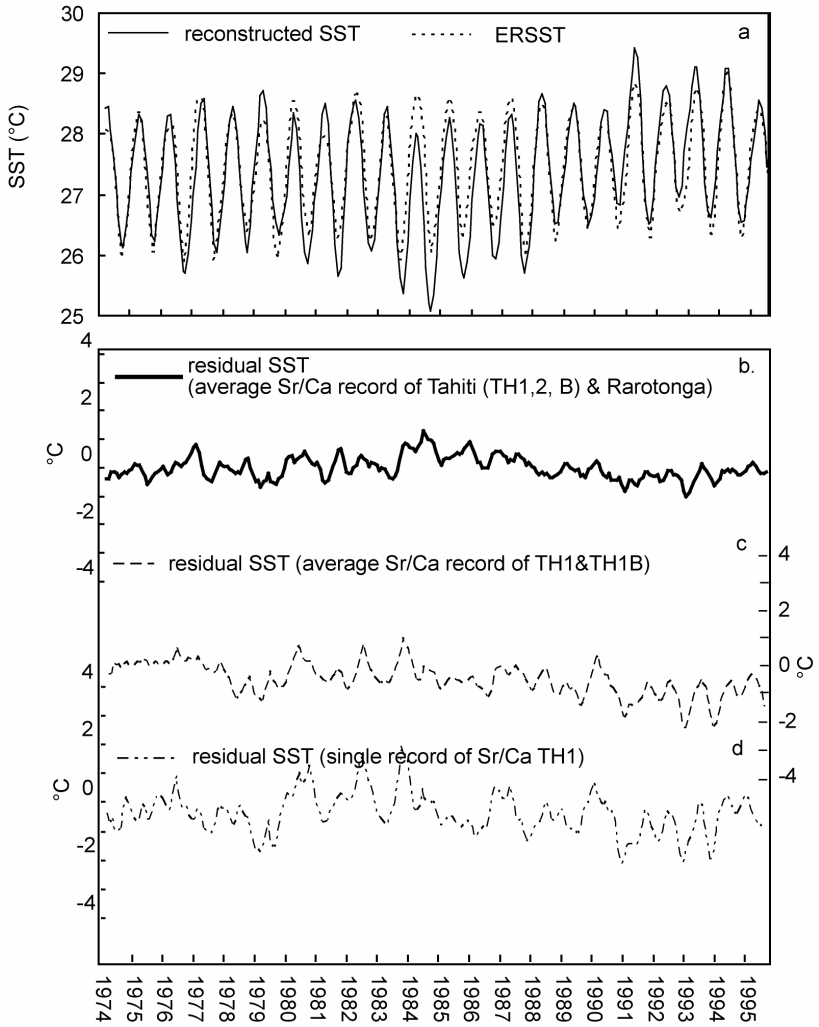

Figure 3.10. (a) Reconstructed SST based on monthly regression of ERSST vs. average Sr/Ca data from Tahiti and Rarotonga records (R = 0.88; eq.1, Table 9). Comparison of the residual SST for the regression (b) SST vs. averaging proxy Tahiti & Rarotonga records (R= 0.88; eq. 1, Table 9), (c) vs. average proxy records from the same coral colony (TH1 & TH1B) (R = 0.82; eq. 1, Table 7) and (d) vs. single record from core TH1 (R = 0.69; eq. 1, Table 4).

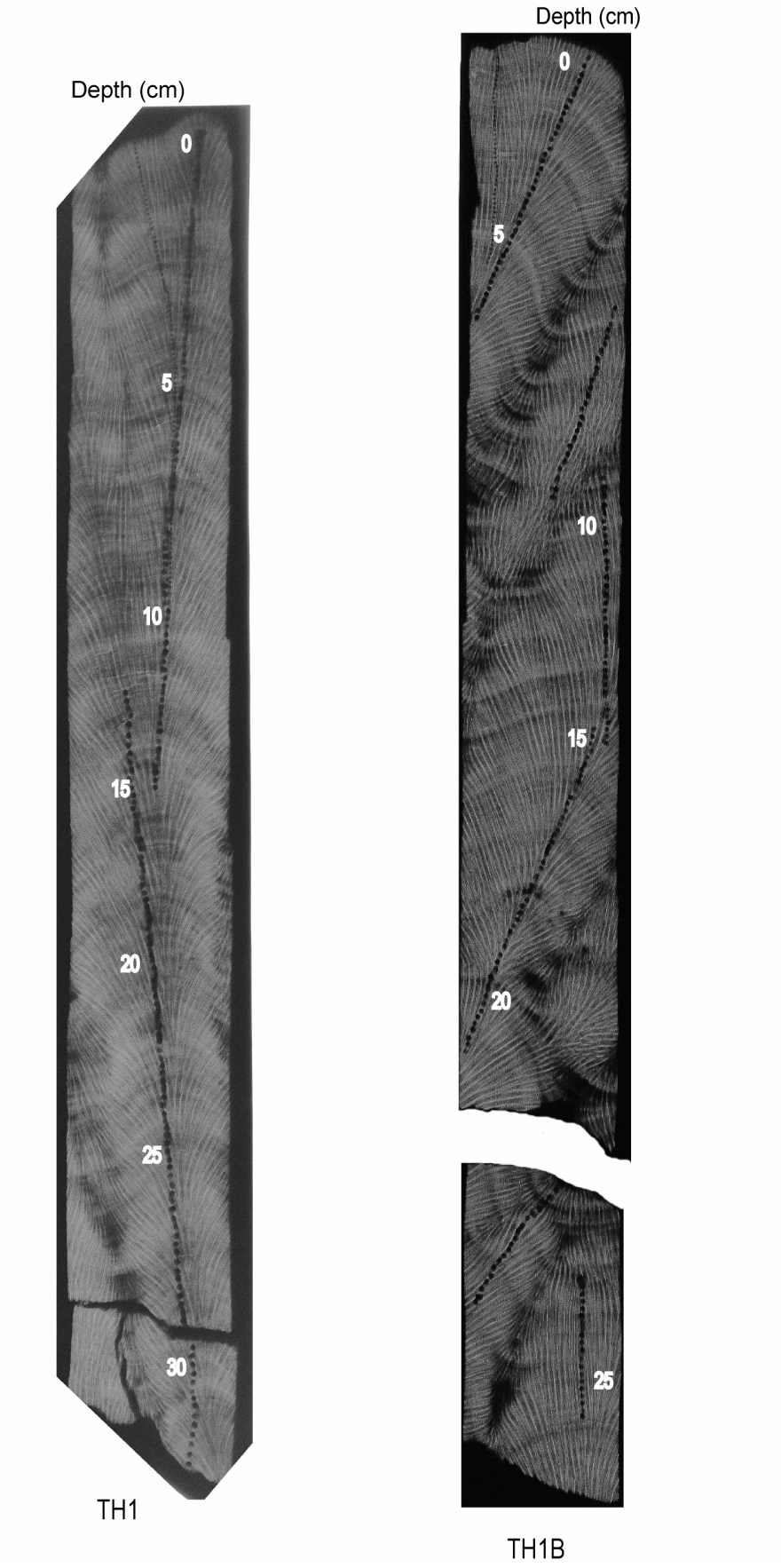

Figure 3.11. X-ray images of the coral slabs. Left: the top of vertical core TH1. Right: the horizontal core TH1B.

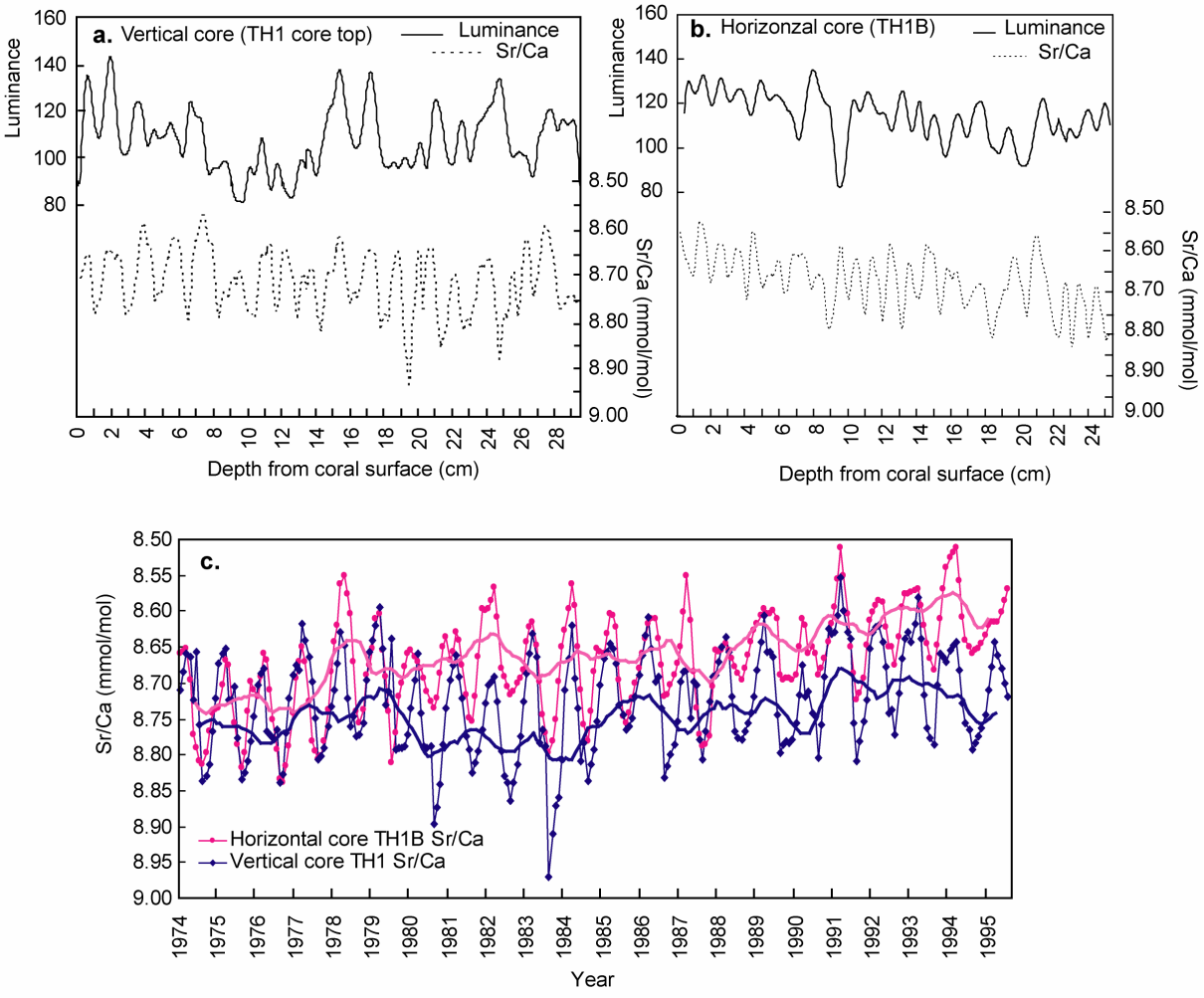

Figure 3.12. (a) High (low) luminance indicates high (low) density band of vertical core TH1 and (b) of horizontal core TH1B. (c) Monthly Sr/Ca ratio of the horizontal (TH1B) and vertical (TH1) cores.Thick lines: 12 points running average.

Our study shows that the Sr/Ca variations of the horizontal core TH1B have a much better correlation with instrumental SST variations than the vertical core (TH1). Therefore, we suggest that the extension rate and the calcification rate do not significantly influence Sr/Ca ratios in these cores. The apparent offset is perhaps only due to "noise". However, several years (eg. 1974-1977) show more or less identical Sr/Ca values (Figure 3.12c). Hence, we can not identify a constant shift toward higher or lower Sr/Ca ratios in one of the cores. We suggest, that a reproducible temperature signal can only be recorded by Sr/Ca values measured from multiple coral cores. Nevertheless, we should not ignore possible vital effects in the coral Sr/Ca ratios since there are at present still many different Sr/Ca vs. SST calibrations (e.g. Marshall and Mc Culloch, 2002; Linsley et al., 2004).

4.6 Annual mean coral Sr/Ca calibration

In order to obtain an annual calibration equation, the annual Sr/Ca is regressed against the annual mean SST data. We use the period data of 1974-1995 to obtain the same length of data. The annual mean is acquired by averaging data from August to July in the following years. Table 3.10 shows the annual regression equation of single Sr/Ca records (TH1,TH1B and TH2) vs. ERSST data.

	Regression equation				R
1. Sr/Ca $_{TH1}$ vs. ERSST	Sr/Ca = -0.08 SST + 11.177	σ =0.03	n=22	(1)	0.28
2. Sr/Ca$_{TH1B}$ vs. ERSST	Sr/Ca = -0.218 SST + 14.621	σ =0.03	n=22	(2)	**0.79**
3. Sr/Ca$_{TH2}$ vs. ERSST	Sr/Ca =-0.051 SST + 10.265	σ =0.04	n=22	(3)	0.21
4. Sr/Ca $_{TH1\text{-}TH1B}$ vs. ERSST	Sr/Ca = -0.151 SST + 12.815	σ =0.02	n=22	(4)	**0.71**
5. Sr/Ca $_{TH12B}$ vs. ERSST	Sr/Ca = -0.089 SST + 11.173	σ =0.02	n=22	(5)	0.55

Table 3.10. The annual mean calibration of the Tahiti records: single coral record (1-3) and average records (4-5) ($p < 0.001$ for all analysis).

In the mean annual scale calibration, the correlation coefficients of annual calibration of SST vs. single Sr/Ca record from TH1 and TH2 are low (Table 3.10; eq.1 & eq.3). The correlation coefficient on an annual mean scale from the single Sr/Ca records TH1B is the highest. However, the slope is much higher than published slopes of the coral Sr/Ca-SST relationships. The linear regression of the average coral Sr/Ca records vs. ERSST shows lower correlation coefficients (see equation 4 & 5 Table 3.10) than TH1B records.

We used the monthly coral Sr/Ca-SST regression to convert the proxy to SST. This approach is justified, because the incorporation of Sr/Ca in coral skeleton is governed by thermodynamic laws on monthly as well as on annual time scales. We find that on an annual mean scale the variation of reconstructed SST is much larger than indicated by grid-SST (Figure 3.13). The variance is larger for single records ($\sigma = 1.14$ for TH2, $\sigma = 0.6$ for TH1, $\sigma = 0.79$ for TH1B) than for the average record ($\sigma = 0.58$ for average TH1-TH1B and $\sigma = 0.53$ for average TH1-TH2-TH1B). Importantly, the differences in the variance between the proxy and grid-SST do not seem to depend on the strength of correlation between the proxy and SST. The gridded SST data ussually have a lower SST variation than the local SST data as the result of average SST observation within the grid box. Each location then can show a slightly different temperature therefore by averaging those values, it will be possible to reduce the site-specific variability and retain the common grid average value. The larger the grid, the

more can the individual values differ from each other. This problem cause the variation of reconstructed SST from Sr/Ca from Tahiti is higher than the variation of grid SST. This problem may overcome by averaging the proxy. Averaging the proxy records will remove local SST signal. The larger grid SST the more proxy records should be averaged.

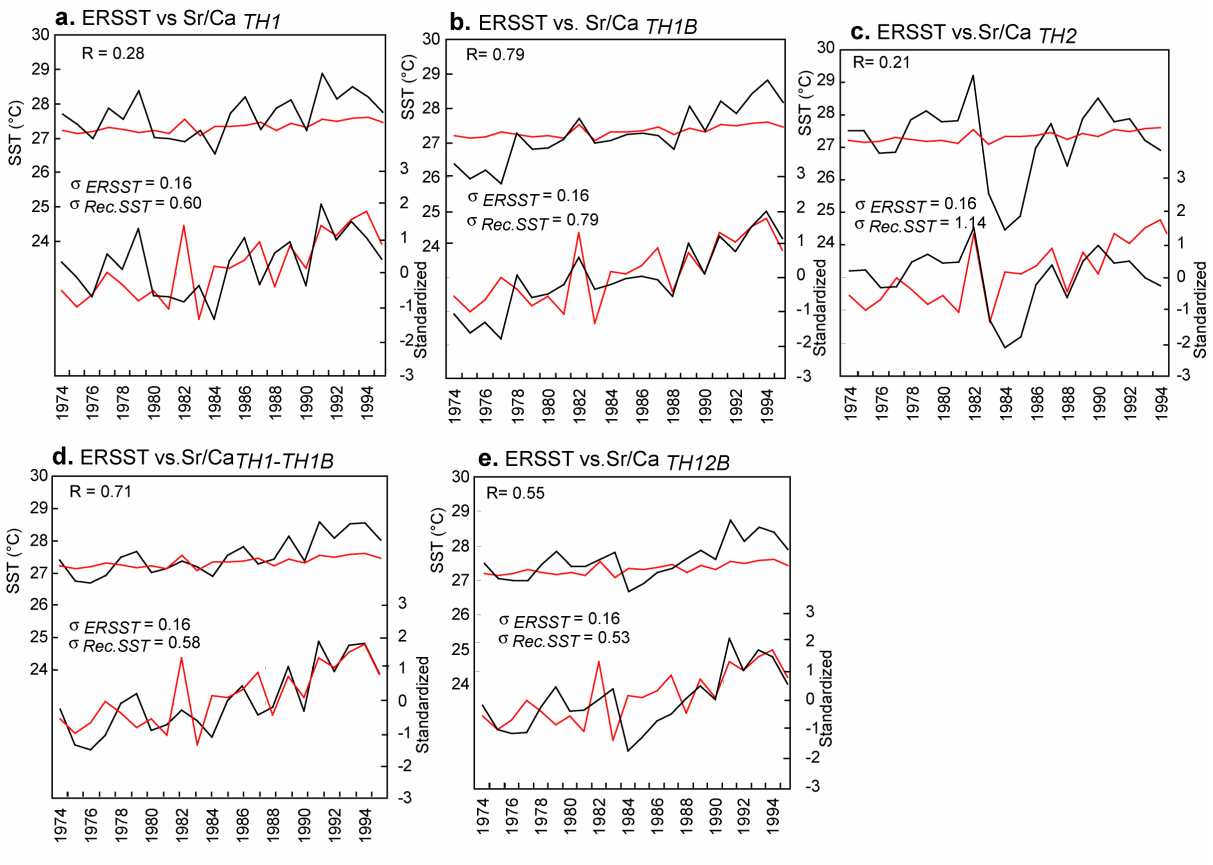

Figure 3.13. Annual means of ERSST (red solid lines) compare to annual means of reconstructed SST (dark solid lines) (top). Below: annual means normalized to unit variance. Reconstructed SST is based on the regression of ERSST vs. Sr/Ca of the single records (a) TH1, (b) TH1B and (c) TH2 and (d) average Sr/Ca of TH1 & TH1B and (e) of TH1,TH2 & TH1B.

5. Concluding remarks

The grid derived SST data are often regional averages using a large area. Grid-SST can not capture the small-scale SST variations at given coral sites. Therefore, that is portrayed by the proxies. However, coral-based Sr/Ca SST reconstructions are developed with the aim to reconstruct large-scale historical SSTs. Therefore, a comparison between the proxy record and grid-SST is critical to assess the fidelity of coral records as monitors of large-scale climate anomalies.

In order to obtain a better correlation between the coral proxy and SST, the peak matching method is usually applied to develop the chronology. In our study, developing chronologies based on peak matching do not always result in a higher correlation (high R value) between SST and the relevant proxy compared to the anchor point method. It seems that both methods itself do not affect the result of the calibrations. However, we should keep in mind that the R only represents the best fit of the data.

Several previous studies applied the regression equation considering temperature as the dependent variable (Gagan et al., 1998, 2000; Ayliff et al., 2004). In this study, we used temperature as the independent variable considering that the regression error (σ) is small. However, the lower σ values do not mean that the estimated temperature variations, which are calculated from this equation, are more representative of the true temperatures. The lower σ values only show that the deviation of calculated temperatures based on the regression equation of coral Sr/Ca vs. grid SST is small. The slope values of the monthly coral Sr/Ca - SST relationship are consistent with published estimates for the Sr/Ca-SST relationship, but the slope values obtained by the annual mean calibration are not. This means that variances are different. This outcome will have important implications for reconstructing SST variation from fossil corals.

Some previous studies suggest that growth and calcification rate affects coral Sr/Ca (e.g., de Villiers et al., 1994), while others find that these effects are minor (e.g Crowley et al., 1999). In our study, it seems that the extension rate does not significantly influence our coral Sr/Ca record. De Villiers et al. (1994) showed that higher Sr/Ca ratios are associated with lower extension rates. We find the opposite: the horizontal core has lower Sr/Ca ratios (mean = 8.671 mmol/mol) and lower extension rates (0.974 cm/year), while the vertical core has higher Sr/Ca ratios (mean = 8.725 mmol/mol) and higher extension rates (1.337 cm/year). These differences lead to an offset in the intercept Sr/Ca vs. SST regression equation of the horizontal and vertical core. However, the offset between the horizontal and the vertical core does not appear to be systematic. We, therefore, suggest that this is simply caused by "noise" e.g. Sr/Ca heterogeneities within the coral colony. This seems to be more problematic in the vertical core. However, extension and calcification rate-related Sr/Ca variations need to be better understood, especially at longer time scales, and potential vital effects on coral Sr/Ca ratios should not be ignored.

The quality of the Sr/Ca-SST regression is often assessed solely based on the correlation coefficient. The higher the correlation coefficient, the better the Sr/Ca-SST relationship. However, a high correlation coefficient of the regression equation does not necessarily mean that the equation is accurate enough to reconstruct SST. It is also important to look at the residual SST (e.g. difference between the SST dataset and reconstructed SST based on coral Sr/Ca). In order to essentially improve the correlation coefficients of the proxy-SST relationship, the variances of the reconstructed SST and to minimize the residual SST, we propose to average the proxy measurements from multiple coral colonies taken from different locations in a given region. We suggest that SST reconstruction from average proxy records are more representative of regional SST variations. At Tahiti, SST reconstructions from intercolony averaged coral proxy records resulted in a better correlation coefficient and reduced the residual SST compared to single proxy records. The average proxy record calculated from multiple colonies taken from two sites (Tahiti and Rarotonga) resulted in a better correlation coefficient and in a further reduction of the residual SST compared to averaged coral proxy records from one site (Tahiti).

The SST reconstruction from Tahiti coral Sr/Ca records shows much larger interannual variations than the grid-SST, i.e., the variance of the annual mean SST reconstruction differ from instumental grid-SST. This poses a serious problem to any attemps to assess the magnitude of interannual SST variations from fossil corals taken at Tahiti. Besides calibrating coral proxy with the local SST measurement, developing multiple coral proxy records are also needed to improve the calibration of proxy-SST.

Acknowledgement

We are grateful for the support of the Deutscher Akademischer Austauschdienst (DAAD) (grant A/02/21403) and the Deutsche Forschungsgemeinschaft (Leibniz award to Prof. Wolf-Christian Dullo). We are grateful to Dieter Garbe-Schönberg for discussion about Sr/Ca analysis. We also thank Lutz Haxhiaj, Karin Kiessling and Ana Kolevica for their assistance in the isotope and trace element laboratory.

CHAPTER IV

Reconstructing seawater $\delta^{18}O$ from paired coral $\delta^{18}O$ and Sr/Ca ratios: Methods, Error Analysis and Problems, with examples from Tahiti (French Polynesia)

Sri Yudawati Cahyarini, Miriam Pfeiffer, Oliver Timm and Wolf-Chr. Dullo

(submitted to Journal of Geophysical Research-Oceans)

Abstract

We compare several statistical routines that may be used to calculate $\delta^{18}O_{sw}$ and SSS from paired coral Sr/Ca and $\delta^{18}O$. The relationship between coral $\delta^{18}O$, SST and SSS can be described in a general linear regression model ($\delta^{18}O_{coral} = \gamma_1 SST + \gamma_2 SSS + \gamma_o + e_{\delta^{18}O_{coral}}$). Typically, the $\delta^{18}O_{coral}$-SST relationship is estimated by linear regression of coral $\delta^{18}O$ vs. SST, i.e., it is assumed that γ_2=0. This is a methodological error, because if SST and SSS co-vary, the estimate of γ_1 will be biased. Ideally, a multiple linear regression (MLR) of coral $\delta^{18}O$ vs. SST and SSS should be used. The MLR, however, assumes that the independent variables are free of error, which they are not. Since the slope of the $\delta^{18}O_{coral}$ - temperature relationship is known, we propose to insert this value for γ_1 in the regression models. This requires that the constant values are removed from the regression equations. To omit the constant, it has been proposed to compute the instantaneous changes of the proxies. We propose to center the regression equations (i.e., to remove the mean values from the variables). The statistical error propagation is calculated to assess our ability to resolve past variations in $\delta^{18}O_{sw}$ (SSS). At Tahiti, we can not resolve the seasonal cycle of $\delta^{18}O_{sw}$ (SSS), since its amplitude equals the combined analytical uncertainties of coral $\delta^{18}O$ and Sr/Ca. On an annual mean scale, however, the analytical uncertainty reduces, and variations in SSS are larger. We find a significant correlation between reconstructed $\delta^{18}O_{sw}$ and SSS. Both show a freshening in 1977/78.

1. Introduction

The oxygen isotopic composition of seawater ($\delta^{18}O_{sw}$) is related to the hydrological balance (precipitation-evaporation (P-E)) and, by extension, to sea surface salinity (SSS) (e.g., Craig and Gordon, 1965; Schmidt, 1999; Delaygue et al., 2000). Both are important climatic parameters. Therefore, reconstructing $\delta^{18}O_{sw}$ is an important aspect of coral

paleoclimatology. The main objective of coral-based $\delta^{18}O_{sw}$ reconstructions is to reconstruct past variations of SSS on time scales ranging from seasonal to centennial (e.g., Ren et al., 2002; Hendy et al., 2002). The statistical methods that should be used for $\delta^{18}O_{sw}$ calculations, however, have been a matter of intense debate over the past few years (Gagan et al., 1994, 1998; Ren et al., 2002; Huppert and Solow, 2004; Kilbourne et al., 2004). Also, the reliability of $\delta^{18}O_{sw}$ reconstructions inferred from paired coral Sr/Ca and $\delta^{18}O$ measurements is difficult to assess due to the lack of continuous time series of $\delta^{18}O_{sw}$ and the poor quality of instrumental salinity datasets currently available (e.g., Kilbourne et al., 2004).

Coral $\delta^{18}O$ ($\delta^{18}O_{coral}$) is influenced both by temperature and $\delta^{18}O_{sw}$ (Ren et al., 2002; Pfeiffer et al., 2004; Correge et al., 2004), while Sr/Ca is believed to be influenced by SST only (Beck et al., 1992; McCulloch et al., 1994; Shen et al., 1996; Alibert and McCulloch, 1997; Marshall and McCulloch, 2002). Therefore, $\delta^{18}O_{sw}$ can be reconstructed by removing the effect of SST from $\delta^{18}O_{coral}$ using paired measurements of coral $\delta^{18}O$ and Sr/Ca ratios. Because $\delta^{18}O_{coral}$ and Sr/Ca have different units, they are both converted to SST, in order to subtract the temperature contribution inferred from coral Sr/Ca. However, coral $\delta^{18}O$ and Sr/Ca ratios are complicated by so-called 'vital effects' that result in absolute offsets of the proxies measured in different coral colonies (McConnaughey, 1989; de Villiers et al., 1995; Linsley et al., 1999; Marshall and McCulloch, 2002). These offsets are believed to remain constant within a given coral colony, provided that the coral is sampled along the main growth axis (McConnaughey, 1989; Alibert and McCulloch, 1997), and the coral $\delta^{18}O$ (Sr/Ca)-temperature relationship for a given coral can be obtained by calibrating the coral proxies with instrumental data. The most commonly used technique to calculate $\delta^{18}O_{sw}$ is to estimate the linear regression equation in the form $Y(t) = MX(t) + B + e(t)$ between coral $\delta^{18}O$ (Sr/Ca) and local SST (e.g., Gagan et al., 1994,1998). Because the absolute values of coral $\delta^{18}O$ and Sr/Ca are not very reliable, Ren et al. (2002), have proposed to omit the intercept value of the $\delta^{18}O_{coral}$ (Sr/Ca)-SST regression by calculating the first derivatives of the two proxies. Thus, only the relative changes of the proxies are used to calculate relative changes of $\delta^{18}O_{sw}$. Kilbourne et al. (2004) and Huppert and Solow (2004), however, have shown that the results obtained with the method of Ren et al. (2002) and Gagan et al. (1994,1998) are basically the same

(except for a constant offset). Both methods will fail if SST-covariant changes in $\delta^{18}O_{sw}$ and SSS occur (Huppert and Solow, 2004), because coral $\delta^{18}O$ is calibrated with SST only and changes in $\delta^{18}O_{sw}$ would bias the slope of the $\delta^{18}O_{coral}$ -SST regression.

In this paper, we will compare and discuss the methods proposed for $\delta^{18}O_{sw}$ reconstructions from corals, and suggest to use a simpler, well established statistical method to omit the intercept values from the $\delta^{18}O$ (Sr/Ca)-SST regression equation. We also explore how SST covariant changes in $\delta^{18}O_{sw}$ and SSS would affect coral-based reconstructions and how we could avoid this potential problem in the future. We will illustrate the various approaches with paired $\delta^{18}O$ and Sr/Ca records from modern Tahiti corals. For all approaches, the error propagation of calculated $\delta^{18}O_{sw}$ and SSS is discussed. $\delta^{18}O_{sw}$ (SSS) reconstructions are compared and validated with SSS data from the Simple Ocean Data Assimilation (SODA) model (Carton et al., 2000).We will also highlight problems that need to be addressed in future studies in order to achieve reliable $\delta^{18}O_{sw}$ and SSS reconstructions from corals.

2. Climatic and oceanographic setting of Tahiti

Modern coral cores were drilled in the lagoon of Tahiti (149°20' W 17°4`E), which is part of the Society archipelago, French Polynesia (Figure 4.1). Tahiti is a large (~1042 sq km) and high volcanic island (~2241 m and ~1323 m) located in the Southwestern tropical Pacific (24°S-10°S; 160°E-140°W). This region is characterized by a major salinity front that separates the high salinity waters formed in the subtropical region (120°W, 20°S) where evaporation exceeds precipitation, from the low salinity waters formed in the warm pool area, where precipitation exceeds evaporation (Gouriou and Delcroix, 2002). Tahiti lies in the path of the South-Equatorial Current that advects high salinity water from the central south Pacific. Seasonal variability is apparent in climatological SSS data, with an average amplitude of ± 0.3 psu (Carton et al., 2000; Gouriou and Delcroix, 2002) (Figure 4.2). The Southwestern tropical Pacific also displays substantial interannual salinity variations, which are clearly linked to ENSO (Gouriou and Delcroix, 2002). ENSO-related SSS variations are twice as large as seasonal variations (Gouriou and Delcroix, 2002). Mean seasonal SST varies from 27°C to 28.5°C during November-April and from 26°C to

28°C during May-October (Figure 4.2). For SST, the amplitude of interannual, ENSO-related variations are an order of magnitude smaller than the seasonal signal (Gouriou and

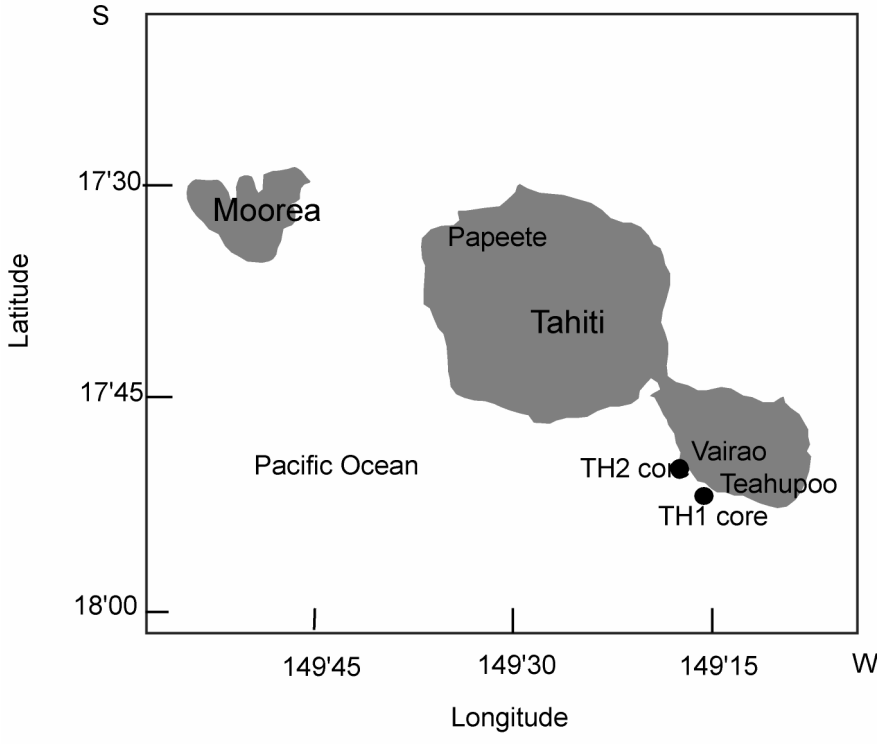

Figure 4.1. Map of Tahiti, French Polynesia, with location of coral cores (black dots).

Delcroix, 2002). Thus, SST covariant changes in SSS (and $\delta^{18}O_{sw}$) occur on seasonal and interannual time scales, but on interannual time scales the effects of SSS on coral $\delta^{18}O$ should be proportionally larger.

3. Material and Methods

3.1. Sample collection and analytical procedures

In July 1995, we drilled two coral cores from massive colonies of genus *Porites* growing in the lagoon of Tahiti. Core TH1 was taken at Teahupoo (Figure 4.1), in the south-eastern part of the lagoon. The core was drilled vertically along the major axis of growth and is 1.80 m long. Core TH2 was drilled at Vairao (Figure 4.1). The core is 3.4 m long.

The coral cores were then slabed to a thickness of 4 mm. These slabs were cleaned in an Ultrasonic bath and dried at 50°C for 24 hours. The X-radiographs of the slabs show clear

annual density bands that allow a precise chronology. The average annual extension rate is approximately 1-2 cm/year. A sampling transect that follows the main growth axis was

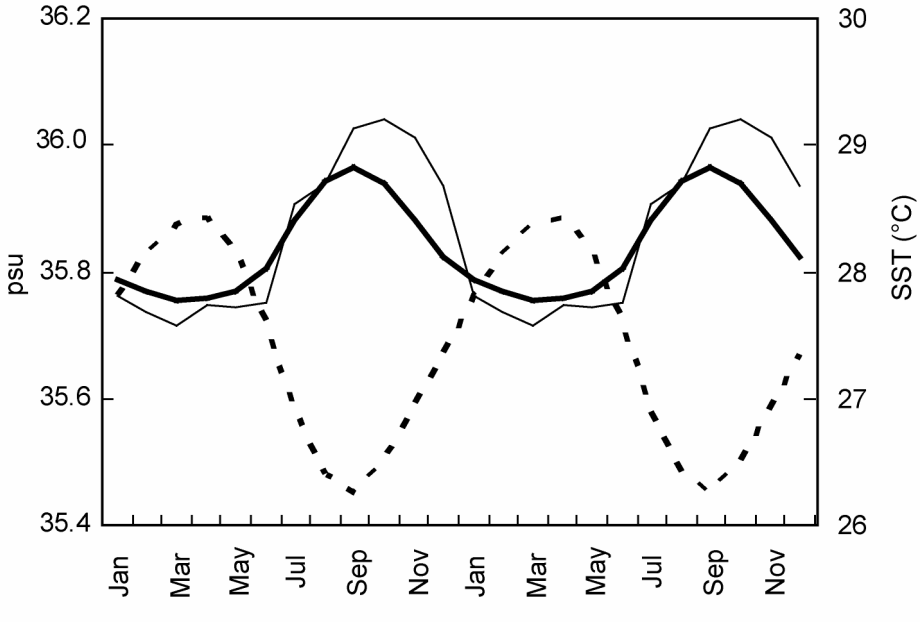

Figure 4.2. Tahiti climatology of SSS from SODA (bold black line) (Carton et al., 2000), SSS from Delcroix et al (1996) (black line) and SST from SODA v.1.2 (dashed line).

choosen. Slabs were subsampled with a dental drill using a drilling bit of 1 mm. Powdered samples were taken every 1 mm to get monthly resolved proxy records. The powdered samples were split for stable oxygen isotope ($\delta^{18}O$) and trace element (Sr/Ca ratios) analysis.

We measured Sr/Ca ratios on an inductively coupled plasma optical emission spectro-photometer (ICP-OES) at the University of Kiel following a combination of the techniques described by Schrag (1999) and de Villiers et al. (2002). The sample solution is prepared by dissolving approximately 0.5 mg of coral powder in 1.00 mL HNO_3 70%. The working solution is prepared by serial dilution of the sample solution with HNO_3 2% to get a concentration of ca. 8 ppm Ca. Standard solution is prepared by dilution of 1.00 mL of the stock solution (0.52 grams of coral powder from an in-house standard in 250 mL HNO_3 2%) with 2.00 mL HNO_3 2%. Sr and Ca lines, which are used for this measurement, are 407 nm and 317 nm respectively. Analytical precision on Sr/Ca determinations is 0.15% RSD or 0.01 mmol/mol (1σ).

The stable oxygen isotopic composition ($\delta^{18}O$) was analyzed at IFM-GEOMAR. Core TH1 was analysed using a Finnigan Mat 251 mass spectrometer. A Thermo Finnigan Gasbench

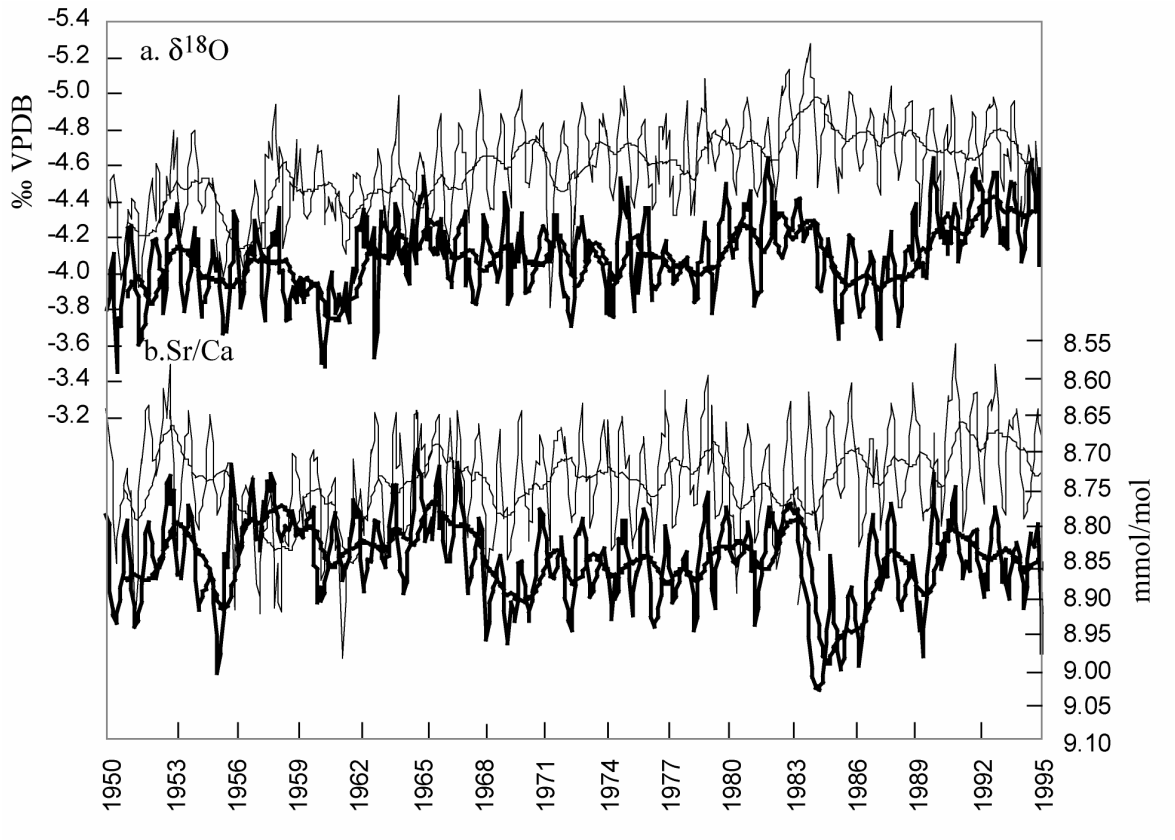

Figure 4.3. Monthly coral $\delta^{18}O$ (a) and Sr/Ca (b) time series from Tahiti cores: TH1 (thin black lines) and TH2 (thick black lines) for the period 1950-1995, with 12 points running averages.

II Delta Plus was used for the analysis of core TH2. The isotope ratios are reported in ‰ VPDB relative to NBS 19. The analytical uncertainty is less than 0.06‰ (1σ) for $\delta^{18}O$ measurements.

The chronology of TH1 and TH2 was constructed by linear interpolation between anchor points that were tied to the seasonal minima (maxima) of the Sr/Ca records. It is assumed that the minimum (maximum) skeletal Sr/Ca corresponds to the maximum (minimum) SST. The annual maximum (minimum) Sr/Ca is tied to August (March), which is on average the coolest (warmest) month in Tahiti. The uncertainty of the age model is approximately 2 months in any given year. Since the aim of this study is to validate the proxies with salinity data from the SODA reanalysis, we only use the proxy data back until 1950 (Figure 4.3).

3.2 Historical data

Instrumental records of past salinity variations are scarce. Delcroix et al., (1996) and Gouriou and Delcroix (2002) have published a monthly salinity time series for the Southwestern tropical Pacific extending back until 1976 from ship-of-opportunity measurements. This dataset is averaged over 2° latitude x 10° longitude. The Simple Ocean Data Assimilation reanalysis of ocean climate variability provides monthly averaged SST and SSS data covering the past 50 years mapped onto a uniform 0.5° x 0.5° grid (Carton et al., 2000). The SODA model uses input data from the World Ocean Database 2001, hydrographic data, satellite and in situ SST and altimetry from Geosat, ERS-1 and TOPEX/Poseidon (Carton et al., 2000). In this study, we use SODA 1.2 which uses the surface wind products from the NCEP/NCAR reanalysis. This product may be biased by the introduction of satellite observations in the mid-1970s, but it does not require correction of the mean stress (like the ECMWF ERA 40 product, which was used in the newer versions of SODA), which is particularly problematic in the tropics (Carton et al., 2000). Figure 4.4 compares the SODA data for the 0.5° x 0.5° grid including Tahiti with the historical salinity record of Gouriou and Delcroix (2002). We note that the correlation between the two time series is relatively low (R = 0.39). For this study, however, we decided to use the SODA data because it extends back until 1950 and is long enough for a comparison with our coral proxy data on an annual mean scale.

4. The reconstruction of $\delta^{18}O$ seawater

4.1 Methodologies

The most commonly used technique to calculate $\delta^{18}O_{sw}$ is to estimate the linear regression equation of coral $\delta^{18}O$ - SST, as well as coral Sr/Ca - SST. The general linear regression equation is:

$$Y(t) = MX(t) + B + e(t) \quad (1)$$

where the vector $Y(t) = (y_1(t), y_2(t), ...y_m(t))^T$, M is the m x n matrix, and $X = (x_1(t), x_2(t), ...x_n(t))^T$. t denotes the time dependence of dependent (Y) and independent (X) variables. B is the vector containing constants, and $e\ (t)$ is the vector containing the errors of the dependent variables.

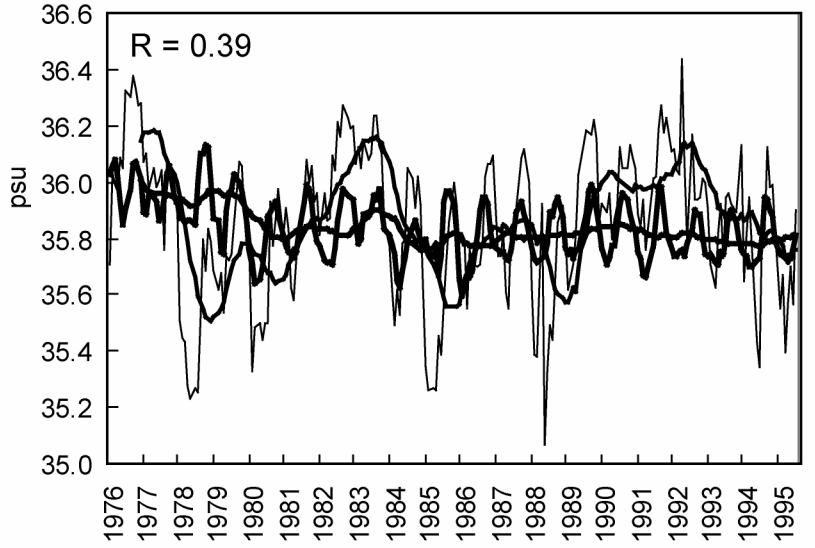

Figure 4.4. Monthly SSS data from the SODA v.1.2 model (thick black lines) (σ= 0.11) (Carton et al. 2000) and Delcroix et al. (1996) (black lines) (σ=0.26) with 12 points running average.

In this version, it is assumed that the independent variables are free of error. We are aware, however, that the SST datasets, which are used as independent variables are not free of error. We omit the explicit expression of time dependence hereafter. This is the general form of a multiple linear regression (MLR) problem, and the estimation of the regression parameters is standard (e.g., Draper and Smith, 1981). We will discuss how the problem of reconstructing $\delta^{18}O_{sw}$ fits into this model (equation 1). The abstract variables are related with the physical variables by:

$$x_1 \equiv SST \tag{2}$$

$$x_2 \equiv \delta^{18}O_{sw} \sim (P-E) \sim SSS \tag{3}$$

$$n = 2 \tag{4}$$

$$y_1 \equiv \delta^{18}O_{coral} \tag{5}$$

$$y_2 \equiv Sr/Ca \tag{6}$$

$$m = 2 \tag{7}$$

The ~ sign means that the variables are assumed to be linearly related. The MLR equation consists of two equations. The specific form of the matrix (equation 1) accounts for the fact that $\delta^{18}O_{sw}$ (SSS) and SST influence $\delta^{18}O_{coral}$ but that $\delta^{18}O_{sw}$ (SSS) does not influence Sr/Ca ($\beta_2 = 0$):

$$\delta^{18}O_{coral} = \gamma_o + \gamma_1 SST + \gamma_2 SSS + e_{\delta^{18}O_{coral}} \quad (8)$$

$$Sr/Ca = \beta_o + \beta_1 SST + \beta_2 SSS + e_{Sr/Ca} \quad (9)$$

The matrix *M* in the general MLR (equation 1) that is associated with equation 8, 9 is invertable and thus it is possible to reconstruct SST, SSS from the two proxies provided that the constants of regressions are known.

4.1.1. The method of Gagan et al. (1994, 1998)

Gagan et al. (1994, 1998) estimated the linear regression equations of coral $\delta^{18}O$ and Sr/Ca vs. SST. These equations are used to convert both proxies to temperature units. $\delta^{18}O_{sw}$ is then calculated by subtracting Sr/Ca-SST from $\delta^{18}O_{coral}$ -SST. This method uses equation 8 of the MLR model with $\gamma_2 = 0$:

$$\delta^{18}O_{coral} = \gamma_o + \gamma_1 SST_{\delta c} + e \quad (10)$$

where $\delta^{18}O_{coral}$ is measured coral $\delta^{18}O$, $SST_{\delta c}$ is sea surface temperature calculated based on the regression equation of coral $\delta^{18}O$ vs. measured SST, γ_o is the intercept, γ_1 is the slope of the regression equation, and *e* is the error. Using equation 10 coral $\delta^{18}O$ can be converted to unit temperature.

The regression equation of Sr/Ca vs. SST considering SST as independent variable is:

$$Sr/Ca = \beta_o + \beta_1 SST_{Sr/Ca} + e \quad (11)$$

where *Sr/Ca* is measured coral Sr/Ca, $SST_{Sr/Ca}$ is sea surface temperature calculated based on the regression equation of coral Sr/Ca vs. measured SST, β_o is the intercept and β_1 is the slope value of regression equation of Sr/Ca vs. SST, and *e* is the error. Equation 11 is used to convert Sr/Ca to unit temperature.

$\delta^{18}O_{sw}$ is calculated by subtracting $SST_{Sr/Ca}$ from $SST_{\delta c}$:

$$\delta^{18}O_{sw} = [1/\gamma_1 (\delta^{18}O_{coral} - \gamma_o)] - [1/\beta_1 (Sr/Ca - \beta_o)] \quad (12)$$

4.1.2 The method of Ren et al. (2002)

Ren et al. (2002) saw the major problem in separating the SST and SSS signal is in the estimate of the intercept. Therefore, Ren et al. (2002) proposed to look at what they called the instantaneous changes of the proxies to omit the intercept values from the calculation of $\delta^{18}O_{sw}$:

$$\Delta x = x(t_{i+1}) - x(t_i) \quad (13)$$

Where t_i, t_{i+1} is the time index for two consecutive data points in a time series and x is one of the variables (SST, SSS, $\delta^{18}O_{coral}$, Sr/Ca). Ren et al. (2002) define the instantaneous changes of coral $\delta^{18}O$ ($\Delta\delta^{18}O_{coral}$) at a given time as a sum of two components: one represents the contribution caused by instantaneous changes in SST ($\Delta\delta^{18}O_{sst}$) whereas the other is the contribution caused by the instantaneous changes in seawater $\delta^{18}O$ ($\Delta\delta^{18}O_{sw}$) (equation 14).

$$\Delta\,\delta^{18}O_{coral} = \Delta\delta^{18}O_{sst} + \Delta\delta^{18}O_{sw} = (\partial\delta^{18}O_{coral}/\partial\mathrm{SST})\,\Delta SST + (\partial\delta^{18}O_{coral}/\partial\delta^{18}O_{sw})\Delta\delta_{sw} \quad (14)$$

$\partial\delta^{18}O_{coral}/\partial$SST and $\partial\delta^{18}O_{coral}/\partial\delta^{18}O_{sw}$ are the partial derivatives of coral $\delta^{18}O$ with respect to SST and $\delta^{18}O_{sw}$, respectively. They represent the rate of change in coral $\delta^{18}O$ with respect to the change of one variable, while the other variable is constant. The partial derivative of $\delta^{18}O_{coral}$ and Sr/Ca with respect to SST are the slopes of the proxy-SST regression equations, i.e. γ_1 and β_1, respectively (see equation 8, 9). $\partial\delta^{18}O_{coral}/\partial$SST can be estimated from the linear regression of coral $\delta^{18}O$ versus measured SST, provided that seawater $\delta^{18}O$ does not change over this calibration interval. Similarly, ∂Sr/Ca/∂SST, the partial derivative of Sr/Ca with respect to SST, can be estimated.

The instantaneous changes of Sr/Ca (Δ *Sr/Ca*) are calculated as follows:

$$\Delta\,Sr/Ca = (\partial\mathrm{Sr/Ca}/\partial\mathrm{SST})\,\Delta SST = \beta_1\,\Delta SST \quad (15)$$

$\Delta\delta^{18}O_{sst}$ in equation 14 can be expressed as:

$$\Delta\delta^{18}O_{sst} = \gamma_1\Delta SST \quad (16)$$

and the instantaneous changes of $\delta^{18}O_{sw}$ can be calculated as:

$$\Delta\delta^{18}O_{sw} = \Delta\,\delta^{18}O_{coral} - \gamma_1 / \beta_1\,(\Delta\,Sr/Ca) \quad (17)$$

Absolute values of reconstructed $\delta^{18}O_{sw}$ are obtained by adding up all the instantaneous contributions to an arbitrary reference:

If $reconstructed\ \delta^{18}O_{sw\,(o)} = reference\ value + \Delta\delta^{18}O_{sw}$

then

$$reconstructed\ \delta^{18}O_{sw\,(i)} = reconstructed\ \delta^{18}O_{sw\,(i-1)} + \Delta\delta^{18}O_{sw\,(i+1)} \quad (18)$$

i = 1,2,3,....i

4.1.3 The Centering method

In order to omit the intercept value (constant of regression), we can center the linear regression equation by removing the mean value of its variables (Draper and Smith, 1981). For the linear regression equation

$$Y = \beta_o + \beta_1(X) + e, \tag{19}$$

The omission of β_o means that the regression line passes through $X = 0$ and $Y = 0$, that is the line has zero intercept $\beta_o = 0$ at $X = 0$. Note, however, that the physical removal of β_o from the model by centering the data is quite different from setting $\beta_o = 0$ (Draper & Smith, 1981). For the straight-line model of equation 19, the centered mathematical model can be written as

$$Y_i - \overline{Y} = \beta_1(X_i - \overline{X}) + e \qquad \text{i} = 1,2,\ldots\text{n} \tag{20}$$

where $\overline{Y}$ is the mean value of Y and $\overline{X}$ is the mean value of X. β_1 is the slope of the straight-line model. For $\delta^{18}O_{sw}$ reconstructions, centering the data is the easiest way to remove the intercept from the calculation. If measured coral $\delta^{18}O$ is $\delta^{18}O_{coral}$, the SST contribution to $\delta^{18}O_{coral}$ is $\delta^{18}O_{sst}$ and the seawater $\delta^{18}O$ contribution to $\delta^{18}O_{coral}$ is $\delta^{18}O_{sw}$, we can define the relative variations of $\delta^{18}O_{coral}$ relative to its mean value (hereafter referred to as $\Delta\ \delta^{18}O_{c\text{-}centre}$) as the sum of $\delta^{18}O_{sst}$ relative to the mean value of $\delta^{18}O_{sst}$ (hereafter referred to as $\Delta\delta^{18}O_{sst\text{-}centre}$) and $\delta^{18}O_{sw}$ relative to the mean value of $\delta^{18}O_{sw}$ (hereafter referred to as $\Delta\delta^{18}O_{sw\text{-}centre}$). We write equation 14 as:

$$\Delta\ \delta^{18}O_{c\text{-}centre} = \Delta\delta^{18}O_{sst\text{-}centre} + \Delta\delta^{18}O_{sw\text{-}centre} \tag{21}$$

By centering the data equation 21 can be defined as:

$$\delta^{18}O_{coral_i} - \overline{\delta^{18}O_{coral}} = \delta^{18}O_{sst_i} - \overline{\delta^{18}O_{sst}} + \delta^{18}O_{sw_i} - \overline{\delta^{18}O_{sw}} \tag{22}$$

i = 1,2,…n

where $\delta^{18}O_{coral}$ is measured coral $\delta^{18}O$, and $\overline{\delta^{18}O_{coral}}$ is the mean value of measured coral $\delta^{18}O$. $\delta^{18}O_{sw}$ are the variations of coral $\delta^{18}O$ with respect to seawater $\delta^{18}O$, $\overline{\delta^{18}O_{sw}}$ is the mean value of $\delta^{18}O_{sw}$, $\delta^{18}O_{sst}$ are the variations of coral $\delta^{18}O$ with respect to SST, and $\overline{\delta^{18}O_{sst}}$ is the mean value of $\delta^{18}O_{sst}$.

Assuming that Sr/Ca is only influenced by temperature, the variations of coral Sr/Ca relative to its mean value can be written as:

$$Sr/Ca_i - \overline{Sr/Ca} = \beta_1(SST_i - \overline{SST}) \quad (23)$$

Where *Sr/Ca* is measured Sr/Ca and $\overline{Sr/Ca}$ is the mean value of measured Sr/Ca. β_1 is the slope of the regression equation of coral Sr/Ca vs. SST. $\delta^{18}O_{sst\text{-}centre}$ can be written as:

$$\delta^{18}O_{sst_i} - \overline{\delta^{18}O_{sst}} = \gamma_1(SST_i - \overline{SST}) \quad (24)$$

Inserting equation 23 into equation 24, $\Delta\delta^{18}O_{sst\text{-}centre}$ can be expressed as:

$$\Delta\delta^{18}O_{sst\text{-}centre} = \delta^{18}O_{sst_i} - \overline{\delta^{18}O_{sst}} = \gamma_1\left(\frac{Sr/Ca_i - \overline{Sr/Ca}}{\beta_1}\right) \quad (25)$$

Where γ_1 is the slope of the regression equation of coral $\delta^{18}O$ vs. SST.

Thus, $\Delta\delta^{18}O_{sw\text{-}centre}$ (equation 22) can be written as:

$$\Delta\delta^{18}O_{sw\text{-}centre} = (\delta^{18}O_{coral_i} - \overline{\delta^{18}O_{coral}}) - \gamma_1/\beta_1(Sr/Ca_i - \overline{Sr/Ca}) \quad (26)$$

Where $\Delta\delta^{18}O_{sw\text{-}centre}$ is $\delta^{18}O_{sw}$ relative to the mean value of $\delta^{18}O_{sw}$, Sr/Ca is measured coral Sr/Ca, $\overline{Sr/Ca}$ is the mean value of measured Sr/Ca, γ_1 is the regression slope of coral $\delta^{18}O$ vs. SST and β_1 is the regression slope of coral Sr/Ca vs. SST. $\delta^{18}O_{coral}$ is measured coral $\delta^{18}O$, and $\overline{\delta^{18}O_{coral}}$ is the mean value of measured coral $\delta^{18}O$.

4.1.4 Multiple linear regression

Assuming that coral $\delta^{18}O$ is influenced by SST and $\delta^{18}O_{sw}$, that $\delta^{18}O_{sw}$ is linearly related to SSS and that Sr/Ca is influenced by SST only, we can reconstruct $\delta^{18}O_{sw}$ and SSS using a multiple linear regression (equation 1).

The relationship of coral $\delta^{18}O$ versus SST and SSS can be expressed with equation 8 ($\gamma_2 \neq 0$):

$$\delta^{18}O_{coral} = \gamma_o + \gamma_1 SST + \gamma_2 SSS + e \quad (27)$$

The relationship of Sr/Ca versus SST can be expressed with equation 9 ($\beta_2 = 0$):

$$Sr/Ca = \beta_o + \beta_1 SST + e \quad (28)$$

Combining equation 27 in 28 we obtain:

$$\delta^{18}O_{coral} = \gamma_o + \gamma_1\left(\frac{Sr/Ca - \beta_o}{\beta_1}\right) + \gamma_2 SSS \quad (29)$$

Thus, absolute values of SSS can be calculated with the following equation:

$$SSS = \frac{\delta^{18}O_{coral} - \gamma_o - \frac{\gamma_1}{\beta_1}(Sr/Ca - \beta_o)}{\gamma_2} \tag{30}$$

4.1.5 Centering of multiple linear regression equations

Equation 30 contains two constants: one of the multiple linear regression equation of coral $\delta^{18}O$ - SST, SSS and one of the linear regression equation of Sr/Ca - SST. We can center the MLR to calculate SSS so that all data are regarded as anomalies with respect to their mean and the constants in the MLR can be ommited. The centered MLR of coral $\delta^{18}O$ - SST, SSS can be defined as:

$$\delta^{18}O_{coral} - \overline{\delta^{18}O_{coral}} = \gamma_1(SST - \overline{SST}) + \gamma_2(SSS - \overline{SSS}) \tag{31}$$

The centered regression equation of the Sr/Ca-SST relationship is given in equation 23. Inserting equation 23 into equation 31, we obtain:

$$\delta^{18}O_{coral} - \overline{\delta^{18}O_{coral}} = \gamma_1\left(\frac{Sr/Ca - \overline{Sr/Ca}}{\beta_1}\right) + \gamma_2(SSS_i - \overline{SSS}) \tag{32}$$

Thus, we can calculate relative variations of SSS:

$$SSS_i - \overline{SSS} = \frac{1}{\gamma_2}\left[(\delta^{18}O_{coral_i} - \overline{\delta^{18}O_{coral}}) - \frac{\gamma_1}{\beta_1}(Sr/Ca_i - \overline{Sr/Ca})\right] \tag{33}$$

4.2 Error Propagation

The error is termed one standard error (σ), which implies that 67 % of the data lie within $\pm 1\sigma$ of the mean. The individual errors of the measured physical parameters propagate through any calculation. If $Y = f(x_1, x_2, ... x_i)$ and each of X_i has its own associated standard error σ_{xi}, the squared error propagation of Y is given by (see e.g., Bevington, 1969; Press et al., 1990):

$$\sigma^2 Y = \sum_{i=1}^{n}\left(\frac{\partial f}{\partial Xi}\right)^2 \sigma^2 X_i \tag{34}$$

When calculating $\delta^{18}O_{sw}$ from measured coral $\delta^{18}O$ and Sr/Ca, the covariance between the two variables can be neglected, because the measurement accuracy of coral $\delta^{18}O$ and Sr/Ca is un-related to each other. Based on equation 34, we can calculate the error of

reconstructed $\delta^{18}O_{sw}$ for (1) the method of Ren et al. (2002) and the centering method, (2) the multiple linear regression:

4.2.1 Error calculation for the method of Ren et al. (2002) and centering

The $\delta^{18}O_{sw}$ contribution to coral $\delta^{18}O$ for the method of Ren et al. (2002) is given in equation 17. The $\delta^{18}O_{sw}$ contribution to coral $\delta^{18}O$ for the centering method is given in equation 25. We can write both equations as:

$$Y = x_1 - \frac{\gamma_1}{\beta_1} x_2$$

the error propagation can be calculated using equation 34:

$$\sigma_y^2 = \sigma_{x1}^2 (\frac{\partial y}{\partial x_1})^2 + \sigma_{x2}^2 (\frac{\partial y}{\partial x_2})^2$$

$$\sigma_y^2 = \sigma_{x1}^2 + (\frac{\gamma_1}{\beta_1})^2 \sigma_{x2}^2$$

Thus, the equation for the error propagation of Ren et al. (2002) and centering is:

$$\sigma_{\delta sw}^2 = \sigma_{\delta c}^2 + (\frac{\gamma_1}{\beta_1})^2 \sigma_{sr/ca}^2 \qquad (35)$$

Where $\sigma_{\delta sw}$ is the error of reconstructed $\delta^{18}O_{sw}$, $\sigma_{\delta c}$ is the error of measured $\delta^{18}O_{coral}$, $\sigma_{Sr/Ca}$ is the error of measured Sr/Ca, γ_1 and β_1 are the slopes of the linear regression of $\delta^{18}O$ vs. SST and Sr/Ca vs. SST, respectively. Note that the error contributions from the means are negligible when averaged over a large sample size.

4.2.2 Error calculation for the multiple linear regression

The multiple linear regression equation for reconstructing sea surface salinity (SSS) is given in equation 30. We can write this equation as:

$$Y = \frac{1}{\gamma_2}\left[x_1 - \gamma_o - \frac{\gamma_1}{\beta_1}(x_2 - \beta_o) \right]$$

$$<=> Y = \frac{\gamma_1}{\beta_1 \gamma_2}\beta_o - \frac{\gamma_o}{\gamma_2} + \frac{x_1}{\gamma_2} - \frac{\gamma_1}{\beta_1 \gamma_2} x_2$$

if $\frac{\gamma_1}{\beta_1 \gamma_2}\beta_0 - \frac{\gamma_o}{\gamma_2}$ is a constant c, $Y = c + \frac{x_1}{\gamma_2} - \frac{\gamma_1}{\beta_1 \gamma_2} x_2$ and the equation for the error propagation of *Y* becomes:

$$\sigma_y^2 = \sigma_{x1}^2(\frac{\partial y}{\partial x_1})^2 + \sigma_{x2}^2(\frac{\partial y}{\partial x_2})^2 + \sigma_c^2(\frac{\partial y}{\partial c})$$

$$<=> \sigma_y^2 = \frac{\sigma_{x1}^2}{\gamma_2^2} + \frac{\sigma_{x2}^2\gamma_1^2}{\beta_1^2\gamma_2^2} + \sigma_c^2$$

Thus, the error for absolute SSS estimates can be calculated:

$$\sigma_{sss}^2 = \frac{\sigma_{\delta c}^2}{\gamma_2^2} + \frac{\sigma_{sr/ca}^2\gamma_1^2}{\beta_1^2\gamma_2^2} + \sigma_c^2 \quad (36)$$

4.2.3 Error calculation for the centered multiple linear regression

The equation for the centered multiple linear regression for reconstructing SSS is given in equation 33. We can write this equation as:

$$y = \frac{1}{\gamma_2}(x_1 - \frac{\gamma_1}{\beta_1}x_2)$$

the error propagation of *Y* is

$$\sigma_y^2 = \frac{\sigma_{x1}^2}{\gamma_2^2} + \frac{\sigma_{x2}^2\gamma_1^2}{\gamma_2^2\beta_1^2}$$

Thus, the error for relative salinity variations calculated with the centered multiple linear regression is:

$$\sigma_{sss}^2 = \frac{\sigma_{\delta c}^2}{\gamma_2^2} + \frac{\sigma_{sr/ca}^2\gamma_1^2}{\gamma_2^2\beta_1^2} \quad (37)$$

where σ_{sss} is the error of relative SSS variations. $\sigma_{\delta c}$ is the error of measured coral $\delta^{18}O$, $\sigma_{Sr/Ca}$ is the error of measured Sr/Ca, γ_1 and γ_2 are the slopes of the multiple regression for $\delta^{18}O$ vs. SST, SSS respectively and β_1 is the slope value of the Sr/Ca vs. SST regression.

5. Discussion

5.1. Examples: Tahiti records

In this section, we reconstruct $\delta^{18}O_{sw}$ from paired $\delta^{18}O$ and Sr/Ca measurements of the Tahiti corals to illustrate and compare the methodologies described in this paper. We will not only discuss the statistical procedures, but also the main ideas underlying the various approaches. Statistical error estimates are calculated to constrain our ability to resolve $\delta^{18}O_{sw}$ (SSS) variations.

5.1.1. Calibration: seasonal coral Sr/Ca ($\delta^{18}O$) variations vs. SST

The skeletal Sr/Ca ($\delta^{18}O$) was regressed against SST using points defining seasonal maxima and minima in the records. For the sake of keeping the manuscript short, we will only use the averaged proxy records of TH1 and TH2 (hereafter referred to as Sr/Ca_{TH12} and $\delta^{18}O_{TH12}$). This should reduce the noisiness of the proxy records as, for example, site-specific effects may bias single-core reconstructions. The regression equation (with 95% confidential levels) for monthly Sr/Ca_{TH12} vs. SST (SODA) is:

$$Sr/Ca = -0.063\pm0.004\ SST + 10.53\pm0.12 \quad (R = 0.86, p< 0.001) \tag{38}$$

The linear regression of monthly $\delta^{18}O_{TH12}$ vs. SST (SODA) is:

$$\delta^{18}O_{coral} = -0.19\pm0.016\ SST + 0.815\pm0.437 \quad (R = 0.78, p< 0.001) \tag{39}$$

Both the slope of the Sr/Ca- and the $\delta^{18}O$-SST relationships are consistent with published estimates.

5.1.2. Reconstructing seawater $\delta^{18}O$ using the method of Ren et al. (2002) and centering

In this illustration we will show that $\delta^{18}O_{sw}$ changes calculated using the Ren et al. (2002) method and the centering method are identical. We use paired Sr/Ca_{TH12} and $\delta^{18}O_{TH12}$ to calculate seawater $\delta^{18}O$. For Sr/Ca, we use the slope of the monthly regression of Sr/Ca_{TH12} vs. SODA SST (β_1=-0.063 mmol/mol/°C). The published regression slope of $\delta^{18}O$-SST in biological carbonates ranges from -0.17 ‰/°C to -0.23 ‰/°C (O 'Neil et al., 1969; Bemis et al., 1998; von Langen et al., 2000; Spero et al., 2003). Corals show more or less the same range of $\delta^{18}O$-SST relationships i.e., -0.18 ‰/°C -0.22 ‰/°C (Weber and Woodhead, 1972; Gagan et al., 1994; Wellington et al., 1996, Juillet-Leclerc and Schmidt, 2001). We use the published regression slope γ_1=-0.18 ‰/°C (Gagan et al., 1994; Spero et al., 2003) for the coral $\delta^{18}O$-SST relationship.

Using the method of Ren et al. (2002), we calculate the instantaneous changes of $\delta^{18}O_{sw}$ ($\Delta\delta^{18}O_{sw}$) with equation 17 and reconstructed $\delta^{18}O_{sw}$ with equation 18. In this example we set the arbitrary reference value to 0. The reference value only determines the absolute values of $\delta^{18}O_{sw}$, not the relative variations. The results are shown in Figure 4.5. Using the centering method, we calculate $\delta^{18}O_{sw}$ with equation 26 (Figure 4.6). We compare the results of the Ren et al. (2002) and centering method (see table 1): we subtract the mean value from reconstructed $\delta^{18}O_{sw}$ of Ren et al. (2002) (Figure 4.5e). The result (Δ

reconstructed $\delta^{18}O_{sw}$) will be identical to reconstructed $\delta^{18}O_{sw}$ from centering ($\Delta\delta^{18}O_{sw\text{-}centre}$) (compare Figure 4.5e and Figure 4.6c, see also Table 4.1). Using the centering method is much simpler than Ren et al. (2002).

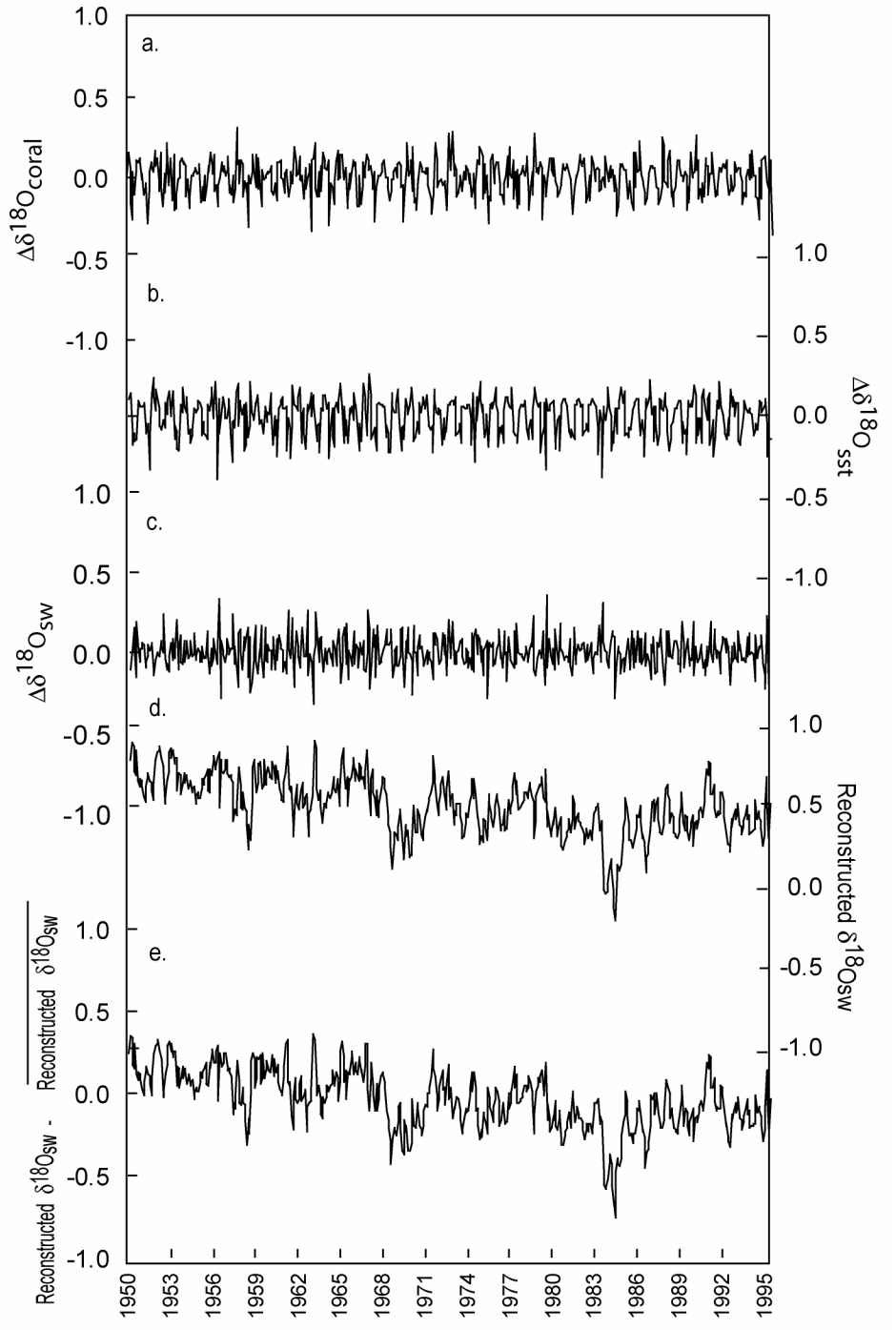

Figure 4.5. $\delta^{18}O_{sw}$ reconstruction using the method of Ren et al. (2002) derived from Sr/Ca_{TH12} and $\delta^{18}O_{TH12}$. Instantaneous changes of (a) $\delta^{18}O_{coral}$ ($\Delta\delta^{18}O_{coral}$), (b) SST contribution ($\Delta\delta^{18}O_{sst}$), (c) $\delta^{18}O_{sw}$ contribution ($\Delta\delta^{18}O_{sw}$). (d) Reconstructed $\delta^{18}O_{sw}$, and (e) variation of reconstructed d18Osw minus its mean value.

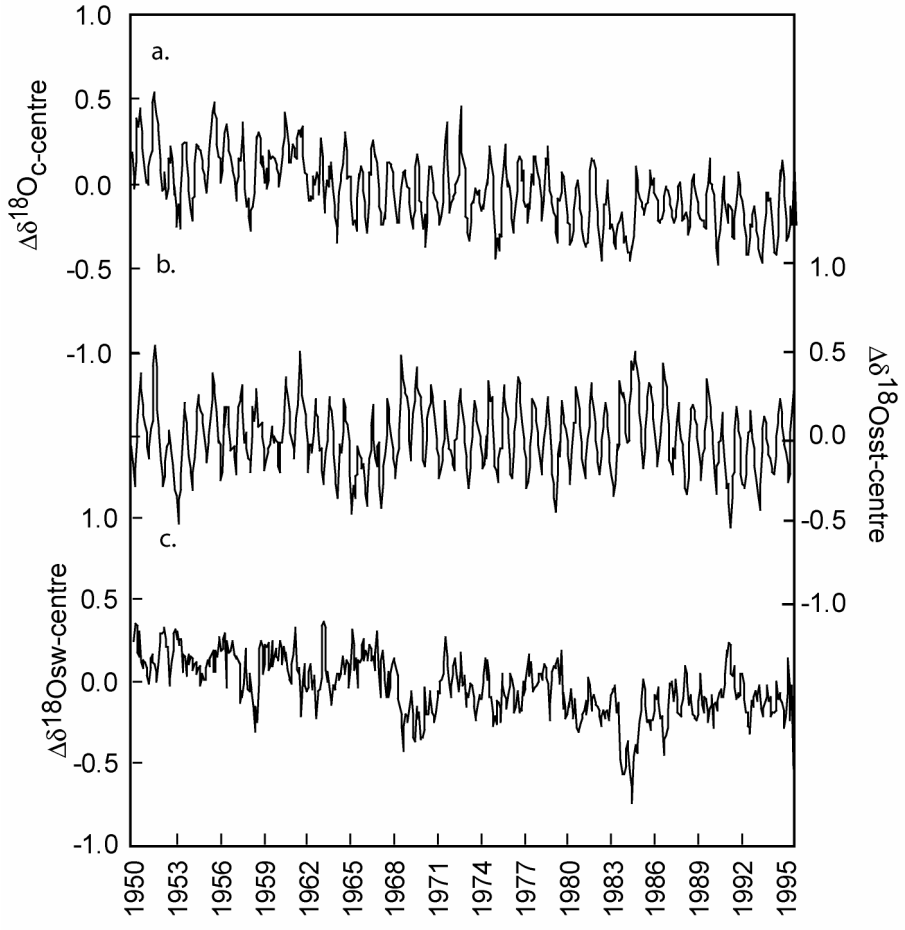

Figure 4.6. $\delta^{18}O_{sw}$ reconstruction from $\delta^{18}O_{TH12}$ and Sr/Ca_{TH12} calculated with the centering method (see text for discussion).

Ren	Centering	correlation Ren and Centering
see eq. 14 to calculate $\Delta\,\delta^{18}O_{coral}$	see eq. 21 to calculate $\Delta\,\delta^{18}O_{c\text{-}centre}$	$\Delta\,\delta^{18}O_{coral} = \Delta\,\delta^{18}O_{c\text{-}centre} - \overline{\delta^{18}O_{c-centre}}$
see eq. 16 to calculate $\Delta\delta^{18}O_{sst}$	see eq. 25 to calculate $\Delta\delta^{18}O_{sst\text{-}centre}$	$\Delta\delta^{18}O_{sst} = \Delta\,\delta^{18}O_{sst\text{-}centre} - \overline{\delta^{18}O_{sst-centre}}$
see eq. 12 to calculate rec. $\delta^{18}O_{sw}$	see eq. 26 to calculate $\Delta\delta^{18}O_{sw\text{-}centre}$	$rec.\delta^{18}O_{sw-\mathrm{Re}n} - \overline{rec.\delta^{18}O_{sw-\mathrm{Re}n}} = \Delta\delta^{18}O_{sw\text{-}centre}$

Table 1. Correlation of Ren et al. (2002) and centering methods.
Note: Δ Ren = $x_{i+1} - x_i$**, Δ Centering =** $x_i - \bar{x}$ **.**

5.1.3. Error Propagation: Ren et al. (2002) and centering methods

The error propagation of $\delta^{18}O_{sw}$ (σ) is calculated based on the regression equations used to calculate $\delta^{18}O_{sw}$ from paired Sr/Ca and $\delta^{18}O$ measurements. This is a statistical error estimate and does not necessarily reflect the true error of our $\delta^{18}O_{sw}$ reconstruction. The true error (e) would be the sum of noise (ε) (e.g., the sum of all non-climatic factors that may influence the proxies) and the error propagation (σ). It is impossible to estimate the noise component of the proxies (although averaging two or more independent proxy records should reduce the noise), and therefore it is also impossible to calculate the true error. However, the measurement error propagation should provide important constraints on the limitations of $\delta^{18}O_{sw}$ reconstructions: we can definitely not resolve $\delta^{18}O_{sw}$ variations that are smaller than the combined analytical uncertainties of coral $\delta^{18}O$ and Sr/Ca measurements. In this example, we calculate the error for the $\delta^{18}O_{sw}$ reconstruction obtained from Sr/Ca_{TH12} and $\delta^{18}O_{TH12}$.

For both the method of Ren et al. (2002) and centering, the error propagation for $\delta^{18}O_{sw}$ is calculated from the standard deviation of the $\delta^{18}O$ and Sr/Ca measurements and the slope values of the $\delta^{18}O$- and Sr/Ca-SST relationship (equation 35). The standard deviation of coral $\delta^{18}O$ is $\sigma_{\delta c}$ = ±0.06 ‰ (1σ), and the standard deviation of Sr/Ca is $\sigma_{Sr/Ca}$ = ±0.01mmol/mol (1σ). For the $\delta^{18}O$-SST relationship we used γ_1 = -0.18 ‰/ °C (Gagan et al., 1994; Spero et al., 2003). For Sr/Ca-SST we used the slope estimate of Sr/Ca_{TH12} – SODA SST (β_1 = -0.063 mmol/mol/°C). The statistical error for $\delta^{18}O_{swTH12}$ calculated with the method of Ren et al. (2002) and centering is (equation 35):

$\sigma^2_{\Delta\delta sw} = \sigma^2_{\delta c} + \sigma^2_{Sr/Ca}(\gamma_1/\beta_1)^2 = 0.06^2$ ‰$^2 + 0.01^2$(mmol/mol)^2(-0.18 ‰/-0.063 mmol/mol)^2 = ±0.0044 ‰^{2}

thus, $\sigma_{\Delta\delta sw}$ = ±0.066 ‰

Figure 4.7 shows the relative $\delta^{18}O_{sw}$ variations derived from Sr/Ca_{TH12} and $\delta^{18}O_{TH12}$ (centering method) with the error propagation. Since we omit the intercept values of the linear regression equations from the $\delta^{18}O_{sw}$ calculation using either the method of Ren et al. (2002) or centering, we also omit the intercept error. This results in a relatively small statistical error of the $\delta^{18}O_{sw}$ reconstruction. Note, however, that this error only applies to relative variations of $\delta^{18}O_{sw}$. Furthermore, the true error is larger because of the ommited effects of the error in slopes and the non climatic noise.

5.1.4. Example of multiple linear regression analysis

For multiple linear regression analysis, we calibrate Sr/Ca_{TH12} and $\delta^{18}O_{TH12}$ with SST and SSS from the SODA dataset (Carton et al., 2000) using points defining maxima and minima in the records. The multiple regression equation (95% confidential level) of coral $\delta^{18}O$ vs. SST and SSS from SODA is:

$$\delta^{18}O_{coral} = -0.16\pm0.02\ SST + 0.46\pm0.15\ SSS - 16.738 \quad (R= 0.78,\ p < 0.001) \qquad (40)$$

and for Sr/Ca vs. SST SODA see equation 38.

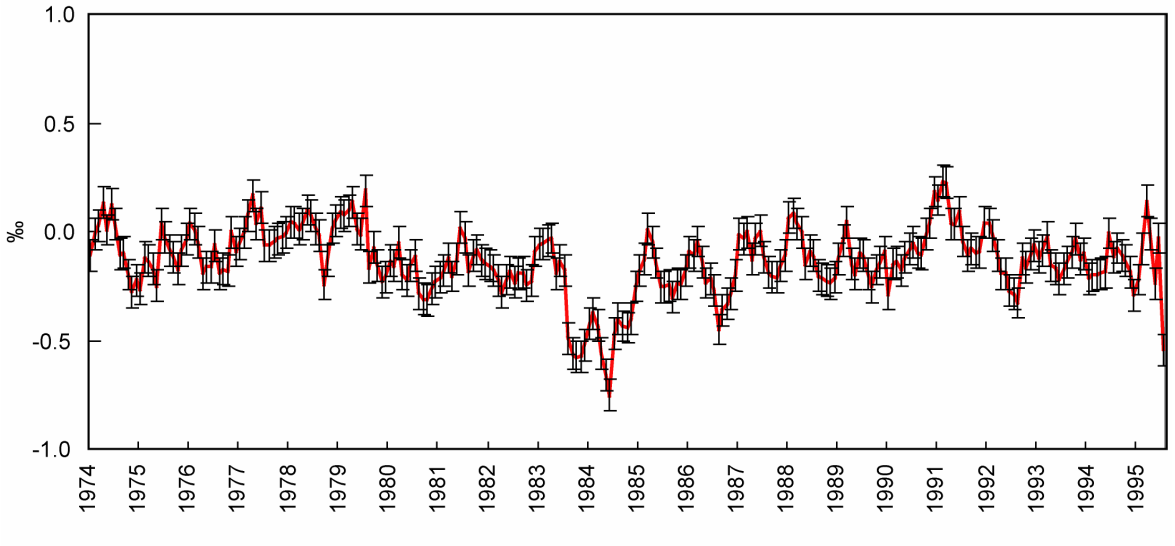

Figure 4.7. Monthly $\delta^{18}O_{sw}$ and error propagation (σ = 0.066 permil) derived from paired $\delta^{18}O_{TH12}$ and Sr/Ca_{TH12} using the centering method for the period 1974 to 1995.

Adding the errors, $\delta^{18}O$ - SST could be -0.18 ‰/°C (e.g., Weber and Woodhead, 1972; Gagan et al., 1994; Wellington et al., 1996), it is consistent with published slopes. We applied equation 30 into equation 40 to calculate absolute values of SSS (Figure 4.8a) and equation 33 (e.g., the centered MLR) to reconstruct relative variations in SSS (Figure 4.8b). Relative variations of SSS (Figure 4.8b) equal reconstructed SSS (Figure 4.8a) minus its mean value, provided that the same slope values are used. We re-calculate SSS by prescribing the known slope of coral $\delta^{18}O$ vs. SST (-0.18 ‰/°C), the estimated slope of $\delta^{18}O_{sw}$ vs. SSS for the southern Pacific (0.47 ‰/psu) (Delaygue et al., 2000), and the slope of the Sr/Ca-SST relationship estimated with the SODA dataset (-0.063 mmol/mol/°C). This can only be done in the centered MLR. The result is shown in Figure 4.8c. The $\delta^{18}O_{sw}$

reconstruction calculated with the centered, univariate linear regression (Figure 4.6c) will be identical to the curve in Figure 4.8c if the latter is divided by the factor used for the $\delta^{18}O_{sw}$ –SSS relationship (0.47 ‰/psu) in the centered MLR.

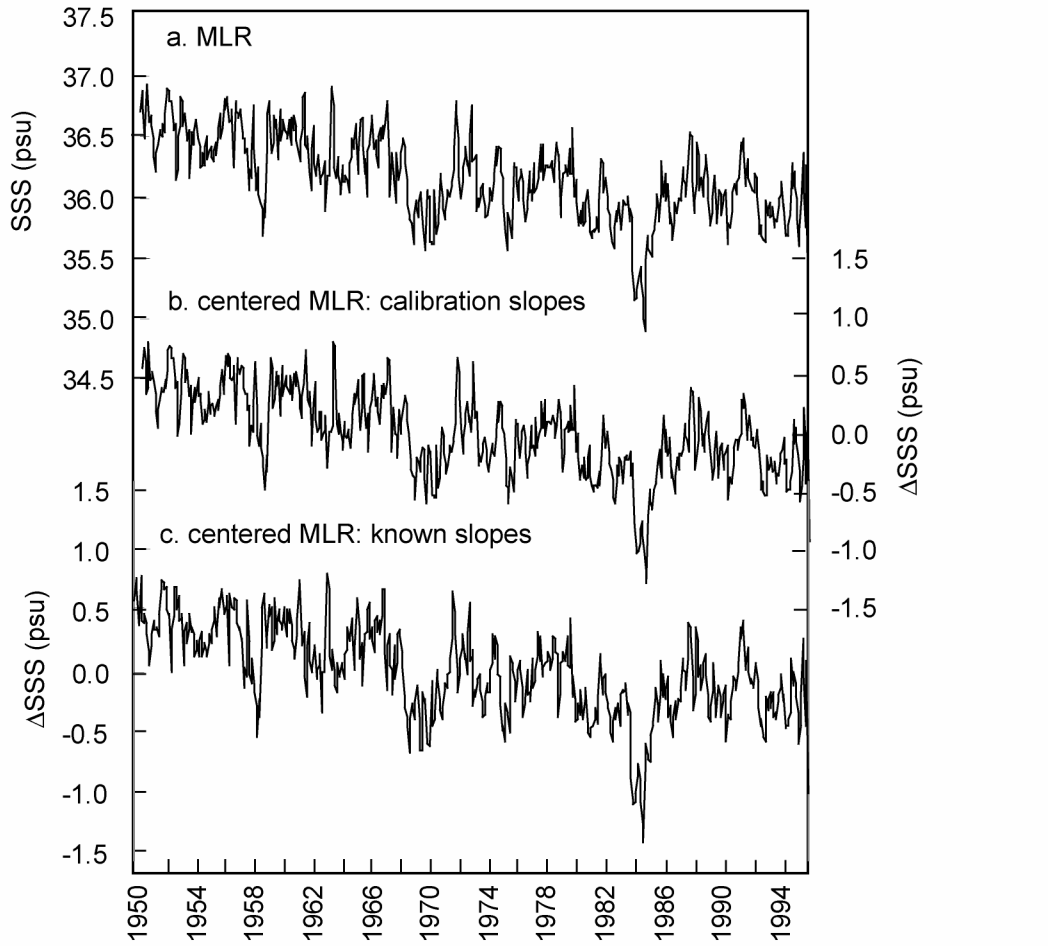

Figure 4.8. (a) Reconstructed SSS using the multiple linear regression (MLR) approach, (b,c) using centered multiple linear regression. (b) Regression slope are estimated by MLR (γ1 = -0.16 ‰/°C, γ2 = 0.46 ‰/psu, β1 = -0.063 mmol/mol/°C), (c) known slope are used (γ1= -0.18 ‰/°C and γ2 = 0.47 ‰/psu).

The error propagation for relative SSS variations (centered multiple linear regression) can be calculated with equation 37:

$$\sigma_{sss}^2 = \frac{\sigma_{\delta c}^2}{\gamma_2^2} + \frac{\sigma_{srca}^2 \gamma_1^2}{\beta_1^2 \gamma_2^2}$$

$= (0.06^2\ ‰^2)/(0.47^2\ ‰^2/psu^2) + [0.01^2\ mmol/mol^2*(-0.18)^2\ ‰^2/°C^2] / [(-0.063)^2\ mmol/mol^2/°C^2 *0.47^2\ ‰^2/psu^2] = 0.02\ psu^2$

$\sigma_{sss} = \pm 0.14$ psu

5.2. Reconstructed $\delta^{18}O_{sw}$ (SSS) vs. sea surface salinity (SSS)

The main objective of coral-based $\delta^{18}O_{sw}$ reconstructions is to reconstruct past variations of SSS on time scales ranging from seasonal to centennial (e.g., Ren et al., 2002; Hendy et al., 2002). However, the reliability of $\delta^{18}O_{sw}$ reconstructions inferred from paired coral Sr/Ca and $\delta^{18}O$ is often not clear due to the lack of continuous $\delta^{18}O_{sw}$ measurements. Also, the quality of instrumental salinity data is at present difficult to assess (see also Kilbourne et al., 2004). Here, we compare the $\delta^{18}O_{sw}$ reconstructions from the Tahiti corals with sea surface salinity data taken from the SODA dataset (Carton et al., 2000):

(1) We derive $\delta^{18}O_{sw}$ using the centering method (equation 26). We calculate $\delta^{18}O_{sw}$ from paired Sr/Ca and $\delta^{18}O$ records of Tahiti (Sr/Ca_{TH12} and $\delta^{18}O_{TH12}$) using a published value to describe the $\delta^{18}O$-SST relationship (Gagan et al., 1994; Spero et al., 2003). We then correlate this record with SSS from the SODA dataset. We find that the correlation between monthly $\delta^{18}O_{sw\text{-}TH12}$ and SSS from SODA is low (R = 0.33) (Figure 4.9a). The low correlation coefficient of the monthly time series reflects the simple fact that we can not resolve the seasonal cycle of SSS with our $\delta^{18}O_{sw}$ reconstruction (Figure 4.9a). This is not surprising: the combined analytical error of $\delta^{18}O$ and Sr/Ca ($\sigma_{\Delta\delta sw}$ = ±0.066 ‰) almost equals the mean seasonal cycles of $\delta^{18}O_{sw}$ expected based on climatological data of salinity (0.3 psu or 0.14 ‰) (Figure 4.9b). Note, however, that the slope obtained in our seasonal $\delta^{18}O_{TH12}$-SST calibration (-0.19 ‰/°C) could incorporate a small seasonal $\delta^{18}O_{sw}$ contribution to coral $\delta^{18}O$. To check if our unability to resolve the seasonal cycle could be due to the uncertainties of the Sr/Ca-SST relationship, we insert a range of slope values for β_1 (-0.05, -0.08 and -0.2 mmol/mol/°C) in equation 26, and re-calculate $\delta^{18}O_{sw}$ (Figure 4.9c). Using slope values ranging from -0.05 or -0.08 mmol/mol/°C, which bracket the wide range of published Sr/Ca-SST relationships (see Marshall and McCulloch, 2002), does not significantly change the shape of the seasonal $\delta^{18}O_{sw}$ curve. Only if a slope value of -0.2 mmol/mol/°C is used, which is much larger than any published Sr/Ca-SST estimate, the shape of the $\delta^{18}O_{sw}$ curve changes (Figure 4.9c).

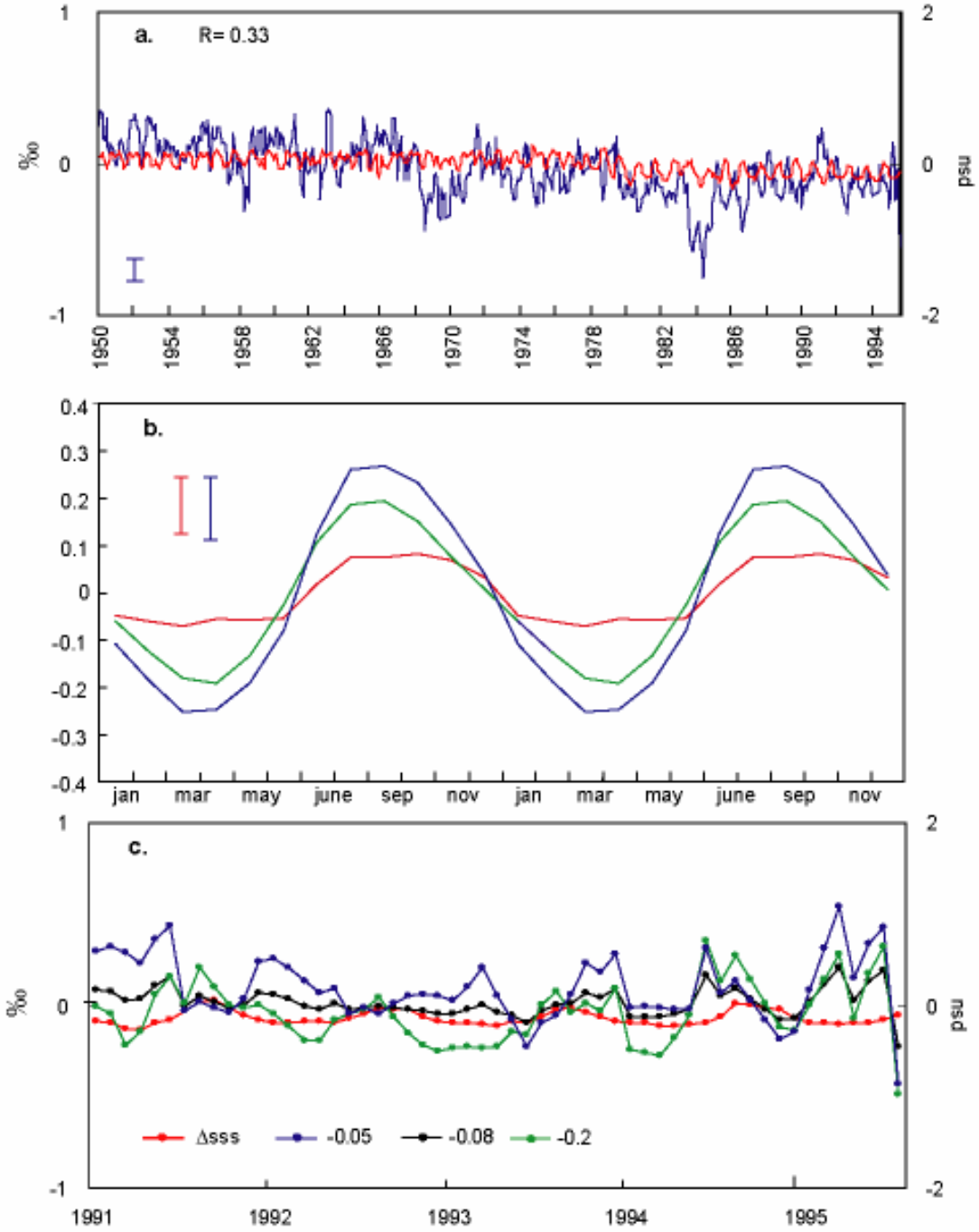

Figure 4.9. (a) Monthly timeseries of $\delta^{18}O_{sw}$ derived from paired coral Sr/Ca_{TH12} and $\delta^{18}O_{TH12}$ (blue) and monthly SSS from SODA (red) for the time period from 1950 to 1995. (b) Climatology of SSS contribution (red), SST contribution to coral $\delta^{18}O$ (green) and expected $\delta^{18}O_{coral}$ (blue). Data is centered to the mean value.The analytical error for coral $\delta^{18}O$ is 0.06 ‰ (blue bar) and the combined error for reconstructed d18Osw is 0.066 ‰ (green bar) (c) $\delta^{18}O_{sw}$ computed by inserting several slope values for Sr/Ca-SST: -0.05 mmol/mol/°C (blue), -0.08 mmol/mol/°C (black), -0.2 mmol/mol/°C (green), and centered-SSS from SODA (red).

In the Southwestern tropical Pacific, interannual variations of SSS are proportionally larger with respect to SST than on a seasonal scale (Gouriou and Delcroix, 2002). Also, annual mean $\delta^{18}O_{sw\text{-}TH12}$ is computed from a number of independent $\delta^{18}O_{sw}$ estimates, and thus the analytical uncertainty of annual mean $\delta^{18}O_{sw\text{-}TH12}$ reduces according to the formula: $\sigma_{Total}=(\sigma^2/N)^{1/2}$, where σ is the analytical error of the single measurements, and N is the number of independent measurements (e.g Bevington, 1969). Thus, the analytical uncertainty for annual mean $\delta^{18}O_{sw\text{-}TH12}$ reduces to ±0.019 ‰ or ±0.04 psu (if we assume that annual mean $\delta^{18}O_{sw\text{-}TH12}$ is calculated from 12 independent measurements; for 24 independent measurements the analytical uncertainty would be even lower). The standard deviation of annual mean SSS from SODA is ±0.07 psu for the 1976-1995 periods (±0.08 psu for the 1950-1995 periods), and for the historical record of Gouriou and Delcroix (2002) σ = ±0.19 psu. Therefore, annual mean SSS variations should measurably affect the skeletal chemistry of the Tahiti corals. The correlation between annual mean $\delta^{18}O_{sw\text{-}TH12}$ with SSS from SODA is high ($R = 0.61$, $p < 0.001$), and $\delta^{18}O_{sw\text{-}TH12}$ co-varies with SSS from SODA (Figure 4.10a). Both series show an abrupt shift towards lower salinity/$\delta^{18}O_{sw}$ in 1977/78 which indicates a freshening of surface waters.

(2) We reconstruct SSS using multiple linear regression of coral $\delta^{18}O$ vs. SST, SSS from the SODA dataset and linear regression of Sr/Ca vs. SST from SODA. The multiple linear regression will estimate the $\delta^{18}O$-SST, SSS slopes to obtain the best fit with SST, SSS. Again, we find that the correlation between the monthly time series of reconstructed SSS vs. instrumental SSS is lower ($R= 0.45$, $p< 0.001$, using a slope of -0.16 ‰/°C for the $\delta^{18}O$-SST relationship) than the correlation between the annual mean time series ($R=0.61$, $p<0.001$) (Figure 4.10b). However, on an annual mean scale the variance of the instrumental SSS is lower than the variance of SSS reconstructed from the coral proxies (Figure 4.10).

(3) We calculate SSS using the centered multiple linear regression model. We use the published slope of $\delta^{18}O$-SST relationship (-0.18 ‰/°C) (Gagan et al., 1994; Spero et al., 2003), and a slope value of 0.47 °/$_{oo}$/psu for $\delta^{18}O_{sw}$ vs. SSS (Delaygue et al., 2000). Because we used the same slope for $\delta^{18}O$-SST, the SSS reconstruction is equivalent to the $\delta^{18}O_{sw}$ reconstruction calculated with the centering method (Figure 4.10a) (the latter can be

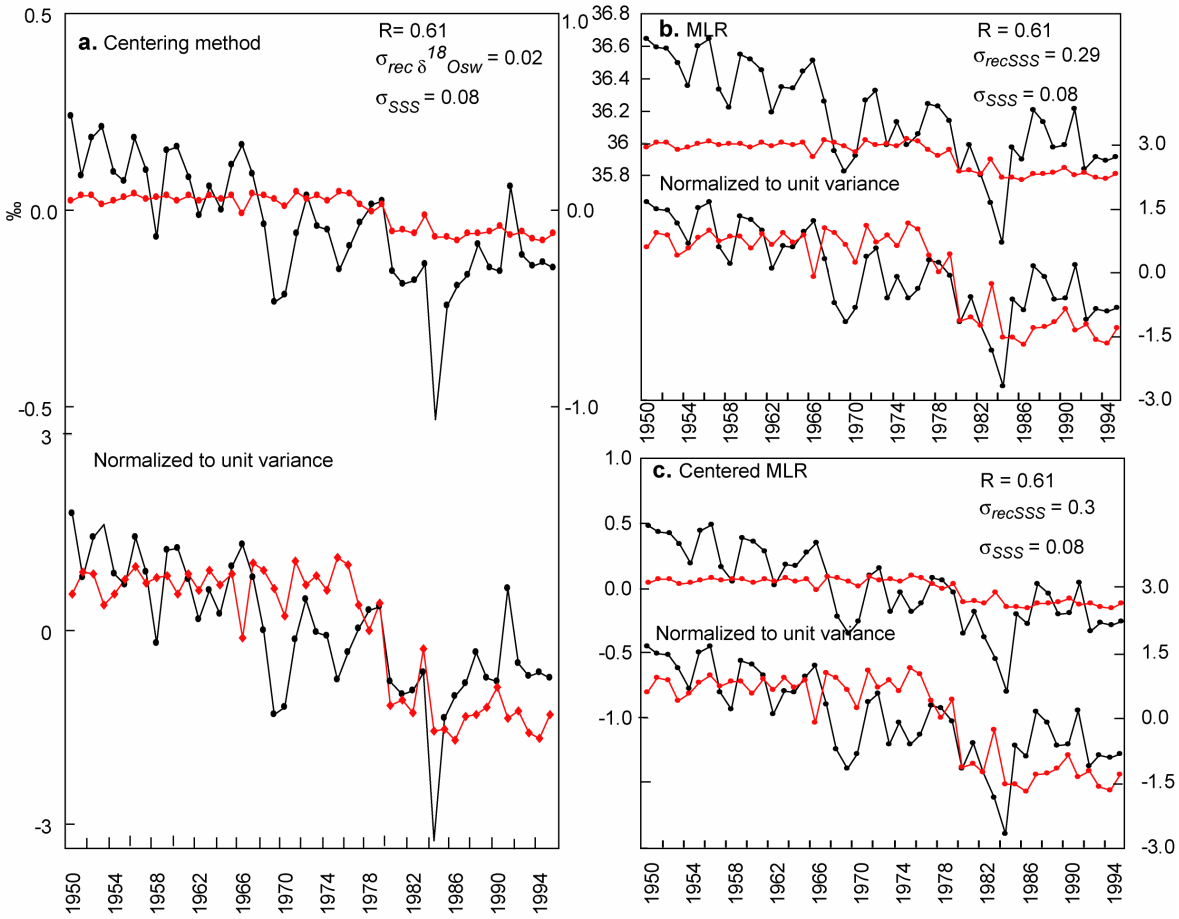

Figure 4.10. (a) Annual mean reconstructed $\delta^{18}O_{sw}$ (black) and SSS SODA (red) calculated with the centering method. (b) Annual mean reconstructed SSS (black) and SSS SODA (red) calculated with MLR, using the calibration slopes for the calculation. (c) Annual mean reconstructed SSS calculated with centered MLR, using the known slopes: -0.18 ‰/°C for $\delta^{18}O$ -SST and 0.47 ‰/psu for $\delta^{18}O_{sw}$ -SSS. (see text for discussion).

converted to SSS by dividing the series with 0.47‰/psu). Again, we find a clear relationship between annual mean SSS estimated from the corals and SSS from SODA. However, we note that the variance of annual mean SSS reconstructed from the corals is larger than the variance of SSS from the SODA model (Figure 4.10). For coral-based reconstructions, using the known and presumably correct slope for the SST contribution to coral $\delta^{18}O$, as well as for the $\delta^{18}O$-salinity relationship should yield the correct variations of local $\delta^{18}O_{sw}$ and salinity. However, the discrepancies may reflect differences in the spatial scales represented by SODA-SSS and the local, coral-based SSS reconstruction. Also, the variance of SODA is low compared to the Gouriou and Delcroix (2002) SSS series, which was averaged over a 2°x10° grid, indicating that the variance in the SODA reanalysis is too low.

In summary, we must admit that the reconstruction of seasonal-scale variations of SSS and $\delta^{18}O_{sw}$ from Tahiti corals is not possible because the combined analytical uncertainties of the $\delta^{18}O$ and Sr/Ca measurements are too large ($\sigma_{\Delta\delta sw}$ = ±0.066 ‰). The seasonal-scale variations of SSS (0.3 psu; Carton et al., 2000; Gouriou and Delcroix, 2002), and hence expected $\delta^{18}O_{sw}$ variations (0.14 ‰) almost equal the analytical error. On an annual mean scale, variations of SSS at Tahiti are proportionally larger than on a seasonal scale (Gouriou and Delrcoix, 2002), and annual mean $\delta^{18}O_{sw\text{-}TH12}$ is computed from 12 independent $\delta^{18}O_{sw}$ estimates, so that the analytical error of annual mean $\delta^{18}O_{sw\text{-}TH12}$ is lower. Annual mean variations of $\delta^{18}O_{sw\text{-}TH12}$ follow the SSS data from SODA. Both series show an abrupt shift towards lower salinity/$\delta^{18}O_{sw}$ in 1977/78 which indicates a freshening of surface waters. However, the variance of annual mean SSS from the SODA dataset is lower than the variance of reconstructed SSS from the corals, although, using the known (and presumably correct) slope for the coral $\delta^{18}O$-SST, as well as for the $\delta^{18}O_{sw}$ -salinity relationship should yield the correct variations of local $\delta^{18}O_{sw}$ and salinity. Clearly, if we want to reduce the uncertainties of quantitative $\delta^{18}O_{sw}$ and SSS reconstructions from corals, we need much better instrumental data that can only be obtained during long-term monitoring programs.

5.3. Methods of reconstructing $\delta^{18}O_{sw}$

As shown in previous studies (Huppert and Solow, 2004; Kilbourne et al., 2004), published methods of $\delta^{18}O_{sw}$ reconstructions (Gagan et al., 1994,1998; Ren et al., 2002) result in equivalent $\delta^{18}O_{sw}$ changes if the same slope parameters are used for the $\delta^{18}O$ (Sr/Ca)-SST relationship, and are offset from each other in a predictable way. The same applies to the centering method proposed in this study. Salinity reconstructions derived from the centered multiple linear regression can be converted to $\delta^{18}O_{sw}$-units with the factor used for the $\delta^{18}O_{sw}$-SSS relationship, and will equal $\delta^{18}O_{sw}$ derived with the centering method. However, the logic behind the various methods proposed is different, and only if we use a logically correct approach the method will be universally applicable.

To obtain absolute values of SST and $\delta^{18}O_{sw}$, coral $\delta^{18}O$ (Sr/Ca) must be calibrated with instrumental data, because coral aragonite is offset from equilibrium with respect to $\delta^{18}O$

(McConaughey, 1989) and also with respect to Sr/Ca (de Villiers et al., 1995; Marshall and Mc Culloch, 2002). In most studies, coral $\delta^{18}O$ is calibrated vs. SST only (e.g., McCulloch et al., 1994; Gagan et al., 1994, 1998, 2000), i.e., equation 8 is used with $\gamma_2 = 0$. This is a methodological error, because coral $\delta^{18}O$ is influenced concomitantly by SST and $\delta^{18}O_{sw}$ (SSS). If $\delta^{18}O_{sw}$ (SSS) variations are independent of SST, the effect of $\delta^{18}O_{sw}$ (SSS) can be understood as an additional error and a constant (time-independent) shift in the constant. However, in the tropical oceans SST and $\delta^{18}O_{sw}$ (SSS) often co-vary (e.g., Gouriou and Delcroix, 2002), and thus the partial regression coefficient γ_1 in the MLR will be different from the regression coefficient in the simple linear regression case of Gagan et al. (1994, 1998), which estimates γ_1 only from SST and coral $\delta^{18}O$. Thus, in the Gagan et al (1994, 1998) method, γ_1 includes SST-covariant $\delta^{18}O_{sw}$ (SSS) variations and this biased parameter is used to calculate the 'residual' $\delta^{18}O_{sw}$. It is not solely the intercept, but the bias in the regression coefficient γ_1 that causes problems in separating $\delta^{18}O_{sw}$ (SSS) and SST variability.

Ren et al. (2002) saw the major problem of separating the SST and $\delta^{18}O_{sw}$ (SSS) signal in the estimates of the intercept (constant of regressions), therefore they proposed to look at what they called 'instantaneous changes' (see equation 13). The application of the first differencing operation to the time series and their use in an MLR makes the constants of the MLR arbitrary and thus they can be set to equal zero. The same can be achieved by centering the data, i.e., the removal of the mean values from the variables of the linear regression (see section 4.1.3), which is more straightforward and a standard method in linear regression analysis (e.g., Draper and Smith, 1981). For both the method of Ren et al. (2002) and centering, the estimate of γ_1 from observations in a univariate linear regression ($\gamma_2 = 0$) would be biased in regions where SST and $\delta^{18}O_{sw}$ (SSS) co-vary (see also Huppert and Solow, 2004, for a discussion), i.e., theoretically the two methods have the same problem as the method of Gagan et al. (1994, 1998). In practice, however, it is generally accepted that the relative changes of coral $\delta^{18}O$ and Sr/Ca are not influenced by vital effects and follow the thermodynamic laws (e.g., Linsley et al., 1999; Ren et al., 2002). That means, we know γ_1 (estimates of the $\delta^{18}O$-SST relationship range from -0.18 to -0.22 ‰/°C) (e.g., Weber and Woodhead, 1972; Gagan et al., 1994; Wellington et al., 1996) and β_1 (estimates of the Sr/Ca-SST relationship range from -0.04 and -0.08 mmol/mol/°C). We

can insert these estimates in the equations of Ren et al. (2002) and centering, and we can calculate relative changes of $\delta^{18}O_{sw}$ from paired proxy measurements of any given coral. If we assume that Sr/Ca shows SST only, we can calibrate the Sr/Ca time series with SST to check the quality of the coral core: this slope value should always match published estimates.

The method of Gagan et al. (1994, 1998), in contrast, requires that coral $\delta^{18}O$ and Sr/Ca of any given coral is calibrated with local SST, because in addition to γ_1 and β_1 we need to estimate the intercepts, and will fail at sites where SST-covariant changes in $\delta^{18}O_{sw}$ (SSS) occur. Only if the calibration slope matches the known slope of the $\delta^{18}O_{coral}$-SST relationship (i.e., only if $\delta^{18}O_{sw}$ changes are too small to measurably affect coral $\delta^{18}O$), the Gagan et al. (1994, 1998) method will produce the correct temporal variations of $\delta^{18}O_{sw}$. The Gagan et al. (1994, 1998) method is therefore not appropriate to separate SST and $\delta^{18}O_{sw}$ (SSS).

A better approach for salinity reconstructions from corals would be to use a multiple linear regression of coral $\delta^{18}O$ vs. SST, SSS. The partial regression coefficients of the MLR are defined in equation 8. The regression parameters obtained by applying the MLR are thus able to take the covariance between SST and SSS into account. The MLR is optimal in a least squares sense, however there is an important deficit that must be overcome in the future: The instrumental datasets, which are used as independent variables (SST, SSS) are not free of error. The MLR is based on the assumption that the independent variables are free of error or that the error are negligible compared to the error of the dependent variables. If the errors in the proxy measurement are low and all parameters are known, inclusive the constants of the MLR equations, it is possible to reconstruct the absolute values of SST and SSS. In practice, the constants (or intercepts) are barely known, which makes it difficult to obtain absolute values. Besides, time series of past SSS variations are rare and, given the discrepancies often observed between datasets (Figure 4.4) probably not free of error (see also Kilbourne, et al., 2004). This is a serious problem for calibration/validation exercises of coral-based $\delta^{18}O_{sw}$ reconstructions.

Alternatively, it is possible to center the MLR, so that the constants are removed from the regression model and all variables are regarded only as anomalies with respect to their mean value. In the centered MLR model we can also insert the known slope values for the $\delta^{18}O$ (Sr/Ca)-SST relationships. In the centered MLR, we can estimate the slope of $\delta^{18}O_{sw}$ vs. SSS (γ_2), or insert published estimates from the literature. Note, however, that only relative variations of SSS are calculated.

6. Conclusions

The method proposed by Gagan et al. (1994, 1998) for deriving $\delta^{18}O_{sw}$ from paired coral proxy $\delta^{18}O$ and Sr/Ca measurements contains a methodological error (coral $\delta^{18}O$ is calibrated with SST only) and can not be used in areas where SST-covariant variations in $\delta^{18}O_{sw}$ and SSS occur, because these would be incorporated in the slope of the $\delta^{18}O$-SST relationship. This would lead to a systematic bias of $\delta^{18}O_{sw}$ and SSS reconstructions.

The method of Ren et al. (2002) and the centering method proposed in this study omit the intercept value of the $\delta^{18}O$-SST and Sr/Ca-SST regression equation from the calculation of $\delta^{18}O_{sw.}$ Thus, it is possible to insert the known slope of the $\delta^{18}O$ (Sr/Ca)-SST relationship and we can calculate $\delta^{18}O_{sw}$ for any given coral record. The method of Ren et al. (2002) and the centering method give practically the same results. However, the Ren et al. (2002) method requires much more complicated mathematical calculations than centering, which is a standard method in linear regression analysis.

The multiple linear regression between coral $\delta^{18}O$, SST and SSS should be the correct approach for the reconstruction of salinity from corals. This would allow us to estimate the slope of the coral $\delta^{18}O$-SST and coral $\delta^{18}O$-SSS relationship and also enable us to estimate the simultaneous contribution of $\delta^{18}O_{sw}$ (SSS) and SST to coral $\delta^{18}O$. We can then calculate $\delta^{18}O_{sw}$ even in regions where SST-covariant $\delta^{18}O_{sw}$ variations occur, e.g., at sites that are influenced by major oceanic salinity fronts (like Tahiti), or by the Intertropical Convergence Zones. Unfortunately, however, reliable time series of past SSS variations are scarce, and those that do exist are averaged over large areas. This is a serious problem in coral paleoclimatology.

The true error of $\delta^{18}O_{sw}$ (e) calculated from paired proxy measurements is the sum of the error propagation based on the linear relation of the proxy vs. SST (σ) and the error due to noise (ε). Only the statistical error propagation can be calculated. The error propagation (σ) of $\delta^{18}O_{sw}$ calculated from coral $\delta^{18}O_{coral\text{-}TH12}$ and Sr/Ca_{TH12} is $\sigma = \pm 0.066‰$. This is larger than the seasonal cycle of $\delta^{18}O_{sw}$ expected based on climatological data of SSS. Therefore, seasonal-scale variations of $\delta^{18}O_{sw}$ can not be resolved. However, on an annual mean scale, the error of $\delta^{18}O_{sw\text{-}TH12}$ reduces because we average a large number of independent estimates. Also, interannual variations of SSS are larger, and should measurably affect coral $\delta^{18}O_{sw}$. Annual mean $\delta^{18}O_{sw\text{-}TH12}$ clearly follows SSS from SODA, and both records indicate a freshening of surface waters in 1977/78. We note that the variance of SSS inferred from the corals is higher than in the SODA dataset. This may reflect the different spatial scales represented by the coral-based salinity reconstructions and SSS from the SODA dataset, or problems in the SODA reanalysis. In order to obtain reliable, quantitative salinity reconstructions from corals we will need much better instrumental data of $\delta^{18}O_{sw}$ and SSS that can only be obtained through long-term monitoring programs.

Acknowledgements

We are grateful to the support of the Deutscher Akademischer Austauschdienst (DAAD) (grant A/02/21403) and the Deutsche Forschungsgemeinschaft (Leibniz award to Prof. Wolf-Christian Dullo). We thank Dieter Garbe-Schönberg and Jens Zinke for discussions. We also thank Lutz Haxhiaj, Karin Kiessling and Ana Kolevica for their assistance in the isotope and trace element laboratory.

CHAPTER V

Assessing the fidelity of coral $\delta^{18}O$ and Sr/Ca ratios from modern Tahiti corals as recorders of interannual and interdecadal climate variability in the tropical Pacific

Abstract

We analyze coral $\delta^{18}O$ and Sr/Ca ratios of massive coral cores drilled at Tahiti. Sr/Ca ratios are used to reconstruct SST and paired measurements of coral $\delta^{18}O$ and Sr/Ca are used to reconstruct seawater $\delta^{18}O$ (SSS). We correlate coral Sr/Ca ($\delta^{18}O$) with SST and several climate indices, e.g. the Southern Oscillation Index (SOI), Niño 3.4, and Niño 4 SST. Calibration of coral Sr/Ca-SST confirms that Sr/Ca is a good temperature proxy. The calibration of coral $\delta^{18}O$-SST, SSS using multiple linear regression confirms that coral $\delta^{18}O$ is influenced by SST and SSS. The correlation of coral Sr/Ca ($\delta^{18}O$) with the SOI and the Niño 3.4 index is low. Systematic changes of SST related to ENSO can not be inferred from coral Sr/Ca ratios of Tahiti corals. This is confirmed by instrumental SST records from Tahiti that also show a low correlation with the SOI and Niño 3.4. Tahiti is located in a transitional zone of the El Niño -related SST and SSS anomaly response in the tropical Pacific (warm in the eastern equatorial Pacific and cold in the West Pacific Warm Pool). This makes it extremely difficult to identify El Niño or La Nina events from SST or SSS records in this area. However, SST anomalies in the Niño 4 region are captured by coral Sr/Ca from Tahiti. This shows that the decadal mode of SST in the tropical Pacific can be recorded by coral Sr/Ca ($\delta^{18}O$) since the leading mode of SST in the Niño 4 region is decadal. This is confirmed by coral Sr/Ca which correlates with the Pacific Decadal Oscillation (R = 0.46). We also found that SSS reconstructed from the corals is a better record of decadal variability in the region. The results of this study provide important constraints for future paleoclimatic reconstructions based on fossil corals from Tahiti.

1. Introduction

Geochemical proxies measured in corals are a promising tool to extent the instrumental record of sea surface temperature (SST) and sea surface salinity (SSS) back in time. Living massive colonies of *Porites* are the most widely used coral genus for paleoclimatic reconstructions and can be up to 500 years old. The rapid growth of *Porites* corals allows the development of monthly resolved proxy records, and annual density bands provide a basis for a precise chronologies. The most important proxies measured in corals are the stable oxygen isotopes

($\delta^{18}O$) and Sr/Ca ratios. Although vital effects may bias the absolute values of the coral proxies (McConnaughey, 1989 a,b), time-dependent variations were shown to follow the thermodynamic laws and are linearly related to environmental parameter (McCulloch et al, 1994) provided that the corals are sampled along the main growth axis. Coral $\delta^{18}O$ and Sr/Ca are linearly related to temperature. Coral $\delta^{18}O$ is also linearly related to $\delta^{18}O$ seawater, which co-varies with salinity. Based on paired coral Sr/Ca and $\delta^{18}O$ measurements, it is possible to reconstruct seawater $\delta^{18}O$ and sea surface salinity (SSS) (e.g McCulloch et al, 1994; Gagan et al., 1998; Ren et al., 2002).

Several proxy coral $\delta^{18}O$ records were developed from sites lying in the South Pacific Convergence Zone (SPCZ). An annual mean coral $\delta^{18}O$ spanning AD 1997-1780 and AD 2001-1776 from Fiji was shown to be coherent with the PDO, particularly between 1880 and 1950 (Bagnato et al., 2005). A 271 years, monthly resolved coral Sr/Ca record from Rarotonga also clearly displays interdecadal variability that is coherent with the PDO (Linsley et al., 2000), supporting the idea that interdecadal variability in the extra-tropical Pacific is symmetric about the equator, which would suggest a tropical origin of this signal (Evans et al., 2002). Several coral studies have shown that coral proxies record ENSO (Charles et al., 1997; Cobb et al., 2003a; Kilbourne et al., 2004; Zinke et al., 2004; Timm et al., 2005).

The El Niño Southern Oscillation (ENSO) is a predominantly interannual phenomenon centered in the tropical Pacific, that has important consequences for global climate. During normal periods, the eastern equatorial Pacific is cold because of equatorial upwelling driven by the easterly trade winds. Surface waters in the Western Pacific Warm Pool (WPWP), in contrast are warm (> 28°C). El Niño is the warm phase of ENSO. The south-easterly trade winds weaken, and the eastern equatorial Pacific warms, while the WPWP cools. During La Nina, the cool phase of ENSO, the southeasterly trade winds strengthen and the eastern equatorial Pacific is cooler than normal, while the WPWP is even warmer. The tropical Pacific also features pronounced decadal, ENSO-like variability (e.g. Latif et al., 1997; Cobb et al., 2001; Evans et al., 2002). A better understanding of decadal and long-term ENSO-like variability is an important topic in present climate research. However, longer records are needed in order to assess low-frequency modulations of ENSO and their relationship to extra-tropical climate modes such as the Pacific Decadal Oscillation (PDO) (Mantua et al., 1997; Salinger et al., 2001; Folland et al., 2002)

The south western tropical Pacific (SWTP) (24°S-10°S and 160°E-140°W) is characterized by a salinity front that separates the south-eastward oriented tongue of fresh, warm water that underlies SPCZ from the westward oriented tongue of high salinity water formed in the center of the subtropical gyres which is advected westward by the southern branch of the South Equatorial Current (Gouriou and Delcroix, 2002). The salinity front is the result of the concurrence of the high salinity waters formed in the subtropical south Pacific region (20°S, 120°W), where evaporation exceeds precipitation, with the low salinity waters formed in the WPWP, where precipitation exceeds evaporation. SSS variations in the SWTP result from the displacement of this salinity front, which lie at the south-eastern margin of the WPWP (170°W-15°S). Interannual variations are clearly linked to ENSO. On longer time scale, the SWTP exhibits prominent interdecadal climate fluctuations (e.g Deser et al., 2004; Linsley et al., 2004; Bagnato et al., 2005; Asami et al., 2005). Interdecadal fluctuations in SST and rainfall are coherent with interdecadal variability over the extra-tropical North Pacific (Deser et al., 2004).

The Southern Oscillation Index (SOI) is defined as the normalized sea level pressure (SLP) difference between Tahiti and Darwin (Australia). Therefore, Tahiti corals are believed to be promising recorders of past ENSO variability, and the International Ocean Drilling Project (IODP) Tahiti sea-level expedition will drill fossil corals for paleo-ENSO reconstructions. However, the coral proxies do not record SLP but SST, $\delta^{18}O_{sw}$ and SSS. Tahiti is located at a transitional zone, i.e. close to the zero lines of the ENSO-related SST anomaly response in the tropical Pacific (Figure 5.1). The island also lies at the eastern border of SWTP where ENSO may lead to a displacement of the salinity front and to precipitation anomalies due to the movement of SPCZ. Since Tahiti is located on the southern margin of SPCZ, the coral proxies could also be influenced by interdecadal variations in the SWTP which were shown to be coherent with the subtropical North Pacific (Power et al., 1999; Evans et al., 2002; Folland et al., 2002, Bagnato et al., 2005).

In this study, we present the first detailed assessment of the fidelity of modern corals from Tahiti as recorders of climate variability in the tropical Pacific. We have measured monthly Sr/Ca and $\delta^{18}O$ from three modern coral cores covering the past 20 to 90 years. Two of these cores were drilled from the same coral colony. $\delta^{18}O$ seawater and salinity is reconstructed from the paired proxy measurements. We compare coral Sr/Ca, $\delta^{18}O$ and reconstructed SSS with the Niño 3.4 index and the PDO index as well. The results of this study can be used as

basis for any paleoclimatic study using fossil corals from Tahiti that are being drilled as a part of the IODP-Tahiti sea level Expedition 2005.

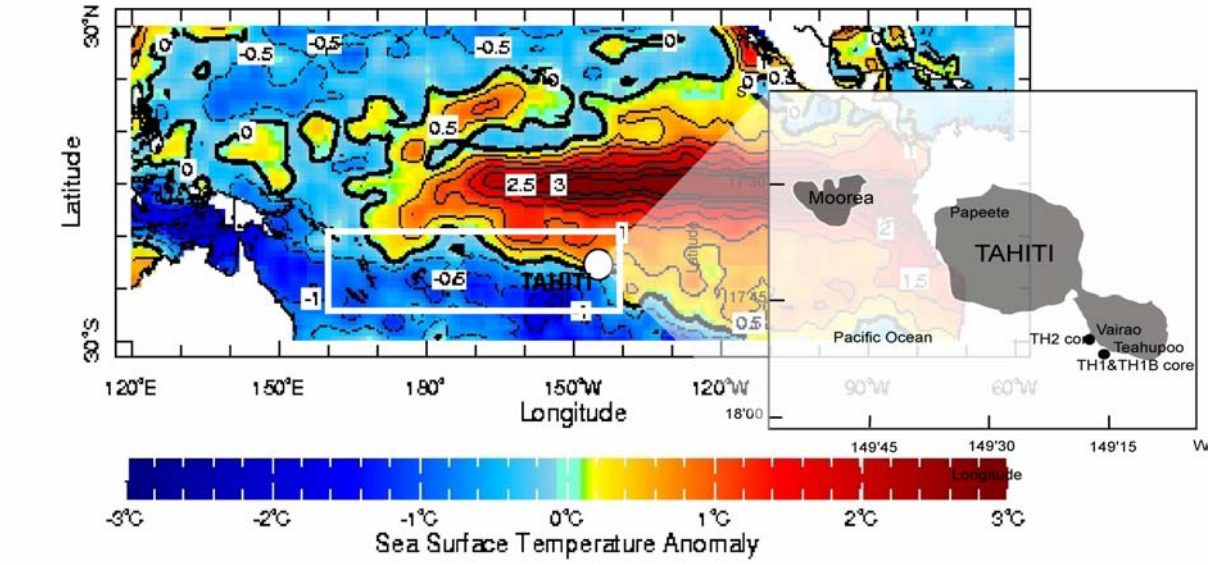

Figure 5.1. SST anomalies in November 1982 (colors) and location of the south western tropical Pacific (SWTP) region (white box). Tahiti is located close to zero line of the SST anomaly pattern. Coral drilling locations are indicated by black dots, see inset. SST data is taken from the NCEP dataset, (http:// iridl. Ldeo. columbia. edu/ sources/ NOAA/ NCEP/ EMC/ CMB/ GLOBAL/ Reyn_SmithOIv2/ monthly/ ssta).

2. Oceanic and climate setting of Tahiti

Tahiti is located at the eastern margin of the SWTP (Figure 5.1). The seasonal displacement of the salinity front that separates the low salinity water of the WPWP from the high salinity waters formed in the subtropical south Pacific results in seasonal SSS variation on the order of 35.8-36 psu at Tahiti (149°20' W 17°4`E) (Gouriou and Delcroix, 2002). During austral summer, the 36 psu contours lies to the east of Tahiti, while during austral winter it lies to the west of Tahiti (Rougerie et al., 1993). At Tahiti, maximum SST and precipitation as well as minimum SSS occurs during November-April, the warm, rainy season. The cool and dry season lasts from May to October, and minimum SST and precipitation coincide with maximum SSS. Based on the climatological cycle of SST at Tahiti the maximum (minimum) SST occurs in March (August) (Figure 5.2). Mean seasonal SSTs during the rainy season range from 27° to 28°C (November-April) and from 26° to 28°C during the dry season (May-October).

3. Material and methods

Three cores from two massive colonies of *Porites* were drilled on July 1995 at Teahupoo (TH1 and TH1B) and at Vairaoo (TH2). Core TH1 and TH1B were drilled from the same

colony. Core TH1 was drilled vertically 180 cm long, core TH1B was drilled horizontals and is 26 cm long. Core TH2 was drilled vertically and is 380 cm long but we only use the upper 110 cm long in this study. The coral cores were slabed to a thickness of 4 mm. These slabs were rinsed in an Ultrasonic bath and dried at 50^{o} C for 24 hours. The X-radiographs of the

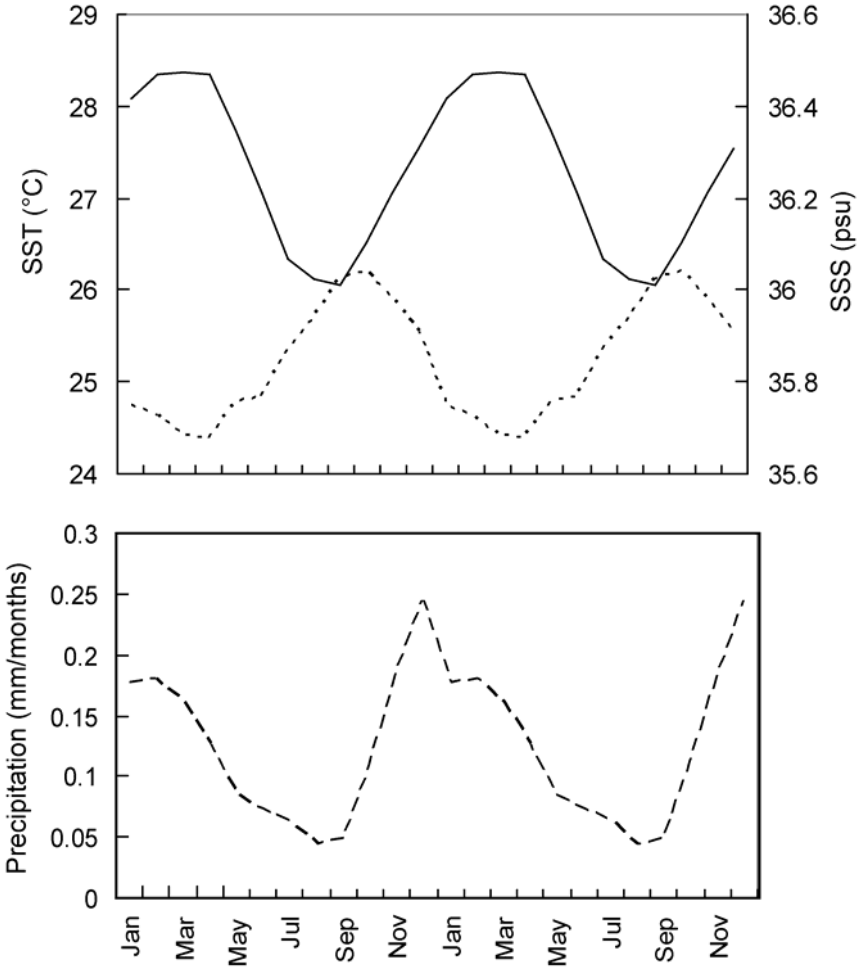

Figure 5.2. The monthly mean of (a) SST (solid line), and SSS (dashed line) and (b) precipitation at Tahiti. Data from Delcroix et al. (1996, 2002)

coral slabs (Figure 2.1 see Chapter II) show pronounced annual density bands that allow the development of precise chronology. The average annual extension rate is approximately 1-2 cm/ year. A transect that follows the main growth axis is selected for sub-sampling. The slabs are sampled to get coral powder using a drilling bit of 1 mm. Powdered samples are taken every ±1 mm to get monthly resolved proxy data. The powdered samples of TH1 and TH2 are then splitted for stable isotope ($\delta^{18}O$ and $\delta^{13}C$) and trace element (Sr/Ca ratio) analysis. $\delta^{18}O$ and Sr/Ca of TH1B are measured at sub sample from two parallel sampling transects.

We measured Sr/Ca ratios on an inductively coupled plasma optical emission spectrophotometer (ICP-OES) at the university of Kiel following a combination of the techniques from Schrag (1999) and de Villiers (2002). The relative standard deviation (RSD) of multiple measurements is about 0.15% or 0.01 mmol/mol (1σ). The stable isotopic composition of $\delta^{18}O$ and $\delta^{13}C$ of TH1 is analysed using a Finnigan Mat Mass spectrometer 251 at the IFM-GEOMAR. A Thermo Finnigan Gasbench II Delta Plus is used for the stable isotope measurement of TH2 and TH1B. The isotope ratios are reported in ‰VPDB relative to NBS 19. The analytical uncertainty is less than ±0.06 ‰ (1σ) for $\delta^{18}O$ measurements.

The chronology is constructed using linear interpolation based on anchor points tied to the seasonal cycle of the Sr/Ca records. It is assumed that the minimum (maximum) skeletal Sr/Ca correspond to the maximum (minimum) SST. The maximum (minimum) Sr/Ca is tied to August (March), which is on average the coolest (warmest) month at Tahiti. The anchor points defined based on Sr/Ca are also used for the interpolation of coral $\delta^{18}O$. This method takes into account that the seasonal extremes of coral $\delta^{18}O$ may not coincide with the Sr/Ca extremes, as the $\delta^{18}O_{sw}$ minima (maxima) do not necessarily coincide with SST minima. Note that the precipitation maximum leads the SST maximum by approximately 2 months (Figure 5.2). Since coral $\delta^{18}O$ and Sr/Ca were measured at the same samples, they have the same ages and, logically this should be the correct approach for the age determination of $\delta^{18}O$. For TH1B, because of lack of coral sample powder, the sample is not splitted for coral $\delta^{18}O$ and Sr/Ca analysis. The anchor points were chosen for coral $\delta^{18}O$ and Sr/Ca separately. The maximum (minimum) $\delta^{18}O$ in any given year is tied to August (March) and the maximum (minimum) Sr/Ca is also tied to August (March). Thus, seasonal extremes coincide with the Sr/Ca extremes, the age uncertainty of $\delta^{18}O$ relative to Sr/Ca is approximately 2 months in any given year. The age models are developed based on the proxies confirm that TH1 extends from February 1923 until July 1995, TH1B extends from January 1974 to July 1995, and TH2 from July 1903 until July 1995. The uncertainty of the age model is approximately 2 months in any given year. Figure 5.3 shows the monthly coral $\delta^{18}O$ and Sr/Ca ratios measured from TH1, TH2 and TH1B.

We use SST from the Extended Reconstructed global Sea Surface Temperature (ERSST) of Smith & Reynolds (2004) for calibration the proxy since the ERSST provides long time series of SST extending from January 1854 until present with 2°x2° resolution. We also use SST

and SSS from the Simple Ocean Data Assimilation (SODA) reanalysis to calibrate coral $\delta^{18}O$ and reconstructed SSS (seawater $\delta^{18}O$). The SODA reanalysis of ocean climate variability provides monthly averaged SST and SSS data covering the past 50 years mapped onto a uniform 0.5° x 0.5° grid (Carton et al., 2000). The SODA model uses input data from the World Ocean Database 2001, hydrographic data, satellite and in situ SST and altimetry from

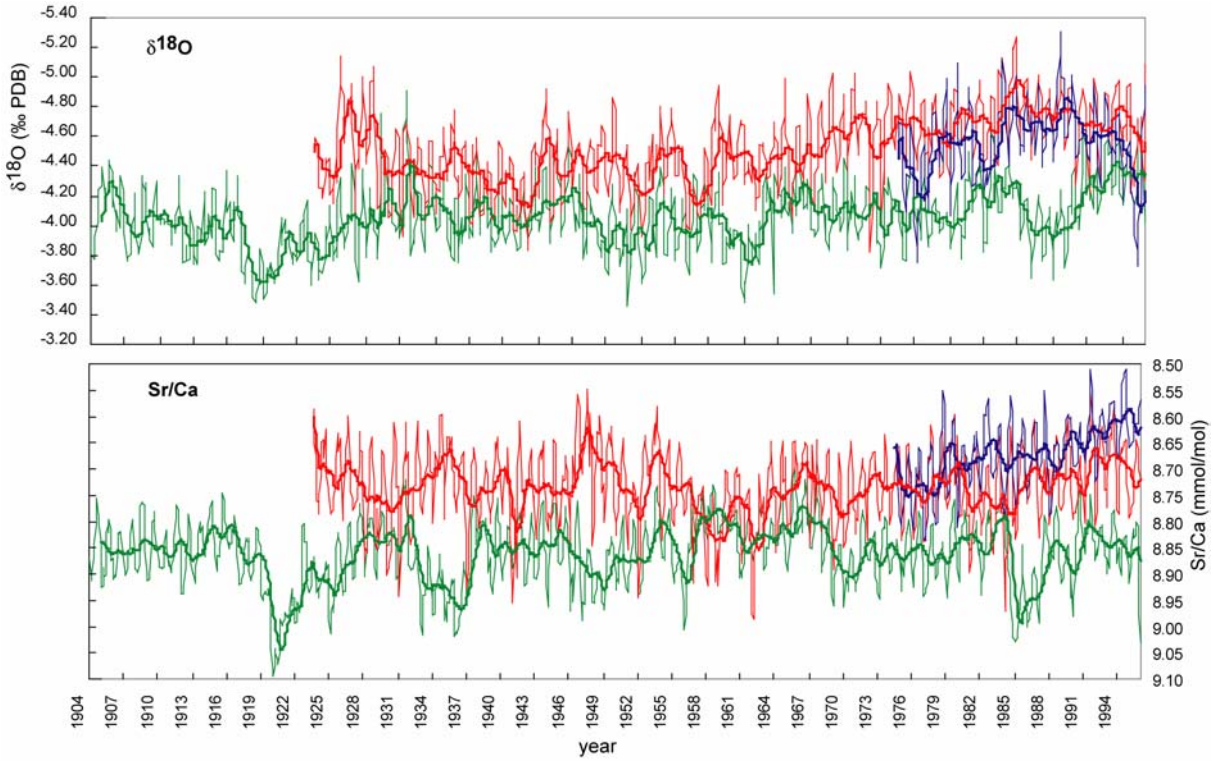

Figure 5.3. Monthly coral $\delta^{18}O$ and Sr/Ca from Tahiti cores: TH1 (red line), TH2 (green line) and TH1B (blue line). Bold lines are 12 points running averages.

Geosat, ERS-1 and TOPEX/Poseidon (Carton et al., 2000). In this study, we use SODA 1.2 which uses the surface wind products from the NCEP/NCAR reanalysis. This product may be biased by the introduction of satellite observations in the mid-1970s, but it does not require correction of the mean stress (like the ECMWF ERA 40 product, which was used in the newer versions of SODA), which is particularly problematic in the tropics (Carton et al., 2000).

The Analyseries software package is used to interpolate the proxy data (Paillard et al., 1996) and for statistical analysis. We also use statistical time series analysis tools available in the world wide web provided by the Royal Netherlands Meteorological Institute (KNMI) (http://www.knmi.nl) (Oldenborgh and Burgers, 2005). Grinsted et al. (2004) provide a software package for the computation of wavelet power spectra and wavelet coherence spectra. Multi Taper Method (MTM) spectral analysis is performed with the single spectrum

analysis (SSA)-MTM toolkit (Dettinger et al., 1995). SSA is used to get the power spectrum in the certain frequency.

4. Results and Discussion

4.1 Coral Sr/Ca

The basic statistical of measured Sr/Ca from Tahiti cores i.e TH1, TH1B, TH2 and average Sr/Ca from TH1, TH2 and TH1B cores (column avTH12B) and average Sr/Ca from TH1 and TH2 cores (column avTH12) are shown in Table 4.1.

	TH1	TH1B	TH2	avTH12B	avTH12
Min	8.549	8.510	8.698	8.604	8.651
Max	8.985	8.838	9.096	8.882	8.943
Mean	8.735	8.671	8.862	8.753	8.796
Std.Deviation	0.072	0.068	0.063	0.052	0.053
Variance	0.005	0.005	0.004	0.003	0.003
points	870	259	1105	259	870

Table 4.1. Basic statistic of Sr/Ca measured at the Tahiti cores, in mmol/mol.

The reproducibility of Sr/Ca measured at the three Tahiti cores has been assessed using linear regression model. The reproducibility between single Sr/Ca records TH1 - TH1B is good (R = 0.66) for the monthly resolution for period 1974-1995. Despite we found good reproducibility of single Sr/Ca records between TH1B (hereafter mention as Sr/Ca_{TH1B}) and TH1 (hereafter mention as Sr/Ca_{TH1}) in the seasonal scale, but we found that the annual mean correlation of Sr/Ca_{TH1B} - SST and Sr/Ca_{TH1} - SST is different. This can be caused by the different trend of Sr/Ca_{TH1B} and Sr/Ca_{TH1} in the annual scale which possible result in the differences of data distribution between two records. The record of Sr/Ca from TH1B has more similar variation and trend in the interannual scale with the SST from ERSST and Delcroix et al. (1996, 2002) than that of Sr/Ca from TH1 (Figure 5.4), thus it cause the data distribution of Sr/Ca_{TH1B} more fit to SST which is resulted higher correlation of Sr/Ca_{TH1B} - SST (R= 0.73 p <0.001) than Sr/Ca_{TH1} - SST (R=0.69 p <0.001). Compare to other location in the central Pacific i.e Rarotonga (RRT) (Linsley et al., 2000), the reproducibility of Sr/Ca_{TH1} with Sr/Ca from Rarotonga (Sr/Ca_{RRT}) is good (R= 0.66 p <0.001), but not with the other two cores (TH2 and TH1B). TH2 records do not have good reproducibility with any TH1 and TH1B records.

We here performed a linear correlation between monthly coral Sr/Ca and SST (ERSST) to estimate the Sr/Ca - SST relationship. The best single core correlation is obtained for TH1B (Sr/Ca_{TH1B} = -0.054±0.003 SST + 10.144±0.09 R= 0.73 p < 0.001). A better correlation is obtained between Sr/Ca_{TH12B} and SST (R= 0.83 p<0.001). The slope of the monthly Sr/Ca-

SST regression is in good agreement with published estimates which range from -0.04 to -0.08 mmol/mol/°C (e.g., Beck et al, 1992; de Villiers et al., 1994, 2002; Shen, et.al, 1996; Alibert, et al, 2003; Marshal and McCulloch, 2002; Mitsuguchi et al, 2003). Three cores

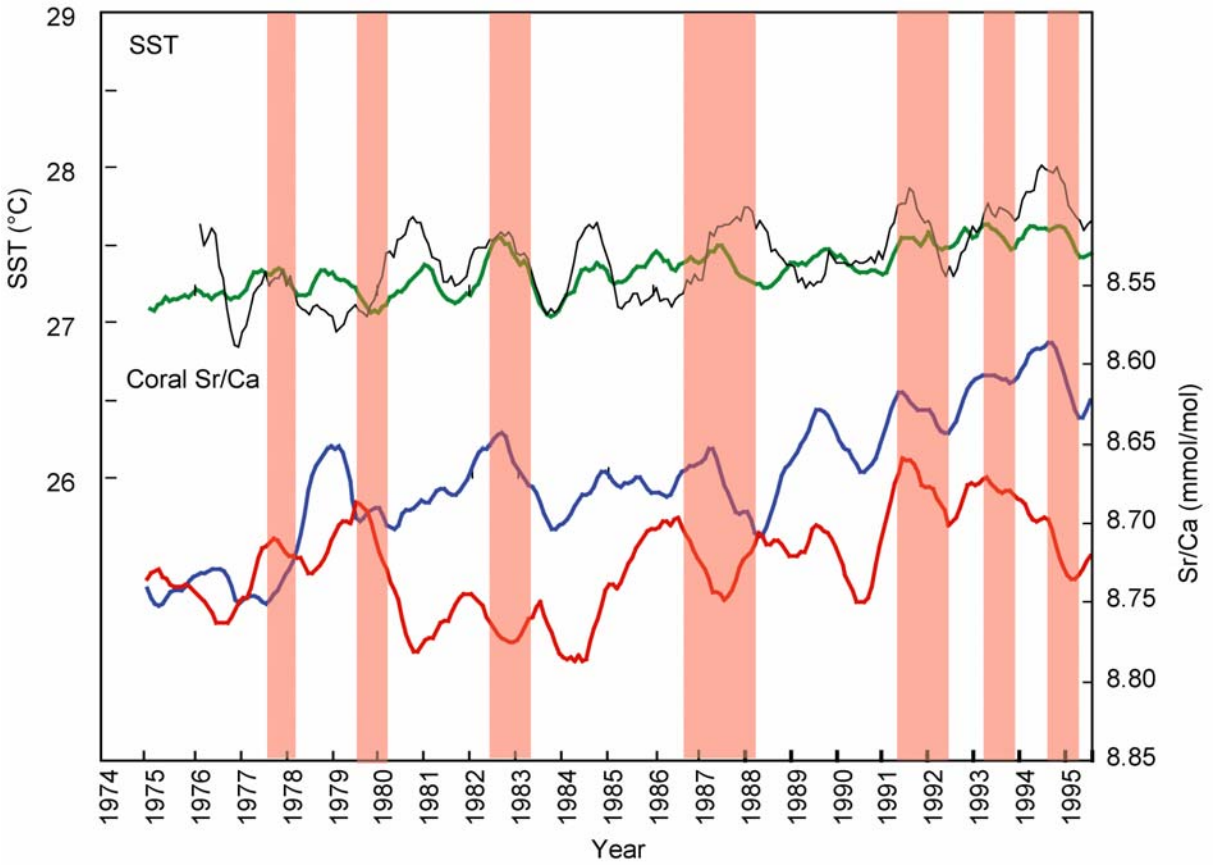

Figure 5.4. SST from ERSST (green line) and Delcroix et al. (1996, 2002) (black line) compared to 12 points running average of Sr/Ca of TH1 (vertical core) (red line) and Sr/Ca of TH1B (horizontal core) (blue line). Red shading indicates El Niño events (Trenberth, 1997).

average of TH1, TH2 and TH1B will used to infer large-scale climate signal recorded at Tahiti.

We also compare the annual mean Sr/Ca records with annual mean SST. Annual means are computed by averaging the data from August to July in the following year (Figure 3.13 see chapter III). The horizontal core TH1B has the best correlation (R= 0.796) with SST on an annual mean scale. The other two single core records have a low correlation with grid-SST (TH1: R=0.27 p<0.001; TH2: R=0.21 p<0.001). This is surprising, because most coral paleoclimatologist believe that corals should be drilled vertically to obtain the best climate reconstruction. The average Sr/Ca record computed from the three cores (Sr/Ca_{TH12B}) correlate well with grid-SST (R=0.55 p<0.001). Since the monthly Sr/Ca-SST calibration should

provide the best statistical estimate of the Sr/Ca-SST relationship, we use this calibration to convert the Sr/Ca records to SST. We then compute annual means from these monthly SST reconstructions. We find that on an annual mean scale the variation of reconstructed SST is much larger than indicated by grid-SST (σ_{ERSST} = 0.16°C). This will have implication of any climate study using fossil coral from Tahiti, because the modern Tahiti coral records from this study do not show the variance right in the annual mean scale. The variance of single records is larger (σ = 1.14°C for TH2°C, σ = 0.6°C for TH1, σ = 0.79°C for TH1B) than for the average record (σ = 0.58°C for average TH1-TH1B and σ = 0.53°C for average TH1-TH2-TH1B). Importantly, the differences in the variance between the proxy and grid-SST do not seem to depend on the strength of the correlation between the proxy and SST.

To further assess the fidelity of coral Sr/Ca as a proxy for SST on longer time scales, we calculate running correlations between the single Sr/Ca records of TH1 and TH2 vs ERSST. The time series are averaged over 12 months (August -July), and a 31 years running window is used. The results show that the correlation of Sr/Ca from TH1 with SST is low near the core top. This suggests that the Sr/Ca record of TH1 maybe more less reliable at the top. Prior to 1960 TH1 shows a stable correlation with grid-SST. As TH1B does show a high correlation with SST, we replace the core top of TH1 with TH1B records. However, the correlation coefficient does not improve much, because TH1B is too short. Sr/Ca_{TH2} does not show any significant correlation in any period of time with SST (Figure 5.5).

4.2 Coral $\delta^{18}O$

Oxygen isotopes ($\delta^{18}O$) in coral aragonite are believed to be a function of both seawater $\delta^{18}O$ ($\delta^{18}O_{sw}$) and temperature (Charles, et al., 1997; Quinn, et al., 1998; Gagan, et al., 2000; Juillet-Leclerc and Schmidt, 2001). The mean $\delta^{18}O$ of coral aragonite is offset from isotopic equilibrium, most likely due to biological processes (McConnaughey, 1989b). Assuming that this disequilibrium is constant in time, the relationship between coral $\delta^{18}O$, SST and seawater $\delta^{18}O$ will be linear. In this study, the linear regression between the average coral $\delta^{18}O$ from TH1,TH1B and TH2 records (hereafter $\delta^{18}O_{TH12B}$) and SST only yields a slope value of -0.14‰/°C (R= 0.76, p<0.001). Using TH1B only, which seems to be the best single core record of climate at Tahiti, the calibration slope of $\delta^{18}O_{TH1B}$ -SST (-0.15 ‰/°C, R= 0.54, p<0.001) is more or less the same as obtained with the average proxy TH1,TH1B and TH2. These regression slopes are lower than the known slope of the $\delta^{18}O$ - SST relationship in biological carbonate that ranges from -0.18‰/°C to -0.22 ‰/°C (Weber and Woodhead,

1972; Gagan et al., 1994; Wellington et al., 1996; Juillet-Leclerc and Schmidt, 2001). However, a high correlation coefficient based on the fitting of coral $\delta^{18}O$ with measured temperature does

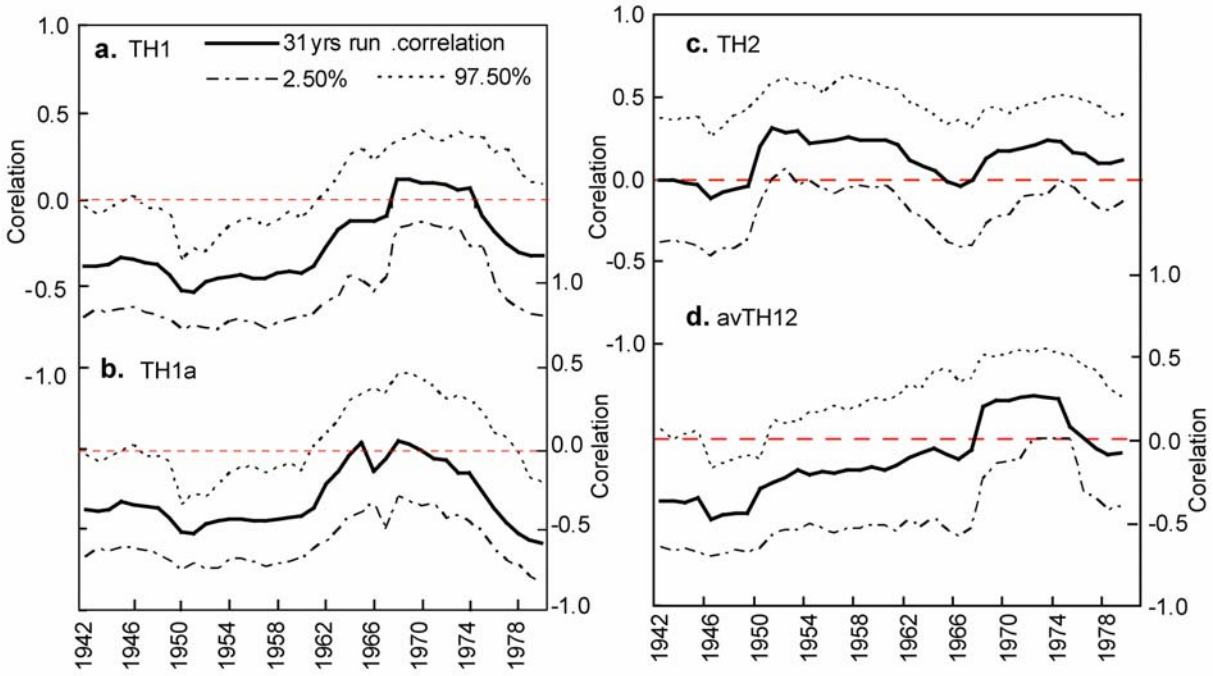

Figure 5.5. Running correlation of (a) Sr/Ca_{TH1} vs. ERSST, (b) Sr/Ca_{TH1a} vs. ERSST. The Sr/CaTH1a records is obtained by replacing the core top of Sr/CaTH1 with Sr/Ca_{TH1B}. (c) Sr/Ca_{TH2} vs. ERSST and (d) Sr/Ca_{TH12} vs. ERSST. Confidence level are calculated with bootstrap method.

not necessarily reflect the dependence of $\delta^{18}O$ on temperature. Coral $\delta^{18}O$ could be influenced by SST- covariant changes in the isotopic composition of the seawater. The correct calibration approach should be the use of multiple linear regression (MLR) to estimate the $\delta^{18}O$-SST relationship. Assuming that seawater $\delta^{18}O$ is linearly correlated with SSS, we can use the MLR of coral $\delta^{18}O$ vs. SST, SSS to estimate the coral $\delta^{18}O$ - SST, SSS relationship. We use the averaged coral $\delta^{18}O$ from TH1 and TH2 and the SST and SSS from the SODA reanalysis for calibration. TH1B and average proxy from TH1, TH2, TH1B are too short to provide time series. We obtain the multiple regression equation (95% confidential level) of coral $\delta^{18}O_{TH12}$ vs. SST and SSS from SODA: $\delta^{18}O_{coral}$ = -0.16±0.02 *SST* + 0.46±0.15 *SSS* -16.738 (R= 0.78, $p < 0.001$). Taking into account the statistical uncertainty of the slope value, the regression slopes are in agreement with published estimates slope of the coral $\delta^{18}O$ - SST (e.g. Weber and Woodhead, 1972; Gagan et al., 1994; Wellington et al., 1996, Juillet-Leclerc and Schmidt, 2001) and with the seawater $\delta^{18}O$ -SSS relationship at Tahiti (Delaygue et al., 2000). The annual mean MLR correlation of coral $\delta^{18}O_{TH12}$ vs. SST and SSS from SODA is low (R =

0.33), and the regression slopes of coral $\delta^{18}O_{TH12}$ -SST and seawater $\delta^{18}O$- SSS is not in agreement with published estimates. The uncertainty in the proxy and the instrumental datasets appear to be too large for calibration with MLR in annual mean scale. Table 4.2 shows the basic statistical of measured coral $\delta^{18}O$ from Tahiti cores i.e TH1, TH1B, TH2 and average $\delta^{18}O$ from TH1,

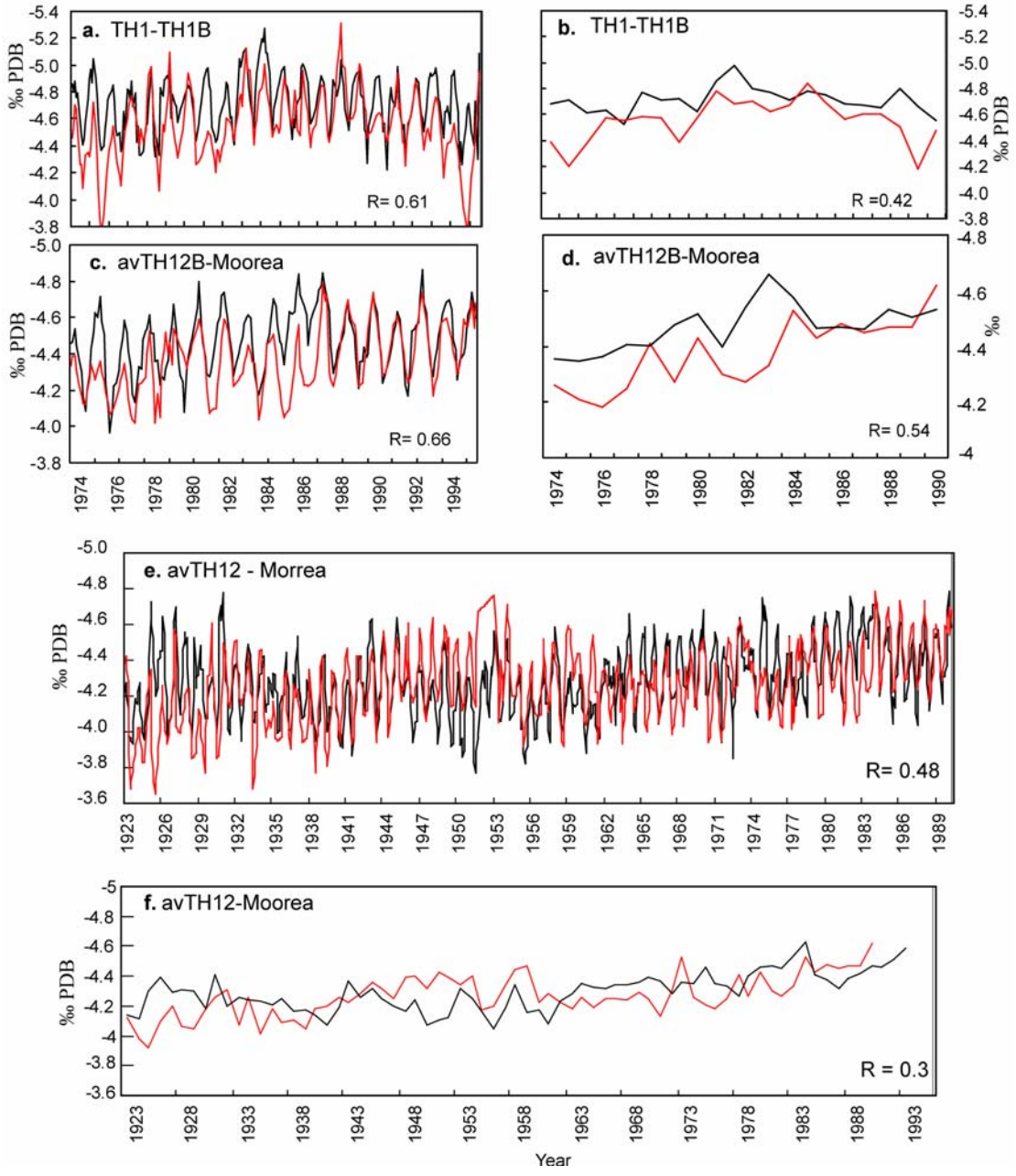

Figure 5.6. (a) Monthly and (b) annual mean variations of coral $\delta^{18}O$ from TH1 (black line) and TH1B (red line). (c) Monthly and (d) annual mean variations of coral $\delta^{18}O$ from average coral TH1,TH2 and TH1B from Tahiti (black lines) compared to coral $\delta^{18}O$ record from Moorea (Boiseau et al., 1998) (red line). (e) monthly and (f) annual mean of coral $\delta^{18}O_{TH12}$ (black) and coral $\delta^{18}O_{Moorea}$ (red) for the period 1923-1990.

TH2 and TH1B cores (column avTH12B) and average coral $\delta^{18}O$ from TH1 and TH2 cores (column avTH12).

	TH1	TH1B	TH2	avTH12B	avTH12
Min	-5.274	-5.108	-4.906	-4.861	-4.784
Max	-3.817	-3.792	-3.456	-3.967	-3.769
Mean	-4.520	-4.559	-4.054	-4.475	-4.301
Std.Deviation	0.260	0.237	0.219	0.172	0.200
Variance	0.069	0.056	0.048	0.030	0.040
points	870	259	1105	259	870

Table 4.2. Basic statistic of coral $\delta^{18}O$ measured at the Tahiti cores, in ‰PDB.

A good reproducibility is found between single coral $\delta^{18}O$ records from the same colony (TH1-TH1B) (R= 0.61, p <0.001) (Figure 5.6). The reproducibility for coral $\delta^{18}O$ TH1-TH2 is low (R= 0.41, p <0.001,) and coral $\delta^{18}O$ for TH2 and TH1B it is even lower. Compared to other coral $\delta^{18}O$ studies in the central Pacific area e.g. Moorea (25 km from Tahiti) (Boiseau et al., 1998), the reproducibility is good. We obtained a good correlation between monthly $\delta^{18}O$ record from Moorea, the closest published record, and average coral proxy from Tahiti: $\delta^{18}O_{TH12B}$ - $\delta^{18}O_{moorea}$ (R = 0.66, p <0.001), and coral $\delta^{18}O_{TH12}$ - $\delta^{18}O_{moorea}$ (R=0.48). In the annual mean scale the reproducibility is low: $\delta^{18}O_{TH12B}$ - $\delta^{18}O_{moorea}$ (R = 0.54, p <0.001), $\delta^{18}O_{TH12}$ - $\delta^{18}O_{moorea}$ (R= 0.3, p <0.001). Figure 5.6 compares the variations of coral $\delta^{18}O$ from Tahiti and Moorea for the period 1974-1990.

4.3 Reconstructed seawater $\delta^{18}O$ (sea surface salinity)

We reconstruct seawater $\delta^{18}O$ or sea surface salinity (SSS) using the centering MLR method (see chapter IV for detail methods). We insert the known slope of coral $\delta^{18}O$ vs. SST (-0.18 ‰/°C), the estimated slope of $\delta^{18}O_{sw}$ vs. SSS for the southern Pacific (0.47 ‰/psu) (Delaygue et al., 2000), and the slope of the Sr/Ca-SST relationship estimated with the SODA dataset (-0.063 mmol/mol/°C) into the equation of the MLR. We use the proxy average from TH1 and TH2 to get longer time series proxy data. The SSS reconstruction for periof 1950-1995 is shown in Figure 5.7

Salinity reconstructions derived from the centered multiple linear regression can be converted to $\delta^{18}O_{sw}$-units with the factor used for the $\delta^{18}O_{sw}$-SSS relationship, and will equal $\delta^{18}O_{sw}$ derived with the centering method (see chapter IV for detail discussion). $\delta^{18}O_{sw}$ reconstructions are still relatively uncertain, because combined analytical uncertainties of

$\delta^{18}O$ and Sr/Ca measurements are large ($\sigma_{\Delta\delta sw} = \pm 0.066$ ‰, see chapter 4 section 5.1.3 for the calculation of the error). The seasonal-scale variations of SSS (0.3 psu; Carton et al., 2000; Gouriou and Delcroix, 2002), and hence expected $\delta^{18}O_{sw}$ variations (0.14 ‰) almost equal the

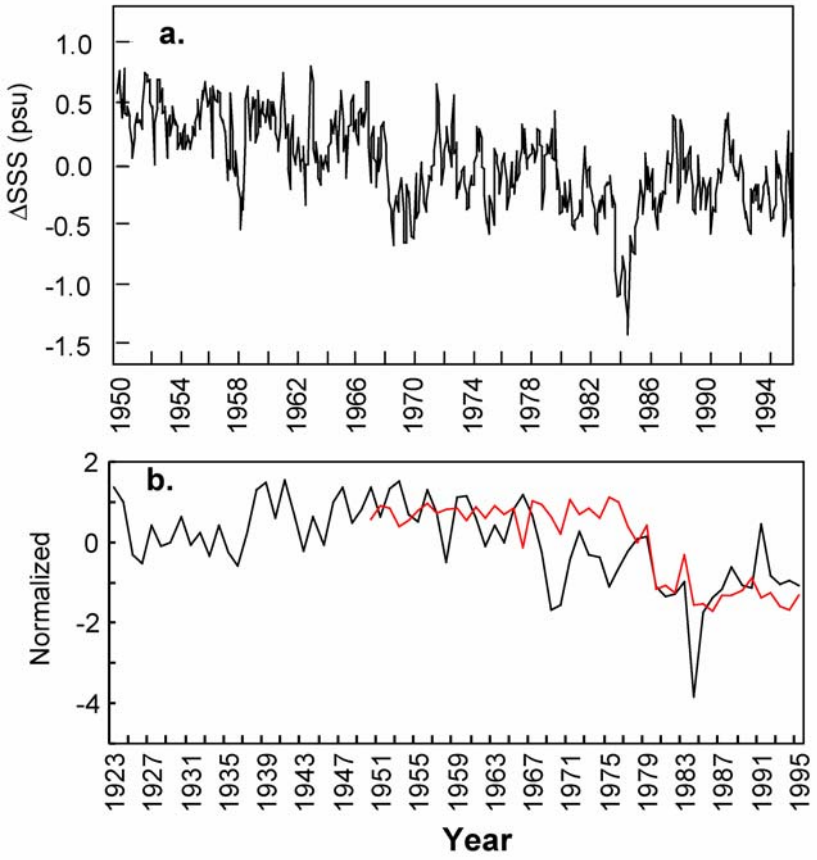

Figure 5.7. (a) Monthly variations of reconstructed SSS for the period 1950-1995. SSS reconstruction is calculated using the centered multiple linear regression. Published values slope are used ($\gamma 1$ = -0.18 ‰/°C and $\gamma 2$ = 0.47 ‰/psu). (b) Annual mean variation of reconstructed seawater $\delta^{18}O$ (black) and SSS from SODA (red). Data is normalized to unit variance.

analytical error. This makes the reconstruction of seasonal-scale variations of SSS and $\delta^{18}O_{sw}$ from Tahiti corals is impossible. The annual mean $\delta^{18}O_{sw\text{-}TH12}$ (Figure 5.7b) is computed from a large number of independent $\delta^{18}O_{sw}$ estimates, and thus the analytical uncertainty of annual mean $\delta^{18}O_{sw\text{-}TH12}$ reduces to ±0.19 ‰ or ±0.04 psu if we assume the annual mean $\delta^{18}O_{sw\text{-}TH12}$ is calculated from 12 independent measurements. The correlation between annual mean $\delta^{18}O_{sw\text{-}TH12}$ with SSS from SODA for 1950-1995 period is high ($R = 0.61$, $p < 0.001$), and $\delta^{18}O_{sw\text{-}TH12}$ co-varies with SSS from SODA. Both series show an abrupt shift towards lower salinity/$\delta^{18}O_{sw}$ in 1977/78 which indicates a freshening of surface waters.

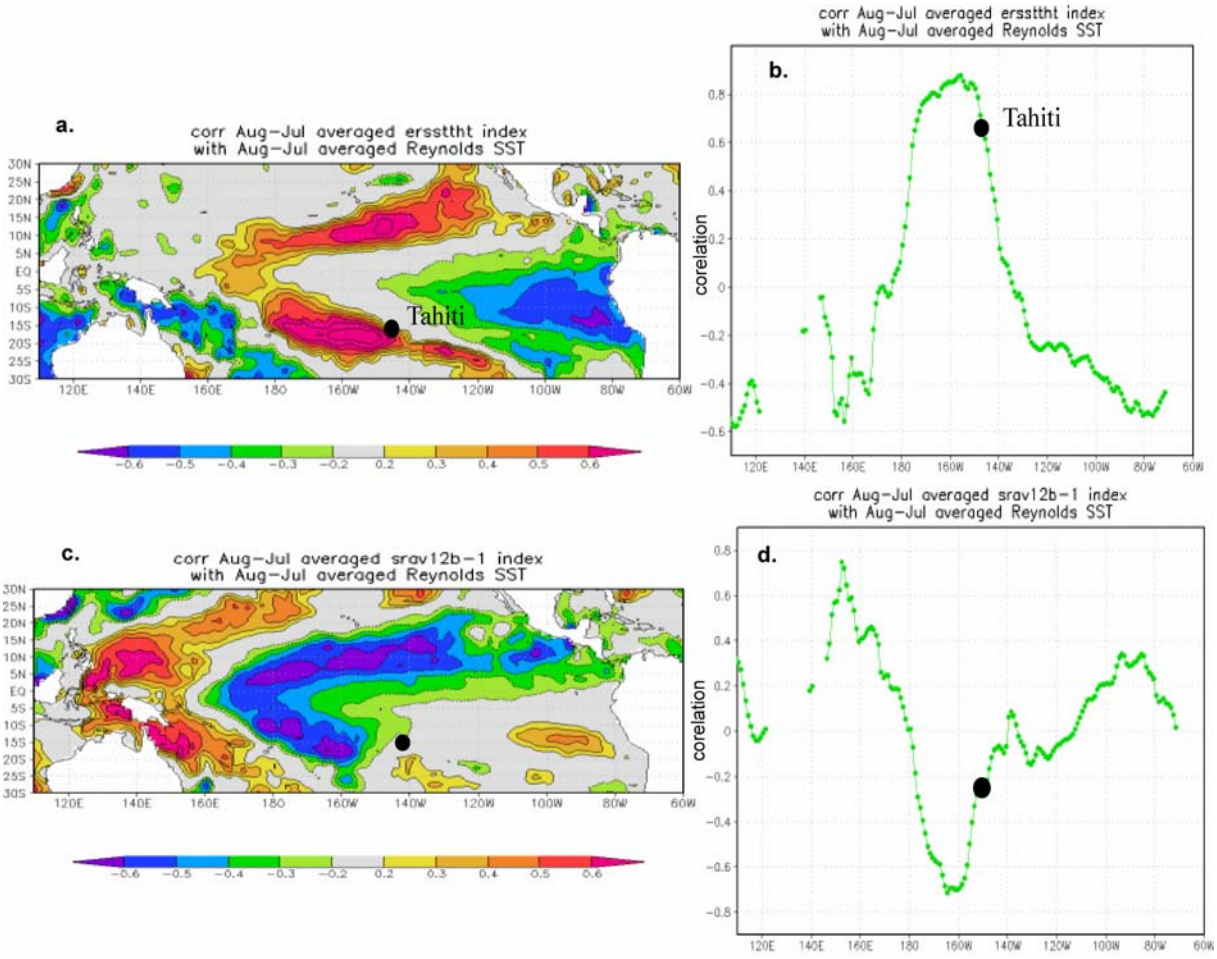

Figure 5.8. (a) Field correlation between ERSST data at Tahiti (149°2W 17°4S) with the tropical Pacific SST field (NCEP data set, 1982-1995) and (b) cross section showing correlation coefficients along 17°4 S. (c) Field correlation of Sr/Ca$_{TH12B}$ with SST field (NCEP data set, 1982-1995). (d) Cross section showing correlation coefficients along 17°4 S. All time series are averaged over 12 months (August to July). Map created at http://climexp.knmi.nl/.

4.4 Coral Sr/Ca ($\delta^{18}O$) and ENSO

The geographical location of Tahiti in the tropical Pacific more or less directly at a zero line of the ENSO-induced SST and rainfall anomalies should make it really difficult to obtain a reliable record of past ENSO events from Tahiti corals.

We computed spatial correlations of Tahiti SST and Sr/Ca$_{TH12B}$ with the SST field in the tropical Pacific using the KNMI time series analysis page (http:/climexp.knmi.nl/) (Oldenborgh and Burgers, 2005). The correlation between Tahiti-SST and tropical Pacific SST shows the tropical El Niño pattern. Correlations are positive in the subtropics and negative in the eastern equatorial Pacific and the WPWP (Figure 5.8). However, Tahiti lies

close to the zero line of the ENSO-related SST anomaly response, where correlations change from positive to negative (Figure 5.8). Sr/Ca shows more or less the same correlation pattern (that the correlation coefficients have opposite signals because of the inverse relationship of coral

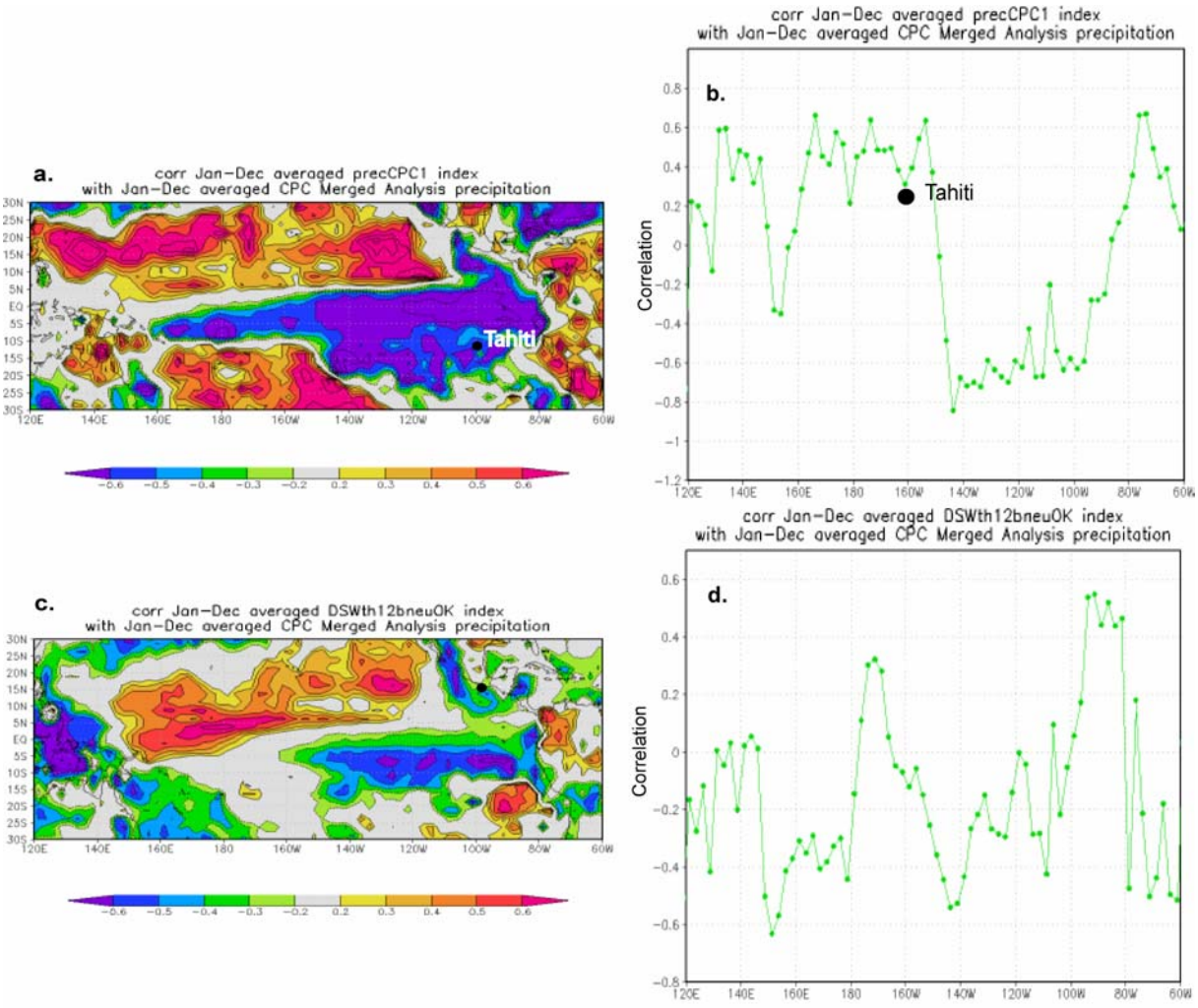

Figure 5.9. (a) Field correlation of precipitation at Tahiti (149°2 W 17°4 S) and precipitation field in the tropical Pacific. (b) Cross section showing correlation coefficients at 17°4 S. (c) Field correlation of $\delta^{18}O_{sw}$ derived from paired coral $\delta^{18}O$ and Sr/Ca with precipitation field in the tropical Pacific. (d) Cross section showing correlation coefficients at 17°4S. Tahiti location is indicated by a black dot. Precipitation data is taken from the Climate Prediction Center (CPC) (Xie and Arkin, 1996).

Sr/Ca with local SST). Correlation coefficients are negative in the subtropical and positive in the WPWP. However, the correlation of Sr/Ca with SST in the eastern equatorial Pacific is weak, while correlations in the WPWP are higher. Again, Tahiti lies close to the zero line of the SST anomaly response where correlations change from positive to negative. This should make it difficult to obtain a clear ENSO signal from SST or SST reconstruction of Tahiti.

To asses the spatial coherence between $\delta^{18}O_{sw}$ and precipitation, we do a field correlation of $\delta^{18}O_{sw}$ derived from paired coral $\delta^{18}O$ and Sr/Ca from Tahiti cores and precipitation in the tropical Pacific. The results do not shown clear ENSO pattern and in the southern Pacific, where Tahiti is located the correlation is low (Figure 5.9). Higher precipitation leads to a depletion in the oxygen isotopic composition of seawater and to a freshening (=lower salinity) of surface waters (Fairbanks et.al, 1997). If we assume that the oxygen isotopic composition of seawater is recorded by coral $\delta^{18}O$, coral $\delta^{18}O$ (and $\delta^{18}O_{sw}$ inferred from paired proxies) could also record ENSO-induced precipitation anomalies. A field correlation of precipitation

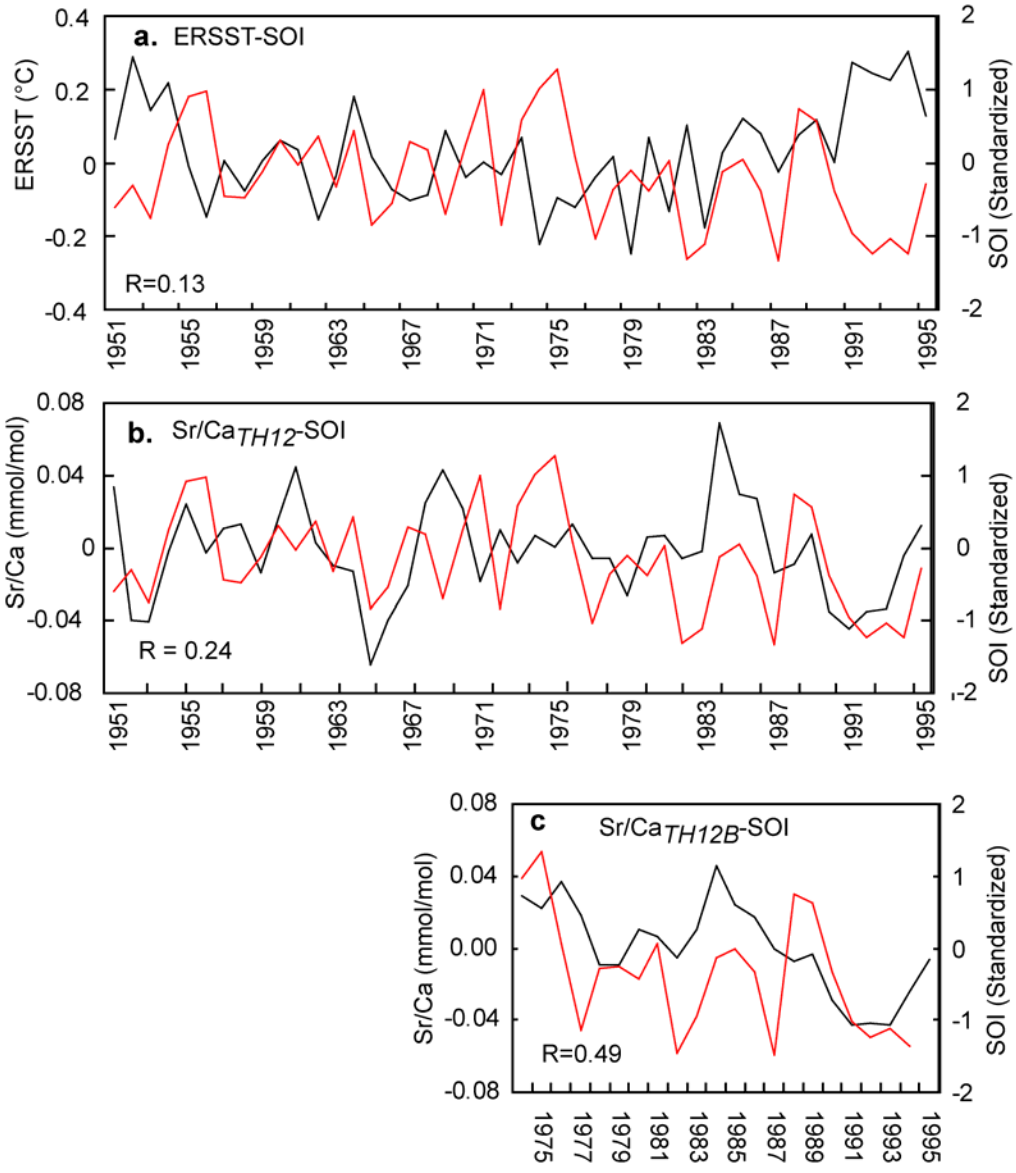

Figure 5.10. Annual mean (January-December) of (a) SST (ERSST) (black line), (b) Sr/Ca of TH1 and TH2 average (black line), (c) average Sr/Ca of TH1, TH2 and TH1B (black line) and annual mean of SOI (red line).

data from Tahiti (149°2 W 17°4 S) with the precipitation-field of tropical Pacific (data from Climate Prediction Centre (CPC) (Xie & Arkin, 1996) shows the tropical pattern of the ENSO-induced rainfall anomaly response in the tropical Pacific. However, Tahiti is located close to zero line of the ENSO-induced rainfall anomalies, where correlations change from negative to positive (Figure 5.9a). We also computed correlations between annual mean $\delta^{18}O_{sw}$ and precipitation in the tropical Pacific (Figure 5.9c). The pattern is similar to the pattern obtained with instrumental data.

The cross section map along 17°4 S showing the correlation of Tahiti $\delta^{18}O_{sw}$ and precipitation, again shows that Tahiti lies close to zero line (Figure 5.9b, d). A negative correlation is obtained in the region extending from the western coast of south America to the central tropical Pacific, the center of ENSO, while positive correlations are obtained in the north-western equatorial Pacific (Figure 5.9). These results suggest that $\delta^{18}O_{sw}$ inferred from Tahiti corals could record ENSO-related precipitation (salinity) changes. However, the fact that Tahiti lies close to the zero line of the ENSO pattern should make it difficult to use these cores as monitors of past ENSO archives.

Further asses the ability of coral Sr/Ca to capture ENSO related SST, we correlate the proxy with Southern Oscillation Index (SOI) and the Niño 3.4 index. The time series are averaging over 12 months. On longer time scales, we use the averaged TH1 and TH2 record and for shorter periods (back until 1974) the averaged TH1, TH2, TH1B record. For the 1951-1995 calibration periods, the highest correlation of Sr/Ca_{TH12} vs. SOI is obtained for annual means taken from January-December (R = 0.24). For the period of 1974-1995, we found a higher correlation of Sr/Ca_{TH12B} -SOI (R= 0.49) (Figure 5.10). The largest Sr/Ca variation changes are found during the El Niño of 1982-1983, and during the El Niño of 1991 which apparently lead to large changes in SST at Tahiti. Grid- SST at Tahiti also shows a low correlation with the SOI (R= 0.08-0.1) (Figure 5.10a). This confirms that the ENSO signal can not be clearly captured in coral Sr/Ca from Tahiti. However, spectral analysis of coral Sr/Ca_{TH12} does show significant coherence with the SOI in the frequency band of 0.18 cycle/yrs (5.5 yrs) (Figure 5.11). Similar results are obtained using wavelet coherence analysis, which also show that Sr/Ca is coherent with the SOI at periods of 4-8 years.

We also correlate the coral proxy with the Niño 3 and 3.4 indices, which capture the SST anomalies in the eastern equatorial Pacific. Ideally since SST anomalies (SSTa) in the Niño 3.4 and Niño 3 region are very similar, the correlation of any time series with both indices should be very similar. However, it was suggested that the Niño 3.4 index is a more robust index of ENSO, since the standard deviation of the monthly Niño 3.4 index (0.77°C) is lower than the standard deviation of the Niño 3 index (0.79°C) (Trenberth, 1997). For the 1974 to 1995 period, the correlation of Sr/Ca_{TH12B} vs. Niño 3.4 is computed for 4 months averages (all

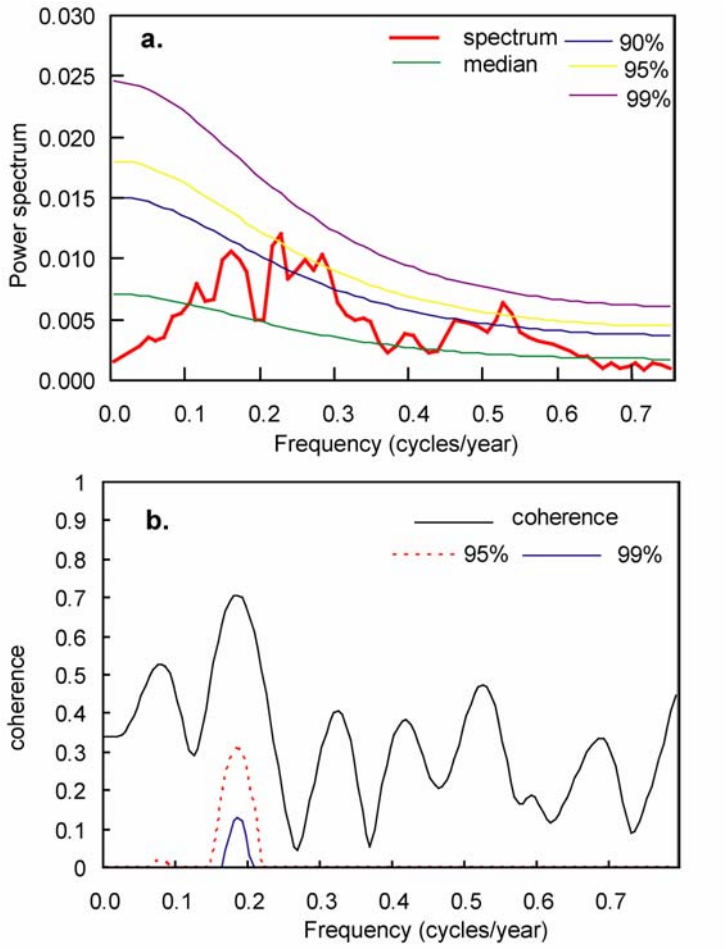

Figure 5.11 (a) MTM single spectrum analysis of Sr/Ca_{TH12}. Significant power is centered at 0.22 cycles/year (4.5 yrs), 0.25-0.3 cycles/year (4-3 yrs) and 0.53 cycles/year (1.8 yrs). (b) Coherency spectrum between SOI and Sr/Ca_{TH12}, showing significant coherency in the frequency band of 0.18 cycles/yr (5.5 yrs).

months). The correlation ranges from R = 0.18 to 0.51. The highest correlation is obtained for the January to April averaged (R =0.51). Similarly, for the 1974 to 1995 period the SST (ERSST) dataset for Tahiti (149°2S 17°4 S) shows an even lower correlation with Niño 3.4 (R = 0.01 -0.36) than coral Sr/Ca- Niño 3.4. For the 1923 to 1995 period, the correlation of Sr/Ca_{TH12} vs. Niño 3.4 is low (R = 0.1-0.3), similarly it is shown by the SST dataset (R= 0.1-

0.4) (Figure 5.12). For annual mean scale, 1923-1995 period, the correlation of Sr/Ca_{THI2} vs. Niño 3.4 is low (R=0.2-0.23), SST shows even a lower correlation (R = 0.13-0.17) (Figure 5.12). The correlation of coral $\delta^{18}O$ with Niño 3.4 is also low for any time period (R=0.054-0.17).

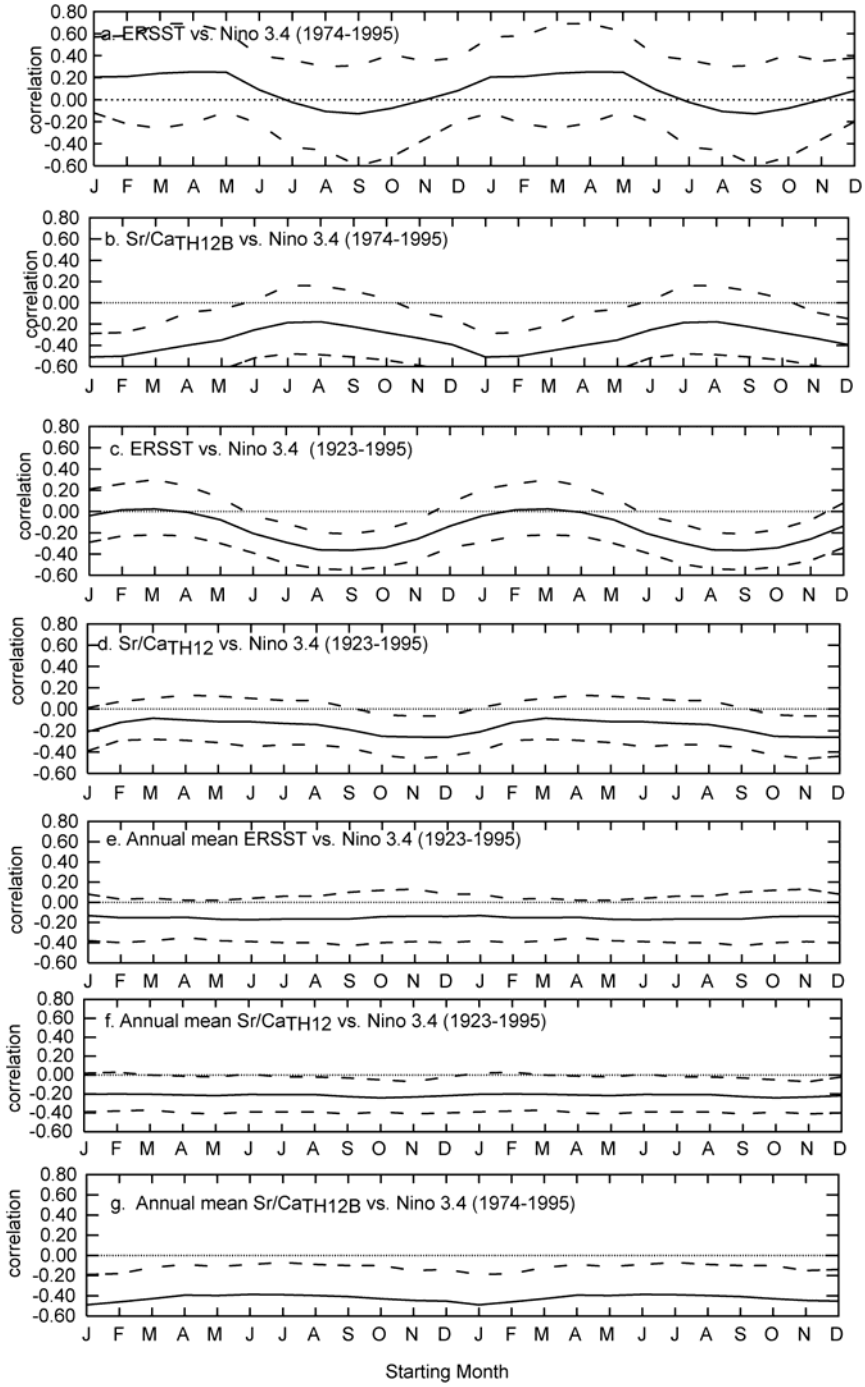

Figure 5.12 (a) Correlation of ERSST vs. Niño 3.4 and (b) of Sr/Ca_{THI2B} vs. Niño 3.4 for the period 1974-1995, 4 months running averages. (c) Correlation of ERSST vs. Niño 3.4 for the periods 1923-1995 and (d) of Sr/Ca vs. Niño 3.4 for the period 1974-1995, 4 months running averages. Correlation of annual mean (e) ERSST vs. Niño 3.4, (f) Sr/Ca_{THI2} vs. Niño 3.4 and (g) Sr/Ca_{THI2B} vs. Niño 3.4. The band around the correlations (solid black lines) indicates the 95% confidence limits (dashed line).

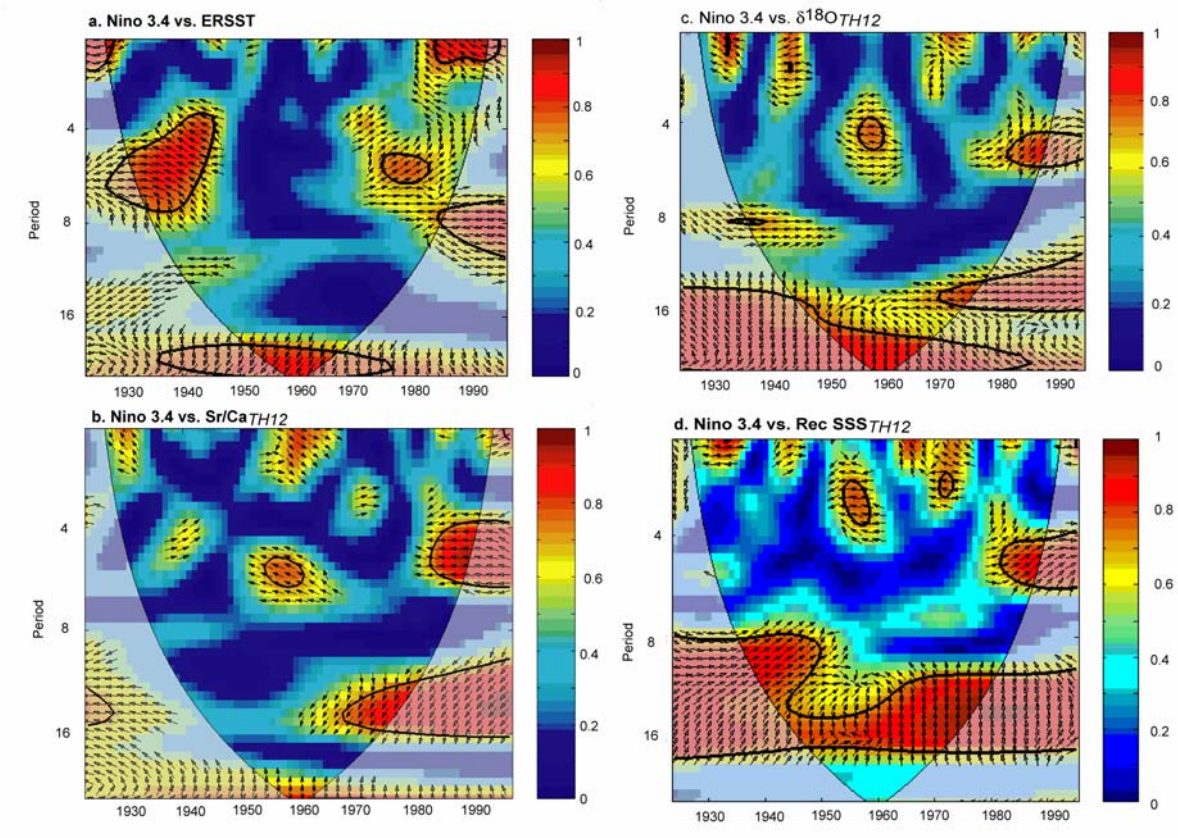

Figure 5.13 Wavelet coherence between the Niño 3.4 index and (a) ERSST, (b) Sr/Ca_{TH12} ,(c) $\delta^{18}O_{TH12}$, and (d) Reconstructed SSS. The data is processed using the wavelet coherence package from Grinsted et al. (2004) (see text for discussion). The thick black contour indicates the 5% significance level against red noise. The relative phase relationship is shown as arrows (with in-phase pointing right, anti-phase pointing left and Niño 3.4 leading salinity by 90° pointing straight down). Note: the large coherency between reconstructed SSS and the Niño 3.4 index at decadal/interdecadal periods.

The results of the correlation analysis above show that coral Sr/Ca from Tahiti is a poor recorder of ENSO, which is confirmed by the low correlation of Tahiti SST with ENSO indices. Furthermore, Tahiti coral Sr/Ca shows non-systematic changes of SST during ENSO years (Figure 5.14c,d). Tahiti is located in a transitional zone, i.e., Tahiti lies close to the zero line of the ENSO related-SST anomalies in the tropical Pacific and also at the eastern border of south western Pacific salinity front (Gouriou and Delcroix, 2002). The displacement of the salinity front due to precipitation and SST variations in the SPCZ during the ENSO years alter the SSS and SST in Tahiti region. Thus, surface water at Tahiti are influenced by complex processes, and not only by atmospheric phenomena, but also by oceanic advection. Thus, each ENSO event can leave a different signature at Tahiti (e.g. positive or negative SST/SSS anomalies). The wavelet cross coherence between Sr/Ca and Niño 3.4 (Figure 5.13) shows that the two signals are coherent at 4-8 yrs and 8-16 yrs periods. Similarly, the SST shows

significant coherence with Niño 3.4 at the 4-8 yrs and 8-16 yrs periods. The large coherence in decadal/interdecadal periods is shown between reconstructed SSS and Niño 3.4 (Figure 5.13d).

We correlate the Sr/Ca_{TH12B} with Niño 4 index. We compute 12 months averages for all month. For 1974-1995 periods, the annual mean correlation of Sr/Ca_{TH12B} - Niño 4 ranges from R= 0.6 to 0.7 (Figure 5.14b). High annual mean correlations are obtained for October-September averages to January-December averages. The highest correlation between coral Sr/Ca_{TH12B} - Niño 4 is obtained by averaging January to December (R=0.7). For 1923-1995 periods, the correlation of Sr/Ca_{TH12} - Niño 4 for monthly means is low (R= 0.1-0.3). The highest correlation is obtained for January (R=0.3). The annual mean correlation for 1923-1995 periods of Sr/Ca_{TH12} with Niño 4 is low (R= 0.24-0.3). For period 1923-1995, the annual mean correlation between coral $\delta^{18}O_{TH12}$ vs. Niño 4 is low (R=0.22-0.25). We suggest that involving horizontal record of TH1B, the high correlation of Sr/Ca- Niño 4 can be obtained. However, the annual mean correlation of Tahiti coral Sr/Ca vs. Niño 4 is statistically significant (Figure 5.14a,b). In the short time window (1974-1995) used for calibration, Sr/Ca vs. Niño 4 shows an even higher correlation than Sr/Ca vs. Niño 3.4. The leading mode of SST variability in the western equatorial Pacific (the Niño 4 region) is a decadal mode (Lohmann and Latif, 2005). The higher correlation of coral Sr/Ca from Tahiti with Niño 4 may indicate that coral proxy records from Tahiti may capture decadal variability of the tropical Pacific. Since the leading mode of SST in the Niño 4 region is a decadal mode (Lohmann and Latif, 2005), we also correlate the corals time series with Niño 4 index. The running correlation of coral Sr/Ca ($\delta^{18}O$) computed with a 21 years running window is low for annual averages (Figure 5.14).

4.5 Interdecadal coral Sr/Ca ($\delta^{18}O$) variations

Sr/Ca of Tahiti corals show a better correlation with SST in the subtropics and the WPWP, than with the eastern equatorial Pacific. The correlation with the Niño 4 index also higher than the correlation with Niño 3 and Niño 3.4. The leading mode of SST variability in the Niño 4 region is decadal mode, so the Tahiti corals may record decadal variability of the Pacific oceans. To further evaluate the decadal signal in the Tahiti coral Sr/Ca ($\delta^{18}O$) records, we correlate coral Sr/Ca ($\delta^{18}O$) with the Pacific Decadal Oscillation (PDO) index (The PDO index is the leading principle componen of monthly SST anomalies in the North Pacific Ocean, poleward of 20°N (see detail in Zhang et al., 1997; Mantua et al., 1997). We compute

running correlations of Sr/Ca vs. PDO using 21 years running windows. The correlation is low in the most recent decade. An increasing positive and statistically significant correlation is found from 1950 backward. The ERSST data for Tahiti vs. PDO mirrors the Sr/Ca vs. PDO

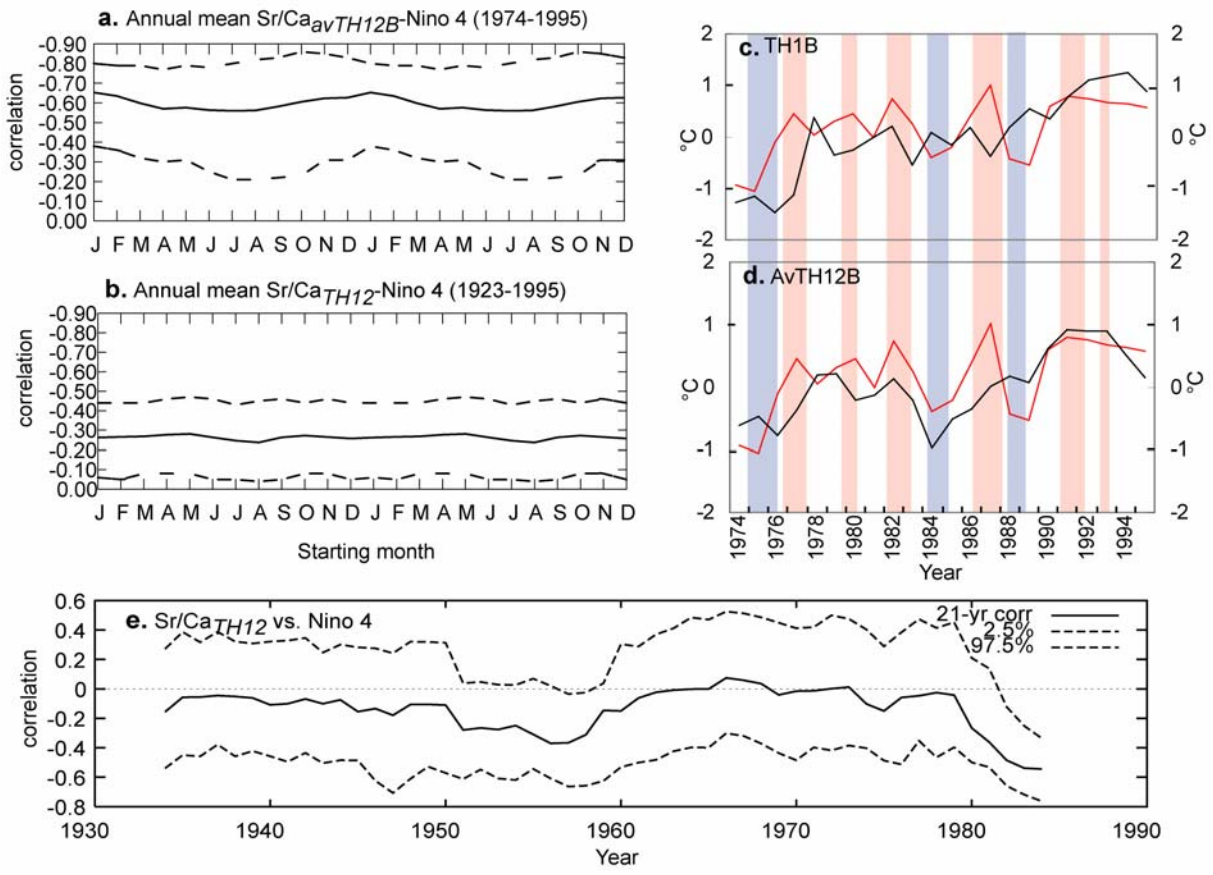

Figure 5.14. Annual mean correlation of (a) Sr/Ca$_{TH12B}$- Niño 4 index for the period 1974-1995, (b) of Sr/Ca$_{TH12}$-Niño 4 index for the period 1923-1995 period. (c) Annual mean reconstructed SST$_{Sr/CaTH1B}$ (black line), and Niño 4 index (red), (d) reconstructed SST$_{Sr/CaTH12B}$ (black) and Niño 4 (red). ENSO years are indicated by red (El Niño event) and blue shading (La Nina event) according to Trenberth (1997). (e) Running correlation of Sr/Ca$_{TH12}$ and Niño 4 for annual means computed from January to December, 21 year running window.

correlation, which shows the same increasing correlation with PDO from 1950 backward (note that the sign of the correlation is opposite to Sr/Ca-PDO correlation due to the inverse correlation of Sr/Ca with local SST). This confirms the running correlation of Sr/Ca vs. PDO reflects the correlation of SST at Tahiti with PDO. The runnning correlation of coral $\delta^{18}O$ vs. PDO shows a similar correlation pattern as Sr/Ca vs. PDO prior to 1970, and a generally higher correlation with PDO than Sr/Ca. The highest correlation of coral $\delta^{18}O$ vs. PDO is found near the core top (1970-1995), we also find a high correlation between reconstructed SSS vs. PDO in this interval (Figure 5.15). The global wavelet power spectrum of these two proxies does not show significant variability at decadal periods. However, the ~ 72 year

records of coral Sr/Ca ($\delta^{18}O$) are not long enough to asses the statistical significance of the spectral peak at interdecadal periods.

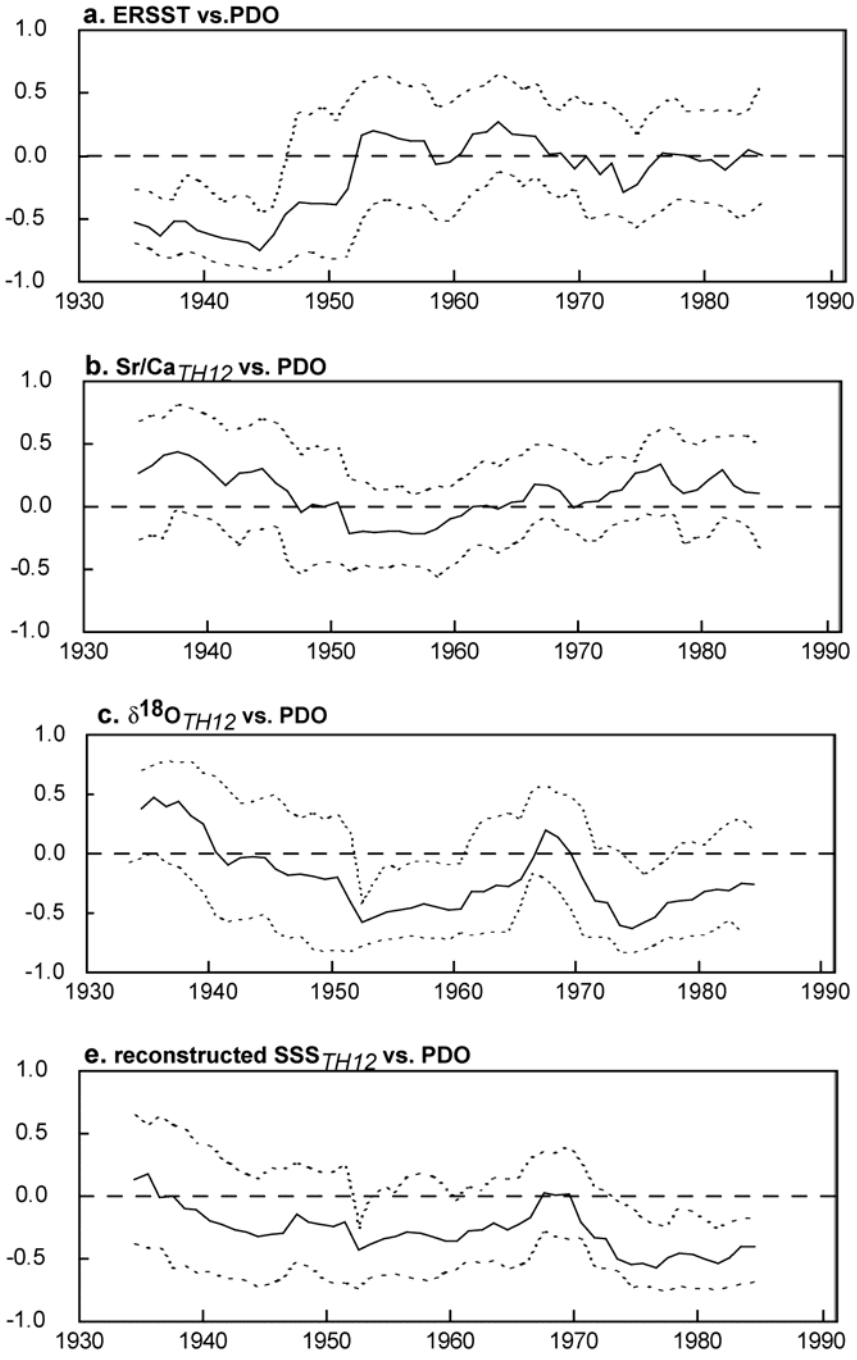

Figure 5.15. Running correlation of (a) ERSST-PDO and (b) Sr/Ca$_{TH12}$-PDO (c) $\delta^{18}O$ -PDO and (e) reconstructed SSS-PDO for 12 months averages (January-December), 21 years window.

The running correlation for 21 years window shows that the correlations of Sr/Ca (ERSST) vs. PDO becomes stronger prior to 1960 (Figure 5.15a,b). These results are consistent with the observations of Folland et al. (2002), who reported a higher variability in the position of the SPCZ prior to 1945. The correlation of Sr/Ca_{TH12}-PDO near the core top (1970 to present) is low, similarly the correlation of the ERSST-PDO. The correlation of $\delta^{18}O_{TH12}$-PDO is low for the period ±1965-1970 (Figure 5.15c). Reconstructed SSS - PDO correlation pattern is similar with the correlation pattern of $\delta^{18}O_{TH12}$ -PDO (Figure 5.15d). Only for the period from 1965 to 1970, the correlation of reconstructed SSS -PDO is weak. However the Reconstructed SSS - PDO correlation seems to be higher than Sr/Ca-PDO correlation. These results suggest that decadal-scale SSS variations in this region are proportionaly larger than decadal SST variations.

5. Conclusions

The correlation of Sr/Ca of Tahiti corals with SST on a monthly and annual mean scale confirms that Sr/Ca is a good proxy for temperature. By adding statistically uncertainties to the slope estimate, the regression slope of coral $\delta^{18}O$-SST in a multiple regression $\delta^{18}O$ vs. SST,SSS is in agreement with published slope estimates for $\delta^{18}O$ - SST (-0.18- -0.22 ‰/°C). This confirms that coral $\delta^{18}O$ records SST and seawater $\delta^{18}O$ (SSS).

The variance of annual mean reconstructed SST from Tahiti coral Sr/Ca is larger than the variance of grid- SST. It is difficult to infer the magnitude of regional SST variations from Tahiti corals in pre-instrumental times.

The potential of coral Sr/Ca ($\delta^{18}O$) to record past ENSO variations is low. There are no systematic changes of Sr/Ca with respect to the SST anomalies in the Niño 3.4 region. This should be taken into account when attempting to reconstruct ENSO from fossil corals drilled at Tahiti. Tahiti is located in a transitional zone between the fresh, warm waters in the western Pacific warm pool and the saltier, colder waters from the southern central Pacific, and lies close to the zero line of SSTa during ENSO years. Therefore, the ENSO signal can not be reliably recorded in coral proxies from Tahiti even if individual El Niño events may lead to large SST anomalies. However, for period 1974-1995 coral Sr/Ca records from Tahiti do show a relationship with SST anomalies in the Niño 4 region on the interannual time scales. In Niño 4 region, the leading mode of SST variability is a decadal mode, and this signal can

be captured in the proxy records from Tahiti. However, our proxy is too short to asses the statistical significance of spectral peaks at decadal periods.

The correlation of Sr/Ca_{TH12} with the PDO is low, similarly shown by instrumental SST. Reconstructed SSS, calculated from coral Sr/Ca and $\delta^{18}O$, shows the higher correlation with the PDO index than the correlation of Sr/Ca-PDO. This suggests that at decadal timescales the SSS signal is proportionally stronger than the SST signal, and is best resolved in reconstructed SSS ($\delta^{18}O_{sw}$). Besides, reconstructed SSS shows coherency with Niño 3.4 at decadal periods.

Acknowledgements

We are grateful for the support of the *Deutscher Akademischer Austauschdienst* (DAAD) (grant A/02/21403) and the *Deutsche Forschungsgemeinschaft* (Leibniz award to Prof. Wolf-Christian Dullo). We are grateful to Oliver Timm for discussion.

CHAPTER VI

Paired coral $\delta^{18}O$ and Sr/Ca measurements at a Timor coral: salinity variations in an exit passage of the Indonesian Throughflow

Abstract

$\delta^{18}O$ and Sr/Ca ratios have been analyzed at a 180 cm coral core (*Porites*) from Timor (Indonesia). The coral core extends from 1914-2004. Measured coral Sr/Ca is a good proxy for temperature, and correlates well with grid SST on a monthly (R = 0.62-0.67) and annual mean scale (R = 0.51-0.54). The monthly correlation of Sr/Ca with local SST measured at Ombai strait is high (R = 0.89). High resolution SST data from satellite measurements (AVHRR) also show high correlation with coral Sr/Ca ratios. Seasonal SSS variations at Timor can be reconstructed from paired coral $\delta^{18}O$ and Sr/Ca measurements. Reconstructed SSS shows a good correlation (R= 0.5) with SSS from the SODA dataset for the period 2000-2004. Coral Sr/Ca shows a significant coherence with Niño 3.4 in the interannual periodicity band. The strong El Niño of 1982/1983 is more easily identified in Timor coral Sr/Ca than the El Niño of 1997/1998. During the El Niño of 1997/1998, the Timor waters are saltier than normal. This is also shown by reconstructed SSS based on coral $\delta^{18}O$ and Sr/Ca measurements, although the magnitude is much smaller than measured SSS at Ombai.

1. Introduction

Indonesia is located in the Western Pacific Warm pool (WPWP), which plays an important role in the global climate system. This region is a major exporter of latent heat to the northern and southern hemisphere. The transport of warm water in and out of WPWP is thought to play an important role in the global climate and also in the modulation and termination of warm El Niño Southern Oscillation (ENSO) events (e.g. Peixoto and Oort, 1992). The exchange of Pacific and Indian Ocean waters through the Indonesian seas, what so called Indonesian Throughflow (ITF) (Figure 6.1) affects both ENSO and the Australasian monsoon (Gordon et al., 2004). On a seasonal scale, the climate of Indonesia is influenced by the Australasian monsoon.

The seasonal movement of the intertropical convergence zone (ITCZ) across the equator causes differences in air pressure between the Asian continent and Australia that shift every 6

months cause a seasonal reversal of the monsoon winds over Indonesia, which in turn drive the surface water currents. The latter influence sea surface temperature (SST) and sea surface

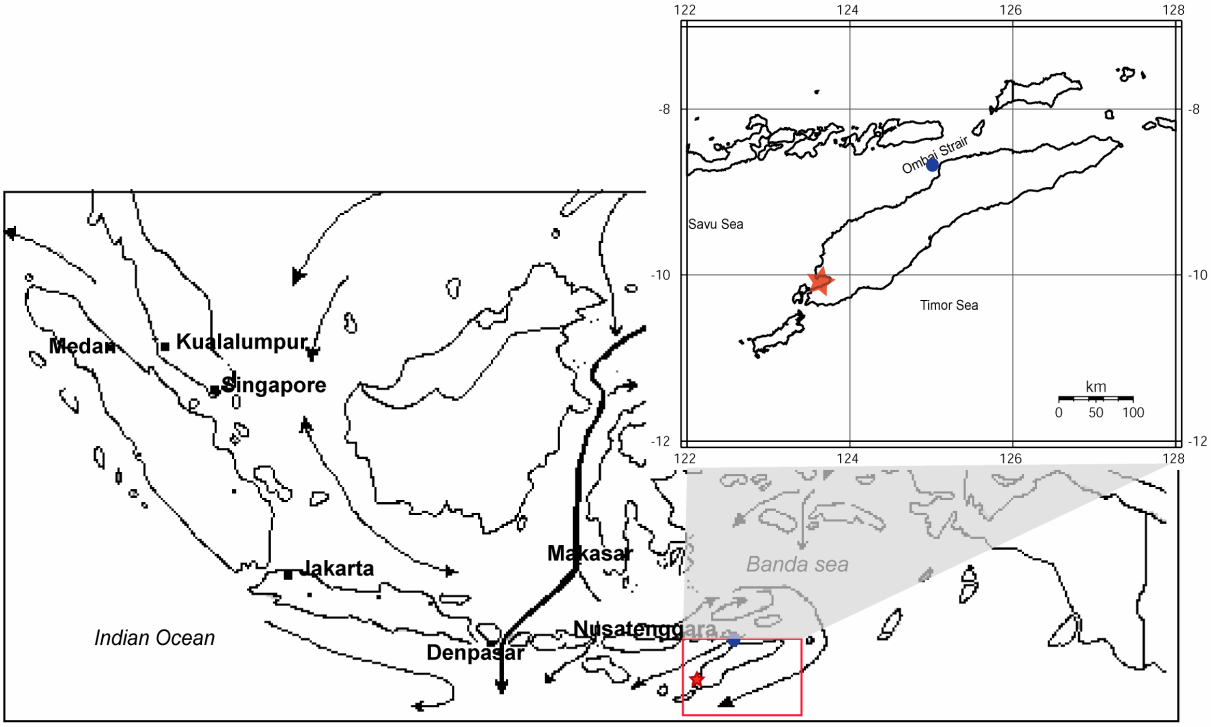

Figure 6.1. Map of Indonesia showing the surface currents of the Indonesian Throughflow (arrows) and the drilling location of KP1 (red star) at Kupang bay (Timor) (inset). SSS measurements were made at Ombai, indicated by the blue dot (Sprintall et al., 2003).

salinity (SSS). On an annual mean scale, the Indonesian region experiences warm and wet conditions. Lowest salinity is found in the western part of Indonesia extending from the Java sea to the South China sea. In the Banda sea, to the north-east of Indonesia, the water is saltier (Figure 6.2). During northern hemisphere summer the Southeast monsoon (SE monsoon) prevails over Indonesia. The SE monsoon is the dry season. The Northwest monsoon (NW monsoon) prevails during northern hemisphere winter and is the rainy season. During the NW monsoon the winds blow from northwest, and the low salinity water from the South China sea and the Java sea move to the southeast of the Indonesian Sea and into the ITF. During the SE monsoon, the prevailing winds blow from Australia, pushing the low salinity waters back into the Java and South China Sea (Gordon et.al., 2004). This water movement influences SSS in the ITF passages. However, in the exit passages of Timor (Ombai strait, Savu sea, Timor sea) (Figure 6.1) the salinity is lower during the SE monsoon than during the NW monsoon. However, the SSS differences between the two season are not very large (Figure 6.3). SST in the Timor region drops as the sun migrates further to the north during the SE monsoon (June-September). This reduces evaporation and as the ITCZ passes over and into the Banda sea rainfall increases. During the NW monsoon the ITCZ moves over northern Australia. In the

NW monsoon season, water vapor evaporated from the warm waters of Timor is transported into northern Australia and induces the rainy season in this region. The changing SST and the position of ITCZ could be sufficient to lead to the observed SSS pattern. However, the complex ocean-atmospheric interaction in the region of Timor makes this region interesting for a detailed climatic study. Coral skeletons contain a suite of isotopic and trace elemental indicators of environmental changes in the tropical ocean. These can be used to reconstruct important climatic variables such as sea surface temperature (SST) and sea surface salinity (SSS) over the past centuries (e.g Beck et al., 1992; Gagan et al., 2000; Ren et al., 2002; Marshall and McCulloch, 2002; Fallon et al., 2003; Mitsuguchi et al, 2003; Kilbourne et al., 2004). Coral $\delta^{18}O$ shows SST and seawater $\delta^{18}O$ variations (Ren et al., 2002; Pfeiffer et al., 2004b; Correge et al., 2004), while coral Sr/Ca shows SST only (Beck et al., 1992; McCulloch et al., 1994; Shen et al., 1996; Alibert and McCulloch, 1997; Marshall and McCulloch, 2002). Paired measurements of coral $\delta^{18}O$ and Sr/Ca are used to reconstruct seawater $\delta^{18}O$ (e.g. Gagan et al., 1994, 1998; Ren et al., 2002). Several coral studies have shown that coral proxies record ENSO (Charles et al., 1997; Cobb et al., 2003a; Kilbourne et al., 2004; Zinke et al., 2004; Timm et al., 2005) and decadal ENSO-like variability (Hughen et al., 1999; Correge et al., 2000; Cobb et al., 2001).

At present there are no continuous paired coral $\delta^{18}O$ and Sr/Ca records from the exit passages of the ITF. Charles et al. (2003) only analyzed coral $\delta^{18}O$ and had problems with the $\delta^{18}O$-SST calibration. Abram et al. (2003) measured coral cores drilled at Sumatra, which are not influenced by the Indonesian Throughflow.

Here we present the first paired coral $\delta^{18}O$ and Sr/Ca record from one of the exit pasages of the ITF (Figure 6.1). Sr/Ca is used to reconstruct SST. We will use coral Sr/Ca to examine the impact of El Niño in Indonesia. The El Niño signal in Indonesia is clearly identified in instrumental oceanographic/climatic data from Indonesia (e.g. Aldrin and Susanto, 2003), and we expect that the El Niño signal will be shown by the coral Sr/Ca. We also reconstruct SSS using paired coral $\delta^{18}O$ and Sr/Ca measurements, which will improve our understanding of the oceanic processes in this area.

2. Climatic and oceanographic setting

The WPWP is characterized by the warmest surface ocean waters of the earth (Levitus et al., 1994) and drives the tropical atmospheric circulation. The influence of large-scale climate

phenomena varies across the Indonesian region due to island topography and/or ocean-atmosphere fluxes. Based on climatological data (1979-2002) the annual mean SST in the Indonesian region varies from 27°C to 30°C with precipitation above 6.5 mm/day over most of Indonesia (Figure 6.2). Annual mean SSS from Levitus et al. (1994) varies from 32 psu to 35 psu (Figure 6.2) in Indonesian region.

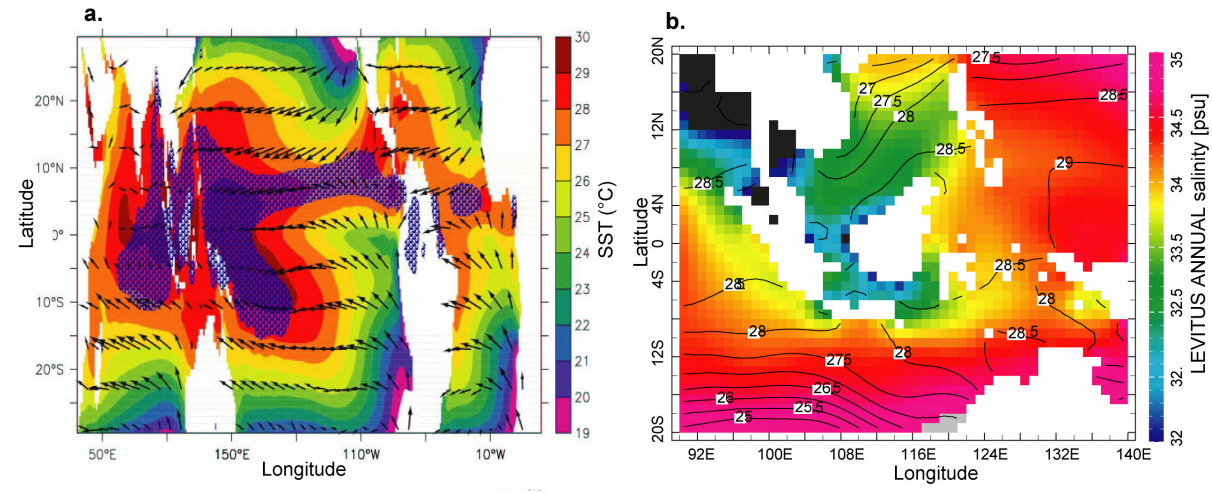

Figure 6.2. (a) Annual mean climatological surface conditions for the period of 1979-2002: SST (colors), wind (vectors) and precipitation higher than 6.5 mm/day (cross-hatched in blue). (b) Annual mean SSS (colors) and SST (contours) from Levitus et al. (1994).

During the NW monsoon (December-March) the northeasterly winds blow north across the equator. SST in Indonesia ranges between ~28.5°C-30°C. During the SE monsoon (June-September), when the prevailing winds blow northwestward from Australia SST ranges between ~26°C-29°C (Figure 6.3a). Precipitation is above 6.5 mm/day over all of Indonesia during the NW monsoon, while during the SE monsoon the precipitation is lower in central-eastern Indonesia. During the SE monsoon, low salinity waters are found further to the east in the Banda sea (Figure 6.3b). At the same time the warmer SSTs in southern Java-Nusatenggara (northern Australia) expand further to the north. During the NW monsoon, the northwesterly winds push the low salinity water from the South China Sea into the Makassar Strait of the ITF main exit passage. This low salinity water is pushed back northwestward to the South China Sea by the southeasterly winds of the following SE monsoon (Gordon et al., 2004) (Figure 6.3c).

The coral was taken from Timor (Indonesia), and is located in Ombai passage (see Figure 6.1). Therefore, SST and SSS may be influenced both by oceanic advection and atmospheric phenomena (e.g. ITCZ movement or monsoon). In the Timor region, SST is high (29°C-30°),

and precipitation is above 6.5mm/day during the NW monsoon. In the transitional period between the NW to the SE monsoon (April-June), Timor SST ranges from 27°C-28°C, and the precipitation is lower. Lowest SSTs occur in the SE monsoon and range from 26°C-

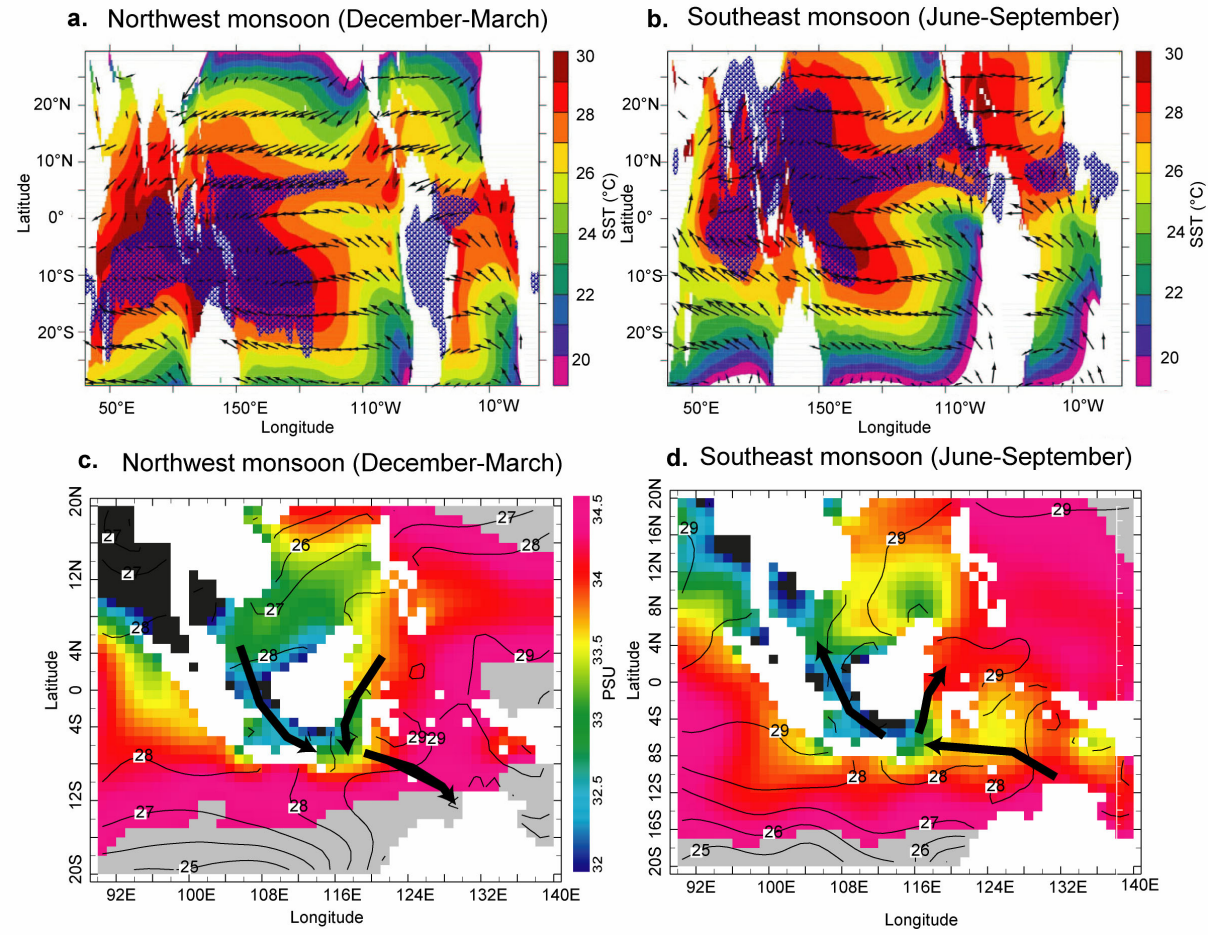

Figure 6.3. Seasonal mean of climatological surface conditions (1979-2002): (top) SST (colors), surface winds (vectors), precipitation 6.5 mm/day (cross-hatched in blue). (bottom) SSS (Levitus et al., 1994) and movement of low salinity waters along the path of Indonesian Throughflow (black arrows)(Figure 6.3c,d redrawn after Gordon et al., 2004). (a) NW monsoon, (b) SE monsoon, (c) NW monsoon, and (d) SE monsoon.

27°C. During the transition from the SE to the NW monsoon (October-December), mean SST at Timor is high (29°C-30°C), and precipitation remains lower than 6.5 mm/day. Climatological salinity data from Timor suggests that SSS is not governed by the precipitation-evaporation balance (Figure 6.4). Maximum SSS (Levitus et al., 1994) occurs in January and minimum SSS is in May, while local precipitation maxima (data from the National Centers for Environmental Prediction (NCEP)) occur in February and minima in April (Figure 6.4). Monthly mean SST at Timor is obtained from the Extended Reconstructed global Sea Surface Temperature (ERSST) dataset (Smith and Reynolds, 2004). Maximum SST is found in December and minimum SST in August (Figure 6.4). The annual cycle

dominates the SST and SSS signal: warmest temperature occurs during the NW monsoon and a distinctive freshening is found in March-May (Sprintall et al., 2003). During the El Niño of 1997/1998, the region is cooler and saltier than normal caused by below-average regional precipitation as well as lower transport of fresh warm Throughflow waters in the region (Sprintall at al., 2003).

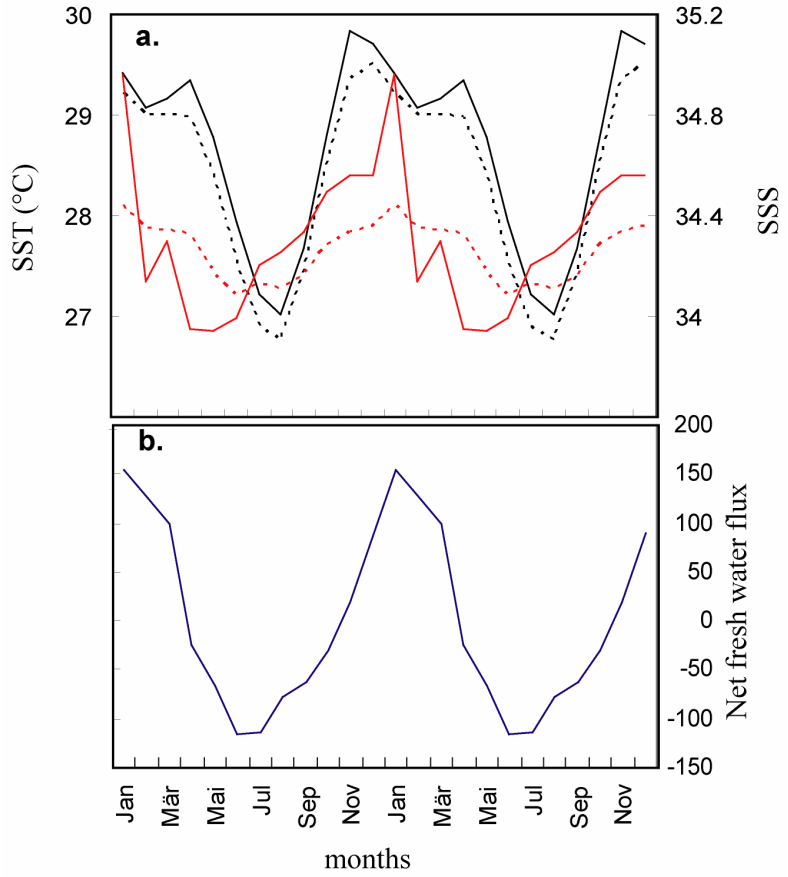

Figure 6.4. (a) Climatological data of SST: ERSST (black dashed line) and NCEP (black solid line), SSS from Levitus et al. (1994) (red solid line) and SODA (combined v.142 and v.143) (red dashed line). (b) Net fresh water flux from Oberhuber (1988).

3. Material and methods

A 180 cm long core (KP1) from a massive colony of *Porites sp*. was drilled in Kupang bay, west Timor island (Indonesia, 10°12'S 123°31'E) in June 2004. The living surface of the colony was about ± 3 m below sea level. The core was cut into 4 mm thick slabs. These slabs were rinsed in an Ultrasonic bath and dried at 50^{o} C for 24 hours. The X-radiographs of the slabs (Figure 2.1c see Chapter II slabs) show pronounced annual density bands that allow the development of a precise chronology. The average annual extension rate is ca 1-2 cm/year. A sampling transect that follows the main growth axis was selected. Slabs are sub sampled to get coral powder using a drilling bit of 1 mm. Powdered samples are taken every ±1 mm to

obtain monthly resolution. The powdered samples are then splitted for stable isotope ($\delta^{18}O$ and $\delta^{13}C$) and trace element (Sr/Ca ratio) analysis. The Sr/Ca ratios are measured on an inductively coupled plasma optical emission sprectro-photometer (ICP-OES) at the University of Kiel following a combination of the techniques from Schrag (1999) and de Villiers et al. (2002). The relative standard deviation (RSD) of multiple measurements is about 0.15%. The stable isotope composition ($\delta^{18}O$ and $\delta^{13}C$) of the samples is analyzed using a Thermo Finnigan Gasbench II Delta Plus. The isotope ratios are reported in ‰VPDB relative to NBS 19. The analytical uncertainty is ± 0.06 ‰ for $\delta^{18}O$ measurements.

The chronology is constructed based on the seasonal cycle of the Sr/Ca data series. It is assumed that the minimum (maximum) skeletal Sr/Ca corresponds to the maximum (minimum) SST. The maximum (minimum) Sr/Ca is tied to August (December), which is the coolest (warmest) month at Timor. For all other values that are not anchor points, ages are assigned by linear interpolation based on these anchor points. A second interpolation is performed to obtain constant time steps with 12 monthly values. For coral $\delta^{18}O$ the same anchor points as for the Sr/Ca records are used. The results confirm that core KP1 extends from May 1914 until June 2004. The uncertainty of the age model is approximately 2 months in any given year. Figure 6.5 shows monthly time series of coral $\delta^{18}O$ and Sr/Ca measured at KP1.

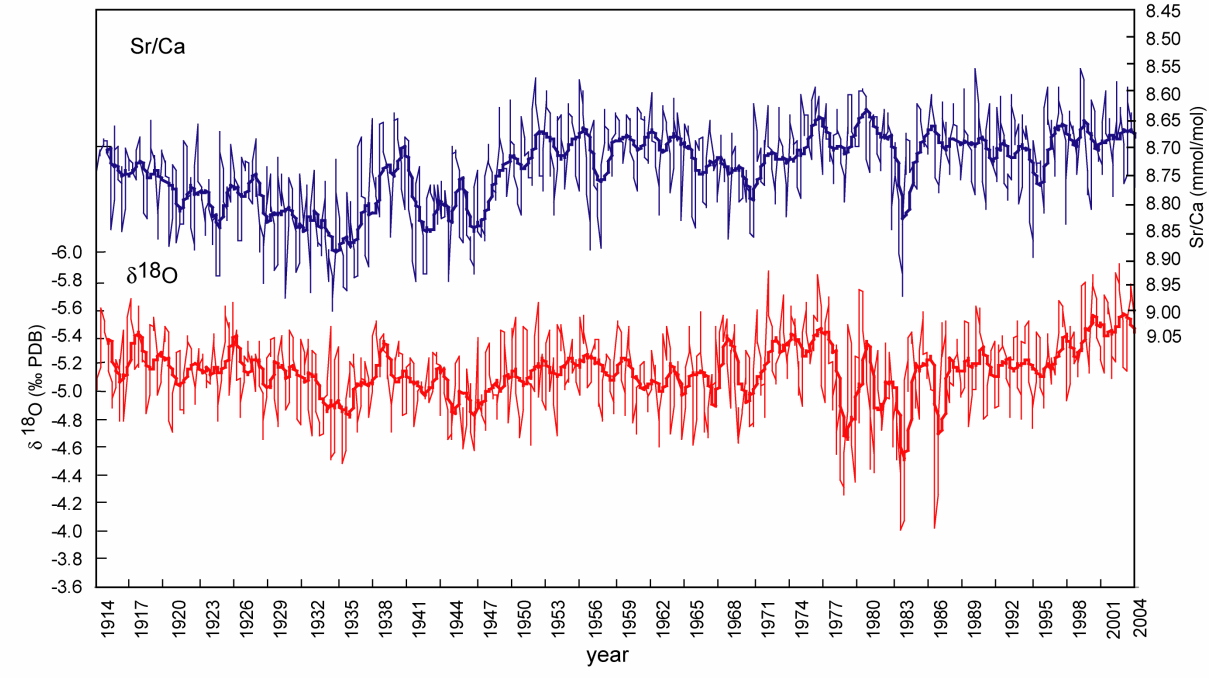

Figure 6.5. Monthly proxy time series of coral $\delta^{18}O$ (red line) and Sr/Ca (blue line) of KP1 from Timor, Indonesia. Bold lines are 12 point running averages.

We use SST from the Extended Reconstructed global Sea Surface Temperature dataset (ERSST) of Smith & Reynolds (2004), the Optimal Interpolation SST from the National Center for Environmental Prediction SST data (NCEP) (Reynold and Smith, 1994), and Advanced Very High Resolution Radiometer SST data (AVHRR) from NASA for calibrating the proxy. The ERSST provides a time series extending from 2004 to 1880 with 2°x2° resolution, while the NCEP data only extends back until 1982. The AVHRR data has a higher spatial resolution (4 km x 4 km) than the ERSST and NCEP datasets. The AVHRR SST is available back until 1985. Local measurements of SST and SSS from Ombai strait (hereafter mention as SSS (SST) Ombai) for the period from January 1996 to March 1998 (Sprintall et al., 2003) are also used in this study. SSS (SST) Ombai is measured data close to the coral site (see Figure 6.1). To calibrate reconstructed salinity from paired coral proxies, we use the grid-data from the reanalysis Simple Ocean Data Assimilation (SODA) model (Carton et al., 2000; Carton & Giese, 2005) which provides the longest monthly time series of sea surface salinity (SSS) available for Timor. SODA is combines field information of temperature, salinity, sea level and wind. The previous version of SODA (v.142) uses the European Center for Medium Range Forecast ERA-40 atmospheric reanalysis. In this version there are possible wind errors in the tropics. To overcome this problem, the latest SODA version (v.143) uses daily wind data from the QuikSCAT scatterometer (Carton & Giese, 2005). We use SODA version 1.4.3 for calibration. Unfortunately the dataset is short (2000 to 2004). To obtain longer SSS time series, we combine both v.142 and 143.

4. Results

4.1 Coral Sr/Ca ($\delta^{18}O$)

Measured coral Sr/Ca of core KP1 varies from 8.556 mmol/mol to 9.003 mmol/mol with a mean value 8.739 mmol/mol. Coral $\delta^{18}O$ varies from -5.94‰ to -4.03‰ with a mean value of -5.17‰. The chronology is determined based on the seasonal cycle of coral Sr/Ca ($\delta^{18}O$), which confirms that the core extents from May 1914 to June 2004.

4.2 Calibration of coral Sr/Ca-SST

Coral Sr/Ca ratios are calibrated with SST from several datasets to estimate the Sr/Ca-SST relationship. SST from the ERSST dataset covers the entire time interval of KP1. SST from the AVHRR has the highest spatial resolution. Local measurements from Ombai strait are available from January 1996 to March 1998 (Sprintall et al., 2003). The calibration equations of Sr/Ca-SST are shown in Table 6.1.

Sr/Ca vs.SST	Regression equation
Sr/Ca - ERSST (1914-2004)	(1) Sr/Ca = -0.05±0.002 SST + 10.148±0.06 (R = 0.6, n = 1082)
Sr/Ca-ERSST(1950-2004)	(2) Sr/Ca = -0.04±0.002 SST + 9.9326±0.06 (R = 0.62, n= 654)
Sr/Ca- AVHRR SST (1985-2004)	(4) Sr/Ca = -0.04±0.002 SST + 9.713±0.07 (R = 0.67, n= 234)
Sr/Ca-Ombai SST (Jan 1996-Mar 1998)	(5) Sr/Ca = -0.06±0.006 SST + 10.277±0.16 (R = 0.89, n= 27)

Table 6.1 Monthly calibration equations of Sr/Ca vs. SST. $p< 0.001$ for all regression equations.

The linear regression of Sr/Ca-ERSST estimated by taking only the maximum and minimum value of the data (e.g. Correge et al., 2004) resulted in Sr/Ca = -0.07±0.04 SST + 10.844 ±0.11 (R = 0.86, p <0.001, n= 108).

For annual mean calibrations, we averaged the Sr/Ca values from September to August of the following year. This resulted in the highest correlation with instrumental ERSST compared to other annual averages. The annual mean calibration of the Timor Sr/Ca record with ERSST (1914-1995 periods) is: Sr/Ca = -0.1±0.02 SST + 11.63±0.47 (R = 0.52, p <0.001, n= 90). For correlation of Sr/Ca with AVHRR SST, the annual mean is taken from March to February: Sr/Ca = -0.04±0.02 SST AVHRR + 9.86±0.43 (R = 0.54 p <0.01 n = 20).

4.3 Calibration of coral $\delta^{18}O$ *-SST*

$\delta^{18}O_{coral}$ is influenced by SST and SST-covariant changes in the isotopic composition of the seawater ($\delta^{18}O_{sw}$). The latter co-varies with salinity (Charles, et al., 1997; Gagan, et al., 2000; Juillet-Leclerc and Schmidt, 2001). The SST contribution $\delta^{18}O_{coral}$ is known as -0.18- -0.22 ‰/°C (Weber and Woodhead, 1972; Gagan et al., 1994; Wellington et al, 1996). The lack of available $\delta^{18}O_{sw}$ data forced most people to use the linear regression of $\delta^{18}O_{coral}$ and SST to represent the relationship of $\delta^{18}O_{coral}$ and SST assuming that $\delta^{18}O_{sw}$ has remained constant. If $\delta^{18}O_{sw}$ and salinity variations influence coral $\delta^{18}O$, the $\delta^{18}O$-SST calibration will have a lower (higher) slope value than expected (e.g. Quinn et al., 1998; Felis et al., 2000).

The monthly $\delta^{18}O_{coral}$ vs. SST calibration of KP1 has a lower slope value (-0.1 to -0.12) than the published slope estimate (e.g Weber and Woodhead, 1972; Gagan et al., 1994; Wellington et al, 1996). The monthly linear regression by taking only the maximum and minimum value of the data (e.g. Correge et al., 2004) resulted in a $\delta^{18}O_{coral}$ - ERSST regression slope of -0. 15 ‰/°C (R = 0.6). Using multiple linear regressions (MLR) model between $\delta^{18}O_{coral}$ and SST, SSS we can take the covariance between SST and $\delta^{18}O_{sw}$ into account. Assuming $\delta^{18}O_{sw}$ is

linearly related to SSS, then the relationship of $\delta^{18}O_{coral}$ and SST can be represented in the MLR of $\delta^{18}O_{coral}$ vs. SSS, SST. The MLR of monthly $\delta^{18}O_{coral}$ vs. SST, SSS is shown in Table 6.2.

$\delta^{18}O_{coral}$ vs SST,SSS	MLR equation
$\delta^{18}O_{coral}$ vs. SSS, SST (SODA v.143) (2000-2004)	(1) $\delta^{18}O_{coral}$ = -0.12±0.02 SST + 0.42±0.14 SSS -16.314 (R = 0.7, n = 53)
$\delta^{18}O_{coral}$ vs. SSS SODA v.143, SST AVHRR (2000-2004)	(2) $\delta^{18}O_{coral}$ = -0.15±0.02 SST + 0.33±0.13 SSS - 12.34 (R = 0.74, n = 53)
$\delta^{18}O_{coral}$ vs. SSS,SST (Ombai)	(3) $\delta^{18}O_{coral}$ = -0.17±0.04 SST -0.01±0.11 SSS - 5.9 (R = 0.69, n = 27)

Table 6.2. Monthly $\delta^{18}O_{coral}$ vs. SSS, SST estimated by MLR model. $p < 0.001$ for all analysis.

The MLR calculated taking only the maximum and minimum values of the monthly data results in lower $\delta^{18}O_{coral}$ - SST slope value (ERSST: γ_1 = -0.12±0.02‰/°C $p < 0.001$ R = 0.70) than the published slope estimate. The MLR calibration with local measurements from Ombai strait (Sprintall et al., 2003) yields a slope ($\delta^{18}O_{coral}$ - SST) consistent with published estimates (γ_1 = -0.17±0.04‰/°C $p < 0.001$ R = 0.69) (e.g Weber and Woodhead, 1972; Gagan et al., 1994; Wellington et al, 1996) if the slope errors are taking into account. The data of SSS SODA v.143 as well as SSS Ombai is too short to calibrate the annual mean time series. For this calibration, we combined SODA v.142 and v.143 (1958-2004). Using this combined SSS dataset, the annual mean correlation coefficient of linear regression of $\delta^{18}O_{coral}$ vs. SSS, SST is low (R= 0.24) for period of 1950-2004.

5. Discussion

5.1 Coral Sr/Ca-SST relationship

The field correlation map between the annual mean of coral Sr/Ca and the ERSST dataset for periods 1914-2004 shows that measured Sr/Ca of KP1 calibrates with the SST in the Indonesian region at R = 0.4-0.6 (Figure 6.6). The field correlation map is calculated with the Royal Netherlands Meteorological Institute (KNMI) climate explorer (Oldenborgh and Burgers, 2005). Coral Sr/Ca shows the highest correlation with central Indonesian waters from Java, Sulawesi, eastern Nusatenggara to Timor (R = 0.5 -0.6) (Figure 6.6a). The result of linear regression of monthly Sr/Ca - SST shows that using the higher resolution SST dataset (AVHRR) resulted in the higher correlation coefficient (R=0.67). The correlation of Sr/Ca and SST from local measurement at Ombai is even higher (R=0.89) (Figure 6.6c). These

results convince us that coral Sr/Ca shows local SST, and the high resolution of SST dataset should have similar variance with coral Sr/Ca (which represent the point measurements) (Figure 6.6b,c). The correlation between SST Ombai and ERSST for local Timor (10°12'S 123°31'E) itself and also with SST AVHRR is low i.e. R= 0.4 and R=0.47 respectively.

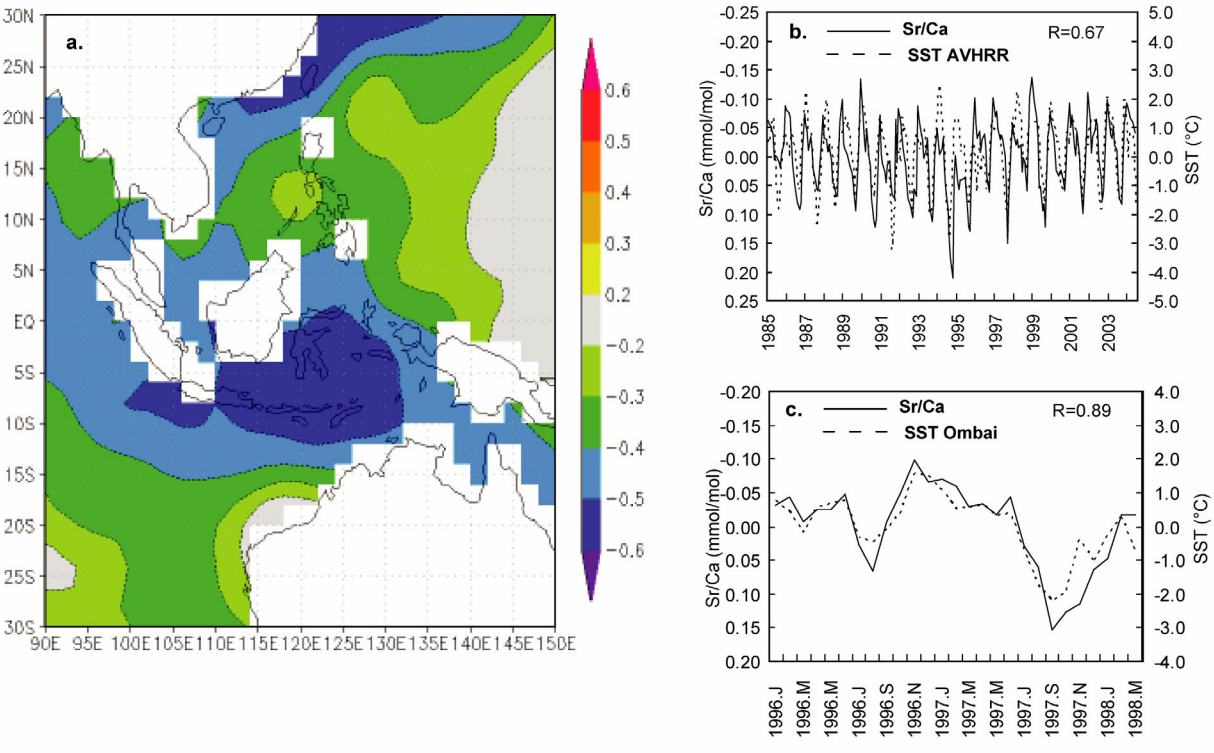

Figure 6.6. (a.) Field correlation of annual mean Sr/Ca$_{KP1}$ vs. ERSST for 1914-2004 calculated with the KNMI webpage (Oldenborgh and Burgers, 2005). (b.) Monthly time series of Sr/Ca$_{KP1}$ (solid lines) and SST from AVHRR (dashed lines) and (c.) Sr/Ca$_{KP1}$ (solid line) and SST from local measurement at Ombai strait (dashed lines).

The calibration equation of Sr/Ca-ERSST for the period of 1950-2004 is used to verify the Sr/Ca record of KP1 prior to 1950. In the validation period, Sr/Ca-SST shows a different trend from the ERSST (Figure 6.7). This can be interpreted as cooling trend which is shown by the coral proxy prior to 1950 that is not captured by global SST products. However, the interpretion of Sr/Ca in terms SST is complicated by possible biological factors such as the changes in the calcification rate, or the growth rate (de Villiers et al., 1995; Cohen et al., 2004). For example, higher mean Sr/Ca ratios from lower skeletal extension rates (de Villiers et al., 1995). Although we do not find any evidence for changes in skeletal extension/calcification in the X-ray images of KP1, these problems can not be ruled out unless the results of KP1 can be replicated with a second core from the region.

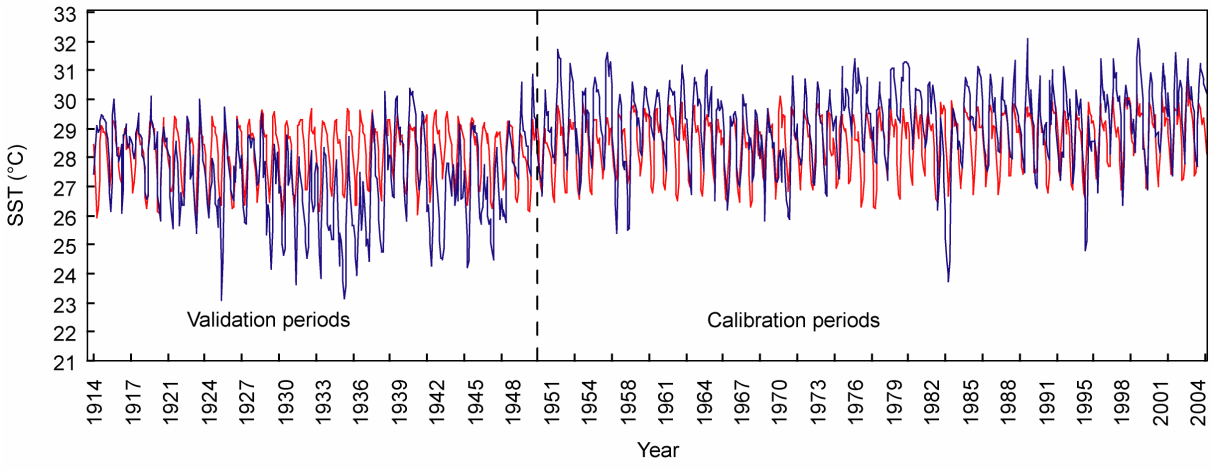

Figure 6.7. Reconstructed SST (blue line) based on the calibration equation of Sr/Ca$_{KP1}$ vs. ERSST for the 1950-2004 period (R = 0.62) and the time series from the ERSST dataset for the grid including Timor (red line)

On an annual mean time scale, the regression slope of KP1 Sr/Ca-ERSST (-0.1 mmol/mol/°C) is much higher than published slopes of the coral Sr/Ca-SST relationships, which range from -0.04 to -0.08 mmol/mol/^{o}C (e.g., Beck et al, 1992; de Villiers et al., 1994, 2002; Shen, et.al, 1996; Alibert, et al, 2003; Marshall & McCulloch, 2002; Mitsuguchi et al, 2003). This shows that variations of annual mean Sr/Ca are much larger than expected based on grid-SST (Figure 6.8). This could reflect the fact that grid-SST is averaged over a large region (ERSST: 2°x2°), therefore grid-SST may have a lower variance than a local point measurement of SST (as represented by coral Sr/Ca from one single core) on interannual time scales. For the period of 1914-2004, the correlation coefficient between annual mean Sr/Ca-ERSST is high (R = 0.52) but after removing the trend the correlation becomes lower (R= 0.1). However, using high resolution SST data from AVHRR SST (1985-2004) the correlation between annual mean Sr/Ca-SST AVHRR (annual means are calculated from March to February in the following year) is high (R= 0.54). By removing the trend, the correlation of Sr/Ca-SST AVHRR remain the same.

The high correlation between Sr/Ca-SST can be caused by similar trends of both time series. This seems to be the case for the correlation between Sr/Ca and ERSST. However, this problem does not affect the correlation of Sr/Ca and SST AVHRR. This suggests that the high resolution SST data better captures the SST variance at the coral site.

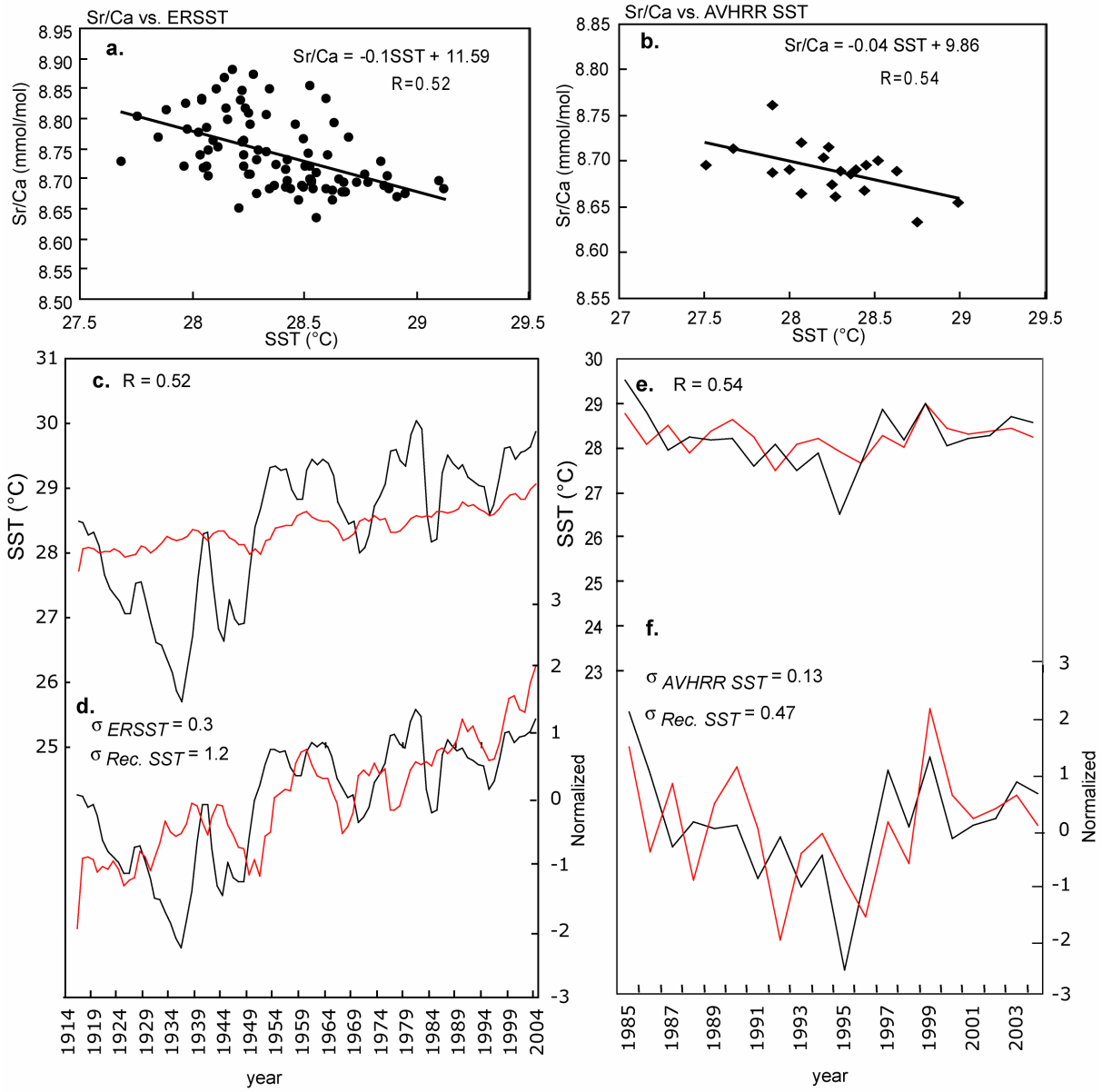

Figure 6.8 (a). Linear regression between Sr/Ca and SST from ERSST and (b) from AVHRR. (c) Variation of annual mean ERSST (red) and reconstructed SST (black) derived from the Sr/Ca-ERSST calibration and (d) plot after normalization to unit variance. (e) Annual mean of SST from AVHRR (red) and reconstructed SST (black) based on the Sr/Ca-SST AVHRR calibration and (f) plot after normalization to unit variance. The correlation coefficient of Sr/Ca-ERSST R=0.1 after detrending the data, but for Sr/Ca-AVHRR, the correlation remains the same after detrending (R=0.54).

The different of data length that is used for calibration may cause the high correlation of Sr/Ca-ERSST occurs in the different annual mean period with Sr/Ca-AVHRR SST i.e. September to August for ERSST and March to February for AVHRR. Using the same data length (1985-2004 periods), both annual mean Sr/Ca-ERSST and Sr/Ca-AVHRR SST calibrations show higher correlation by averaging months from March to February ($R_{Sr/Ca-AVHRR}$ = 0.54, $R_{Sr/Ca-ERSST}$ =0.67) than from September to August ($R_{Sr/Ca-AVHRR}$= 0.31, $R_{Sr/Ca-}$

$_{ERSST}$ =0.42). However, for annual mean Sr/Ca-SST calibration, for 1985-2004 periods, both ERSST and AVHRR SST show the expected slope value i.e -0.04 - - 0.08 mmol/mol/°C. The slope of the annual mean Sr/Ca-ERSST calibration for 1914-2004 periods could be biased by the greater uncertainty of the ERSST dataset on the longer time scales. Figure 6.9 shows plot of slope and intercept of Sr/Ca-SST calibration.

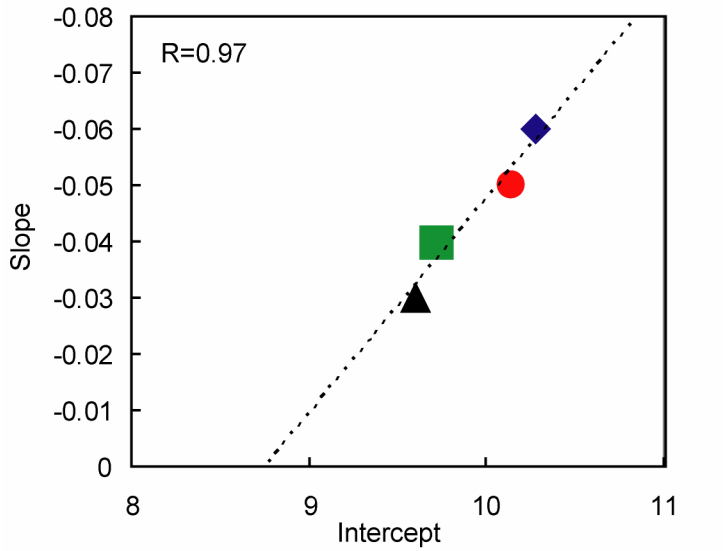

Figure 6.9. Slope and intercept plot of monthly Sr/Ca-SST calibration: Ombai SST (blue), ERSST (red), AVHRR SST (green), and SODA 142,143 SST (black).

5.2 Coral $\delta^{18}O$ variations

The seasonal cycle of salinity should dampen the seasonal cycle of SST in coral $\delta^{18}O$, as warm (cold) SSTs coincide with high (low) salinity (Figure 6.4). Thus we expect that the slope of the monthly SST calibration of KP1 using SST only will be lower (<0.18 ‰/°C) than the published $\delta^{18}O_{coral}$- SST relationship. The calibration slopes of monthly $\delta^{18}O_{coral}$- SST calibration ranges from 0.1 to 0.12‰/°C, regardless of the SST dataset used. A calibration using only the maxima (minima) values in any given year also yielded slope values lower than 0.18 ‰/°C.

Ideally $\delta^{18}O_{coral}$ should be calibrated vs. SST and $\delta^{18}O_{sw}$ using the multiple linear regression (hereafter mention as MLR). Assuming that $\delta^{18}O_{sw}$ linearly correlates with SSS, the MLR of $\delta^{18}O_{coral}$ vs. SSS, SST can be used to estimate the $\delta^{18}O_{coral}$ - SST relationship. The slope value of the $\delta^{18}O$-SST in the MLR of $\delta^{18}O_{coral}$ vs. SSS, SST (-0.15±0.02 ‰/°C) from SODA is lower than the published slope estimates for coral $\delta^{18}O$- SST i.e. 0.18-0.22 ‰/°C (Weber and Woodhead, 1972; Gagan et al., 1994; Wellington et al, 1996). However, including the slope

error, the slope of $\delta^{18}O$- SST in the MLR regression of $\delta^{18}O_{coral}$ vs SSS SODA, SST AVHRR is still consistent with published $\delta^{18}O$- SST relationship of biological carbonates, which range from -0.17 ‰/°C to -0.23 ‰/°C (O 'Neil et al., 1969; Bemis et al., 1998; von Langen et al., 2000; Spero et al., 2003). Using SST and SSS measured directly at Ombai strait, we obtain a $\delta^{18}O_{coral}$ - SST slope of -0.17±0.04‰/°C using MLR, consistent with published slope estimate (e.g Weber and Woodhead, 1972; Gagan et al., 1994; Wellington et al, 1996) especially when taking into account the slope error of the regression. The slope of $\delta^{18}O_{coral}$ - SSS Ombai in the MLR is low (0.01±0.11 ‰/psu) and the slope error of the regression is large. The Ombai dataset is very short and the SSS variations are relatively small in the interval measured. A better and longer dataset is needed for a reliable of $\delta^{18}O_{sw}$ and SSS. The estimate slope for $\delta^{18}O_{sw}$ - SSS from Delaygue model (2003) for Timor region could be around 0.1-0.3 ‰/psu.

$\delta^{18}O_{coral}$ shows positive anomalies during the ~1977-1986 periods, when the mean value (-4.9 ‰) is larger than normal (-5.17 ‰). The $\delta^{18}O_{coral}$ measurements of this interval have been repeated to ensure that the anomalies are reproducible and not due to analytical problems. Theoretically, $\delta^{18}O_{coral}$ can be biased by coral growth or diagenesis. However, these problems should both also influence coral Sr/Ca. In fact, coral Sr/Ca appears to be even more sensitive to anomalous coral growth and/or diagenesis (de Villiers et al., 1994; McGregor & Gagan, 2003). Therefore it is unlikely that the $\delta^{18}O_{coral}$ anomalies are related to problems of our coral case. The other coral environmental causes, e.g. anomalous freshwater fluxes can not be ruled out since the sampling location lies close to a river mouth, although this river is rather small. However, the values of measured $\delta^{18}O_{coral}$ in the period of ~1977-1986 is still in range value of $\delta^{18}O$ values in corals measured, i.e., ~ -4 to -5 ‰

5.3 Reconstructed SSS

Coral $\delta^{18}O$ (here after mention as $\delta^{18}O_{coral}$) is influenced concomitantly by SST and $\delta^{18}O_{sw}$, while coral Sr/Ca is influenced by SST only. Therefore $\delta^{18}O_{sw}$ can be reconstructed from the paired $\delta^{18}O_{coral}$ and Sr/Ca measurements of KP1 from Timor coral. Assuming that $\delta^{18}O_{sw}$ correlates linearly with SSS, paired $\delta^{18}O_{coral}$ and Sr/Ca measurements can also be used to reconstruct SSS. In this study, SSS is reconstructed from paired $\delta^{18}O_{coral}$ and Sr/Ca using centered MLR (see section 4.2.5 chapter 4 for details regarding this method). The published slope of $\delta^{18}O_{coral}$ -SST (γ_1 = -0.18 ‰/°C), of $\delta^{18}O_{sw}$ -SSS (γ_2 = 0.3‰/psu) (Delaygue et al., 2000) and the estimate slope of coral Sr/Ca-SST AVHRR (β_1 =-0.04 mmol/mol/°C) are used

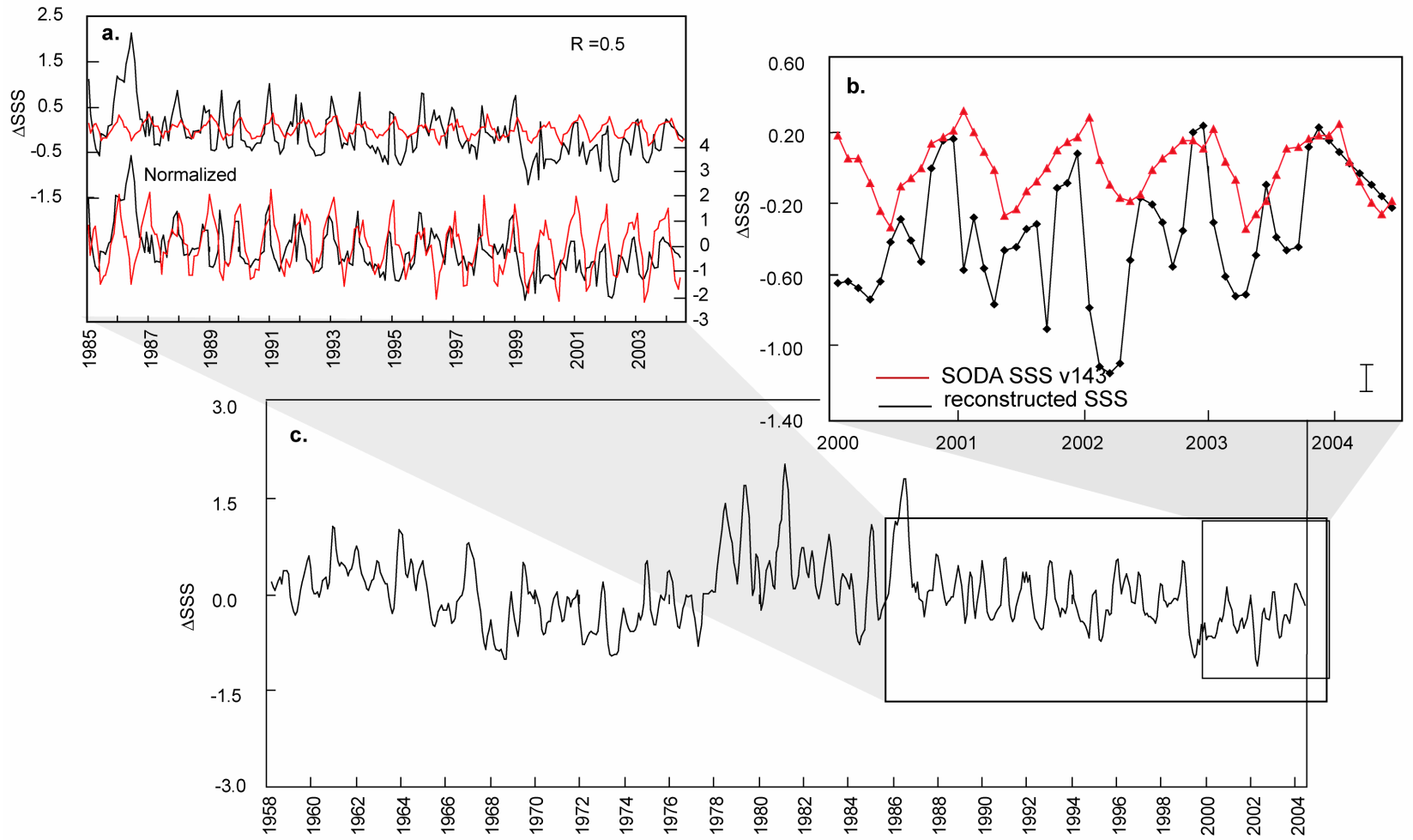

Figure 6.10. Monthly reconstructed SSS from paired $\delta^{18}O$ and Sr/Ca of KP1 using centered MLR ($\gamma 1$ = -0.18 ‰/°C, $\gamma 2$ = 0.3 ‰/psu $\beta 1$ = 0.04 mmol/mol/°C) for (a) the periods of 1985-2005 (black lines); combined SSS from SODA v.142 and v.143 (red line), (b) the period of 1985-2004 (black lines); SSS from SODA v.143 (red line). The error of reconstructed SSS is ±0.18 psu (black bar). (c) Reconstructed SSS for the periods of 1958-2004. Reconstructed SSS shows clear seasonal variations.

in the calculation. The result is shown in Figure 6.10. The error propagation of reconstructed SSS (hereafter mention as rec. SSS) is calculated using equation: $\sigma_{sss}^2 = \frac{\sigma_{\delta c}^2}{\gamma_2^2} + \frac{\sigma_{sr/ca}^2 \gamma_1^2}{\gamma_2^2 \beta_1^2}$ (see section 4.2.3, chapter IV, for details regarding this method), where γ_1 = -0.18 ‰/°C , γ_2 = 0.3 , β_1 = -0.04 mmol/mol/°C. The analytical uncertainty of $\delta^{18}O_{coral}$ is $\sigma_{\delta c}$ = ±0.06 ‰ (σ1) and of Sr/Ca $\sigma_{sr/ca}$ = ±0.01 mmol/mol (σ1). The error propagation of reconstructed SSS is σ_{sss} = ±0.18 psu which would correspond to ±0.07 ‰ $\delta^{18}O_{sw}$.

SSS from SODA v.143 is used to validate reconstructed SSS. The version 143 of SODA should be the most reliable for the calibration of our proxy reconstruction. Since this version performs better in the tropics (Carton & Giese, 2005). On longer time scales, reconstructed SSS shows similar variations as the combined SSS of SODA v.143 and v.142 (see Carton & Giese, 2005 for detailed discussion of SODA v.142 and 143). The seasonal variation of surface salinity of Timor can be resolved (Figure 6.10a). This is as what we expect, since the error propagation of reconstructed SSS (0.18 psu or 0.07 ‰) is much lower than the amplitude of the seasonal cycle of SSS (0.5 psu or 0.2‰). Therefore the seasonal cycle of SSS can be resolved by paired coral proxy measurements at Timor. The chronological error of 1-2 months, however, could lead to errors in the reconstruction of SSS (note that the climatological SST minimum (maximum) varies depending on the dataset). By shifting reconstructed SSS by 1 months (which is within chronological error), the highest correlation of monthly reconstructed SSS and SSS SODA is obtained (R = 0.5 p< 0.001) for periods 2000-2004. A calibration of reconstructed SSS with SSS measured in Ombai strait results in low correlation (R = 0.28 p< 0.001). During the period of 1997-1998, the amplitude of SSS Ombai is much lower (±0.3 psu) than during the period of 1996-1997 (±0.53psu). Hence, the SSS signal of 1997-1998 can not be reconstructed from the coral proxy, because the amplitude of SSS variations is more or less within the error range of reconstructed SSS (±0.18 psu or 0.07‰). After smoothing the time series with a 3 months running average, both SSS Ombai and reconstructed SSS show similar patterns back until June 1996. However, the correlation between SSS SODA for Timor (10°12'S 123°31'E) and SSS Ombai is low (R=0.3, 1996-1998periods).

On the annual mean scale, measured $\delta^{18}O_{coral}$ covaries strongly with the SST contribution to $\delta^{18}O_{coral}$ ($\Delta\delta^{18}O_{sst}$) derived from Sr/Ca ($\Delta\delta^{18}O_{sst}$ = γ/β * ΔSr/Ca) (Figure 6.11). The correlation between $\delta^{18}O_{coral}$ and Sr/Ca for annual means is high (R = 0.47). However, we

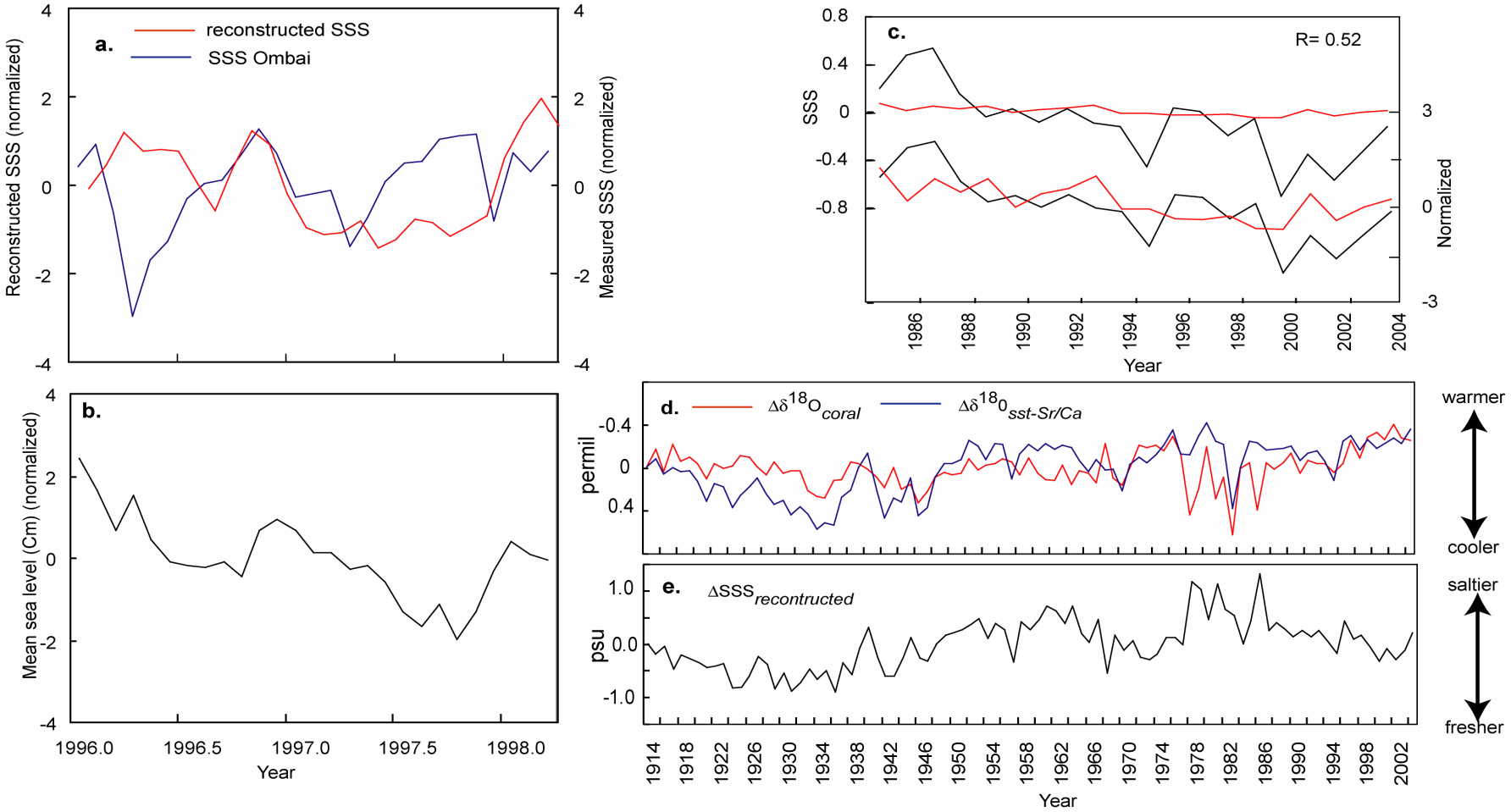

Figure 6.11. (a) Seasonal variation of local SSS (blue) at Ombai strait (Sprintall et al., 2003), reconstructed SSS from paired proxies (red) and (b) mean sea level measured at Timor (Windupranata, 2002). Data is normalized to unit variance. SSS is reconstructed using centered MLR. Regression coefficients are $\delta^{18}O$ vs. SSS, SST Ombai (γ_1 = -0.21 ‰/°C), Sr/Ca vs. SST Ombai (β_1 = -0.06 mmol/mol/°C) (see text for discussion). (c) Annual mean of reconstructed SSS (black line) and SSS from combined SODA v.142 and v.143. Data is normalized to unit variance. (d) Annual mean of coral $\delta^{18}O$ changes (red) and SST contribution to coral $\delta^{18}O$ derived from Sr/Ca (blue), and (e) reconstructed SSS for the periods of 1914-2004 (black).

found that the variation of $\delta^{18}O_{coral}$ is larger than expected based on the SST contribution inferred from Sr/Ca. The larger variation of $\delta^{18}O_{coral}$ suggests that the $\delta^{18}O_{coral}$ signal is enhanced by SST co-variant changes in seawater $\delta^{18}O$, while Sr/Ca shows SST only. We reconstruct the annual mean SSS based on the annual mean Sr/Ca and $\delta^{18}O_{coral}$. Annual means are calculated from September to August of the following year. Annual mean of reconstructed SSS was correlated with SSS SODA over the past 20 years (1985-2004) (R= 0.52). We find that the variance of reconstructed SSS is larger than the variance of SSS SODA (Figure 6.11). The same problem was found when comparing annual mean reconstructed SST and SST. SSS SODA is obtained from reanalysis model and averaged in a grid box scale. The SSS from SODA reanalysis has lower variance than the local SSS observation at Ombai. Thus, local measurements of SSS directly at the site are needed to overcome the variance problem. Unfortunately the SSS Ombai record is too short for a annual mean calibration. However, when both time series are normalized to unit variance, reconstructed SSS shows similar trends as SSS SODA. During the past 20 years, both time series show a freshening in the Timor region (Figure 6.11).

5.4 ENSO signature in Timor coral Sr/Ca

During El Niño events the trade wind in the central Pacific relax, which leads to a deepening of the thermocline in the eastern Pacific and shallowing in the western Pacific warm pool. The warm SST in the central -eastern Pacific, and cool SST in the western Pacific. Since our coral Sr/Ca record is a temperature proxy from the western Pacific, we expect to see the typical El Niño pattern in the spatial correlation map with opposite correlations between the western and eastern Pacific region.

To assess the sensitivity of SST at Timor to ENSO phase changes, we have computed regression plot of global SST - SSTa (anomaly) in the Niño 3 region. The magnitude of SST changes related to Niño 3 in Timor is low, the coefficient regression ranges from 0.1°C to -0.1°C) and the correlation coefficient (R) is lower than 0.31 for an annual mean scale and a monthly mean (Figure 6.12a,b). During December-February, when El Niño peak, the seasonal mean correlation of SST - SSTa Niño 3 is high (R = ±0.63) (Figure 6.12c). During September-October-November (SON), when El Niño events develope, the correlation of SST - SSTa Niño 3 is even higher (R= 0.63-0.77), and the magnitude of SST changes related to SSTa Niño 3 is also higher (the regression slope ranges from -0.1 to -0.6). In June-August (JJA), the magnitude of SST changes at Timor related to SSTa Niño 3 ranges from 0.1°C to

0.35 °C, but the correlation is low (R< 0.31) (Figure 6.12d). Based on the correlation map of global SST and SSTa Niño 3 (Figure 6.12), becomes clear that in the Timor regions, the impact of ENSO on monthly an annual mean is not strong. Only the SON and DJF season clearly ENSO-related SST anomalies.

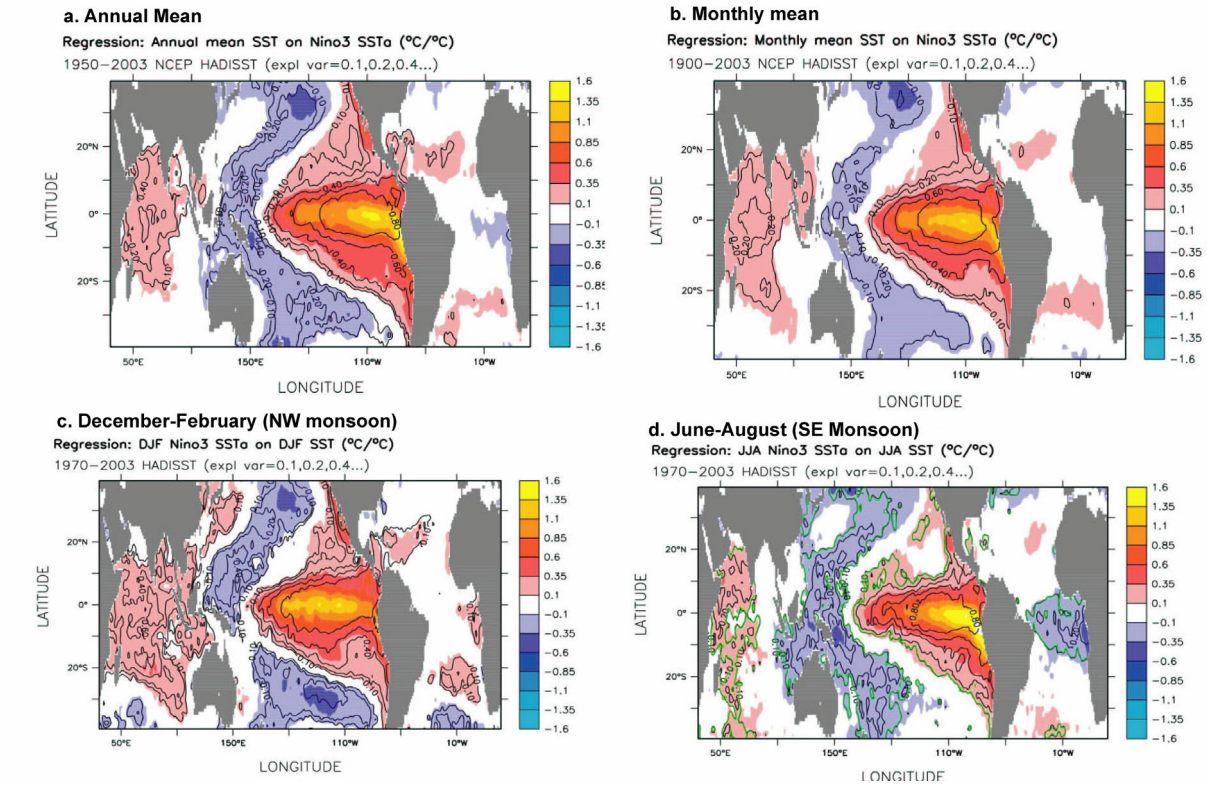

Figure 6.12. Regression coefficient plot (colors) and explained variance (contours) between Niño 3 average SST and global SST for (a) annual means, (b) monthly means, (c) seasonal means of December-February and (d) June-August. Explained variance equals the square of the correlation coefficient.

Field correlations of grid-SSTs (NCEP) from Timor averaged over 4 months also show the El Niño pattern. Similarly field correlation maps are computed with coral Sr/Ca of KP1 (Figure 6.13). The El Niño teleconection is clearly shown by the field correlation between global SST and coral Sr/Ca from Timor. The maps show a negative correlation between coral Sr/Ca -SST in the WPWP (consistent with the inverse relationship of coral Sr/Ca with local SST) and a positive correlation in the central -eastern equatorial Pacific. During the NW monsoon, when the El Niño is strongest, the field correlation of Sr/Ca-SST does show the El Niño pattern more clearly than during the SE monsoon. During the SE monsoon, when the El Niño is weak (SST vs. SSTa Niño 3: R < 0.31) (see Figure 6.12d), the El Niño pattern is not very clearly shown in the field correlation of coral Sr/Ca-SST becomes unclear (Figure. 6.13).

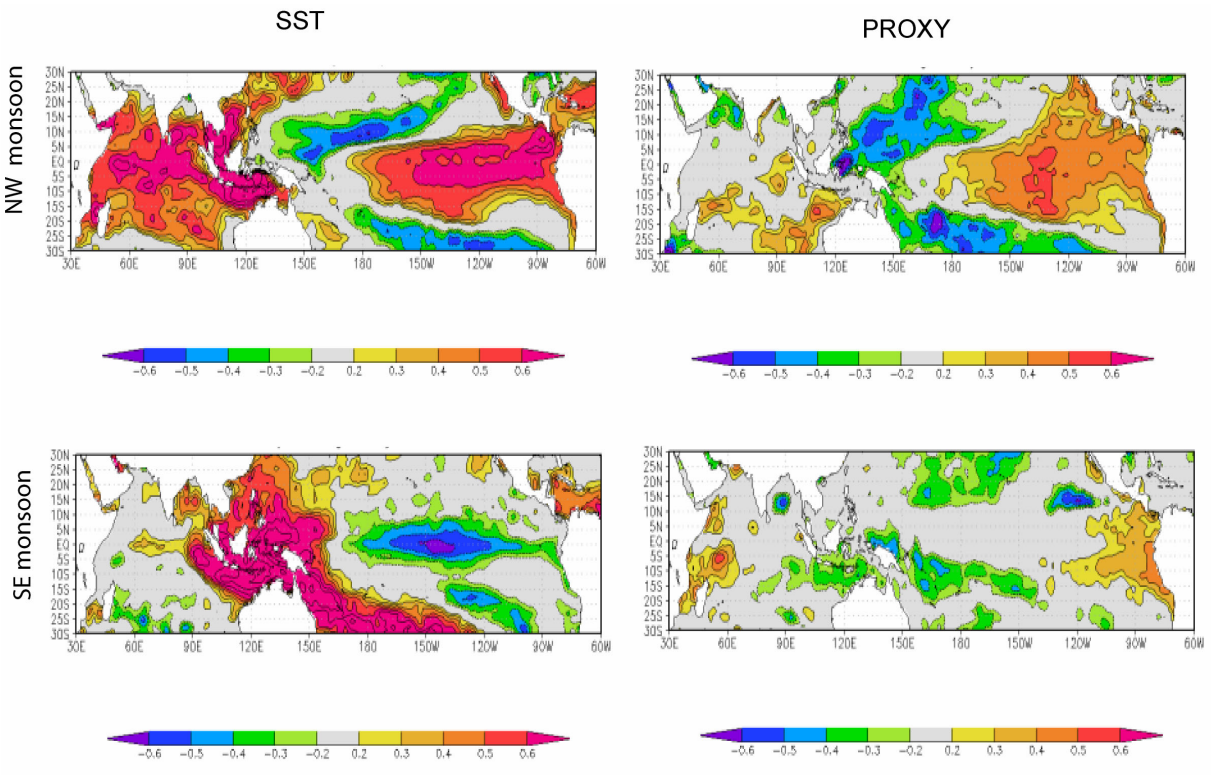

Figure 6.13. Field correlation between SST (NCEP) for Timor (10.12°S 123. 31°W) and the global SST field (NCEP) (left) for periods 1982-2004. Field correlation between SST (NCEP) and Sr/Ca of KP1 for periods 1982-2004 (right). Time series are 4 months seasonal averages: mean December-March (upper panels) and mean June-September (bottom panels). All maps computed at http://www.climexp.knmi.nl/.

The regression plot of grid SST and SSTa from Niño 3 region (Figure 6.12c,d) shows that the impact of ENSO on SST in Timor is small. The variance of ENSO-related SSTa at Timor is low for annual and seasonal mean. The regression coefficient is also low. Thus it should be difficult to get a clear signal of ENSO in this area. To get a clearer El Niño signal from the Timor coral, coral Sr/Ca is filtered in the 2-7 yrs periodicity (the typical El Niño band) using a wavelet bandpass-filter (Torrence and Compo, 1998). The filtered time series is correlated with the unfiltered Niño 3.4 (Niño 3) index. Figure 6.14 compares the filtered Sr/Ca series with Niño 3.4. after normalized to unit variance. The monthly, seasonal and annual mean filtered Sr/Ca is also correlated with Niño 3.4 and Niño 3 index using linear regression. The results show that on a monthly and annual mean scale the correlation of filtered Sr/Ca with Niño 3.4 or Niño 3 index is low. The highest correlation of Sr/Ca and Niño 3 index is obtained for period 1970-2004 i.e. R= 0.24 for annual mean and R = 0.36 for monthly scale. This suggests that Sr/Ca- SSTa Niño 3 are only correlated during the past ~ 30 years (Figure 6.15). On a seasonal mean scale, the best correlation Sr/Ca- Niño 3 index is obtained for December-February averages of the for period 1970-2004 (R=0.4). The linear regression of

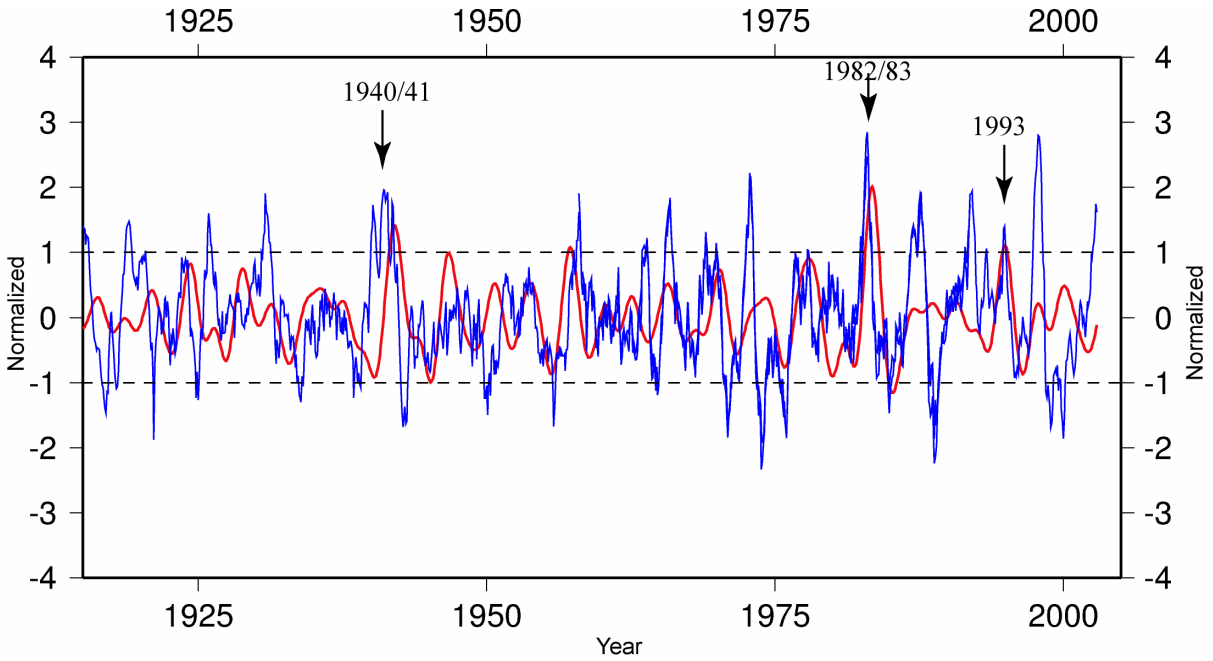

Figure 6.14. Sr/Ca of KP1 filtered in the 2-7 year frequency band using a wavelet bandpass filter (Torrence and Compo, 1988) with the Nino 3.4 index (blue line). Only several El Niño events (i.e 1940/41, 1982/83, 1993) are indicated by Sr/Ca of the Timor coral. Dashed lines: one standard deviation.

Sr/Ca- Niño 3.4 index does not show a good correlation in any calibration period. SSTa in Niño 3.4 and Niño 3 are identical (Trenberth, 1997), thus ideally the correlation of any time series with both indexes should be similar. In our case, the small differences recorded in both El Niño indices appear to influence the correlation Sr/Ca with SST. However, it has been suggested that the Niño 3.4 index is a better indicator of ENSO signal, since the standard deviation of monthly Niño 3.4 (0.77°C) is lower than Niño 3 (0.79°C) (Trenberth, 1997). However, filtered grid-SST of Timor shows similar problems when correlated with Niño 3 and Niño 3.4 indices as coral Sr/Ca (Figure 6.15).

Using a simple linear regression approach, the coral Sr/Ca and Niño 3.4 index do not show a clear statistical relationship. However both coral Sr/Ca and coral SST at Timor show a high correlation with the El Niño indices for recent decades (back until 1970) when El Niño events can be identified (see Fig. 6.14). The different of correlations of coral Sr/Ca vs. the Niño indices are maybe due to the statistical problems. We have obtained positive or negative of

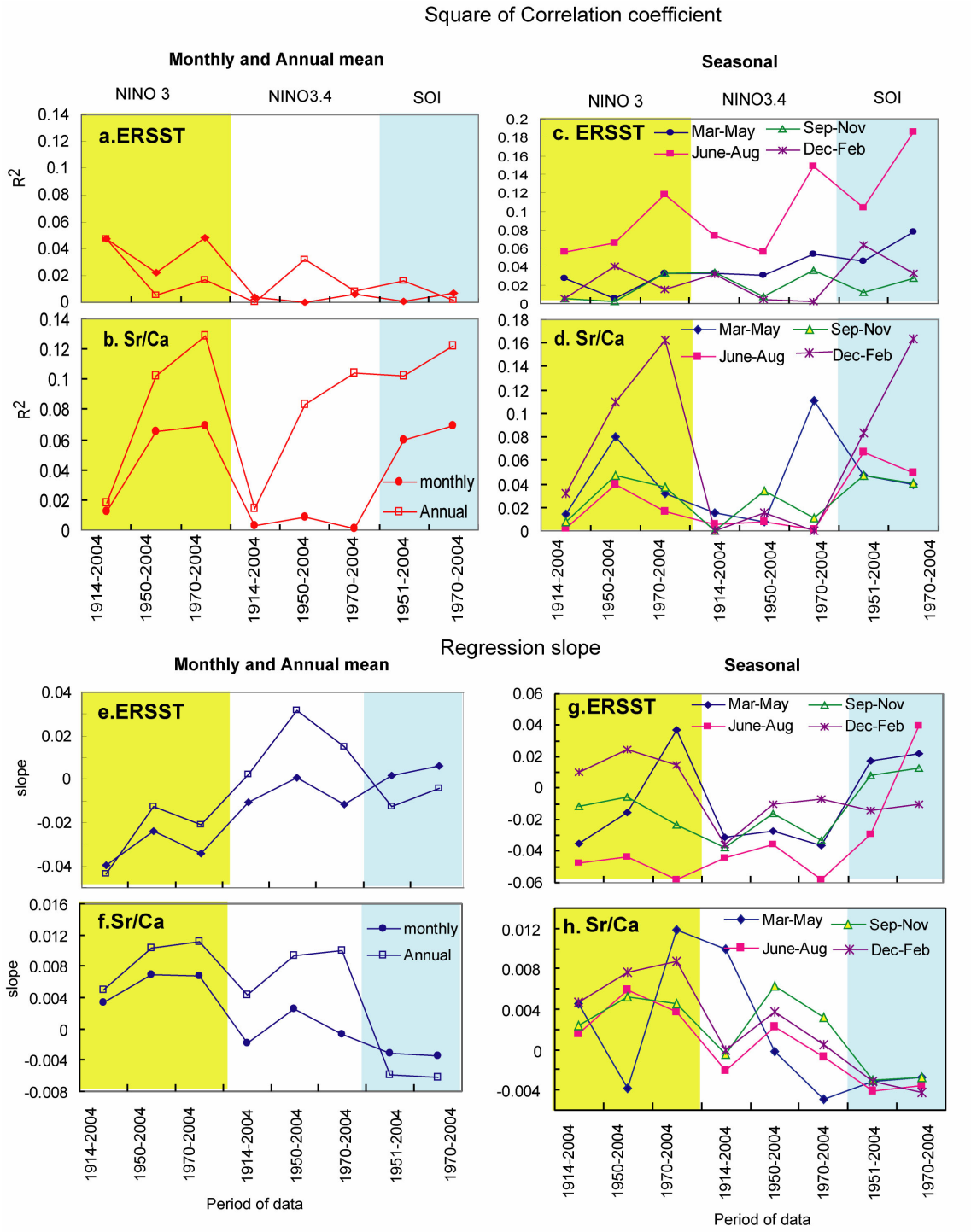

Figure 6.15. Square of correlation coefficients (R^2) for monthly and annual mean regression of (a) ERSST vs. ENSO Indices, (b) Sr/Ca vs. ENSO Indices. R^2 for seasonal mean calibration of (c) ERSST vs. ENSO indices, (d) Sr/Ca vs. ENSO indices. Regression slope of monthly and annual mean of (e) ERSST vs. ENSO Indices and (f) Sr/Ca vs.ENSO indices. Regression slope of seasonal calibration of (g) ERSST vs. ENSO and of (h) Sr/Ca vs. ENSO. Colored shading marks ENSO Indices used: Nino 3 (yellow), Nino 3.4 (white) and SOI (blue).

regression slopes, high and low of correlation coefficient depending on the period of data used. However, coral Sr/Ca and local SST at Timor do always show similar relationship with

ENSO. Besides, coral Sr/Ca shows a good correlation with SST Ombai the only local SST measurement and show good correlation (R= 0.7) but the Ombai dataset is too short i.e. 1996-1998 period. Other physical factors such as the monsoon, oceanic advection or processes internal to the Indian Ocean may also influence the coral proxy. These factors could overprint the ENSO signal in the Timor coral at longer time window. Thus, we need a better understanding of the climatic processes in the Timor region.

Coral Sr/Ca is also correlates with the Southern Oscillation Index (SOI). A high correlation of Sr/Ca vs. SOI is found for mean December-February values for the period 1970-2004 (R = 0.4) (Figure 6.15).

We average the coral Sr/Ca time series from November to February, when the signal of ENSO is strongest and then compute the power spectrum and the coherence spectrum using the wavelet power spectrum and wavelet coherence software package provided by Grinsted et al. (2004). The wavelet power spectrum gives a measure of the time series variance as a function of period and time. The wavelet coherence spectrum estimates the correlation (coherence) of two time series as a function of time and period even though the variance of the common power is low (see Grinsted et al., 2004 for a detailed discussion). The wavelet power spectrum analysis shows that both local SST at Timor (ERSST) and coral Sr/Ca do not show significant variability in the ENSO periodicity band (3-8 years) (Figure 6.16). Coral Sr/Ca has significant power at decadal/interdecadal periodicities (9-10 years). This signal is coherent with Niño 3.4 index during 1920-1970 and 1980-2004 (Figure 6.17b,d). Both local SST at Timor and coral Sr/Ca are coherent with Niño 3.4 at interannual periods from 1950-1960 and 1970-1980. The strong El Niño of 1997/1998 is clearly shown (Figure 6.17a). Coral Sr/Ca clearly shows the strong El Niño of 1982/1983 (Figure 6.17b). The significant and strong decadal coherence is found. However, local SST at Timor does not show any significant decadal/interdecadal variability (Figure 6.16a). This suggests that suggested that the coral proxy is more reliable recorder of decadal El Niño -like SST variability than reconstruction of historical SST from sparse measurements.

5.5 El Niño and SSS at Timor

The wavelet power spectrum of SODA SSS for Timor shows significant variability at

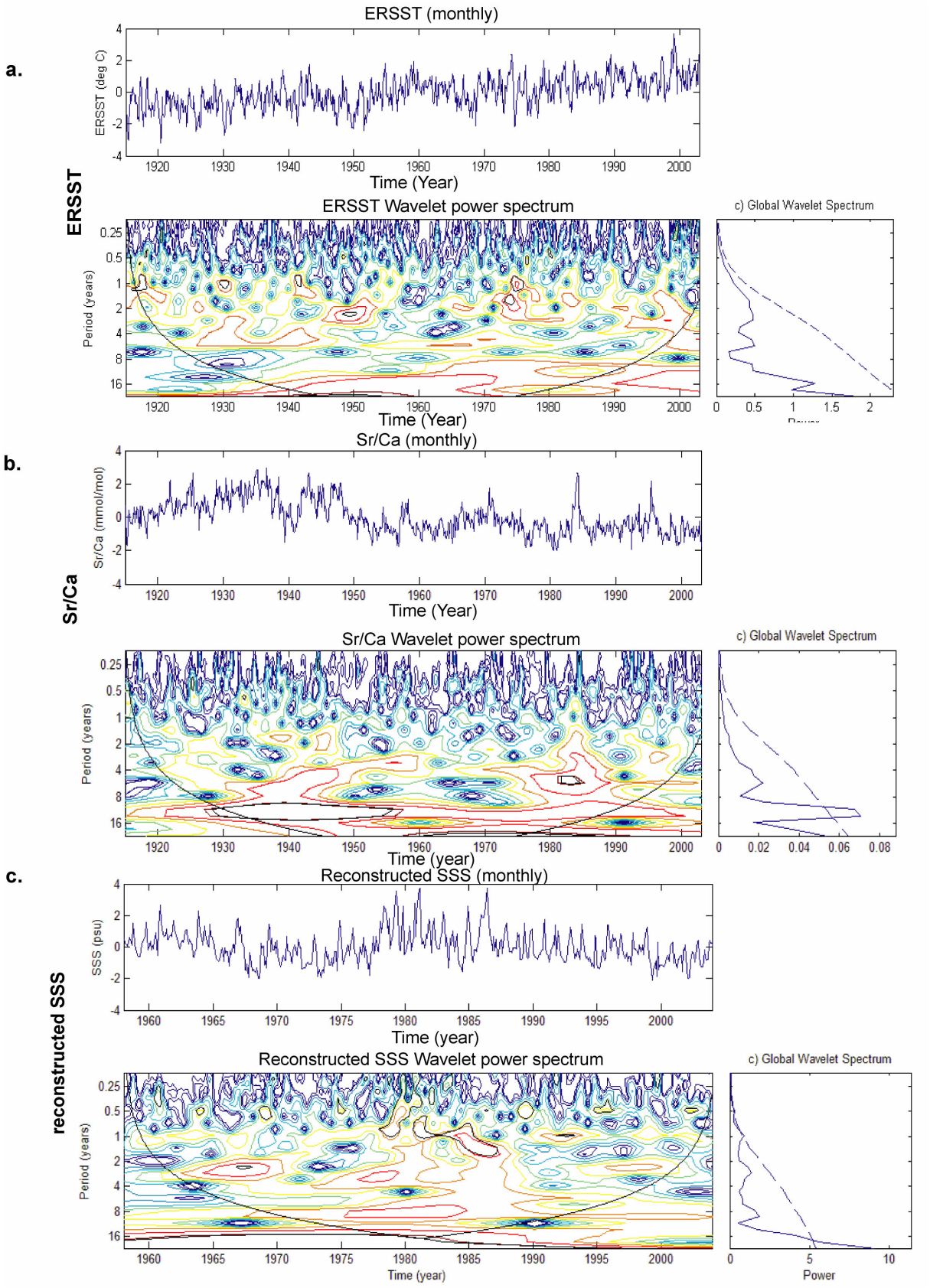

Figure 6.16. (a) Wavelet power spectrum of (a) SST anomalies from ERSST, (b) coral Sr/Ca$_{KP1}$ anomalies, (c) reconstructed SSS from paired proxies of KP1.

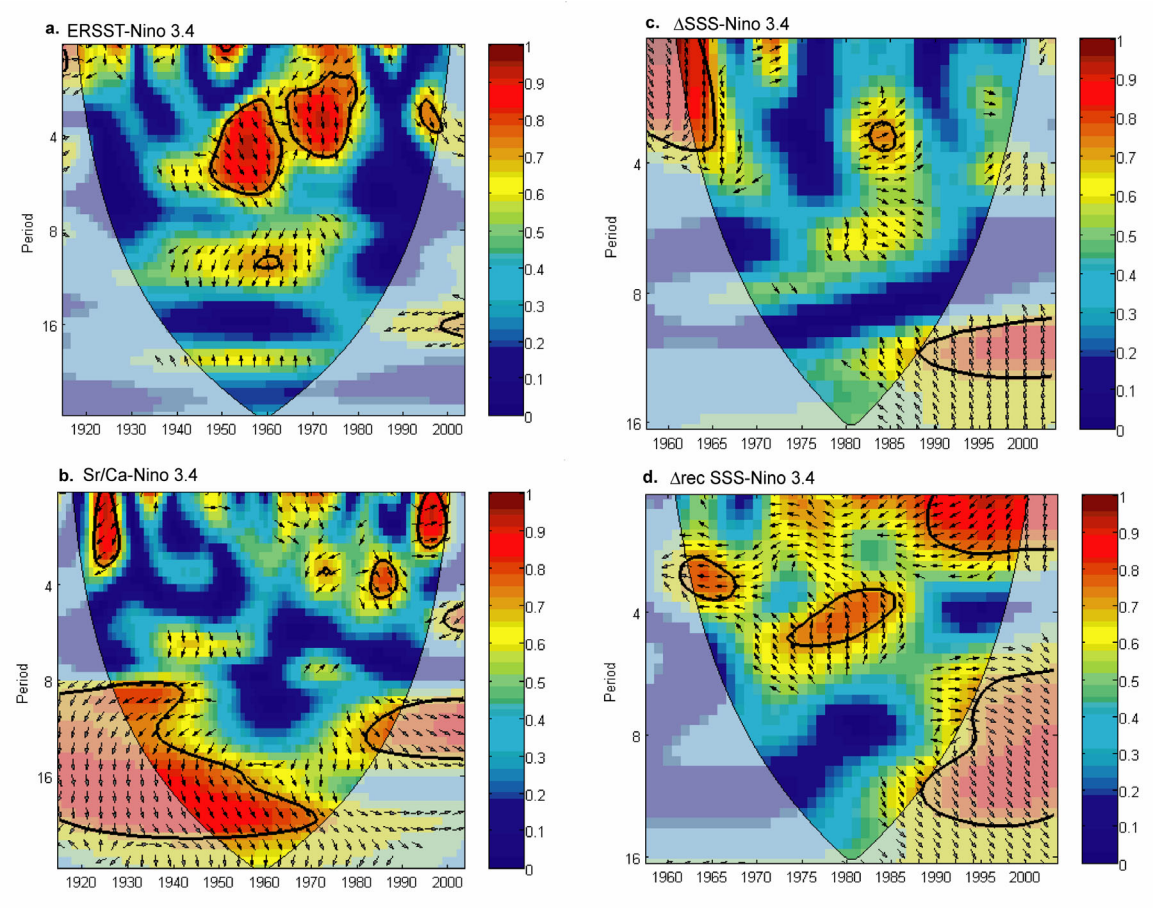

Figure 6.17. Wavelet coherence of (a) SST (ERSST) vs. Nino 3.4, (b) coral Sr/Ca vs. Nino 3.4, (c) SSS of SODA v.142 and v.143 vs. Nino 3.4, and (d) reconstructed SSS vs. Nino 3.4 for seasonal means (November-February). The wavelet coherence spectra are computed using software provided by Grinsted et al. (2004) (see text for discussion). The thick contours indicate the 5% significance level against red noise. The relative phase relationship is shown as arrows (with in-phase pointing right, anti-phase pointing left and Nino 3.4 leading by 90° pointing straight down).

interannual period, while reconstructed SSS shows more power at decadal/interdecadal periods (Figure 6.16c). The SSS SODA for Timor and Niño 3.4 are coherent at interannual periods. The strong El Niño of 1982/1983 is clearly recorded by SODA SSS, but not the El Niño of 1997/1998 (Figure 6.17d). Similarly, reconstructed SSS is coherent with the Niño 3.4 index at interannual time scales and the strong El Niño of 1982/1983 is also recorded by reconstructed SSS. At decadal/interdecadal time scales SODA SSS is coherent significantly with ENSO, as does reconstructed SSS. We suggest that salinity at Timor may be a better indicator of decadal El Niño -like variability than Timor SST, while the interannual ENSO signal seems to be better recorded in the SST. However, local SSS measurements at Ombai strait (Sprintall et al., 2003) still shows similar variations as reconstructed SSS from paired

coral proxies (Figure 6.11) for period 1996-1997. During the El Niño of 1997/1998, the water in the Timor region are cooler and saltier than normal due to the lower regional precipitation, and lower transport of fresh warm Throughflow waters into the Savu sea (Sprintall at al., 2003). The El Niño of 1997/1998 also led to a sea level drop that was measured at Kupang bay (Windupranata, 2002) (Figure 10c). During El Niño events, the warmer waters of the western Pacific warmpool (e.g. Indonesia) move eastward, and SSTs in this region are cooler than normal. The cooling of SST leds to a decreasing in water volume, and hence to a sea level drop (Figure 6.11a,b). The decreasing in water volume corresponds to an increasing in water density (higher salinity) (Pond and Pickard, 1983; Antonov et al., 2002). Local SSS of Ombai increase by 1.2 psu during this period, while reconstructed SSS from paired coral proxies also increases although the magnitude is smaller (0.4 psu) (Figure 6.11a).

5.6 Interdecadal variations of coral Sr/Ca ($\delta^{18}O$) and the Pacific Decadal Oscillation

Since coral $\delta^{18}O$, Sr/Ca and reconstructed SSS show pronounced decadal/interdecadal variations that are coherent with the tropical Pacific, we correlate coral $\delta^{18}O$ (Sr/Ca) and reconstructed SSS the with Pacific Decadal Oscillation (PDO) index. The PDO index is the leading Principal Component (PC) of monthly SST anomalies in the North Pacific Ocean, poleward of 20N (for detail see in Zhang et al., 1997; Mantua et al., 1997). We also correlate grid-SST (ERSST) from the Timor region with the PDO. The time series are smoothed with a 120 months (low pass filter). PDO index is not filtered. Running correlations were computed with a 25 years running window for 4 months seasonal averages (Oldenborg, 2005). For all time series (Sr/Ca, $\delta^{18}O$, SSS, ERSST) highest correlations with the PDO are found for northern hemisphere winter seasonal averages. The running correlation of ERSST vs. PDO and Sr/Ca vs. PDO shows similar variations through time. The correlation decreases during 1950-1960. The same applies to reconstructed SSS and coral $\delta^{18}O$ vs. PDO. Coral $\delta^{18}O$ shows the strongest and most stable positive correlation with the PDO back until 1940 (Figure 6.18). However, coral Sr/Ca shows the most power at decadal/interdecadal periods more than coral $\delta^{18}O$ and reconstructed SSS and even more than than ERSST of Timor. The decadal/interdecadal signal is coherent with the tropical Pacific variability, consistent with other coral records from the western equatorial Indian Ocean (Pfeiffer and Dullo, inpress). It is generally believed that several author have suggested that the decadal/interdecadal variability in the tropical Pacific is forced by the tropic (Evans et al., 2002), hence our Timor coral should also show some relationship with the PDO on longer time scales. Clearly, the decadal/interdecadal variability recorded by our coral requires further investigation.

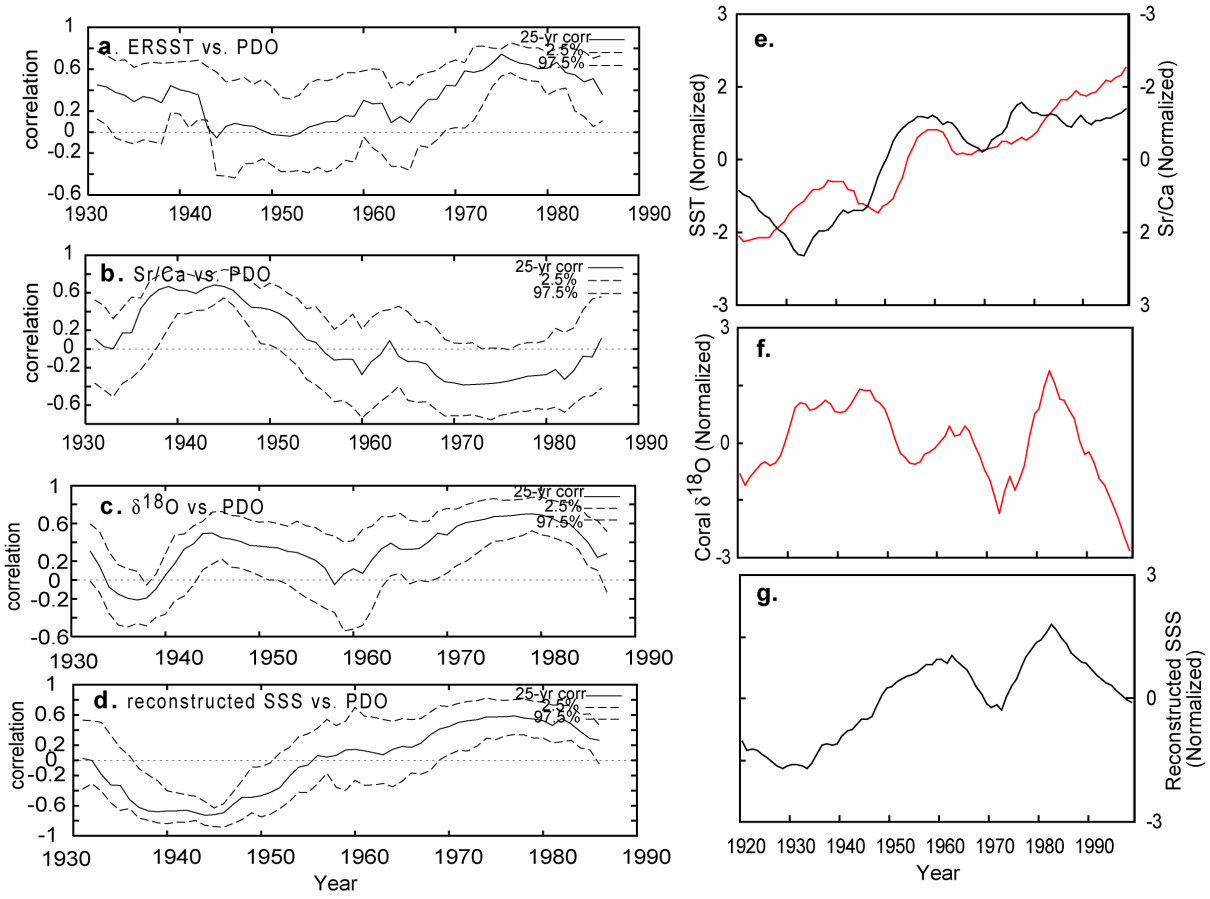

Figure 6.18. The running correlation of (a) ERSST, (b) Sr/Ca, (c) $\delta^{18}O$, (d) reconstructed SSS vs. PDO for Nov-Feb, 25 year running windows. Low pass filtered time series of (e) Sr/Ca (black) and ERSST (red), (f) coral $\delta^{18}O$ and (g) reconstructed SSS. All series are 12 points running averages and normalized to unit variance.

6. Concluding remarks

In the Indonesian region, coral $\delta^{18}O$ is influenced by a multitude of process (e.g. SST, E-P, advection), and this complicates the calibration of $\delta^{18}O_{coral}$ and SST reconstructions based solely on $\delta^{18}O_{coral}$ measurements (e.g. Charles et al., 2003). We have developed the first monthly Sr/Ca record from one of the exit passages of the ITF. Our coral Sr/Ca record from Timor-Ombai passage correlates with SST on seasonal and annual mean scales. The slope values are generally consistent with published Sr/Ca-SST relationships, particularly on a monthly scale. The $\delta^{18}O_{coral}$ -SST relationship can not be estimated by linear regression with SST only, because seasonal variations in $\delta^{18}O_{sw}$/SSS that co-vary with SST bias the $\delta^{18}O_{coral}$ -SST slope. The obtained slope values are too low compared to published estimates. Ideally, the $\delta^{18}O_{coral}$ -SST slope should be estimated by taking SSS ($\delta^{18}O_{sw}$) into account using MLR.

The SST contribution to $\delta^{18}O_{coral}$ in the multiple linear regression of coral $\delta^{18}O$ vs. SST, SSS SODA is -0.12- -0.15 ‰/°C. Using SST and SSS measured at Ombai strait close to the coral site, the slope of $\delta^{18}O_{coral}$ - SST in the MLR is -0.17±0.04‰/°C, which is consistent with published slope estimates of coral $\delta^{18}O_{coral}$ - SST (-0.18--0.22 ‰/°C) when taking the slope error into account. The incorrect slopes obtained in the MLR using the SODA data may be due to the low reliability or the spatial resolution of SST, and SSS data, or reflect the fact that the temporal relationship of $\delta^{18}O_{sw}$ and SSS is more complex.

The seasonal cycle of salinity in Ombai passage can be resolved by reconstructing SSS based on paired coral $\delta^{18}O$ and Sr/Ca, since the seasonal amplitude of SSS is higher (0.5 psu) than the propagation error of reconstructed SSS (±0.18 psu). The correlation of reconstructed SSS vs. SSS SODA v. 1.4.3 is R = 0.5 for the 5 year period from 2000 to 2004. The variance of SSS is consistent with SSS measured at Ombai passage. Annual mean reconstructed SSS, in contrast has a larger variance than grid-SSS from a combination of SODA v.142 and v.143. This could at least partly reflect uncertainties in the SSS from SODA v.142, since this version uses wind data from ERA 40, which may be problematic in the tropics. Also, the differences in variance could result from the different spatial scales represented by SSS reconstructed from the coral and SSS from SODA. However, this problem may be overcome by longer time series of measured SSS at the coral site.

Field correlation maps for over the past 20 years between Sr/Ca and SST show the El Niño pattern. The highest linear regression correlation (R= 0.4) obtained between Sr/Ca and Niño 3 is during the period of 1970-2004 for December-February seasonal means. However, changing the length of the datasets used for linear regression between coral Sr/Ca and Niño 3.4 (i.e., positive or negative regression slopes, varying correlation coefficients greatly influences the results obtained. This may be due to other climatic factors such as monsoonal process, or oceanic advection, which could dampen the ENSO signal at Timor on longer time scale. This seems likely, grid SST at Timor shows a similar response to ENSO. However, the observed changes in correlation could also reflect statistical artifacts. Coral Sr/Ca of our Timor core shows significant coherency with the Niño 3.4 index at interannual periods. The strong El Niño of 1982/1983 is clearly identified in the Timor coral, better than the El Niño of 1997/1998.

Seasonal mean time series of SODA SSS for Timor do not show a clear correlation with ENSO and neither does reconstructed SSS. However, local SSS measurements at Ombai strait do show the El Niño 1997/1998, and reconstructed SSS from paired proxy measurements shows a similar signature. This convinces us that local measurements of SSS and SST close to the coral site could improve the proxy calibration. Local SSS at Ombai shows an increase by 1.2 psu during the El Niño of 1997/1998, while reconstructed SSS from paired coral proxy measurements also shows an increase, although it is smaller (0.4 psu). This increase in SSS corresponds to a sea level drop in this region.

The highest correlation of the Timor proxy time series (Sr/Ca, $\delta^{18}O$, reconstructed SSS) and instrumental SST (ERSST) vs. PDO is found during northern hemisphere winter. Although the local grid-SST at Timor (ERSST) does not show any significant variability at decadal /interdecadal periods, the Sr/Ca power spectrum does show a large and significant signal at those periods. Decadal/interdecadal variability in coral Sr/Ca is coherent with Niño 3.4. This suggests that the coral proxy is a better recorder of decadal El Niño-like variability than grid-SST reconstructed from sparse data. However, the correlation between the coral proxies and the PDO is not statistically stable over time.

Acknowledgement

We are grateful for the support of the Deutscher Akademischer Austauschdienst (DAAD) (grant A/02/21403) and the Deutsche Forschungsgemeinschaft (Leibniz award to Prof. Wolf-Christian Dullo). We thank Noel Kenlyside for discussions. We thank Steffen Hetzinger and Dudi Prayudi for their assistant during field works. We acknowledge Janet Sprintall (National Science Foundation award OCE-9818670) for providing the collection of the salinity and temperature data from Ombai strait.

CHAPTER VII

Summary of chapter III-VI, conclusions and further studies

1. Summary of chapter III-VI

This thesis presents paired coral $\delta^{18}O$ and Sr/Ca records from Tahiti (French Polynesia) and Timor (Indonesia). The methods of seawater $\delta^{18}O$ (SSS) reconstruction proposed by Gagan et al. (1994, 1998) and Ren et al. (2002) are re-examined. Gagan et al. (1994, 1998) convert Sr/Ca and $\delta^{18}O$ to SST using a linear regression of Sr/Ca-SST and $\delta^{18}O$-SST. Seawater $\delta^{18}O$ is then obtained by subtracting $SST_{\delta 18O}$ with $SST_{Sr/Ca}$. With this method, which is used in the most coral studies (e.g., McCulloch et al., 1994; Gagan et al., 1994, 1998, 2000), coral $\delta^{18}O$ is calibrated vs. SST only. This is a methodological error, because coral $\delta^{18}O$ is influenced concomitantly by SST and $\delta^{18}O_{sw}$. Calibrating coral $\delta^{18}O$ with SST only may cause a bias in the regression slope of coral $\delta^{18}O$ vs. SST (γ_1) that will lead to problems in separating $\delta^{18}O_{sw}$ and SST variability. Ren et al. (2002) saw the major problems for the separation of the SST and $\delta^{18}O_{sw}$ (SSS) signal in the estimates of the intercept (constant of regression), therefore they proposed to use only the relative changes of the proxies to calculate relative changes of $\delta^{18}O_{sw}$. Relative changes are estimated by calculating the first derivative of the two proxies. The same result can be achieved by centering the data, which is proposed in this thesis. For the centering method, the mean values are removed from the variables of the linear regression. This method is more straightforward. For both Ren et al. (2002) and centering methods, the calibration estimate of γ_1 (i.e. the slope of the $\delta^{18}O$-SST regression) would be biased in regions where SST and $\delta^{18}O_{sw}$ co-vary, i.e., theoretically the two methods have the same problem as the method of Gagan et al. (1994, 1998). In practice, however, the changes of coral $\delta^{18}O$ relative to SST are known. It is generally accepted the slope values range from -0.18 to -0.22 ‰/°C. Estimates of Sr/Ca-SST relationship range from -0.04 and -0.08 mmol/mol/°C. We can insert these estimates in the equations of Ren et al. (2002) and centering, and the relative changes of $\delta^{18}O_{sw}$ from paired proxy measurements of any given coral can be calculated. Assuming that $\delta^{18}O_{sw}$ is linearly correlated with SSS, we can calibrate coral $\delta^{18}O$ using a multiple linear regression (MLR) of coral $\delta^{18}O$ vs. SST, SSS, as proposed in this thesis. This should be the correct approach to reconstruct SSS. The covariance between SST and SSS is taken into account in the regression parameters of coral $\delta^{18}O$ vs. SST, SSS.

Practically, however, the constants are barely known, which makes it difficult to obtain absolute values. Besides, time series of past SSS variations are rare, averaged over large areas and probably not free of error (see also Kilbourne, et al., 2004). This is a serious problem for the calibration/validation of coral-based $\delta^{18}O_{sw}$ reconstructions. Alternatively, it is possible to center the MLR, thus the constants can be omitted in the calculation and all variables are regarded as anomalies relative to their mean value. SSS reconstruction obtained with the centered MLR can be converted to $\delta^{18}O_{sw}$ units using the factor used for the $\delta^{18}O_{sw}$-SSS relationship, and will equal $\delta^{18}O_{sw}$ derived with the centering method.

At Tahiti the amplitude of the seasonal cycle of $\delta^{18}O_{sw}$ (0.14‰) expected based on climatological data of SSS almost equals the error propagation (σ) of $\delta^{18}O_{sw}$ calculated from paired coral $\delta^{18}O$ and Sr/Ca ($\sigma = \pm 0.066$‰). Therefore, reconstructed SSS ($\delta^{18}O_{sw}$) from modern Tahiti corals can not resolve the seasonal-scale variations of SSS and $\delta^{18}O_{sw}$ at Tahiti. However, on an annual mean scale, $\delta^{18}O_{sw}$ estimates contain a large number of independent coral $\delta^{18}O$ and Sr/Ca measurement, and thus the analytical uncertainty of annual mean $\delta^{18}O_{sw}$ reduces depending on the analytical error of the single proxy measurements and on the number of independent measurements. Also, annual mean variations of SSS at Tahiti are larger than seasonal scale variations. Therefore, $\delta^{18}O_{sw}$ variations are measurable. At Timor, seasonal variations of SSS can be resolved, since the seasonal cycle of SSS (0.5 psu equivalent to 0.2‰) is larger than the error propagation of reconstructed SSS (±0.18 psu or ± 0.07 ‰).

This study also highlights some major problems of coral Sr/Ca-SST reconstructions. At Tahiti, annual mean of SST reconstructions variability inferred from single coral Sr/Ca records are larger than grid-SST. This most likely reflects the different spatial scales represented by coral Sr/Ca and grid SST. Averaged Sr/Ca records from several colonies result in a better correlation of Sr/Ca with grid-SST. This poses a serious problem to any attempt to assess the magnitude of interannual SST variations from single records of fossil corals taken at Tahiti. The same problem is found for annual mean SST reconstructions based on coral Sr/Ca from a Timor coral. However, coral Sr/Ca from both locations shows a good correlation with local grid-SST. SST anomalies in the western and eastern Pacific are generally anti correlated. This is recorded in the coral Sr/Ca records from Tahiti and Timor. Timor (Tahiti) coral Sr/Ca shows a negative correlation with local SST at Timor (Tahiti), and a positive correlation with Tahiti (Timor) SST. This reflects the fact that warm (cool) SST at Timor

coincides with cool (warm) SST at Tahiti. The field correlation of coral Sr/Ca from both locations (Timor and Tahiti) with SST also shows the El Niño SST anomaly pattern pattern. However, the correlation of the coral proxies from both sites with the Niño 3.4 index is low. The coherency of coral Sr/Ca with Niño 3.4 is also low in the ENSO frequency band (2-7 years). Tahiti is located in the transitional zone between the fresh, warm waters of the west Pacific warm pool and the saltier, cold waters from the southern central Pacific, and lies close to a zero line of SSTa during ENSO years. Therefore, it maybe difficult to detect the ENSO signal in Tahiti corals. However, coral Sr/Ca from Tahiti may be able to detect the SST anomaly in the Niño 4 region, indicating that the decadal/interdecadal signal of the tropical Pacific may be recorded in the proxy records from Tahiti. However, our current proxy time series are too short to asses the robustness of decadal/interdecadal signals. Similarly, the coral proxy record from Timor does not show a clear correlation with El Niño. Timor coral Sr/Ca and local grid-SST show similar decadal trends. Despite, it is still difficult to asses the robustness of the decadal signal since the record is relatively short. Nevertheless, coral Sr/Ca shows significant spectral power at the decadal periods.

The modern coral records from Tahiti presented in this thesis can be used as a basis for paleoclimatic studies from fossil corals drilled at Tahiti as part of the IODP-Tahiti sea level Expedition 2005. The Timor proxy records is the first paired coral Sr/Ca and $\delta^{18}O$ time series from an exit-passage of the Indonesian Throughflow (ITF). Our results show that it is possible to reconstruct past SSS variations using coral proxies in the ITF exit passages.

2. Conclusions

(a) Both Tahiti and Timor coral Sr/Ca shows a good correlation with local SST. This confirms that Sr/Ca is a good temperature proxy. The regression slope values of the monthly coral Sr/Ca -SST calibration are consistent with published estimates of the Sr/Ca-SST relationship, while the slope values obtained by the annual mean calibration are not. This means that the variance of annual mean Sr/Ca and grid-SST is different. This most likely reflects the different spatial scales of the proxy and grid-SST, and has important implications for the reconstruction of past SST variations from fossil corals.

(b) Averaging the proxy measurements from multiple coral colonies taken from different locations in a given region will improve the correlation coefficients of the proxy-SST relationship, the variance of the reconstructed SST will be more realistic compared to grid-

SST, and the residual SST will be minimized. SST reconstructions from average proxy records are more representative of regional SST variations.

(c) The method of $\delta^{18}O_{sw}$ reconstruction from paired coral $\delta^{18}O$ and Sr/Ca measurements proposed by Gagan et al. (1994, 1998) contains a methodological error (coral $\delta^{18}O$ is calibrated with SST only) and can not be used in areas where SST-covariant variations in $\delta^{18}O_{sw}$ and SSS occur because this would bias the regression slope of coral $\delta^{18}O$-SST. The method of Ren et al. (2002) and the centering method proposed in this study can be used, as it is possible to insert the known slope of the $\delta^{18}O$-SST relationship. Both methods give the same results. However, the Ren et al. (2002) method requires much more complicated mathematical calculations than centering. The multiple linear regression between coral $\delta^{18}O$, SST and SSS should be the correct approach for SSS reconstructions from corals. The MLR of coral $\delta^{18}O$-SST, SSS can account for covariant changes of SST and SSS and $\delta^{18}O_{sw}$. This MLR method can be used to calculate SSS even in regions where SST-covariant SSS variations occur. Unfortunately, however, reliable time series of past SSS variations are scarce, and those that do exist are averaged over large areas. This is a serious problem in coral paleoclimatology. Besides, the correlation of SSS-$\delta^{18}O_{sw}$ is also still questionable.

(d) If the error propagation (σ) of $\delta^{18}O_{sw}$ derived from coral $\delta^{18}O$ and Sr/Ca is larger than the SSS seasonal amplitude of $\delta^{18}O_{sw}$ (SSS), variations of $\delta^{18}O_{sw}$ can not be resolved from the coral proxies. However, on an annual mean scale, the error of $\delta^{18}O_{sw}$ should reduce because the annual mean is obtained by averaging a large number of independent measurements. Also, at many sites interannual variations of SSS are larger than seasonal variations, and they should measurably affect coral $\delta^{18}O$. However, it is noted that the variance of SSS inferred from the corals in this study is higher than in the SODA dataset. This may reflect the different spatial scales represented by the coral-based salinity reconstructions and SSS from the SODA dataset, or problems in the SODA reanalysis. In order to obtain reliable, quantitative salinity reconstructions from corals we will need much better instrumental data of $\delta^{18}O_{sw}$ and SSS that can only be obtained through long-term monitoring programs.

(e) Tahiti is not an ideal site to reconstruct ENSO from coral proxies because it is located in a transitional zone i.e. (1) close to the zero line of the ENSO related- SST anomaly pattern and (2) at the eastern border of the south western Pacific salinity front (Gouriou and Delcroix, 2002). The displacement of the salinity front, as well as precipitation and SST variations

related to the SPCZ movement during ENSO years alter SSS and SST in the Tahiti region. (3) Tahiti is also located at the south-eastern margin of the SPCZ region. The correlation of the modern Tahiti coral proxy records with the Niño 3.4 index is low. A better correlation is found between Tahiti coral Sr/Ca- Niño 4 index (from R = 0.6 to 0.7) in an annual mean scale for the period of 1974-1995. This suggests that the coral proxies from Tahiti may better record decadal variability in the tropical Pacific, since the leading mode of SST variation in the Niño 4 region is decadal. However, both Sr/Ca and $\delta^{18}O$ from Tahiti do not show significant spectral power at decadal periods.

(f) At Timor, the ENSO signal is not clearly recorded by the coral proxy records. Despite band pass filtering of the proxy data in the 2-7 year periodicity band (the ENSO band) of the proxy, the correlation of the Timor coral proxies with Niño 3.4 is low. However, cross-spectral analysis of Timor coral Sr/Ca with Niño 3.4 shows significant coherence at interannual periods. The highest correlation of coral Sr/Ca from Timor with the PDO index is obtained for northern hemisphere winter monthly averages. However, the coral proxy records from Timor and Tahiti are too short too asses the robustness of the spectral peaks at decadal periods or to interpret their climatic significance.

3. Further Studies

(a) In order to obtain accurate calibrations of coral proxies with SST and to obtain reliable, quantitative $\delta^{18}O_{sw}$ and salinity reconstructions from corals we will need much better instrumental data of local SST at a coral site, $\delta^{18}O_{sw}$ and SSS. Therefore, long-term monitoring programs are needed. It would also be important to reduce the analytical error of coral $\delta^{18}O$ measurements in order to better resolve the often small seasonal $\delta^{18}O_{sw}$ (SSS) variations.

(b) Longer modern and fossil coral records need to be analyzed in order to obtain reliable, long time series that may be used to interpret and asses the importance of decadal/interdecadal climate variability.

(c) It is necessary to develop Master-chronologies by combining several modern and fossil coral records using U/Th dating following the methods of Cobb et al. (2003). This can provide us with accurate, long and continuous coral proxy time series. U/Th is accurate enough to

determine the age of young corals (< thousand years) with an error of approximately 5 yrs (Cobb et al., 2003).

REFERENCES

Abram, N.J., M.K. Gagan, M.T. McCulloch, J. Chappell, W.S. Hantoro (2003), Coral reef death during the 1997 Indian Ocean Dipole linked to Indonesian wildfires, *Science*, 301, 952-955.

Aharon, P. (1991), Recorders of reef environment histories: stable isotopes in corals, giant clams, and calcareous algae, *Coral Reefs*, 10, 71-90

Aldrian, E., and R. D Susanto (2003), Identification of three dominant rainfall regions within Indonesia and their relationship to sea surface temperature, *International Journal of Climatology*, 23,1435-1452.

Alibert C., L. Kinsley, S. J. Fallon, M. T. McCulloch, R. Berkelmans, and F. McAllister (2003), Source of trace element variability in Great Barrier Reef corals affected by the Burdekin flood plumes, *Geochimica et Cosmochimica Acta*, 67 (2), 231-246.

Alibert, C., and M. T. McCulloch (1997), Strontium calcium ratios in modern *Porites* corals from the Great Barrier Reef as a proxy for sea surface temperature: calibration of the thermometer and monitoring of ENSO, *Paleoceanography*, 12, 345-363.

Antonov, J.I., S. Levitus, and T.P. Boyer (2002), Steric sea level variation during 1957-1994: Importance of salinity, *Journal of Geophysical Research*, 107, C12, 8013, doi: 10.1029/2001JC000964.

Asami, R., T. Yamada, Y. Iryu, T. M. Quinn, C.P. Meyer, and G. Paulay (2005), Interannual and decadal variability of the western Pacific sea surface condition for the year 1787-2000: Reconstruction based on stable isotope record from a Guam coral, *Journal of Geophysical Research*, 110, C05018, doi:10.1029/2004JC002555.

Ayliff, L.K., M.I. Bird, M.K. Gagan, P.J. Isdale, H. Scott-Gagan, B. Parker, D. Griffin, M. Nongkas, and M.T. McCulloch (2004), Geochemistry of corals from Papua New Guinea as a proxy for ENSO ocean-atmosphere interactions in the Pacific Warm Pool, *Continental Shelf Research*, 24, 2343-2356.

Bagnato, S., B.K. Linsley, Howe S.S., Wellington G.M., and Salinger J. (2005), Coral oxygen isotope records of interdecadal climate variations in the South Pacific Convergence Zone region, *Geochemistry Geophysics Geosystems*, 6 (6), Q06001, doi:10.1029/2004GC000879.

Beck, W.J., L. R. Edwards, E. Ito, F.W. Taylor, J. Recy, F. Rougerie, P. Joannot, and C. Henin (1992), Sea surface temperature from coral skeleton Sr/Ca ratios, *Science*, 257, 644-647.

Behera, S.K. and T. Yamagata (2001), Impact of the Indian Ocean Dipole on the Southern Oscillation, *Journal of Climate* (submitted)

Bemis, B. E., H. J. Spero, J. Bijma, and D.W. Lea (1998), Re-evaluation of the oxygen isotopic composition of planktonic foraminifera: Experimental result and revised paleotemperature equations, *Paleoceanography*, 13(2), 150-160.

Bevington, P. R. (1969), (Chapter 4) Propagation of error, in *Data reduction and error analysis for the physical sciences*, pp. 56-65, Mc Graw-Hill Book Co., New York, San Francisco, St. Louis, Toronto, London, Sydney.

Boiseau, M., A. Juillet-Leclerc, P. Yiou, B. Salvat, P. Isdale, and M. Guilaume (1998), Atmospheric and oceanic evidence of El Niño southern oscillation events in the south central Pacific Ocean from coral stable isotopic records over the last 137 years, *Paleoceanography*, 13 (6), 671-685.

Burke, L., L. Selig, and M. Spalding (2002), Reefs at risk in Southeast Asia, UNEP-WCMC, Cambridge, UK.

Cane, M.A. (2005), The evolution of El Niño, past and future, *Earth and Planetary Science Letter*, 230, 227-240, doi: 10.1016/j.epsl.2004.12.003.

Carton, J. A., G. Chepurin, and X. Cao (2000), A Simple Ocean Data Assimilation Analysis of the Global Upper Ocean 1950-1995. Part 1 Methodology, *Journal of Physical Oceanography,* 30, 294-309.

Carton, J.A., and B.S. Giese (2005), SODA: A Reanalysis of Ocean Climate, *Journal of Geophysical Research Ocean* (submitted).

Charles C.D., M. D. Moore, and R. G. Fairbanks (1997), Interaction between the ENSO and the Asian monsoon in a coral record of tropical climate, *Science*, 277, 925-928.

Charles C.D., K. Cobb, M. D. Moore, and R. G. Fairbanks (2003), Monsoon-tropical ocean interaction in a network of coral records spanning the 20th century, *Marine Geology*, 201, 207-222.

Cobb, K.M., C.D. Charles and D.E. Hunter (2001), A central tropical Pacific coral demonstrates Pacific, Indian, and Atlantic decadal climate connections, *Geophysical Research Letters*, 28, 2209-2212.

Cobb, K.M., C.D. Charles, H.Cheng, M. Kastner, R.L. Edwards (2003), U/Th-dating of living and young fossil corals from the central tropical Pacific, *Earth and Planetary Science Letters* 210, 91-103.

Cobb, K.M., C.D. Charles, R.L. Edward, H. Cheng, and M. Kastner (2003a), El Niño-Southern Oscillation and tropical Pacific climate during the last millennium, *Nature*, 424, 271-276

Cohen, A. L., S. R. Smith, M.S. McCartney, and J. van Etten (2004), How brain corals record climate: an integration of skeletal structure, growth and chemistry of *Diploria labyrinthiformis* from Bermuda, *Marine Ecology Progress Series*, 271, 147-158.

Cole, J. E., R. G. Fairbanks, and G.T. Shen (1993), Recent variability in the Southern Oscillation : Isotopic results from a Tarawa Atoll coral, *Science*, 260, 1790-1793.

Cole, J.E., and R.G. Fairbanks (1990), The Southern Oscillation recorded in the $\delta^{18}O$ of Corals from Tarawa atoll, *Paleoceanography*, 5 (5), 669-683.

Corrège, T., T. Delcroix, J. Recy, W.J. Beck, G. Cabioch , and F. Le Cornec (2000), Evidence for stronger El Niño-Southern Oscillation (ENSO) events in a mid-Holocene massive coral, *Paleoceanography*, 15 (4), 465-470.

Corrège, T., M. K. Gagan, W. J. Beck, G. S. Burr, G. Cabioch, and F. Le Cornec (2004), Interdecadal variation in the extent of South Pacific tropical waters during the Younger Dryas event, *Nature*, 428, 927-929.

Craig, H., and Gordon, L.I., 1965, Deuterium and Oxygen 18 variation in the ocean and the marine atmosphere, in: E. Tongiorgi (Ed.), Stable isotope in oceanographic studies and paleotemperatures, Consiglio Nazionale delle Ricerche, Laboratorio di Geologia Nucleare, Pisa, Spoleto, p. 9-130.

Crowley, T. J., T. M. Quinn, and W. T. Hyde (1999), Validation of coral temperature calibrations, *Paleoceanography*, 14(5), 605-615.

de Villiers, S., G. T. Shen, and B. K. Nelson (1994), The Sr/Ca temperature relationship in coralline aragonite: Influence of variability in (Sr/Ca) seawater and skeleton growth parameters, *Geochimica et Cosmochimica Acta* , 58 , 197-208.

de Villiers, S., B. K. Nelson, and A. R. Chivas (1995), Biological controls on coral Sr/Ca and $\delta^{18}O$ reconstructions of sea surface temperatures, *Science*, 269, 1247-1249.

de Villiers, S., M. Greaves, and H. Elderfield (2002), An intensity ratio calibration method for the accurate determination of Mg/Ca and Sr/Ca of marine carbonates by ICP-AES, *Geochemistry, Geophysics, Geosystems,* 3, doi. 10.1029/2001GC000169.

Delaygue, G., J. Jouzel, and J.C. Dutay (2000), Oxygen-18 salinity relationship simulated by an oceanic general circulation model, *Earth and Planetary Science Letters*, 178, 113-123.

Delcroix, T. and M. McPhaden (2002), Interannual sea surface salinity and temperature changes in the western Pacific warm pool during 1992-2000, *Journal of Geophysical Research*, 107, C12 8002, doi: 10.1029/2001JC000862.

Delcroix, T., C. Henin, V. Porte, and P. Arkin (1996), Precipitation and sea-surface salinity in the tropical Pacific Ocean, *Deep-Sea Research I*, 43 (7), 1123-1141.

Deser, C., A.S. Philip, and J. W. Hurrell, 2004, Pacific interdecadal climate variability: Linkage between the Tropics and the North Pacific during boreal winter since 1900, *Journal of Climate,* 17, 3109-3124.

Dommenget, D. and M. Latif (2001), A cautionary note on the interpretation of EOFs, *Journal of Climate*, 15, 216-225.

Dettinger, M.D., M. Ghill, C.M. Strong, W. Weibel, and P. Yiou (1995), Software expedites singular-spectrum analysis of noisy time series. *Eos, Trans. American Geophysical Union*, 76(2), 12, 14, 21.

Draper, N. R. and H. Smith (1981), *Applied regression analysis, second edition*, John Wiley & Sons Inc, New York, Chichester, Brisbane, Toronto, Singapore, 709p.

Dunbar, R.B., G.M. Wellington, M.W. Colgan, and P.W. Glynn (1994), Eastern Pacific sea surface temperature since 1600 A.D: The $\delta^{18}O$ record of climate variability in Galapagos corals, *Paleoceanography*, 9, 291-315.

Epstein, S., R. Buchsbaum, H. A. Lowenstamm, and H.C. Orey (1953), Revised carbonate-water isotopic temperature scale, *Geological Society of America bulletin*, 64, 1315-1326.

Evans, M.N., A. Kaplan, and M.A. Cane (2002), Pacific sea surface temperature field reconstruction from coral $\delta^{18}O$ data using reduced space objective analysis, *Paleoceanography*, 17 (1), 1007, doi: 10.1029/2000PA000590.

Fairbanks, R.G., M.N. Evans, J.L. Rubernstone, R.A. Mortlock, K. Broad, M.D. Moore, and C.D. Charles (1997), Evaluating climate indices and their geochemical proxies measured in corals. *Coral Reefs*, 16, 93-100.

Fairbanks, R.G., C.D. Charles, and J.D. Wright (1992), Origin of global meltwater pulses, in: R.E. Taylor, A. Long and R.S. Kra (Eds.), Radiocarbon after four decades: An interdisciplinary perspective, *Springer-Verlag*, New York, pp.473-500.

Fallon, S. J., M. T. McCulloch, and C. Alibert (2003), Examining water temperature proxies in *Porites* corals from the Great Barrier Reef: a cross-shelf comparison, *Coral Reefs*, doi: 10.1007/s00338-003-0322-5.

Felis, T., G. Lohmann, H. Kuhnert, S. J. Lorenz, D. Scholz, J. Pätzold, S.A. Al-Rousan, and S.M. Al-Moghrabi (2004), Increased seasonality in Middle East temperatures during the last interglacial period, *Nature* , 429, 164-168.

Folland, C.K., J.A. Renwick, M.J. Salinger, and A.B. Mullan (2002), Relative influences of the Interdecadal Pacific Oscillation and ENSO on the South Pacific Convergence Zone, *Geophysical Research Letters*, 29(13), 1643, doi:10.1029/2001GL014201.

Gagan, M. K., A. R. Chivas, and P. J. Isdale (1994), High resolution isotopic records from corals using ocean temperature and mass spawning chronometers, *Earth and Planetary Science Letters*, 121, 549-558.

Gagan, M. K., L. K. Ayliffe, D. Hopley, J. A. Cali, G. E. Mortimer, J. Chappel, J., M. T. McCulloch, and M. J. Head (1998), Temperature and surface ocean water balance of mid-Holocene tropical western pacific, *Science*, 279, 1014-1018 .

Gagan, M.K, L. K. Ayliffe, J. W. Beck, J. E. Cole, E. R. M. Druffel, R. B. Dunbar, and D.P. Schrag (2000), New Views of tropical paleoclimates from corals, *Quarternary Science Reviews* , 19, 45-64.

Ghil, M., M.R. Allen, M.D., Dettinger, K. Ide, D. Kondrashov, M.E. Mann, A.W. Robertson, A. Saunders, Y.Tian, F.Varadi, and P.Yiou (2002), Advanced spectral methods for climatic time series, *Reviews of Geophysics*, 40, doi: 10.1029/2001RG000092.

Gordon, A.L., D.R. Susanto, and K. Vranes (2003), Cool Indonesian Throughflow as a consequence of restricted surface layer flow, *Nature*, 425, 824-828.

Gouriou, Y. and T. Delcroix (2002), Seasonal and ENSO variations of sea surface salinity and temperature in the South Pacific Convergence Zone during 1976-2000, *Journal of Geophysical Research*, 107, C12 8011, doi: 10.1029/200IJC000830.

Grumet, N. S., N. J. Abram., J. W. Beck, R. B. Dunbar, M. K. Gagan, T. P. Guilderson, W. S. Hantoro, and B. W. Suwargadi (2004), Coral radiocarbon records of India Ocean water mass mixing and wind-induced upwelling along the coast of Sumatra, Indonesia, *Journal of Geophysical Research*, 109, C05003, doi: 10.1029/2003JC002087.

Grodsky, S.A., J.A. Carton, and R. Murtugude (2001), Anomalous surface currents in the tropical Indian Ocean, *Geophysical Research Letters*, 28 (22), 4207-4210.

Guilderson, T.P., R.G. Fairbanks, and J.L. Rubenstone, J.L. (1994), Tropical temperature variations since 20,000 years ago: modulating interhemisphere climatic change, *Science* , 263: 663-665.

Guilderson, T.P., D.P. Schrag, and M.A. Cane (2004), Surface water mixing in the Solomon Sea as documented by a high-resolution coral ^{14}C record, *Journal of Climate*, 17, 1150-1156.

Grinsted, A., J.C. Moore, and S. Jevrejeva (2004), Application of the cross wavelet transform and wavelet coherence to geophysical time series, Nonlinear Processes in Geophysics, 11, 561-566.

Hamada, J.I., M.D. Yamanaka, J. Matsumoto, S. Fukao, P.A. Winarso, and T. Sribimawati (2002), Spatial and temporal variations of the rainy season over Indonesia and their link to ENSO, *Journal of the Meteorological Society of Japan*, 80(2), 285-310.

Heiss, G.A. and W.-Chr. Dullo (1997), Stable isotope record from recent and fossil *Porites* sp. in the northern Read Sea, *Coral Research Bulletin*, 5, 161-169.

Helmle, K.P., K.E. Kohler, and R.E. Dodge (2002), Relative optical densitometry and the coral X-radiograph densitometry system: CoralXDS, Presented Poster, Int. Soc. Reef Studies 2002 European Meeting. Cambridge, England. Sept. 4-7.

Hendon, H.H., 2003, Indonesian rainfall variability: Impact of ENSO and local air-sea interaction, *American Meteorological Society*, p.1775-1790.

Hendy, E. J., M. K. Gagan, C. A. Alibert, M. T. McCulloch, J. M. Lough, and P. J. Isdale (2002), Abrupt decrease in tropical Pacific sea surface salinity at end of the little ice age, *Science*, 295, 1511-1514.

Hughen, K. A., D. P. Schrag, S. B. Jacobsen (1999), El Niño during the last interglacial period recorded by a fossil coral from Indonesia, *Geophisical Research Letters*, 26 (20), 3129-3132.

Huppert, A., and A. R. Solow (2004), Comment on "Deconvolving the $\delta^{18}O$ seawater component from subseasonal coral $\delta^{18}O$ and Sr/Ca at Rarotonga in the southwestern subtropical Pacific for the period 1726 to 1997 by L. Ren, B.K. Linsley, G.M. Wellington, D.P. Schrag, and O. Hoegh-Guldberg (2003)", *Geochimica et Cosmochimica Acta*, 68, 3137-3138, doi: 10.1016/j.gca.2003.12.020.

Hurrell, J.W. and K. E. Trenberth (1999), Global Sea Surface Temperature Analysis: Multiple Problems and Their Implications for Climate Analysis, Modeling, and Reanalysis, *Bulletin of the American Meteorological Society*, 80 (12), 2661-2678.

Hoefs, J. (1997), Stable Isotope Geochemistry (fourth edition), *Springer-Verlag*, Berlin.

Imbrie, J., A. McIntyre, A. Mix (1989), Oceanic response to orbital forcing in the late Quaternary: Observational and experimental strategie. In: Climate and Geosciences (Ed. By A. Berger et al.), p.121-164, Kluwer Academic Press, Dordrecht. *NATO ASI Series C*.

Jones, P.D., T. J. Osborn, and K. R. Briffa (1997), Estimating sampling error in large-scale temperature averages, *Journal of Climate* , 10, 2548-2568.

Juneng, L., and F. T. Tangang (2005), Evolution of ENSO-related rainfall anomalies in Southeast Asia region and its relationship with atmosphere-ocean variation in Indo-Pacific sector, *Climate Dynamics*, 25, 337-350

Juillet-Leclerc, A. and G. Schmidt (2001), A calibration of the oxygen isotope paleothermometer of coral aragonite from *Porites*, *Geophysical Research Letters*, 28 (21), 4135-4138.

Kilbourne, K. H., T. M. Quinn, F. W. Taylor, T. Delcroix, and Y. Gouriou (2004), El Niño-Southern Oscillation-related salinity variations recorded in the skeletal geochemistry of a *Porites* coral from Espiritu Santo, Vanuatu, *Paleoceanography*, 19, PA4002, doi: 10.1029/2004PA001033.

Kinsman D.J.J., and H.D. Holland (1969), The co-precipitation of cations with CaCO3-IV. The co-precipitation of Sr^{2+} with aragonite between 16° and 96°C, *Geochimica et Cosmochimica Acta* , 33, 1-17.

Kuhnert, H.J., J. Pätzold, B. Schnetger and G. Wefer (2002), Sea surface temperature variability in the 16th century at Bermuda inferred from coral records. *Palaeogeography, Palaeoclimatology, Palaeoecology*, 179, 159-171.

Latif, M., R. Kleeman, and C. Eckert (1997), Greenhouse warming, Decadal variability, or El Nino? An attempt to understand the anomalous 1990s, Journal of Climate, 10 (9), 2221-2239, doi: 10.1175/1520-0442

Levitus, S., R. Burgett, and T. Boyer (1994), World Ocean Atlas 1994, Vol. 3.

Linsley, B. K., R. G. Messier, and R.B. Dunbar (1999), Assessing between colony oxygen isotope variability in the coral *Porites lobata* at Clipperton Atoll, *Coral Reefs*, 18, 13-27.

Linsley, B.K., G. M. Wellington, and D. F. Schrag (2000), Decadal sea surface temperature variability in the subtropical south Pacific from 1726 to 1997 AD, *Science*, 290, 1145-1148.

Linsley, B.K., G. M. Wellington, D. P. Schrag, L. Ren, M. J. Salinger, and A.W. Tudhope (2004), Geochemical evidence from corals for changes in the amplitude and spatial pattern of south Pacific interdecadal climate variability over the last 300 years, *Climate Dynamics*, 22 (1), doi :10.1007/s00382-003-0364-y.

Lohmann, K., and M. Latif (2005), Tropical Pacific Decadal variability and the subtropical - tropical cell, *Journal of Climate* (accepted).

Mantua, N.J. S.R. Hare, Y. Zhang, J.M. Wallace, and R.C. Francis (1997) A Pacific interdecadal climate oscillation with impacts on salmon production, *Bulletin of the American Meteorological Society*, 78, 1069-1079.

Marshall, J.F., and M.T. McCulloch (2002), An assessment of the Sr/Ca ratio in shallow water hermatypic corals as a proxy for sea surface temperature, *Geochimica et Cosmochimica Acta*, 66, 3263-3280.

Mc Crea, J.M. (1950), On the isotopic chemistry of carbonates and a paleotemperature scale, *Journal of Chemical Physics*, 18, 849-857.

McConnaughey, T. (1989a), $\delta^{13}C$ and $\delta^{18}O$ isotopic disequilibrium in biological carbonates: I Patterns, *Geochimica et Cosmochimica Acta*, 53, 151-162.

McConnaughey, T. (1989b), ^{13}C and ^{18}O isotopic disequilibrium in biological carbonates: II In Vitro simulation of kinetic isotope effect, *Geochimica et Cosmochimica Acta,* 53, 163-171.

McCulloch, M. T., M. K. Gagan, G. E. Mortimer, A. R. Chivas, and P. J. Isdale (1994), A high-resolution Sr/Ca and $\delta^{18}O$ coral record from the great barrier reef, Australia and the 1982-1983 El Niño, *Geochimica et Cosmochimica Acta*, 58, 2747-2754.

McGregor, H.V. and M. K. Gagan (2003), Diagenesis and geochemistry of *Porites* corals from Papua New Guinea: Implications for paleoclimate reconstruction, *Geochimica et Cosmochimica Acta*, 67 (12), 2147-2156.

Mitsuguchi, T., E. Matsumoto, and T. Uchida (2003), Mg/Ca and Sr/Ca ratios of *Porites* coral skeleton: Evaluation of the effect of skeletal growth rate, *Coral Reefs*, doi: 10.1007/s00338-003-0326-1.

Mucci, A., Canuel, R., Zhong, S., 1989, The solubility of calcite and aragonite in sulfate-free seawater and the seeded growth kinetics and composition of the precipitates at 25°C, *Chemical Geology*, 74, 309-320.

O 'Neil J.R., R.N. Clayton, and T.K. Mayeda (1969), Oxygen isotope fractionation in divalent metal carbonates, *Journal of Chemical Physics*, 51, 5547-5558.

Oberhuber, J.M. (1998), An atlas based on COADS data set, Tech. Rep. 15, Max-Planck-Instutut für Meteorologie.

Oldenborgh, G.J. and G. Burgers (2005), Searching for decadal variatios in ENSO precipitation teleconnections, *Geophysical Research Letters*, 32, 15, L15701, doi:10.1029/ 2005GL023110.

Paillard, D., L. Labeyrie, and P. Yiou (1996), Macintosh program perform time-series analysis. *Eos Trans*,77,39.

Pfeiffer, M., O. Timm, W. Chr. Dullo, and S. Podlech (2004a), Oceanic forcing of interannual and multidecadal climate variability in the southwestern Indian Ocean: Evidence from a 160 year coral isotopic record (La Reunion, 55°E,21°S), *Paleoceanography*, 19, doi:10.1029/2003PA000964.

Pfeiffer, M., W. Chr. Dullo, and A. Eisenhauer (2004b), Variability of the Intertropical Convergence Zone recorded in coral isotopic records from the central Indian Ocean (Chagos Archipelago), *Quaternary Research*, 61, 245 - 255, doi 10.1016/ j. yqres. 2004. 02. 009.

Pfeiffer, M., and W. Chr. Dullo (2005), Monsoon-induced cooling of the western equatorial Indian Ocean as recorded in coral oxygen isotope records from the Seychelles covering the period of 1840 to 1994 AD, *Quarternary Science Review*, in press

Pond, S and G. I. Pickard (1983), Introductory Dynamic Oceanography, Pergamon Press, 2nd edition, 330 pp.

Power, S., T. Casey, C. Folland, A. Colman, and V. Mehta (1999), Interdecadal modulation of the impact of ENSO on Australia, *Climate Dynamics*, 15(5), 319-324.

Press, W.H., B. P. Flannery, S. A. Teukolsky, and W. T. Vetterling (1990), Numerical recipes, Cambridge Univ. Press, New York.

Quinn, T. M., F. W. Taylor, T. J. Crowley, and S. M. Link (1996), Evaluation of sampling resoultion in coral stable isotope records: A case study using records from New Caledonia and Tarawa, *Paleoceanography*, 11 (5), 529-242.

Rao, A.S., S.K. Behera, Y. Masumoto, T. Yamagata (2002), Interannual variability in the subsurface Indian Ocean with special emphasis on the Indian Ocean Dipole. *Deep-Sea Research* II, 49, 1549-1572.

Rayner, N.A., D. E. Parker, E. B. Horton, C. K. Folland, L.V. Alexander, D.P. Rowell, E.C. Ken and A. Kaplan (2003), Globaly complete analysis of sea surface temperature, sea ice and night marine air temperature, 1871-2000. *Journal of Geophysical Research*, 108, 4407, doi: 10.1029/2002JD002670.

Ren, L., B. K. Linsley, G. M. Wellington, D. P. Schrag, and O. Hoegh-Guldberg (2002), Deconvolving the $\delta^{18}O$ seawater component from subseasonal coral δ18O and Sr/Ca at Rarotonga in the southwestern subtropical Pacific for the period 1726 to 1997, *Geochimica et Cosmochimica Acta*, 67, 1609-1621.

Reynolds, R. W. and T. M. Smith (1994), Improved global sea surface temperature analyses, *Journal of Climate* , 7, 929-948.

Rougerie, F., Wauty, B. (1993), l'oceanographie du Pacifique Central Sud. In Atlas de Polynesie Francaise, ORSTOM Edition, 20-21.

Saji, N. H., B. N. Goswami, P. N. Vinayachandran, and T. Yamagata (1999), A dipole mode in the tropical Indian Ocean, *Nature*, 401, 360-363.

Salinger, M.J., J.A. Renwick, and A.B. Mulan (2001), The Interdecadal Pacific Oscillation and South Pacific climate, *International Journal of Climatology*, 21, 1705-1721.

Schmidt, G. A. (1999), Error analysis of paleosalinity calculations, *Paleoceanography*, 14 (3), 422-429.

Schmidt, G. A. (1998), Oxygen-18 variations in a global ocean model, *Geophysical Research Letters*, 25(8),1201-1204, doi:10.1029/98GL50866

Schrag, D. P. (1999), Rapid analysis of high-precision Sr/Ca ratio in corals and other marine carbonates, *Paleoceanography*, 14, 97-102.

Shen, C.C., T. Lee, C. Yun chen, C. Ho Wang, C. Feng Dai, and L. An Li (1996), The calibration of D(Sr/Ca) versus sea surface temperature relationship for *Porites* corals, *Geochimica et Cosmochimica Acta*, 60 (20), 3849-3858.

Shen, G.T., L.J. Linn,T.M. Campbell, J.E. Cole, and R.G Fairbanks (1992), A chemical indicator of trade wind reversal in coral from the western tropical Pacific, *Journal of Geophysical Research*, 97,12,689-12,698.

Smith, T.M. and R. W. Reynolds (2004), Improved Extended Reconstruction of SST (1854-1997), *Journal of Climate*, 17, 2466-2477.

Solow, Q.R, and A. Huppert (2004), A potential bias in coral reconstructions of sea surface temperature, *Geophysical Research Letters* , 31, doi: 10.1029/2003GL019349.

Spero, H. J., M. M. Koreen, E. M. Kalve, D. W. Lea, and D. K. Pak (2003), Multispecies approach to reconstructing eastern equatorial Pacific thermocline hydrography during the past 360 kyr, *Paleoceanography*, 18(1), 1022, doi:10.1029/2002PA000814.

Sprintall, J., J.T. Potemra, S. Hautala, A.B. , Nancy, and W.W. Pandoe (2003), Temperature and salinity variability in the exit passages of the Indonesian Throughflow, *Deap-Sea Research Part II*, 50, 2183-2204.

Suzuki A., K. Hibino, A. Iwase, and H. Kawahata (2005), Intercolony variability of skeletal oxygen and carbon isotope signatures of cultured *Porites* corals: Temperature-controlled experiments, *Geochimica et Cosmochimica Acta*, 69 (18), 4453-4462, doi: 10.1016/ j.gca. 2005.05.018.

Timm, O., M. Pfeiffer M., and W.C. Dullo (2005), Nonstationary ENSO-precipitation teleconnection over the equatorial Indian Ocean documented in a coral from the Chagos Archipelago, *Geophysical Research Letters* ,32, L02701 doi:10.1029/2004GL021738.

Torrence, C. and G. P. Compo (1998), A Practical guide to wavelet analysis, *Bulletin of the American Meteorological Society*, 79, 61-78.

Tomczak, M. and J.S. Godfrey (2003), Regional Oceanography: an Introduction, 2nd edition, 390p, Elsevier Science Ltd. England, New York, Tokyo.

Trenberth, K.E. (1997), The definition of El Nino, *Bulletin of the American Meteorological Society*, 2771-2777.

UNEP/IUCN, 1988, Coral reefs of the world. Volume 3: Central and Western Pacific. UNEP Regional Seas Directories and Bibliographies. IUCN, Gland, Switzerland and Cambridge, U.K./UNEP, Nairobi, Kenya. 329 p.

von Langen, P. J., D. W. Lea, and H. J. Spero (2000), Effect of temperature on oxygen isotope and Mg/Ca values in *Neogloboquadrina pachyderma* shells determined by live culturing, *Eos*, AGU, 81(48), Fall Meet Suppl., Abstract OS11C-20.

Weber and Woodhead (1972) Temperature dependence of oxygen-18 concentration in reef coral carbonate, *Journal of Geophysical Research* ,77, 463-473.

Weber, J.N., 1973, Incorporation of strontium into reef coral skeletal carbonate, *Geochimica et Cosmochimica Acta*, 37, 2173-2190.

Webster, P.J. and T.N. Palmer (1997), The past and the future of El Niño, *Nature*, 390, 562-564.

Wellington, G.M., R. B. Dunbar, G. Merlen (1996), Calibration of stable oxygen isotope signature in Galapagos corals, *Paleoceanography*, 11 (4),467-480.

Windupranata, W. (2002), Analisis topografi paras laut di perairan Indonesia serta daerah ekuator samudra Hindia dan samudra Pasifik, *Master Thesis*, Institut Teknologi Bandung, 73p.

Xie, P and P. Arkin (1996), Analyses of global monthly precipitation using gauge observation, satellite estimates and numerical model prediction, *Journal of Climate*, 9, 840-885.

Zhang, Y., J.M. Wallace, and D.S. Battisti (1997), ENSO-like interdecadal variability: 1900-93. *Journal of Climate*, 10, 1004-1020.

Zinke J., W.-Chr. Dullo, G.A. Heiss, and A. Eisenhauer (2004), ENSO and Indian Ocean subtropical dipole variability is recorded in a coral record off southwest Madagascar for the period 1659 to 1995, *Earth and Planetary Science Letters*, 288,177-194.